Statistical Methods for the Joint Analysis of Spatial, Sparse or Missing Ecological Data

Marina Jiménez Muñoz

School of Mathematics, Statistics and Actuarial Science
University of Kent

A Thesis submitted for the degree of
Doctor of Philosophy

January 2020

I would like to dedicate this thesis to my Tata, and my Chacha. Two loving women who were part of my upbringing and who sadly are no longer here with us. You are very much missed.

Acknowledgements

This is a very special section of the thesis because it gives me the opportunity to thank some of the people who have been part of my life during the time I have been doing my PhD.

Firstly, I would like to thank my supervisors Dr Diana Cole and Dr Eleni Matechou. I feel truly honoured to have had the opportunity to work with them. They are wonderful women and academics, who time and again stunned me with their ability to be simultaneously supportive and rigorous. I have learnt so much from them and thoroughly enjoyed the time spent with them both in the office, and also on a personal level. I would also like to express my gratitude to Dr Takis Besbeas, Dr Stephen Baillie and Dr Robert Robinson who have also been a key part of my supervisory team. They have played a very important role in the development of this thesis, and of my learning process.

Thank you to my collaborators, Dr Stephen Freeman and Dr Katarzyna Wojczulanis-Jakubas for their comments and contributions to our work.

Thank you to the Engineering and Physical Sciences Research Council (EPSRC) and the University of Kent for funding my work. My gratitude to the British Trust for Ornithology, and the long running data collection volunteers and ecologists who have made this work possible.

I would like to thank Helen Smith for sharing with me her beautiful starling pictures, particularly the one I chose for the cover for this thesis.

My sincere gratitude to my examiners, Professor Ruth King and Dr Rachel McCrea, for making the time to assess this work and provide their feedback.

Thank you to Claire Carter, the administration team, and the colleagues who have helped me and have contributed to making SMSAS a friendly environment.

To all the people who have contributed to the world of Science, particularly, I would like to thank all the inspiring women in the field who have set an example and have showed that through determination and hard work anything is possible.

I have been blessed with a very big family of whom I am very proud. They have always given me their unconditional love and support. I can hardly find the words to express my gratitude. To my parents, M. Carmen and Narciso, for being patient, encouraging and always being there no matter what. Mum, you are the most loving, courageous and generous person

I know. Dad, thank you for always giving me your time and your help, you are an excellent father. To my sister Elena who is my best friend. As an older sister, she has always cared for me, has been someone to look up to, and has teased me at every possible time. To my grandma, who is the kindest, and cheekiest person in the world. To my aunties, Charqui, Inma and Pili who are very inspiring, hard-working and loving women who have taught me so much. To Jose for taking good care of me during our summer holidays and for still maintaining that care in the distance, always keeping in touch and sending me the most hilarious messages. To my uncles, and my cousins, I am so lucky to have you all in my life and I love you all.

I would like to thank all the friends who have shared this journey with me. To my friends María, Dani, David, Perry, Licia and Sou who have been my international family and with whom I have spent the most amazing times. To my very best friend Marta with whom even from the distance I have shared many years of my life and wonderful holidays. To my friend Bela with whom I have had many good times and inspiring conversations. To my friend Elena who is an incredible strong woman who has shared so much with me. To my housemate and good friend Aurélie with whom I have shared many guilty pleasures and laughs. To Jocelyne who started her PhD with me, and who I truly admire for being her wonderfully eccentric self and who always amazes me with her advice. To Karen, a friend and colleague who has always been so supportive, and kind. To Mario with whom I started my MSc in Stats and with whom I have a great friendship which has taken us around the world. To Alfredo because he is a unique person who always makes me laugh. To my friend, former housemate and officemate Alan with whom I have spent many fun times discussing any possible topic that would come to our minds. To my dear friends and colleagues Joe, Helder and Peter for the good usually quiet and not so quiet times that we have spent together. It has meant the world to me to have you all in my life.

Last but of course not least, I would like to thank my beloved partner Giacomo, for always making everything better and for brightening my world every single day. From the endless silly conversations, to the endless Mathsy discussions. Life is never boring with him. He who has the warmest heart and who is always willing to help me develop my craziest ideas. He has edited the thesis cover and created from scratch the bird animation of this thesis. I am so proud of you.

I hope you can all join me in celebrating this achievement of which I feel you are all part. Thank you, thank you, thank you!

Abstract

To mitigate biodiversity loss, we need to understand the environmental and demographic causes of changes in the distributions and abundances of species. Bird populations are in a continual state of flux; these fluctuations can be explained by changes in vital rates, such as survival and productivity (breeding success).

This thesis is the result of three different ecological projects for which we have developed statistical methods that combine different types of data together. In particular, in this thesis we describe, implement, and develop statistical models that can be applied to different types of ecological data such as census, ring-recovery, and capture-recapture data.

In the first project we use data from the British Trust for Ornithology (BTO), which has developed an extensive historical data set of the total number of birds ringed in Britain and Ireland, dating back to 1909. However, until 2000 the data were submitted by ringers in paper form. The way in which such archival data were collected and stored means that the total number of birds ringed in different age categories is difficult to obtain. Bird survival changes with age, with younger birds being more vulnerable. Missing information on the age at ringing compromises our ability to understand historic variation in survival rates. We examine suitable methods and propose a new model for enhancing the use of such data. Using blackbird (*Turdus merula*) and sandwich tern (*Thalasseus sandvicensis*) data we show the rigour of our model in estimating unknown age proportions for different species, allowing the BTO and other European institutions to fully utilise their historical data.

Bi-parental care is crucial in the reproduction success of the little auk (*Alle alle*) which we study in the second project. For this species, typically, the female deserts the brood before the male does. Hypotheses which considered that females left the nest earlier in order to increase their remating success or to secure their good body conditions have been rejected. As a result, a biological explanation for this unusual trait has not been found yet. We investigate whether the length of time that females stay in the nest in a given breeding season may have an impact on their survival probability in the period following breeding. We combine capture-recapture data from two sites and use sparse continuous covariates data to study if the survival of the female little auk is affected by the time spent in the brood guarding the chicks.

Animals are affected by local environmental conditions that vary with space. In the third project, we incorporate detailed local spatial information, such as geographical coordinates and land cover type data, into an spatially-explicit integrated population model. This involves supplementing census data with ring-recovery data to study demographic rates, while also incorporating detailed local spatial information into integrated population models. Bird count data are typically modelled at large scales using state-space models. In classical analysis, the time-series likelihood component has traditionally been approximated using a Kalman filter methodology, which is computationally efficient but relies on the assumption of the suitability of Gaussian approximations.

Rather than one single nation-wide time-series of counts, spatial census data consist of multiple time-series associated to specific locations. These data are particularly challenging to model because of the presence of very small counts at some locations, which violates the Gaussian assumption of the Kalman filter. To address this issue, we consider hidden Markov models, which are ideally suited to the analysis of very small counts, as their validity does not rely on Gaussian approximations. Both methodologies, the Kalman filter and hidden Markov models, are combined in a flexible algorithm which adapts to the varying sample sizes at different locations—it is therefore able to accommodate data sets of different sizes for many bird species. We illustrate our methods using starling (*Sturnus vulgaris*) data.

Table of contents

List of figures

List of tables

Chapter 1

Introduction

Animal populations are in a continuous state of change. It is for this reason that it is important to understand and to monitor the underlying demographic processes that cause population fluxes (Robinson et al., 2012). This thesis is focused on building statistical models to detect and quantify changes in biodiversity. It is the result of three different ecological projects that combine different types of data together.

Firstly, in this introductory chapter we provide the ecological and statistical background for the work carried out in this thesis. In Section 1.1 we describe the different types of data considered. In Section 1.2 we present the background for the models that we use throughout this thesis. Then, in Section 1.3 we give details about the methods used to fit and compare our models.

In Chapter 2 we present the work of Jiménez-Muñoz et al. (2019) on analysing historical age-aggregated ring-recovery data sets to estimate age-dependent survival. Bird ring-recovery data have been widely used to estimate demographic parameters such as survival probabilities since the mid-twentieth century. However, while the total number of birds ringed each year is usually known, historical information on age at ringing is often not available. A standard ring-recovery model, for which information on age at ringing is required, cannot be used when historical data are incomplete. We develop a new model to estimate age-dependent survival probabilities from such historical data when age at ringing is not recorded; we call this the historical data model. An alternative to the historical data model is the conditional model of McCrea et al. (2012) which conditions on the numbers of recovered individuals. We conduct a simulation study to examine the performance of the historical data model and compare it with other models including the standard and conditional ring-recovery models. Simulation studies show that the historical data model yields similar parameter estimates to the standard model but without requiring knowledge of the age at time of ringing. Parameter redundancy results show that the newly developed historical data model is comparable to

the standard ring-recovery model, in terms of which parameters can be estimated, and has fewer identifiability issues than the conditional model. We illustrate the new proposed model using blackbird (*Turdus merula*) and sandwich tern (*Thalasseus sandvicensis*) data. The new historical data model allows us to make full use of historical data and estimate the same parameters as the standard model without the need to fully computerise the data. In so doing, we can detect potential changes in demographic parameters further back in time.

In Chapter 3 we present work on the timing of female brood desertion and survival in the little auk (*Alle alle*). For this small seabird bi-parental care is crucial to raise the single chick successfully (Kidawa et al., 2012). However, at the end of the nesting period, the females desert their broods, leaving the male counterpart to continue the care alone (Wojczulanis-Jakubas and Jakubas, 2012). The reason why the female leaves the brood first is unclear. Using capture-recapture data, we first examine if the survival of this species is affected by their sex and/or by the site in which they breed. Additionally, using capture-recapture data with the addition of information on the time-to-brood desertion, termed presence data, we aim to understand if the length of stay of the female birds in the brood during breeding affects their survival. The sparse presence data contain a large number of missing values, and to deal with this, algorithms can become computationally very expensive making it difficult to implement the flexible capture-recapture methods containing continuous covariates that have already been developed (see, for example, Bonner et al., 2010; Langrock and King, 2013; Worthington et al., 2015). Thus, we use a deterministic algorithm to impute the missing data making possible the capture-recapture analysis with continuous presence covariates. We take a similar approach to Bonner et al. (2010) who used linear interpolation between an individual's first and last capture. We perform a simulation study to check the validity of our imputation method, and we find that the accuracy of our method depends on the sample size. From analysing the capture-recapture data on their own we find that survival is site dependent, with no apparent sex differences in survival. However, the sparse continuous covariate data do not allow us to reach any strong conclusions regarding the effect of the length of stay of the female in the brood on its survival probability. Thus, our results in this case are inconclusive, but will be updated once more data become available.

Chapters 4 and 5 are directly linked. The British Trust for Ornithology (BTO) collects data through several complementary schemes. These schemes include those recording data on uniquely identifiable animals (ringing data), and on counts of the number of animals observed (census data). While census data are used to estimate abundance, ringing data are used to estimate survival probabilities. Integrated population models (IPMs) combine these two types of data into one single analysis, making it possible to also estimate productivity, which is unobtainable from either type of data alone (Besbeas et al., 2002). Additionally,

results from IPMs are more reliable than those derived from separate analyses (Abadi et al., 2010).

Chapter 4 presents the methodology needed to implement discrete state-space models (SSMs) for population census data of different sizes. A popular approach for fitting SSMs for bird census data is the use of Poisson, or binomial-Poisson non-stationary processes, or appropriate approximations to normal processes (see, for example, Besbeas et al., 2002). We describe how to fit this SSM using the Kalman filter (KF). Additionally, we describe how the SSM can be fitted using these discrete distributions directly, without the need for approximations using, hidden Markov models (HMMs) (Besbeas and Morgan, 2019). We implement both methods within a frequentist framework. We run a simulation study, using an IPM to compare both methods, under different sample sizes, and we find that if time-series containing small counts are used, a systematic negative bias appears in the estimation of the productivity parameter, ρ. This bias is more pronounced when the KF is used to fit time-series data sets. The KF is computationally faster than using HMMs. As this bias reduces when we increase the sample size, we recommend to use the KF to fit time-series data when the average count size is at least 40, and HMMs otherwise. In an additional simulation study, we examine the effect of the systematic negative bias when combining time-series data sets of different sizes. We find that when multiple time-series data sets are combined, the bias in the estimation of the productivity parameter decreases.

In Chapter 5 we develop a spatially-explicit integrated population model (SE-IPM), which is formed from the combination of spatial ring-recovery and census data. We do this by adding spatial information in the form of geographical coordinates and/or land cover data to the survival parameters of the ring-recovery and the SSMs. In the discussion of Chapter 5 we argue that other types of spatial information can be easily incorporated to this SE-IPM, and that in the presence of extensive spatial census data, we could also add spatial dependencies to the productivity parameter. We use starling (*Sturnus vulgaris*) data to illustrate the SE-IPM and show that the model is able to incorporate spatial data at different resolutions.

Finally, in Chapter 6 we discuss the topics covered in this thesis, and outline avenues for planned and possible future work.

1.1 Data Types

1.1.1 Marking Data

Marking individuals is a widely used technique to identify wild animals in ecological studies. Individuals can be marked through the attachment of a neck band, ear tag, wing clip, leg

(a) Great crested newts, (*Triturus cristatus*) ©B.Lewis

(b) Straw-coloured fruit bat (*Eidolon helvum*) ©D.Hayman

(c) Rings for marked birds ©J.Lahoz-Monfort

(d) Semipalmated sandpipers, (*Calidris pusilla*) ©B.Brown

Fig. 1.1 Examples of marked individuals. (a) shows the unique belly patterns of two crested newts; (b) shows a marked straw-coloured fruit bat with a radio-transmitter collar; (c) shows a picture of plastic rings for marking seabirds; (d) shows a group of sandpipers, with the third from the left being marked using a green ring with alpha-numeric code.

ring etc. In some cases individuals possess physical characteristics that make them uniquely identifiable, for example, this is the case of great crested newts or grey whales. Figure 1.1 shows examples of different marking techniques.

Although in quantitative ecology marking data can be used for several purposes (see, for example, McCrea and Morgan, 2015), in this thesis we use marking data to estimate demographic rates, such as survival. We study the impact of different variables that might affect individual survival such as age (see Chapter 2), or sex and location of breeding (see Chapter 3). Additionally in Chapter 5 we combine marking data with census data to obtain spatially-explicit survival estimates.

Data on marked individuals can be collected by capturing individuals while they are alive; we refer to this as capture-recapture (CR) data. Data on marked individuals can also be collected upon the individual's death; we refer to this as mark-recovery (MR) data. In some cases marking data can be collected both when individuals are alive and upon the individual's death; we refer to this as mark-recapture-recovery (MRR) data.

In this section we provide a description of these three marking schemes that will be used throughout the thesis. For further literature on marking data, and other applications we refer the reader to Williams et al. (2002), King et al. (2009) and McCrea and Morgan (2015).

Mark-Recovery/ Ring-Recovery Data

In mark-recovery studies a group of individuals are marked, each with a unique mark that allows for individual identification, and are released in a given year or season, with the expectation of recovering these individuals upon their death. In such a way, when a marked individual is found dead, if the attached mark is returned to the organisation that oversees the study, and its age at ringing was known, the length of the individual's life can be calculated (Rydzewski, 1962).

Mark-recovery data can also be referred to as ring-recovery data, tag-recovery data, and band-recovery data. Ring-recovery (RR) is the terminology used for birds, as usually a ring is attached to the bird's leg, and mark-recovery is a general term that comprises marking for all types of animals (see, for example, Chapter 16, Williams et al., 2002). Tag-recovery and band-recovery are American terminology, which are often associated with a different parameterisation (see, for example, Hoenig et al., 2005). In this thesis we consider bird data, for this reason, from now on we shall refer to the term ring-recovery data.

Ring-recovery data consist of the occasion at time of ringing and occasion at time of recovery for each individual. Typically, data are collated on a yearly time scale and then summarised in an upper triangular matrix. The (i, j)th entry in the matrix corresponds to the total number of birds ringed in year i and recovered in year j (McCrea and Morgan, 2015).

Table 1.1 Ring-recovery data for starlings, 1990-1995.

Year of ringing	Number ringed	Year of recovery						Never recovered
		90	91	92	93	94	95	
1990	3101	52	2	1	2	2	0	3042
1991	1454		10	10	3	2	1	1428
1992	1748			10	8	2	1	1727
1993	1725				8	2	1	1714
1994	1227					2	1	1224
1995	309						1	308

For example, Table 1.1 shows six years of the ring-recovery study for starlings (*Sturnus vulgaris*) carried out by the BTO. The first column in the table contains the year in which the birds were ringed; the second column shows the total number of starlings ringed in each year of study; the following six columns represent how many birds were found and reported dead in each year of the study; and the last column contains the total number of birds that were ringed and never recovered dead—these may either have died within the study and not been recovered; or still be alive at the end of the study. For example, in 1990, 3101 birds

were ringed of which 52 were recovered dead in the same year, 2 in 1991, and so on. From the 3101 birds ringed in 1990, by the end of the study 3042 birds were not recovered. Then in 1991, 1454 birds were ringed of which 10 were recovered dead in the year, and 10 in the following year, and so on. Out of the 1454 birds ringed in 1991, by the end of the study, 1428 birds were not recovered.

Birds can be ringed at different ages. The British Trust of Ornithology classifies them into three age cohorts according to their age: nestlings, juveniles, or adults. Nestlings are newly born birds that have not yet flown the nest, and so they are easier to catch and mark. Juveniles are free-flying birds in their first year. Adults are all birds in their second or later calendar year. The category free-flying birds is used to refer to both juveniles and adults (BTO-Website, 2017).

In ring-recovery studies, covariate information about the ringed individuals can also be collected and its effect on survival can be accounted for. In Chapter 5 we provide a case study for ring-recovery data in the presence of spatial covariates.

Capture-Recapture Data

In capture-recapture studies (also referred to as mark-recapture studies), a group of individuals is marked, each with a unique mark that allows for individual identification, and then released in a given year or season, with the aim of following them during consecutive years or seasons. The individuals can be followed in the form of physical captures or by visual resightings. Note that we use the term "recaptures" to include both physical recaptures and resightings. Capture-recapture studies are different from ring-recovery studies, as capture-recapture information on individuals is collected when they are recaptured alive. In contrast, in ring-recovery or mark-recovery studies, information on a ringed individual is only available if the individual is found dead.

Capture-recapture data contain information on the specific occasions on which a marked individual was captured alive. Typically an occasion is a year. Each individual marked has a documented capture history ($\mathbf{h}_i$) in which a 1 is recorded each year in which the individual is captured or recaptured, and a 0 if the individual is not recaptured. Table 1.2 shows an example data set of a capture-recapture study for the little auk (*Alle alle*), in Magdalenefjorden, a fjord in the Norwegian island of Spitsbergen. This table provides the capture-recapture histories of three marked birds. Table 1.2 can be read as follows: individual 13711 was first captured in 2007, the first year of the study in Magdalenefjorden, it was subsequently recaptured in 2010, but it was not recaptured in 2008, 2009 or 2011. Thus, during this study the last time individual 13711 was seen and recorded was in 2010. Thus, after 2010 the individual could be dead or alive. Similarly, individual 41876, in the third row, was first captured in 2010

and it was subsequently recaptured in 2011, the last year of the capture-recapture study for Magdalenefjorden, so is known to be alive in 2011.

Table 1.2 Example of capture-recapture histories for three little auks, in Magdalenefjorden, for years 2007-2011. The first column contains the specific identification number for each individual. The remaining columns provide the capture-recapture histories for all individuals.

Individual number	Year captured				
	2007	2008	2009	2010	2011
13711	1	0	0	1	0
38980	1	0	1	1	0
41876	0	0	0	1	1

Capture-recapture data can also be summarised in an array, traditionally known as m-array. Table 1.3 shows the capture-recapture m-array for little auks in Magdalenefjorden for the years 2007-2011. Here, the first column represents the year in which individuals were released, and the second column the number of individuals released in every year. The number of individuals released contains information on both the number of individuals that were first captured, and the number of individuals that were recaptured in a particular year. This is true for all years of study, except for the first in which we only have first captures. For example, in Table 1.3 in 2007, 62 individuals were released, these represent only first captures as 2007 is the first year of study. Then, in 2008, 69 individuals were released, these 69 individuals consist of individuals captured for the first time and individuals recaptured from the previous year of study. Additionally, in Table 1.3 columns 3-6 contain information on the first recaptures after each release, and column 6 contains the number of individuals that were never recaptured. For example, from the cohort of individuals released in 2007, 7 were first recaptured in 2009, 2 in 2010, and no individuals were first recaptured in 2011. Additionally from the same cohort, 53 individuals were never recaptured. Similarly, from the cohort of birds released in 2008, 32 were recaptured for the first time (after their release in 2008) in 2009, 4 in 2010, and 1 in 2011. From this same cohort, 32 were never recaptured.

In capture-recapture studies, covariate information about the marked individuals can also be collected. These covariates can be defined as global if they affect all individuals, for example the weather conditions, or they can be defined as individual covariates if they are unique to each specific individual, for example weight. Due to the nature of these data, in capture-recapture studies it is common to have missing covariate values, especially when these are collected at a time-varying individual level. For example the weight of individual 13711 in Table 1.2, could only be measured in 2007 and 2010, when the individual was

Table 1.3 Capture-recapture m-array for little auks in Magdalenefjorden, for years 2007-2011. These data were collected by D. Jakubas and K. Wojczulanis-Jakubas.

Year of study	Number released	Number recaptured 08	09	10	11	Never recaptured
2007	62	0	7	2	0	53
2008	69		32	4	1	32
2009	124			69	2	53
2010	128				47	81

captured and recaptured. Thus, the years in which the individual was not recaptured would result in missing covariate information. Moreover, even if the individual was recaptured, this information could be missing for other reasons such as the covariate not being observed, for example if the individual was resighted rather than physically captured. In Chapter 3 we present a case study for capture-recapture data in the presence of individual covariates.

Mark-Recapture-Recovery Data

Mark-recapture-recovery data are the result of the combination of mark-recovery and capture-recapture data. Although none of the studies in this thesis use this data collection technique, in Chapter 3 we discuss literature developed for mark-recapture-recovery data. Thus, for completeness we briefly describe the characteristics of these data here. In mark-recapture-recovery studies, a group of individuals are marked, each with a unique mark that allows for individual identification, and released in a given year or season, with the aim of following them during consecutive years or seasons, as well as recovering their tags upon their death.

Mark-recapture-recovery data contains information on the specific occasions on which a marked individual was captured alive or recovered dead. Typically an occasion is a year. Each individual marked has a documented capture history ($\mathbf{h}_i$) in which a 1 is recorded each year in which the individual is captured alive or recaptured, a 2 is recorded if the individual is found dead and a 0 is registered if the individual is not recaptured.

Table 1.4 shows a toy example of a five year mark-recapture-recovery study. We show the histories for three individuals marked in different years. Individual 00001 was first captured in 2007, the first year of this mark-recapture-recovery study. It was subsequently recaptured alive in 2009, and it was finally recovered dead in 2010. Individual 00002, was first captured in 2008 and it was subsequently recaptured in 2010. This individual was not recaptured alive or reported dead after 2010, so it may be dead or alive in 2011.

Table 1.4 Example of mark-recapture-recovery histories for three birds marked in years 2007-2011. The first column contains the year in which these birds were first marked. The second column contains the specific identification number for each individual. The remaining columns specify the recapture and recovery histories. In rows 3-5, number 1 indicates a live capture, while 2 indicates a dead recovery.

Year marked	Individual number	Recapture Years 2007	2008	2009	2010	2011
2007	00001	1	0	1	2	0
2008	00002	0	1	0	1	0
2009	00003	0	0	1	0	2

1.1.2 Population Survey Data

Time-series survey or census data have traditionally been used to measure changes in population abundances across years. Throughout the thesis we use the Common Bird Census (CBC) data, the first scheme developed by the BTO for monitoring population trends among widespread breeding birds (Marchant et al., 1990). This scheme was operated during the years 1962 and 2000, and it has now been replaced by the Breeding Bird Survey (BBS).

The observations obtained from the CBC and the BBS surveys are used to build annual population trends. Traditionally, an annual index that provides a measure of the population level, y_j, has been used. This index is built to accommodate the differences between survey sites and the existence of a considerable amount of missing values in the data. To obtain the annual indexes, a generalised linear model is fitted, with counts assumed to follow a Poisson distribution, and a logarithmic link function, to the combined CBC/BBS data. Additionally, for these indexes, standard errors are calculated via a bootstrapping procedure. When BBS data are collected, a weight is applied to account for differences in density sampling. However, no weight was introduced when the CBC data were collected. Therefore, whenever these two survey methods are used in combination, a weight is also given to the CBC counts. This weight is just the average of the overall weights calculated for the BBS data. For more information on how these survey data are usually combined, we refer the reader to Freeman et al. (2007a).

Table 1.5 shows the population abundance indexes for 1990 to 1995 and their corresponding standard errors for starlings. These indexes are given in log-scale and the standard errors are calculated through bootstrapping.

Table 1.5 Annual population indexes in log scale for starlings, 1990-1995.

year	$\log(y_j)$	standard error
1990	6.0189	0.2508
1991	6.0462	0.2465
1992	6.0084	0.2482
1993	5.9715	0.2539
1994	5.6617	0.2236
1995	5.6871	0.2236

1.2 Models

1.2.1 Models for Marking Data

In this section we present the basic capture-recapture and ring-recovery models that will be used and extended throughout this thesis.

General assumptions of mark-recapture and ring-recovery models can be found in Chapters 16 and 17 of Williams et al. (2002), and Chapter 4 of McCrea and Morgan (2015). We list here the relevant assumptions for the models presented in this thesis:

1. The sample is representative of the population.
2. The age and the sex of sampled individuals are correctly determined.
3. Marks are not lost and are registered correctly.
4. Every marked individual present in the population at a specific sampling occasion has the same probability of being recaptured.
5. Every marked individual which has died within an interval of consecutive sampling occasions has the same probability of being recovered dead.
6. Every marked individual present in the population immediately following a sampling occasion has the same probability of surviving until the next sampling occasion.
7. Sampling periods are instantaneous, and recaptured individuals are released immediately.
8. Survival is not affected by the marking.
9. The fate of each marked individual is independent of the fate of every other marked individual.

10. The year in which an individual is found dead is assumed to be the same as the year in which the individual actually died. An individual can only be recovered if it has died in the immediate time preceding recovery (we cannot recover long dead animals).

Ring-Recovery Models

We use a multinomial model for the ring-recovery data because we have assumed that individuals behave independently of one another. We now describe ring-recovery models for different cases: 1.models for which the probabilities are kept constant; 2. models for which the probabilities can vary with time; 3. models for which the probabilities can adopt age and time dependencies.

1. Model with constant probabilities

Suppose there are n_1 years of ringing and n_2 years of recovery, where $n_2 \geq n_1$. The total numbers of individuals ringed in year i, is T_i and the number of individuals ringed in year i that were recovered dead in year j, is R_{ij}, for $i = 1, \ldots, n_1$, and $j = i, \ldots, n_2$. The parameters of interest are:

- ϕ is the probability that an individual survives from one occasion to the next;
- λ is the probability that an individual that dies is recovered and recorded as dead.

The probability of an individual being ringed and recovered is given by

$$P_{i,j} = \begin{cases} (1-\phi)\lambda & \text{if } j = i \\ \\ \phi^{j-i}(1-\phi)\lambda & \text{if } j > i. \end{cases} \tag{1.1}$$

If we make use of the assumption of independence between individuals the likelihood can be modelled by a product of multinomials

$$L(\phi, \lambda) = \prod_{i=1}^{n_1} \left\{ \prod_{j=i}^{n_2} P_{i,j}^{R_{i,j}} \left(1 - \sum_{j=i}^{n_2} P_{i,j}\right)^{T_i - \sum_{j=i}^{n_2} R_{i,j}} \right\}, \tag{1.2}$$

(Cole et al., 2012).

Table 1.6 illustrates the multinomial probabilities for a ring-recovery study which took place during the years 1990 to 1993.

Table 1.6 Ring-recovery cell probabilities for a constant model for the years 1990-1993. Here, $\chi_i = 1 - \sum_{j=i}^{n_2} P_{i,j}$.

Year of ringing	Year of recovery 90	91	92	93	Never recovered
1990	$(1-\phi)\lambda$	$\phi(1-\phi)\lambda$	$\phi^2(1-\phi)\lambda$	$\phi^3(1-\phi)\lambda$	χ_1
1991	-	$(1-\phi)\lambda$	$\phi(1-\phi)\lambda$	$\phi^2(1-\phi)\lambda$	χ_2
1992	-	-	$(1-\phi)\lambda$	$\phi(1-\phi)\lambda$	χ_3
1993	-	-	-	$(1-\phi)\lambda$	χ_4

2. Model with time dependent probabilities

We might be interested in time variations or time trends that might affect our parameters. For example, survival and reporting probabilities could change in time due to weather conditions. We build on the previous case where the probabilities were kept constant. The parameters of interest now are:

- ϕ_i is the annual survival probability for an individual alive at the start of year j;
- λ_j is the annual probability of recovering a dead individual in year j.

The probability of an individual being recovered in year j given it was ringed in year i is given by

$$P_{i,j} = \begin{cases} (1-\phi_i)\lambda_j & \text{if } j = i \\ \prod_{k=i}^{j-1} \phi(1-\phi_j)\lambda_j & \text{if } j > i. \end{cases} \tag{1.3}$$

The likelihood function is still defined by Equation 1.2.

This model is parameter redundant, meaning that not all parameters can be estimated. We discuss parameter redundancy in Section 1.2.4.

3. Model with age and time dependent probabilities

For wild animal populations survival is expected to vary with age, with first-year individuals being more vulnerable than adults. Thus, in order to account for this age variation, the survival probability is divided into first-year survival probability and adult survival probability. The idea of estimating survival from ring-recovery data goes back to (Haldane, 1955). Coulson (1961) published estimates of post-fledging, first-year and adult survival of blackbirds from recoveries assuming a constant reporting rate. These models were further developed by Brownie et al. (1985) and Freeman and Morgan (1992). For example, Freeman and Morgan (1992) incorporated age-dependent parameters in these models for ornithological data, and Catchpole and Morgan (1996) introduced specific notation to distinguish between first-year

and adult survival. Ring-recovery models have since been used and extended by many others (see, for example, Gauthier and Lebreton, 2008; King et al., 2009; McCrea et al., 2013; Thomson et al., 1999).

Suppose there are n_1 years of ringing and n_2 years of recovery, where $n_2 \geq n_1$. The total numbers of individuals ringed in their first-year of life, in year i, is $T_{1,i}$ and the number of first-year individuals ringed in year i that were recovered dead in year j, is $R_{i,j}$, for $i = 1, \ldots, n_1$, and $j = i, \ldots, n_2$. The model depends on the following parameters:

- $\phi_{h,j}$ is the probability that an individual aged h survives to year j of the study, conditionally on being alive in year $j-1$;
- $\lambda_{h,j}$ is the probability of recovering a dead individual aged h in year j of study.

In general, the probability of an individual being recovered in year j given it was marked in year i is given by,

$$P_{i,j} = \left(\prod_{k=i}^{j-1} \phi_{k-i+1,k} \right) (1 - \phi_{j-i+1,j}) \lambda_{j-i+1,j}, \tag{1.4}$$

(Cole et al., 2012).

The likelihood is still given by the product of the multinomial distributions, shown in Equation 1.2.

Table 1.7 illustrates the multinomial probabilities for a ring-recovery study that took place during the years 1990 to 1993. Here, we assume that the first-year survival, ϕ_1, and adult survival ϕ_a are constant, i.e. they do not vary with time, and the reporting probability λ is also constant and is shared for both first-year birds and adults, i.e. it does not have any age dependency.

Table 1.7 Ring-recovery cell probabilities for an age-dependent model for the years 1990-1993. Here, $\chi_i = 1 - \sum_{j=i}^{n_2} P_{i,j}$.

Year of ringing	Year of recovery 90	91	92	93	Never recovered
1990	$(1-\phi_1)\lambda$	$\phi_1(1-\phi_a)\lambda$	$\phi_1\phi_a(1-\phi_a)\lambda$	$\phi_1\phi_a^2(1-\phi_a)\lambda$	χ_1
1991	-	$(1-\phi_1)\lambda$	$\phi_1(1-\phi_a)\lambda$	$\phi_1\phi_a(1-\phi_a)\lambda$	χ_2
1992	-	-	$(1-\phi_1)\lambda$	$\phi_1(1-\phi_a)\lambda$	χ_3
1993	-	-	-	$(1-\phi_1)\lambda$	χ_4

We discuss further ring-recovery models in Chapter 2.

Capture-Recapture Model

Capture-recapture models can be used to estimate abundance or demographic parameters such as survival. In Chapter 3 we use capture-recapture models to analyse the survival of the little auk. Thus, in this section we describe the Cormack–Jolly–Seber model, a capture-recapture model that can be used to estimate demographic parameters. For other uses of capture-recapture models or for alternative model fitting methodologies we refer the reader to Lebreton et al. (1992), Williams et al. (2002), King et al. (2009), and McCrea and Morgan (2015).

The Cormack-Jolly-Seber (CJS) model, was the first capture-recapture model to estimate the probability of survival, rather than to estimate population size from capture-recapture data. This model was developed independently by Cormack (1964), Jolly (1965) and Seber (1965) and considers capture-recapture data conditional on the initial capture of each individual. This model has been extended in several ways. For example, Pollock (1981) extended the CJS model by adding age-dependencies to the survival parameters. Lebreton et al. (1992) provides many examples in which categorical covariates are added to model survival. Several methods for modelling CR data in the presence of continuous covariates are described in Chapter 3. Moreover, Lebreton et al. (1992) performed diagnostic goodness-of-fit tests using as an example the European dipper (*Cinclus cinclus*). Additionally, Cowen and Schwarz (2006) considered the problem of mark loss and incorporated mark-retention parameters. This could be achieved by marking the animals with two marks rather than one.

Suppose there are T years of a capture-recapture study. Individuals are marked in years $t = 1, .., T-1$. These marked individuals may be recaptured in any year after the year in which they were marked for the first time, $t = 2, .., T$. Thus, in T years of capture-recapture studies there are $n_1 = T-1$ years of marking and $n_2 = T-1$ years of recaptures.

The model depends on the following parameters:

- ϕ_j is the probability that an individual alive at time j survives to time $j+1$;
- p_j is the probability that an individual is (re)captured given that it is alive at time j.

Each individual has a capture history, $\mathbf{h}_i$, which is a vector of length T with entry $h_{i,k}$ indicating whether the individual was captured (1) or not (0) at time k. We denote the first year in which the individual is captured as a and the last year in which the individual is recaptured alive as b. The probability of observing capture-recapture history $\mathbf{h}_i$ is

$$Pr(\mathbf{h}_i) = \left\{ \prod_{k=a+1}^{b} \phi_{k-1}(h_{i,k} p_k + \overline{h}_{i,k} \overline{p}_k) \right\} \chi_b, \tag{1.5}$$

where $\overline{x} = (1-x)$, and $\chi_j = \overline{\phi}_j + \phi_j \overline{p}_{j+1}\chi_{j+1}$ is the probability that an individual alive at time j is not recaptured during the study period, with $\chi_T = 1$, and where, if $a = b$, the empty product $\prod_{a+1}^{a}$ is taken to be unity.

For example, the probability of the capture-recapture history $\mathbf{h}_1$=01010 is

$$P(\mathbf{h}_1) = \phi_2 \overline{p}_3 \phi_3 p_4 (\overline{\phi}_4 + \phi_4 \overline{p}_5).$$

Under the assumption of independence between individuals, the likelihood expression is given by the product of the probabilities of all the individual capture-recapture histories, and can be expressed as

$$L(\phi, p; h) = \prod_{i=1}^{N} Pr(\mathbf{h}_i), \tag{1.6}$$

where N is the total number of individuals followed during the capture-recapture study.

1.2.2 Discrete State-Space Model for Census Data

Discrete state-space models (SSMs) are often used to model time-series count data, such as census or survey data. SSMs consist of two discrete stochastic time processes running in parallel: an underlying state process and an observation process. The state process equation is also called the system or transition equation. The observation process equation is also called measurement or output equation. The state process is a first-order Markov process that describes the annual population change. This is modelled by a conditional probability density function (pdf) or probability mass function (pmf) that describes how the state vector changes from time t to time $t+1$. We denote this as g_t. The observation process, f_t, is a conditional process that models the relationship between the collected data or observations $\mathbf{y}_t$ and the state vector $\mathbf{N}_t$ (Newman et al., 2014).

$$\text{Initial state process} : g_0(\mathbf{N}_0|\boldsymbol{\Theta}) \tag{1.7}$$

$$\text{State } t \text{ process} : g_t(\mathbf{N}_{t+1}|\mathbf{N}_t, \boldsymbol{\Theta}) \tag{1.8}$$

$$\text{Observation } t \text{ process} : f_t(\mathbf{y}_t|\mathbf{N}_t, \boldsymbol{\Psi}) \tag{1.9}$$

where $\boldsymbol{\Theta}$ is the vector of parameters of the state model and $\boldsymbol{\Psi}$ is the vector of parameters corresponding to the observation model, and $t = 1, \ldots, T$.

An example of a two-state SSM is given below.

Two States State-Space Model for Census Data

Besbeas et al. (2002) used a two-state SSM for census data on lapwing (*Vanellus vanellus*) birds. This two-state SSM represented two age classes. The data consist of the number of breeding adult birds counted each year. However, the process also needs to account for first-year birds because these transition into adults after their first year of life. We assume that breeding starts at age 2, that only breeding birds are observed, no sex information is available, and that there is no emigration or immigration in the population.

Suppose $N_{a,t}$ is the number of adult individuals (of age ≥ 2) in the population at time t, $N_{1,t}$ is the number of first-year individuals in the population at time t, and $\mathbf{N}_t = (N_{1,t}, N_{a,t})$. The number of observed individuals in both categories in year t is y_t, the time-invariant survival probabilities are ϕ_1 and ϕ_a for first-year and adult birds respectively. The parameter ρ represents the mean number of young per individual recruited into the adult population every year. The state process is

$$N_{a,t+1}|\mathbf{N}_t \sim \text{Bin}(N_{1,t} + N_{a,t}, \phi_a), \tag{1.10}$$

$$N_{1,t+1}|\mathbf{N}_t \sim \text{Pois}(N_{a,t}\phi_1\rho). \tag{1.11}$$

The binomial distribution is used to model survival, and the Poisson distribution to model new arrivals in the population, i.e. births. Figure 1.2 and the following discussion describe the population process in detail.

The observation process is

$$y_t|\mathbf{N}_t \sim \text{Pois}(N_{a,t}), \tag{1.12}$$

as only adult (breeding) birds are observed in the census data.

Figure 1.2 is a graphical representation of the SSM with two states, where we can observe the relation between the states and the observations. Figure 1.2 shows that observations are only made for adult birds in the population. Moreover, Figure 1.2 shows a graphical representation of the underlying processes for both the adult and the first-year populations. At time t, individuals in the adult population, $N_{a,t}$, breed and recruit new chicks. If these chicks survive they become part of the first-year population $N_{1,t+1}$, at time $t+1$. Subsequently, the adult population at time $t+1$ is comprised of those adults and first-year individuals that were alive at time t and survive to time $t+1$.

The state equations are a stochastic version of the matrix projection models (Caswell, 2001). Following Buckland et al. (2004) and Newman et al. (2014) we can use first-order

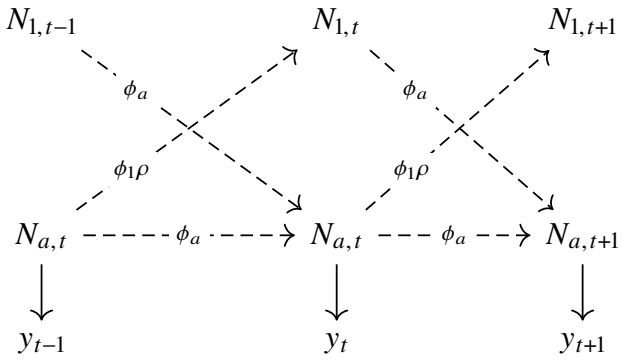

Fig. 1.2 Diagram of the SSM with two states. It shows the life cycle of the population, and the connection between the underlying adult population size $N_{a,t}$ and the number of individuals observed at time t, y_t.

Markovian transition matrices to represent animal population dynamics. Equations (1.10) and (1.11) can be conveniently rewritten as a population matrix using the following Leslie matrix (Leslie, 1945),

$$\begin{pmatrix} N_{1,t+1} \\ N_{a,t+1} \end{pmatrix} = \begin{pmatrix} 0 & \rho\phi_1 \\ \phi_a & \phi_a \end{pmatrix} \begin{pmatrix} N_{1,t} \\ N_{a,t} \end{pmatrix}. \tag{1.13}$$

The observation process of equation (1.12) can also be written as an observation matrix

$$y_t = (0,1) \begin{pmatrix} N_{1,t} \\ N_{a,t} \end{pmatrix}. \tag{1.14}$$

Different distributions can be used to model both the observation process, (see, for example, Knape et al., 2011), and the state process (see, for example, King et al., 2008b). Moreover, extensions or variations of the model to include productivity and more or fewer states are also possible. In Chapter 4 we provide an alternative one-state model.

A general explicit form of the likelihood, $L_{SSM}(\phi_1, \phi_a, \rho)$, does not exist. To make inference on the estimates for the SSM, different approaches have been developed. Traditionally, the time-series likelihood for the census SSM has been approximated using Kalman Filter methodology, for which normal approximations are required (see, for example, Besbeas et al., 2002; Besbeas and Morgan, 2012). Alternatively, Brooks et al. (2004) use a Bayesian approach which does not require the normal approximations needed in the KF. More recently, Besbeas and Morgan (2018) have introduced the use of HMMs to fit the time-series likelihood using either a frequentist or a Bayesian approach. We discuss in detail these different methodologies in Chapter 4.

For this two-state SSM, two of the parameters, ϕ_1 and ρ, are confounded, so that it is only possible to estimate them as a product. This is known as parameter redundancy (see, for example, Cole et al., 2010). The model remains parameter redundant even if the number of first-year birds is observed (Catchpole et al., 2001). To solve the parameter redundancy problem, Besbeas et al. (2002) combined the SSM with a ring-recovery model into an IPM. IPMs are discussed in Section 1.2.3 and parameter redundancy is discussed in Section 1.2.4.

1.2.3 Integrated Population Models

Traditionally, separate studies have been carried out to assess animal demographic processes which include studies to model productivity, survival and movement. These studies could use capture-recapture, ring-recovery, nest records, or census data, for example, to account for population changes and abundance. However, ecological data can be sparse, limiting the ability for analysis, due to problems in parameter estimation, such as parameter redundancy (Catchpole et al., 2001; Cole and McCrea, 2016). To tackle this problem, and obtain self-consistent parameter estimates, some studies have jointly analysed several data sets simultaneously: Catchpole et al. (1998a); King and Brooks (2002a); Jiménez-Muñoz et al. (2019) combine several capture-recapture or ring-recovery data sets; King and Brooks (2002b); King and Brooks (2003) combine multisite capture-recapture data sets.

IPMs consist of the combination of population count data and demographic data into one single analysis that gives information about population trajectories, and facilitate consistent analyses of population processes. Particularly, in this thesis we describe and implement IPMs that combine census data, such as population time-series counts, with demographic data such as ring-recovery into a unified analysis. These types of IPMs were developed by Besbeas et al. (2002) and have since been widely implemented and extended to include more types of data both within the frequentist (see, for example, Besbeas et al., 2002; Besbeas and Freeman, 2006; Besbeas and Morgan, 2012) and the Bayesian (see, for example, Brooks et al., 2004, King et al., 2008b, Abadi et al., 2010) paradigms.

In this section we provide information on the evolution of IPMs, listing here in chronological order some of the relevant publications in this area. As their implementation is continuously growing for ecological studies, we focus on studies that have involved the statistical development of IPMs, centering our attention on those IPMs that combine census and marking data.

Besbeas et al. (2002), showed that by combining a SSM for census data with ring-recovery data one can obtain productivity estimates which would not be available from any of the data sets on their own. They provided two case studies, one for a SSM with two states, similar to that presented in Section 1.2.2, and another for a three-state SSM. In these, they assumed

that the underlying population processes, for example, $N_{a,t}$ and $N_{1,t}$, described in Equations (1.10) and (1.11), can be approximated by normal distributions. Moreover they assumed the observation process, y_t, to be normally distributed. As a result, they were able to maximise the likelihood equation using the KF.

Brooks et al. (2004) provided a Bayesian approach to combining census and demographic data, in which the assumption of normality can be relaxed. Rather than using normal approximations in the state process, the binomial and Poisson distributions can be used directly. Amongst the benefits of this Bayesian approach was the ability to analyse census data with smaller counts, as no normal approximations are needed. In Chapter 4 we provide a case study on different SSM fitting methodologies when different sample sizes are used.

Typically, when collecting census data, especially at large scales, species are observed through surveys of samples of the populations at different sites and times. For this reason, to account for the differences in sampling when using large populations, Besbeas et al. (2002) used a derived index of the population to model abundance. Besbeas et al. (2005) combined count data from different sites with different types of habitats jointly with ring-recovery data for an entire population and obtained habitat-specific productivity estimates. Additionally, Besbeas and Freeman (2006) proposed an alternative approach, modelling the data using a log-linear Poisson distribution that accounted for the site and the years in which each observation was recorded. In Chapter 5 we develop an SE-IPM which allows us to obtain spatially-explicit demographic estimates.

Schaub et al. (2007) applied IPMs to estimate demographic parameters from sparse data from a colony of greater horseshoe bats (*Rhinolophus ferrumequinum*) in Switzerland. They implemented an extension of the IPMs presented in Besbeas et al. (2002) and Brooks et al. (2004) by incorporating capture-recapture and count data into a Bayesian IPM. They considered two age classes, and a sex-specific survival. In so doing they obtained estimates of fecundity that could not be estimated otherwise, as well as more accurate estimates of population growth and survival.

Freeman et al. (2007b) implemented an IPM to national and regional data on starlings (*Sturnus vulgaris*) and found that the steep decline in the number of starlings after the 70s was due to a reduction in survival, particularly, first-year survival. In Chapter 5 we use data on starlings to illustrate our models. Our findings are similar to those presented in Freeman et al. (2007b).

King et al. (2008b) extended the existing work on Bayesian IPMs by changing the measurement error in the observation process N_t from constant to time dependent. Moreover, they provided model-averaged inference to help to inform management policies.

Baillie et al. (2009) used a Bayesian IPM to analyse the causes of decline of the British song thrush (*Turdus philomelos*) and discussed the utility and the direction of IPMs.

McCrea et al. (2010) developed a multi-site integrated population model for the joint analysis of capture-recapture and census data. They used data for great cormorants *Phalacrocorax carbo* in three colonies (sites) in Denmark. Moreover, through a simulation study they demonstrated that parameter estimation was improved when site-specific census data are combined with demographic data.

Schaub and Abadi (2011) provided a review on 25 existing IPMs which consisted of the joint modelling of counts and one or several types of demographic data. They reviewed publications that use IPMs to study birds or mammals, and excluded fisheries studies as in the latter the data were different. In this thesis, we use IPMs with a focus on birds, but with slight variations our models could also be applied to study mammals.

In their review, Schaub and Abadi (2011) remarked that the main benefit of the types of IPMs that we describe here is that they are able to provide estimates of productivity. Furthermore, they found that in all the reviewed publications the use of IPMs resulted in an increased precision of the parameter estimates.

The IPM's assumptions are the union of each of the models' assumptions separately. In this case these are, the ring-recovery's assumptions, together with the correct use of the population models (in this case Leslie matrix), in which the population processes are described. Additionally, there are two IPM specific assumptions: 1. the demography of the individuals included in the different data sets is assumed to be the same; 2. the data sets used in conjunction in the IPM should be independent to each other to avoid overestimated precision of the estimates (Schaub and Abadi, 2011).

Abadi et al. (2010) tested the assumption of independence for an IPM containing three data sources: population census data, capture-recapture, and reproductive success data with different degrees of non-independence. They found that if these three types of data are combined into one single analysis, the lack of independence between data sets had almost no effect in the accuracy of parameter estimates. In contrast, Besbeas et al. (2009) compared the effect of combining census and ring-recovery data into an IPM, under dependence and independence scenarios. They found that if dependent data sets were combined, the estimates were considerably less accurate, and higher mean square errors were obtained than if the data sets combined were independent. Thus, they warned that caution should be taken when combining dependent ring-recovery and census data sets. The difference in the effect of dependence in both studies might be given by the nature of the data sets incorporated in both studies. Abadi et al. (2010) suggested that if the independence assumption is violated, this would have stronger impact on parameter accuracy if ring-recovery data are used instead of

capture-recapture data. They reason that this happens as in contrast with ring-recovery data, the capture-recapture data dominate the survey data to provide information about common parameters. Further, Abadi et al. (2010) suggest that if the level of dependence is higher, by combining data sets in which the same animals have been observed or recorded, serious bias in parameter estimation is expected.

Besbeas and Morgan (2012) evaluated a new method for initialising the KF, the so-called stable age method (SA), for IPMs. This approach was already introduced in Besbeas et al. (2009), however it was not fully developed, and it had not been used to analyse real data, but simulated data. The SA method incorporates ring-recovery parameter estimates in the Leslie matrix to derive the SA distribution. Moreover, if productivity data were available these would contribute to the estimation of the parameter ρ as well. Besbeas and Morgan (2012) compared the SA method to the following initialising methods: approximate diffuse initialisation (AD), the exact diffuse initialisation (ED) and maximum likelihood initialisation (ML). Through a simulation study they found that all the initialising methods perform well, and they highlighted the simplicity of the SA method. However they recommended the SA method for initialising the KF when it is used to form a likelihood for a SSM in ecology, specifically when using IPMs, as one can add extra information to the estimation of the parameters.

Robinson et al. (2012) extended IPMs by adding direct estimation of brood size and nesting success to the model. To do this, they incorporated data on brood sizes and the daily probability of nest failure together with census and ring-recovery data for blackbirds (*Turdus merula*). They used a Bayesian approach to add productivity data into an IPM for the first time.

Moreover, Robinson et al. (2014) used IPMs to estimate demographic parameters from incomplete data sets both across and within 17 species. For some of these species not all the demographic processes were quantified directly, so they introduced a scaling parameter to account for unmeasured variation. In so doing, they were able to reinforce the value of the volunteer-based monitoring programmes for the understanding of the demographic processes driving animal populations.

Finke et al. (2019) proposed an efficient particle Monte Carlo methodology to estimate the demographic parameters of IPMs formed by a SSM for the noisily observed population sizes as well as other components, such as capture-recapture or nest success models. Moreover, they developed strategies for model comparison by incorporating the MCMC algorithm into a sequential Monte Carlo sampler. They demonstrated the methodology on two different applications: little owls and grey herons previously explored by Abadi et al. (2010) and Besbeas and Morgan (2012) respectively. For the owls, they found no evidence in favour of

some of the more complex models proposed in the literature and for the herons they showed that existing models did not describe the data well.

Plard et al. (2019) developed an integrated integral projection model that combined an integrated population model and an integral projection model. This model can estimate demographic parameters and predict population dynamics, and can be viewed as the extension of an IPM which links individual traits to demographic rates and their inheritance.

Riecke et al. (2019) examined, within a Bayesian framework, the effect on parameter estimates when the following model assumptions of the capture-mark-recapture-recovery were violated: marker-induced mortality or marker loss and unmodelled heterogeneity of survival probabilities among individuals. They found that if these assumptions are violated, estimation of additional, previously unidentifiable, parameters may be biased.

Besbeas and Morgan (2019) proposed a new method to model discrete SSMs, the use of HMMs. This new method avoids the KF approximations and Bayesian Monte Carlo simulations. The analysis of SSMs using HMMs is the main topic of Besbeas and Morgan (2018). We evaluate the KF and the HMM in the presence of different time-series sample sizes in Chapter 4 and implement them in a spatial context in Chapter 5.

In this context, the general form of the likelihood equation, and the one that we shall be using in this thesis, is given by the product of the ring-recovery and the SSM likelihoods

$$L_{IPM}(\phi_1, \phi_a, \lambda_t, \rho) = L_{RRM}(\phi_1, \phi_a, \lambda_t) \times L_{SSM}(\phi_1, \phi_a, \rho),$$

where IPM stands for integrated population model, RRM for ring-recovery model, and SSM for state-space model.

The main benefits of using such IPMs, as listed in Schaub and Abadi (2011), are: 1. being able to estimate additional parameters without explicit data; 2. their implementation has been shown to improve the estimation of demographic parameters (Besbeas et al., 2002; Abadi et al., 2010); different temporal lengths or data sets with time periods can be combined and missing data can be incorporated (Brooks et al., 2004; Schaub et al., 2007) 3. flexibility in the model set up. For these reasons, IPMs are increasingly being developed and implemented. In Chapter 5 we present for the first time an SE-IPM consisting of the combination of several census and ring-recovery data sets.

1.2.4 Parameter Redundancy

In ecological studies it is frequent to have two parameters in a model that only appear as a product, and hence cannot be estimated independently (see, for example, Chapter 10, McCrea and Morgan, 2015). This estimation issue is called parameter redundancy. Alternatively, a

model in which not all the parameters can be independently estimated is described as not identifiable. Methods for detecting parameter redundancy were described by Catchpole and Morgan (1997), Gimenez et al. (2004), Cole et al. (2010) and Choquet and Cole (2012). Parameter redundancy results for ring-recovery models are given in Cole et al. (2012) and Jiménez-Muñoz et al. (2019). Parameter redundancy results for capture-recapture models are given in Hubbard et al. (2014). Methods for investigating parameter redundancy in discrete SSMs and IPMs are given in Cole and McCrea (2016). In particular, Cole and McCrea (2016) demonstrated that through the joint analysis of data sets identifiability issues may be solved.

In general, to determine parameter redundancy, symbolic algebra is used to determine the rank of a matrix derived by differentiating the probability of each event occurring with respect to the parameters in the model (Cole et al., 2010). The rank is the number of parameters that can be estimated in the model. A model is parameter redundant when the rank is smaller than the total number of parameters in the model. Alternatively, as in Choquet and Cole (2012) a hybrid symbolic-numeric method can be used to find the rank numerically. To overcome parameter redundancy, models could be reparameterised into a smaller number of parameters or constraints on the models could be used (Jiménez-Muñoz et al., 2019).

Parameter redundancy can also be caused by the data. In ring-recovery models this can occur when there are several $R_{i,t}$ equal to zero, as zero values are equivalent to missing data. Cole et al. (2012) showed that one $R_{i,t}$ for $t = i, \ldots, n_2$ can be zero for each t, and parameter redundancy results will always remain unchanged. Other patterns of zeroes can, but do not always, result in parameter redundancy, as demonstrated in Cole et al. (2012).

Models can also behave as if they were parameter redundant for certain data sets. This is known as near-parameter redundancy, and normally occurs if there exists a nested parameter redundant model, and the maximum likelihood parameter estimates are close to those of the nested model (Catchpole et al., 2001). Catchpole et al. (2001) showed how near-parameter redundancy can be detected by examining the standardised eigenvalues, i.e computing the ratio of all the eigenvalues over the smallest eigenvalue of the Hessian matrix. A value that is close to zero indicates near-parameter redundancy. Chis et al. (2016) define a Hessian matrix as sloppy if $\lambda_{\min}/\lambda_{\max} < 0.001$, where $\lambda_{\min}$ is the smallest eigenvalue and $\lambda_{\max}$ is the largest eigenvalue. Similarly, Zhou et al. (2019) and Cole (2019) used the same ratio of smallest and largest eigenvalues to investigate near-parameter redundancy. In Chapter 2 the sparse sandwich tern data set is used to explore the potential effects of near-parameter redundancy on the models presented here. We do not recommend using near-parameter redundant models.

1.3 Model Fitting and Model Comparison

The maximisation of the likelihood and computation of the information matrix are performed with the optim() function, which is part of the stats package in R (R Core Team, 2018). If the demographic parameter estimates are the result of a logistic function, the associated standard errors are obtained by employing the delta method using the deltamethod() function in the msm package in R (Jackson, 2011).

The parameter estimates obtained from maximum likelihood estimation enjoy an *invariance* property. Suppose, the parameterisation of a model is changed from $\boldsymbol{\theta}$ to $\boldsymbol{\eta} = \psi(\boldsymbol{\theta})$. For example, if we use a logistic transformation, ψ, on $\boldsymbol{\theta}$, the maximum likelihood estimate of $\boldsymbol{\eta}$ is $\hat{\boldsymbol{\eta}} = \psi(\hat{\boldsymbol{\theta}})$. If η is a scalar function, an approximation for the variance of can be found via the delta method.

The delta method states that,

$$Var(\hat{\eta}) \approx \boldsymbol{a'Sa}, \tag{1.15}$$

where $\boldsymbol{S}$ represents the variance-covariance matrix for $\hat{\boldsymbol{\theta}}$ and $\boldsymbol{a'} = \left(\frac{\partial \eta}{\partial \theta_1}, \frac{\partial \eta}{\partial \theta_2}, \ldots, \frac{\partial \eta}{\partial \theta_n}\right)$, evaluated at $\hat{\boldsymbol{\theta}}$. We refer the reader to Morgan (2008) for a more detailed explanation of the delta method.

In the presence of small data sets, the delta method might be insufficient. Throughout this thesis we analyse some small data sets, for example, in Chapters 4 and 5 we make use of small valued time series census data. These data are however jointly modelled with ring-recovery data, which in contrast are abundant, hence together they provide sample sizes for which the asymptotics are likely to be satisfied. Additionally in Chapter 3 we use a small capture-recapture data set for female little auks. To check our results for these data we performed a bootstrap, which resulted in results similar to those we are reporting here. As these are the same, we do not present the bootstrap results in this thesis. However, the bootstrap results are available in Wojczulanis-Jakubas et al. (2019).

In the presence of continuous covariates, we standardise them when needed using the scale() function in R which is part of the R base package (R Core Team, 2018). The standardisation consists of calculating the mean and standard deviation of the entire vector of covariates, and then "scaling" each element by those values by subtracting the mean and dividing by the standard deviation.

For model comparison we use the Akaike Information Criterion (AIC) developed by Akaike (Akaike, 1974). The AIC of a model is defined as:

$$AIC = -2\log L(\hat{\theta}; x) + 2d, \tag{1.16}$$

where d is the number of parameters estimated, and $L(\hat{\theta};x)$ is the maximised likelihood. This general approach provides a versatile procedure to compare models fitted using maximum likelihood using the same data.

Traditionally in ecological studies AIC, or variations such as AICc, have been used to perform model selection. Specifically, in IPMs (which are one of the main focuses of this Thesis) AIC is currently the most commonly employed method for model selection (see for example, Besbeas and Morgan, 2019). There are however some disadvantages of using AIC. For example, when the sample size is small, there is a substantial risk that AIC will select models that have too many parameters. As an alternative, AICc is recommended in theses cases (Anderson and Burnham, 2004). Unfortunately, given the nature of IPMs, it is not straightforward to find simple corrections of AIC as these depend on the notion of sample size, which is not easy or even possible to define for IPMs, given the use of multiple heterogeneous data sets. Model selection methods for IPMs is the topic of Besbeas et al. (in prep.) and their recommendations should be implemented in future work.

Chapter 2

Estimating Age-Dependent Survival from Age-Aggregated Ring-Recovery Data

Forward

This chapter summarises the work presented in Jiménez-Muñoz et al. (2019) where ring-recovery methods are extended to maximise the use of historical ringing records. The material in Jiménez-Muñoz et al. (2019) is the result of a joint collaboration between all the authors, for which I contributed in the development of the methodology. I wrote the computer code, performed the simulation study, and analysed the data and led the writing of the manuscript assisted by all authors. The work on parameter redundancy was carried out by Dr. Cole.

We mostly use the same wording as the paper but add in links to relevant parts of the thesis. The section on parameter redundancy has changed to highlight just the results that are relevant to the thesis. The methods to derive the parameter redundancy results are given in the paper.

2.1 Introduction

Ringing schemes have been running for a long period of time, and for example in Europe and North America they date back to the early 20th century (Greenwood, 2009). Due to their long history, abundant literature for these methods can be found (see, for example, Williams et al., 2002). Initially data were recorded in paper form. Although the process of digitising these data started two decades ago, there are still many ringing records that have not been

computerised. The way in which this historical data was collected and stored means that the total number of fledged birds ringed in different age categories is difficult or often impossible to obtain, due to the sheer size and heterogeneity of the records.

Younger birds tend to have a lower probability of survival than adult birds (Martin, 1995; Péron et al., 2016). Moreover, as behaviour and habitat use change with age, the probability of recovering an individual after death may also be age-dependent. These variations should be taken into account when building models. It is possible to include this information when the numbers of birds ringed annually in the various age classes is known, which is usually the case for most recent studies (see, for example, the Standard ring-recovery model in Section 1.2.1). However, for historical data information on the age of the individual at ringing is often not available. When these totals are unknown, a model that is conditional on the number of birds recovered can be used. The most commonly used model assumes a constant probability of reporting after death for all members of the cohort (Seber, 1971), but this can result in biased parameter estimates (McCrea et al., 2012).

As an alternative to the conditional model, which ignores the annual numbers ringed, Robinson (2010) described a model for when the annual number of pulli (chicks) and fledged birds are separately known, but the latter includes both fully mature, breeding birds and juvenile birds of the year, which will have very different survival prospects. Robinson (2010) estimated survival by assuming that a fixed proportion of the birds ringed as fledged birds were juveniles.

In this chapter, we present a model where the proportion of juveniles is treated as an unknown parameter. In Section 2.2 we introduce the reader to the two data sets, blackbirds (*Turdus merula*) and sandwich terns (*Thalasseus sandvicensis*), used to illustrate our methods. In Section 2.3 we describe the existing ring-recover models, and present the historical ring-recovery models developed in Jiménez-Muñoz et al. (2019). We provide model fitting details and summarise these models in Section 2.4. In Section 2.5 we show the parameter redundancy results obtained in Jiménez-Muñoz et al. (2019). In Section 2.6 we perform a simulation study to show that this model gives similar parameter estimates to the standard model that requires that all the ringing totals are known. We provide an analysis on blackbirds and sandwich terns to show the relevance of the proposed model for different types of data in Section 2.7. Finally in Section 2.8 we provide a discussion of the work presented in this chapter.

2.2 Data

The BTO has been collecting ringing data on the total number of birds ringed in Britain and Ireland for several species since 1909. However until 2000 the data were submitted in paper form. Starting in 2010 we can find digitized data distinguishing three age groups: pulli, juveniles, and adults. Although ringing data have been digitized for the years before 2010, only two age categories have been registered: pulli, which are first-year birds, and fledged birds, which refers to fledged birds of unknown age, including juveniles (also first-year birds) and adults. We refer to the digitized data with two categories as historical data. It would be possible to fully computerise historic data, or find ringing totals for the three age categories, however this would be time consuming. This has been stated for several species (Robinson, 2010). Figure 2.1 illustrates the three age categories in which birds are ringed.

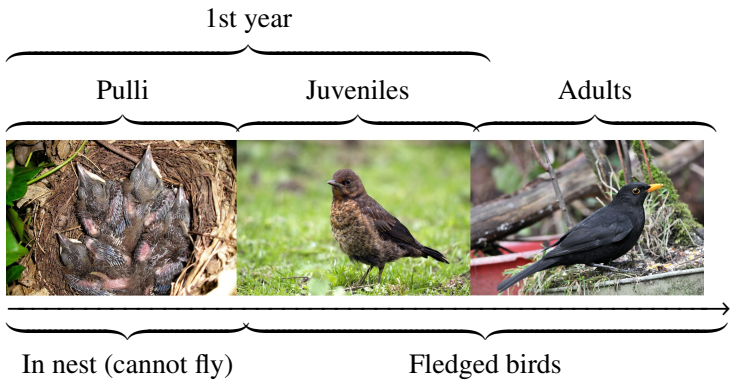

Fig. 2.1 Diagram of the three age categories in which birds are ringed. For this illustration we use pictures of blackbirds. From left to right the pictures were taken by: Simon Thurgood, John Harding, and Tommy Holden.

To illustrate the methods described in this chapter we analyse data provided by the BTO for two different bird species: blackbirds and sandwich terns. We describe these species and the data collected for them in Sections 2.2.1 and 2.2.2 respectively.

2.2.1 Blackbird Data

The blackbird (*Turdus merula*) is a common passerine that occurs throughout Britain. The blackbird data set contains ring-recovery data for birds ringed as pulli, juveniles and adults during the breeding season (April to September) for the years 1964-1983. These data are taken from Robinson et al. (2012), and can be found in Appendix A.1. For this data set the total numbers of birds ringed for all three age categories, pulli, juvenile and adults, are

separately known. We use this data set, as well as the simulated data sets to compare the existing methods and the methods developed in Jiménez-Muñoz et al. (2019) to analyse the historical ringing data.

2.2.2 Sandwich Tern Data

The sandwich tern (*Thalasseus sandvicensis*) is a long-lived migrant seabird. Although population fluctuates dramatically among years, the sandwich tern is on the RSPB's amber list (of the second highest conservation priority level) in the UK (Eaton et al., 2015). The sandwich tern ring-recovery data set contains ring-recovery data for birds ringed as pulli and fledged birds during the breeding season (June to August) in the years 1970-1990. The sandwich tern data set contains information on the total number of birds ringed as pulli, however the total numbers of birds ringed for adults and juveniles are are not known separately. Instead, the total number of fledged birds is given. Moreover, the number of recoveries per year contained in each of the three data classes are very small, making the sandwich tern data very sparse. This data set can also be found in in Appendix A.2. We use the sandwich tern data to explore the suitability of the models presented in Jiménez-Muñoz et al. (2019) in terms of parameter redundancy caused by the structure or paucity of data.

2.3 Models

In this section we describe the models that can be fitted to different ring-recovery data sets. In all of the models, we suppose there are n_1 years of ringing and n_2 years of recovery of dead birds. The total numbers of birds ringed in age category c, in year i, is $T_{c,i}$ and the number of birds ringed in age category c, in year i that were recovered dead in year t, is $R_{c,i,t}$, for $i = 1, \ldots, n_1$, and $t = i, \ldots, n_2$. The age category c represents the age at which birds were ringed, which could be pulli, denoted by p, juveniles (j), first-year birds (1), fledged birds (f) , or adults (a). As mentioned in the data section, first-year birds, may be either pulli, or juveniles, and fledged birds may be either juveniles, or adults.

The models depend on the following parameters:

- $\phi_{1,t}$ is the annual survival probability for a first-year bird alive at the start of year t;
- $\phi_{a,t}$ is the annual survival probability for an adult bird alive at the start of year t;
- $\lambda_{1,t}$ is the annual probability of recovering a first-year dead bird in year t;
- $\lambda_{a,t}$ is the annual probability of recovering a dead adult bird in year t.

2.3.1 Standard Model

The standard model refers to the ring-recovery model that estimates the survival and reporting probability of birds that were ringed early in their first year of life. This model is similar to that presented in Section 1.2.1, however for consistency with the following models, we use slightly different parameterisation here.

The probability that a bird ringed in its first year of life in year i is recovered dead in year t is denoted by $P_{1,i,t}$ with,

$$P_{1,i,t} = \begin{cases} (1-\phi_{1,t})\lambda_{1,t} & \text{if } t = i \\ \phi_{1,i}\left(\prod_{k=i+1}^{t-1}\phi_{a,k}\right)(1-\phi_{a,t})\,\lambda_{a,t} & \text{if } t > i \end{cases}$$

for $i = 1, \ldots, n_1$, $t = i, \ldots, n_2$.

Parameters can be estimated using maximum likelihood, and the likelihood function for the standard model for birds ringed in their first year of life is

$$L_S \propto \left\{\prod_{i=1}^{n_1}\prod_{t=i}^{n_2} P_{1,i,t}^{R_{1,i,t}}\right\}\left\{\prod_{i=1}^{n_1}\left(1-\sum_{t=i}^{n_2} P_{1,i,t}\right)^{T_{1,i}-\sum_{t=i}^{n_2} R_{1,i,t}}\right\}. \tag{2.1}$$

Gauthier and Lebreton (2008) demonstrate how a ring-recovery model can be written as a multi-state model so that the program M-Surge (Choquet et al., 2004) could be used to fit this model.

The model of equation (2.1) can be used either for birds ringed as pulli, or for birds ringed as pulli and juveniles, i.e. birds ringed in their first year of life for which we know the ringing totals. While in practice it is not uncommon for data to be available for pulli alone, and thus modelled using equation (2.1), they are unlikely to ever be available for fledged juveniles alone. The latter data will almost always be analysed in conjunction with those of other age-classes, as outlined in the following section.

2.3.2 Standard Combined Model

As stated by Robinson (2010), it is possible to fit a ring-recovery model to the fledged birds' data, with age specific ringing totals, when the total numbers of birds ringed as juveniles and as adults are known. The standard combined model can be used when there is separate data available on the total numbers of birds ringed in two different age classes. These two age classes are: (1) birds in their first year of life (juveniles and/or pulli) and (2) adult birds. We use the word combined, as two different data sets are pooled together, and the likelihood

function is obtained, under the assumption of independence, by multiplying two likelihood functions: the one for birds being ringed in their first year of life and the other for birds ringed as adults.

The probability that a bird ringed in the adult age class in year i is recovered dead in year t is denoted by $P_{a,i,t}$ with,

$$P_{a,i,t} = \left(\prod_{k=i}^{t-1} \phi_{a,k}\right)\left(1-\phi_{a,t}\right)\lambda_{a,t},$$

for $i = 1,\ldots,n_1$, $t = i,\ldots,n_2$.

If the fledged bird data are fully computerised, we have information on the number of birds ringed as juveniles, $T_{1,i}$ and as adults, $T_{a,i}$. Then the likelihood function for the standard combined model is a straightforward product of that in equation (2.1) and that for birds ringed as adults, i.e.,

$$\begin{aligned} L_{SC} \propto \quad & \left\{\prod_{i=1}^{n_1}\prod_{t=i}^{n_2} P_{1,i,t}^{R_{1,i,t}} P_{a,i,t}^{R_{a,i,t}}\right\} \times \left\{\prod_{i=1}^{n_1}\left(1-\sum_{t=i}^{n_2} P_{1,i,t}\right)^{T_{1,i}-\sum_{t=i}^{n_2} R_{1,i,t}} \times \right. \\ & \left.\left(1-\sum_{t=i}^{n_2} P_{a,i,t}\right)^{T_{a,i}-\sum_{t=i}^{n_2} R_{a,i,t}}\right\}, \end{aligned} \tag{2.2}$$

(see, for example, Brownie et al., 1985, and Freeman and Morgan, 1992).

We use the age category (1) for the $T_{j,i} = T_{1,i}$ birds ringed as known juveniles that are by definition in their first year of life. If additional data on ringed pulli were available, this model can be used to fit these two data sets. If we were to add the pulli data, the age category (1) would include now birds ringed as juveniles, (j), and as pulli, (p). This is always assuming that the total numbers of birds ringed in each age category are known, and also that the same 'first-year' survival probability applies to birds ringed as pulli or slightly older fledged juveniles. For a model separately estimating survival probabilities for the period immediately following fledging (see, for example, Thomson et al., 1999).

2.3.3 Historical Data Model

For records that are not computerised, only the total numbers of fledged birds ringed are known rather than the separate total numbers for juveniles and adults. The models developed by Jiménez-Muñoz et al. (2019) for the historical fledged bird data are similar to the standard combined model for ring-recovery data, but with the addition of a parameter that represents the unknown yearly proportion of birds ringed as juveniles. In these models, the proportion

of juveniles ringed can be estimated as a constant parameter for all the years of study, or as a time dependent parameter allowing for variation between years. Robinson (2010) fixed this proportion to the mean observed in recent years, when the age at ringing data are recorded, and then tested sensitivity to this assumption. Here we consider estimating this proportion. As this model is used to analyse historical data, it is termed the historical data model.

In the historical data model, the total numbers of birds ringed as juveniles, $T_{j,i}$, and as adults, $T_{a,i}$ are unknown. We only know the sum of both, $T_{f,i} = T_{j,i} + T_{a,i}$, where $T_{f,i}$ is the total number of fledged birds ringed in each year i, for $i = 1, \ldots, n_1$.

The historical data model has an additional parameter to be estimated

- π_t is the proportion of fledged birds ringed as juveniles in year t, and $(1-\pi_t)$ is the proportion of fledged birds ringed as adults.

The probability that a bird ringed in year i was a juvenile, and was found dead in year t is

$$Q_{j,i,t} = \begin{cases} \pi_t(1-\phi_{1,t})\lambda_{1,t} & \text{if } t = i \\ \pi_i \phi_{1,i} \left(\prod_{k=i+1}^{t-1} \phi_{a,k} \right) (1-\phi_{a,t})\, \lambda_{a,t} & \text{if } t > i \end{cases}$$

for $i = 1, \ldots, n_1$, $t = i, \ldots, n_2$. The probability that a bird ringed in year i was an adult, and was recovered dead in year t is

$$Q_{a,i,t} = \; (1-\pi_i) \left(\prod_{k=i}^{t-1} \phi_{a,k} \right) (1-\phi_{a,t})\, \lambda_{a,t}$$

for $i = 1, \ldots, n_1$, $t = i, \ldots, n_2$. The likelihood function for the historical data model for fledged birds is

$$L_H = \left\{ \prod_{i=1}^{n_1} \prod_{t=i}^{n_2} Q_{j,i,t}^{R_{j,i,t}} Q_{a,i,t}^{R_{a,i,t}} \right\} \times \left[\prod_{i=1}^{n_1} \left\{ 1 - \sum_{t=i}^{n_2} (Q_{j,i,t} + Q_{a,i,t}) \right\}^{T_{f,i} - \sum_{t=i}^{n_2} (R_{j,i,t} + R_{a,i,t})} \right]. \quad (2.3)$$

There has been extensive work on mixture models dealing with unknown ages for capture-recapture data (see, for example, Pledger et al., 2009; Pradel, 2009). Pledger and Schwarz (2002) developed mixture models in band-recovery models (which is a reparameterisation of the ring-recovery model) and McCrea et al. (2013) examined age-dependent mixture ring-recovery models. Both mixture models assumed that the group an individual belongs to, in this case juveniles and adults, is unknown for all individuals, although to be able to estimate parameters McCrea et al. (2013) used a combined model including data of known age. In this chapter however we know which group some individuals belong to (the birds that were marked and recovered dead), but this information is unknown for the birds that were

never recovered. Alternatively, this model could be written in a multi-event format (Pradel, 2005), as demonstrated in Supporting Information Appendix S3 of Jiménez-Muñoz et al. (2019).

2.3.4 Historical Combined Data Model

If there are separate data for birds ringed as pulli, the numbers of these will generally be known and, as in Robinson (2010), it is possible to use a standard model for the pulli data and a historical data model for the fledged birds of unknown age, in one combined analysis. This model will be referred to as the historical combined data model. Let $R_{p,i,t}$ denote the number of pulli ringed in year i that were recovered dead in year t and let $T_{p,i}$ denote the total number of pulli ringed in year i. The probability that a pullus ringed in year i is recovered in year t is $P_{p,i,t} = P_{1,i,t}$. The likelihood function for the historical combined data model is then

$$L_{HC} \propto \left\{ \prod_{i=1}^{n_1} \prod_{t=i}^{n_2} P_{p,i,t}^{R_{p,i,t}} Q_{j,i,t}^{R_{j,i,t}} Q_{a,i,t}^{R_{a,i,t}} \right\} \times \left[\prod_{i=1}^{n_1} \left(1 - \sum_{t=i}^{n_2} P_{p,i,t} \right)^{T_{p,i} - \sum_{t=i}^{n_2} R_{p,i,t}} \times \left\{ 1 - \sum_{t=i}^{n_2} (Q_{j,i,t} + Q_{a,i,t}) \right\}^{T_{f,i} - \sum_{t=i}^{n_2} (R_{j,i,t} + R_{a,i,t})} \right]. \quad (2.4)$$

2.3.5 Conditional Model

In the case of unknown ringing totals, the conditional model, which conditions on the numbers of recovered individuals only, can be considered as an alternative to the historical data model. The conditional probabilities for birds ringed in year i that are recovered in year t, in both age classes are

$$P_{j,i,t}^{C} = \frac{P_{j,i,t}}{\sum_{t=i}^{n_2} P_{j,i,t}} \text{ and } P_{a,i,t}^{C} = \frac{P_{a,i,t}}{\sum_{t=i}^{n_2} P_{a,i,t}}$$

(McCrea et al., 2012). The likelihood function for the conditional model for the fledged birds is

$$L_C = \prod_{i=1}^{n_1} \prod_{t=i}^{n_2} (P_{j,i,t}^{C})^{R_{j,i,t}} (P_{a,i,t}^{C})^{R_{a,i,t}}. \quad (2.5)$$

The conditional model is known to be parameter redundant, except when λ is constant, (see, for example, Cole et al., 2012).

Conditional Combined model

As with the historical combined data model, separate data on pulli can be combined with the data on fledged birds. The standard model can be used for the pulli and the conditional model can be used for fledged birds. This model, which we refer to as the conditional combined model, has likelihood function

$$L_{CC} = \prod_{i=1}^{n_1}\prod_{t=i}^{n_2}(P^C_{j,i,t})^{R_{j,i,t}}(P^C_{a,i,t})^{R_{a,i,t}}P^{R_{p,i,t}}_{p,i,t} \times \prod_{i=1}^{n_1}\left(1-\sum_{t=i}^{n_2}P_{p,i,t}\right)^{T_{p,i}-\sum_{t=i}^{n_2}R_{p,i,t}}. \quad (2.6)$$

2.4 Model Fitting

R code for fitting the historical data model is provided in Supporting Information Appendix S7 of Jiménez-Muñoz et al. (2019). The historical data model could alternatively be fitted in the program E-surge (Choquet et al., 2009), as explained in Supporting Information Appendix S3 of Jiménez-Muñoz et al. (2019).

The models examined in this chapter are summarised in Table 2.1. This can be interpreted as follows: the standard model with likelihood equation (2.1) is implemented when the ringing total numbers available are for birds in their first year of life. The standard combined model, with likelihood function (2.2), is presented in two lines as this model can be used when we have two known separate ringing totals for juveniles and adults, or three known separate ringing totals, for pulli, juveniles and adults. The historical data model, with likelihood equation (2.3), is implemented when the ringing totals available are for fledged birds, thus we do not know the ringing totals for each age class separately. That is, we do not know how many birds were ringed as juveniles and how many birds were ringed as adults, instead we know the sum of both numbers. The historical combined data model, with likelihood function (2.4), results as the combination of the standard and the historical data model. We use this model when the total number of birds ringed as pulli is known, but the total numbers of birds ringed as juveniles and as adults are unknown separately, and instead we only have information on the sum of both numbers. The conditional and the conditional combined

models with likelihood equations (2.5) and (2.6), are the alternative models to the historical and historical combined data models.

Table 2.1 Description of the models defined above and used throughout the chapter. The models in bold are the models developed in this chapter, and have an extra parameter π, the yearly proportion of birds ringed as fledged birds that are juveniles. Likelihood refers to the equation number of the likelihood function given in the chapter. The last column specifies whether the total number of birds ringed per year per age category is known.

Model name	Likelihood	Data on birds ringed as	Totals known?
Standard	(2.1)	first year of life	yes
Standard Combined	(2.2)	fledged (juveniles and adults)	yes
Standard Combined	(2.2)	pulli and fledged	yes
Historical	(2.3)	fledged	no
Historical Combined	(2.4)	All age-categories: pulli and fledged	pulli only
Conditional	(2.5)	fledged	no
Conditional Combined	(2.6)	All age-categories: pulli and fledged	pulli only

2.5 Parameter Redundancy

Jiménez-Muñoz et al. (2019) used parameter identifiability theory to determine which parameters in the historical and combined models can be estimated, and these were compared to the parameters that can be estimated in the standard ring-recovery model, which are given by Cole et al. (2012). These results are given in Table 2.2. They found that all of the models that are identifiable for the standard form of the model are also identifiable in the historical form of the model (Table 2.2). A combined model, formed from pulli data and data on fledging birds, increases the number of models that are identifiable. The combined historical data model is shown to have identical identifiability results to the standard combined model, so in terms of parameter redundancy it does not matter whether or not the data have been fully computerised.

The alternative to the historical data model is the conditional model. However for ring-recovery data most conditional models are parameter redundant. When the pulli data are combined with the data on fledged bird data, the conditional combined model does not do any better than the pulli data alone, in terms of parameter redundancy. Therefore, in terms of parameter redundancy the best model to use for historical data is the historical data model.

Being able to show theoretically that a model is identifiable, however, is no guarantee that for some specific data the model would not be parameter or near-parameter redundant. We also consider parameter redundancy in practice by using simulation and considering

data on two different ring-recovery data sets. In Section 2.6 we run a simulation study and show that the historical data model gives almost identical parameter estimates as the standard model. We explore the blackbird data set, where we know the total numbers of birds ringed by age-class, and compare the performance of the historical data model with the standard model. Then, similarly to Robinson (2010) we use a subset of sandwich tern data, where we do not know these totals.

Table 2.2 Table taken from Jiménez-Muñoz et al. (2019). Parameter redundancy results. The main body of the table gives the deficiency, which is the difference between the number of parameters and the number of parameters that can be estimated. A deficiency of > 0 indicates the model is parameter redundant. A deficiency of 0 indicates the model is identifiable. The first row specifies the type of model, with Stand. short for standard, Cond. short for conditional and Cond. Comb. short for conditional combined. The combined column is applicable for both the combined historical data model and the combined standard model. The second row specifies which types of data the model is suitable for, either pulli, fledged (Fl) or both combined (Pulli + Fl). The third row specifies the proportion parameter, which is either constant (π) or time dependent (π_t), or not included in that type of model (-). The first column specifies the parameters in the model. Results here are for the same number of years of ringing as recovery, $n = n_1 = n_2$.

Model	Stand.	Historical		Combined	Cond.	Cond. Comb.
Data set(s)	Pulli	Fl		Pulli + Fl	Fl	Pulli + Fl
Proportion	-	π	π_t	π or π_t	-	-
ϕ_1, ϕ_a, λ	0	0	0	0	0	0
$\phi_1, \phi_a, \lambda_t$	0	0	0	0	2	0
$\phi_1, \phi_a, \lambda_1, \lambda_a$	1	1	0	0	2	1
$\phi_1, \phi_a, \lambda_{1,t}, \lambda_{a,t}$	1	1	0	0	3	1
$\phi_1, \phi_{a,t}, \lambda$	0	0	0	0	0	0
$\phi_1, \phi_{a,t}, \lambda_t$	0	0	0	0	3	0
$\phi_1, \phi_{a,t}, \lambda_1, \lambda_a$	1	1	0	0	2	1
$\phi_1, \phi_{a,t}, \lambda_{1,t}, \lambda_{a,t}$	2	2	3	1	$n+2$	3
$\phi_{1,t}, \phi_a, \lambda$	0	0	0	0	0	0
$\phi_{1,t}, \phi_a, \lambda_t$	0	0	0	0	2	0
$\phi_{1,t}, \phi_a, \lambda_1, \lambda_a$	0	0	0	0	2	0
$\phi_{1,t}, \phi_a, \lambda_{1,t}, \lambda_{a,t}$	2	2	3	1	$n+1$	3
$\phi_{1,t}, \phi_{a,t}, \lambda$	0	0	0	0	1	0
$\phi_{1,t}, \phi_{a,t}, \lambda_t$	2	1	$2n+1$	1	$n+1$	2
$\phi_{1,t}, \phi_{a,t}, \lambda_1, \lambda_a$	0	0	0	0	3	0
$\phi_{1,t}, \phi_{a,t}, \lambda_{1,t}, \lambda_{a,t}$	$n+1$	3	$n+2$	2	$2n$	$n+2$

2.6 Simulation Study

To compare how the historical data model performs in practice we provide two different simulation studies, which represent data on fledged birds. For all the simulations, all the parameters are kept constant over time. The first simulation study is for a population in which the adult survival is set to be the same for all individuals. For the second simulation study, we consider a population with heterogeneous adult survival. We simulate two types of heterogeneous populations; a heterogeneous population in which adult survival $\phi_{a,i}$, varies individually, where i denotes a logit-normal individual random effect; and a heterogeneous population formed by two sub-populations with two different adult survival probabilities: $\phi_{a,A}$, and $\phi_{a,B}$. The simulation studies for the heterogeneous populations allow us to test how the proposed models perform in practice when there is individual variation in survival caused by factors other than age. Furthermore, or the two simulation scenarios (i.e. for homogeneous and heterogeneous populations), we compare results for different lengths of study, providing results for five, 10 and 20 years of ring-recovery studies, with $n = n_1 = n_2$ (i.e the number of years of ringing is equal to the number of years of recovery).

For the homogeneous population, in each simulation 100 data sets are simulated from the standard combined model with 1000 birds ringed with a constant proportion π of the birds ringed in their first year of life, and $(1-\pi)$ of the birds ringed as adults. In the model there are separate constant survival probabilities for first year and adult birds, ϕ_1 and ϕ_a respectively, and a constant reporting probability, λ. We provide two different types of heterogeneous populations, first we look at a population in which adult survival $\phi_{a,i}$, varies individually, where i denotes a logit-normal individual random effect. We also simulate data for a population formed by two different sub-populations with two different adult survival probabilities $\phi_{a,A}$, and $\phi_{a,B}$.

Both the standard combined model and the historical data model described above are then fitted to each simulated data set. In the standard combined model the total numbers of birds ringed in each of the two age classes are known, whereas in the historical model only the total number of birds ringed is used. Otherwise, the forms of the two models are identical and match the form used in generating the data. We also fit the historical data model with π fixed either to the true value or to an arbitrary wrong value.

The simulation results for 10 years of study for a homogeneous population are given in Table 2.3; further results for five, and 20 years of study can be found in Appendix A.3. The heterogeneous populations results for five, 10 and 20 years of study are given in Appendix A.4. By simulating data for different study lengths we show how the magnitude of parameter bias is affected by the length of the study. We compare model performance by looking at

the bias, the standard deviation and the mean squared error of the parameters across 100 simulations.

Table 2.3 Simulation study for 10 years of ring-recovery data. The first column specifies the type of model, with Stand. Comb. short for standard combined, and Hist. short for historical. In this first column, the last last two rows contain information for the models in which the proportion parameter was fixed and the values used. The remaining columns contain the average parameter estimate (par est) and the average standard error, given in parentheses, along with the mean square error (MSE).

	ϕ_1		ϕ_a		λ		π	
	par est	MSE	par est	MSE	par est	MSE	par est	MSE
True Value	0.50	-	0.60	-	0.05	-	0.40	-
Stand. Comb.	0.50(0.04)	0.0014	0.60(0.02)	0.0005	0.05(0.002)	0.0000	-	-
Hist.	0.50(0.04)	0.0014	0.60(0.02)	0.0005	0.05(0.002)	0.0000	0.40(0.02)	0.0006
Hist. $\pi = 0.40$	0.50(0.04)	0.0014	0.60(0.02)	0.0005	0.05(0.002)	0.0000	-	-
Hist. $\pi = 0.20$	0.46(0.04)	0.0024	0.63(0.03)	0.0010	0.05(0.001)	0.0000	-	-

The simulation studies show that for a homogeneous population, the historical data model gives almost identical parameter estimates for survival and recovery to the standard combined model. The same is true for the heterogeneous populations. Both homogeneous and heterogeneous populations result in unbiased estimates of the proportion of birds ringed in their first year of life, π. This demonstrates that the historical data model can be used to estimate the additional parameter π as well as the survival and recovery parameters as accurately as the standard ring-recovery model, which requires additional information.

If π is fixed at the true value then the historical data model with a fixed π also performs just as well, as would be expected. However if π is not fixed at the true value then there is bias in the estimation of the survival parameters, the mean square error is bigger, and the standard error is higher than in other models. For example, when π is fixed at a lower value than the true value, fewer birds are estimated to survive their first year and, to retain a match to the subsequent numbers recovered, adult survival is increased in compensation. For constant π the bias decreases as the number of years of ringing and recovery increases. It is therefore recommended that the historical data model is used rather than fixing π.

Further simulation studies for different parameter estimates show very similar results and the recommendation from these simulation studies and Table 2.2 is that if total ringing numbers in each category are unavailable it is preferable to use the historical data model and estimate the proportion in each age class.

2.7 Results

Blackbird Case Study

Using the blackbird data set for comparison purposes, we run two different analyses. In the first analysis we assume we only have historical data, for which the total numbers of juveniles and adults ringed every year are unknown. That is, we add together the total of birds ringed in the fledged category. Then we fit historical data models to this data set. In the second analysis we use all the available data (using either two, or three, known ringing totals, i.e. juveniles and adults, or pulli, juveniles and adults), and we fit standard combined models. The parameter estimates for survival and reporting probabilities for the historical and historical combined data model, and their standard errors, are almost identical to those for the standard combined models (Table 2.4). However, the first year survival probability, ϕ_1, is slightly smaller for the models that analyse pulli data. Birds ringed as pulli are younger than those fledged juveniles, thus their survival is likely to be lower. Therefore adding the pulli data to the first year age class brings the survival probability ϕ_1 down.

Table 2.4 Estimates of survival and reporting probabilities for blackbird data using the standard combined, historical and historical combined data model. The parameter estimates are given alongside standard errors in parentheses. The first row specifies the type of model, with Stand. Comb. and Hist. Comb. short for standard and historical combined. The second row specifies the data used for the analysis, with Juv, Ad, and Fl short for ringing totals for juvenile, adult and fledged birds.

Model	Stand. Comb.	Historical	Stand. Comb.	Hist. Comb.
Data set(s)	Juv + Ad	Fl	Pulli + Juv + Ad	Pulli + Fl
ϕ_1	0.5925(0.0085)	0.5933(0.0085)	0.5451(0.0067)	0.5454(0.0067)
ϕ_a	0.6965(0.0050)	0.6958(0.0049)	0.6915(0.0045)	0.6909(0.0044)
λ	0.0375(0.0005)	0.0375(0.0005)	0.0361(0.0004)	0.0361(0.0004)
π		0.5760(0.0066)		0.5741(0.0066)

Tables 2.5 and 2.6 compare the best models in terms of the Akaike information criterion (AIC; Akaike, 1974) for the standard combined and the historical data models. To compare the model selection for the historical and the standard combined models, we check if the dependencies for the survival and recovery parameters for the best models agree. For example, the standard model with parameters (ϕ_1, ϕ_a, λ_t) would be equivalent, demographically, to the historical data models with parameters (ϕ_1, ϕ_a, λ_t, π), and (ϕ_1, ϕ_a, λ_t, π_t). Table 2.5 shows that the best models for the historical and the standard combined agree; the same parameterisation is chosen for the two different models. Moreover Table 2.6 shows that although the same best (demographic) models are chosen for the historical combined and

the standard combined models, the order of preference differs. The best model for the historical combined data model has parameters $(\phi_1, \phi_a, \lambda_{1,t}, \lambda_{a,t}, \pi)$, followed very closely by the models with parameters the $(\phi_{1,t}, \phi_a, \lambda_t, \pi)$ and $(\phi_1, \phi_a, \lambda_t, \pi_t)$; for the standard combined model the best model has parameters $(\phi_1, \phi_a, \lambda_t)$, followed, some distance behind, by the model with parameters $(\phi_1, \phi_a, \lambda_{1,t}, \lambda_{a,t})$. Nonetheless, the difference in AIC between the top historical data models is very small, and seems to show that the age dependency in the recovery probability does not contribute significantly to the model when the proportion of juvenile birds ringed is not known, but estimated. We provide the parameter estimates for all the models presented in Tables 2.5 and 2.6 in Appendix A.5.

Table 2.5 Comparison between the historical ring-recovery and standard combined model selection for blackbirds. The first and the third columns show the models fitted and the parameterisation used.

Historical Fl	Δ AIC	Standard Combined Juv + Ad	Δ AIC
$\phi_1, \phi_a, \lambda_t, \pi_t$	0.00	$\phi_1, \phi_a, \lambda_t$	0.00
$\phi_1, \phi_{a,t}, \lambda_t, \pi_t$	3.68	$\phi_1, \phi_{a,t}, \lambda_t$	11.89
$\phi_1, \phi_a, \lambda_t, \pi$	6.65		
$\phi_1, \phi_{a,t}, \lambda_t, \pi$	18.30		
$\phi_{1,t}, \phi_a, \lambda_t, \pi$	20.30	$\phi_{1,t}, \phi_a, \lambda_t$	23.87
$\phi_{1,t}, \phi_a, \lambda_t, \pi_t$	22.59		
$\phi_1, \phi_a, \lambda, \pi$	148.56	ϕ_1, ϕ_a, λ	140.58

Table 2.6 Comparison between historical combined and standard combined ring-recovery model selection for blackbirds. The first and the third columns show the models fitted and the data used, with Juv, Ad, and Fl short for ringing totals for juvenile, adult and fledged birds.

Historical Combined Pulli + Fl	Δ AIC	Standard Combined Pulli + Juv + Ad	Δ AIC
$\phi_1, \phi_a, \lambda_{1,t}, \lambda_{a,t}, \pi$	0.00	$\phi_1, \phi_a, \lambda_{1,t}, \lambda_{a,t}$	26.48
$\phi_{1,t}, \phi_a, \lambda_t, \pi$	2.30	$\phi_{1,t}, \phi_a, \lambda_t$	38.38
$\phi_1, \phi_a, \lambda_t, \pi_t$	2.60	$\phi_1, \phi_a, \lambda_t$	0.00
$\phi_1, \phi_a, \lambda_{1,t}, \lambda_{a,t}, \pi_t$	5.10		
$\phi_1, \phi_a, \lambda_t, \pi$	5.80		
$\phi_1, \phi_{a,t}, \lambda_t, \pi_t$	17.70	$\phi_1, \phi_{a,t}, \lambda_t$	30.40
$\phi_1, \phi_a, \lambda, \pi$	146.10	ϕ_1, ϕ_a, λ	148.33

Finally, Figure 2.2 shows that the total number of juvenile blackbirds estimated from the fledged bird data set for the best historical combined data model with parameters $(\phi_1, \phi_a, \lambda_t, \pi_t)$ is very similar to the real number of ringed juvenile blackbirds.

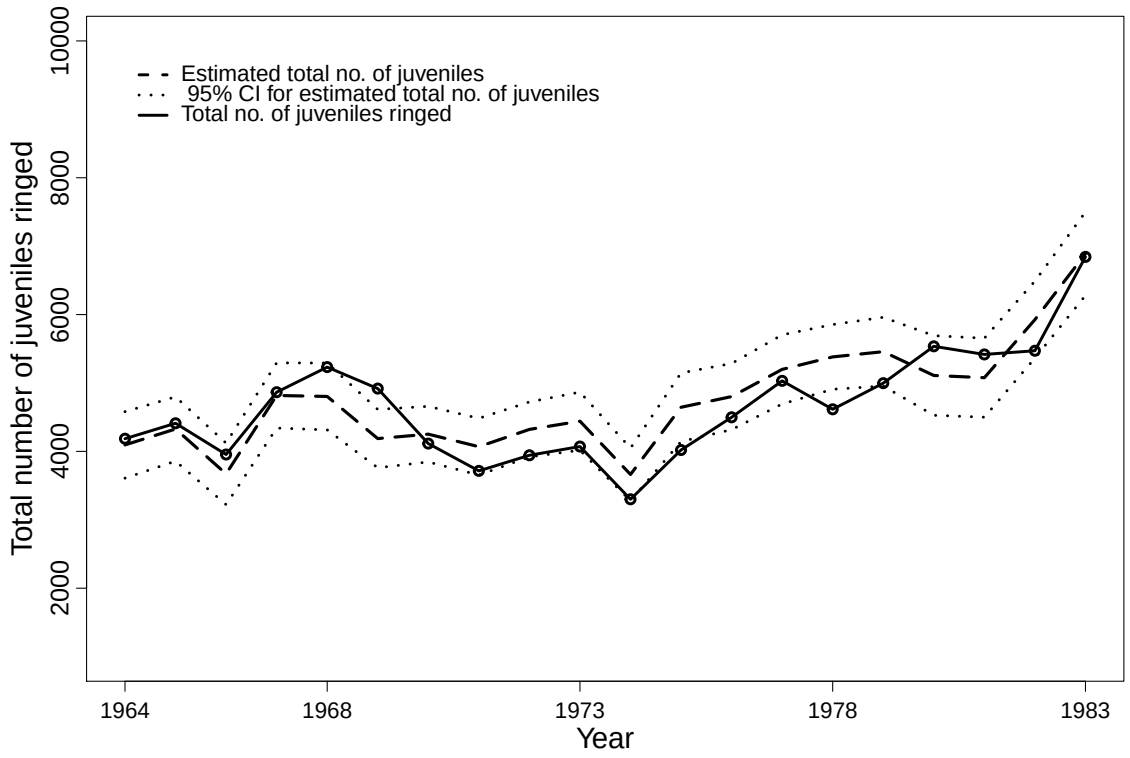

Fig. 2.2 Comparison between the total number of juvenile blackbirds ringed per year, indicated by the continuous line, and the estimated total number of juveniles, indicated by the dashed line, obtained from the time dependent proportion of juveniles (π_t), for the historical combined data model with parameters $(\phi_1, \phi_a, \lambda_t, \pi_t)$. The dotted lines represent the 95 % confidence interval.

Sandwich Tern Case Study

For longer-lived species, juvenile survival may be substantially lower, so we analyse sandwich tern data for which the separate ringing totals are unknown for juveniles and adults. This is a longer-lived species than the blackbird, but it is rarer and the data are consequently sparser. When fitted, most of the historical data models prove to be parameter redundant or near-parameter redundant. In fact, the only model which did not present any identifiability issues, was that in which all the parameters were kept constant. However, when looking at the parameter estimates, the first year survival probability was estimated much higher than the adult survival probability, which does not appear realistic. Moreover, for most of the models we were unable to maximise the likelihood function.

The results described above are a clear example of parameter redundancy caused by the data. The issue of parameter redundancy improved when adding the pulli data to the historical data model by fitting the historical combined data model. As a result, many more models could be fitted, however there were only three models that did not present any sign of parameter redundancy. The parameter estimates for these models can be found in Table 2.7. The parameter estimates for the time dependent parameters can be found in Appendix A.6. Furthermore, when adding the pulli data, the constant model presented more reliable results, with a higher survival probability for adults than for first years, and with parameters estimates closer to those expected based on the results obtained when fitting the standard model to pulli data alone.

Table 2.7 Historical combined ring-recovery model selection and parameter estimates for sandwich terns for the years 1970-1990. The standard errors are given in parentheses. The parameter estimates for these models can be found in Appendix A.6 (Figures A.1 and A.2).

Parameters	Δ AIC	ϕ_1	ϕ_a	λ	π
$\phi_1, \phi_a, \lambda_t, \pi$	0.00	0.74(0.016)	0.87(0.010)	-	0.32(0.076)
$\phi_1, \phi_a, \lambda, \pi$	27.67	0.73(0.015)	0.87(0.010)	0.02(0.001)	0.32(0.076)
$\phi_{1,t}, \phi_a, \lambda, \pi$	34.01	-	0.86(0.010)	0.02(0.001)	0.32(0.076)

Sandwich terns are bigger than blackbirds and most do not begin to breed until their third year of life, thus a more complex age structure may well be more realistic, although these extra parameters may hinder further parameter identifiability. Robinson (2010) explores a model with three age classes, where he estimates survival and reporting probabilities for first-year birds, birds in their second or third year and older birds. We do not have data on ringing totals for birds ringed in their second or third year of life, though these are possibly few as the young birds relocate to West Africa before returning to breed. As for most species, we also do not know the age of the adult sandwich terns at ringing. If this information was known, for this or a similarly long-lived species, a better alternative would be to model this age structure with the approach presented in this chapter in combination with the age-dependent mixture model proposed by McCrea et al. (2013).

2.8 Discussion

We have presented the model from Jiménez-Muñoz et al. (2019) that estimates age-dependent survival probabilities from ring-recovery data where the number of individuals ringed in each age class is unknown. Moreover, Jiménez-Muñoz et al. (2019) used identifiability theory to show that it is possible to estimate the proportion of individuals in each age class. Using

simulation and a data set where the ringing numbers are known by age category we have demonstrated that the historical data model gives almost identical parameter estimates as the standard ring-recovery model. Therefore we have shown that it is possible to fit useful age-dependent survival models to historical ringing data even though the data may not have been fully computerised.

This new model provides an extension to the analysis of UK ringing data of Robinson (2010), where the proportion in each age category was fixed. The new historical data model has the advantage that, by estimating rather than assuming age-specific ratios at ringing, estimates of precision and hypothesis tests are more reliable - if a constraint is imposed unnecessarily, there is bias in estimating survival and the resulting standard errors may overestimate the uncertainty in selecting this value, as demonstrated in the simulation study.

Although these results were motivated by an analysis of UK ringing data (Robinson, 2010), many national ringing schemes, in Europe and North America (Tautin, 2008), face a similar challenge. For European schemes details of birds ringed and subsequently recovered have been routinely collated and are accessible for analysis. The Euring Data Bank (EDB) currently holds in excess of 10 million such records (Du Feu et al., 2016). Moreover, although here we just look at estimating probabilities for two age categories: first year and adult birds, the historical data model can be extended with the addition of an age-mixture model (McCrea et al., 2013) to incorporate other age dependencies that accommodate for differences in breeding age between species.

These results indicate that it is possible to incorporate age-specific variation in models of survival, further unlocking the potential of a valuable historical data archive compiled over several decades to better characterise temporal dynamics in the population processes of many species. Such data are, of course, often the only source of demographic data ever likely to be available as a benchmark against which to compare estimates from more recent years and different climatic and agricultural contexts.

Chapter 3

Analysing Capture-Recapture Data in the Presence of Covariates

3.1 Introduction

The little auk or dovekie (*Alle alle*) is a small bird that breeds on islands in the high Arctic. Bi-parental care is crucial for successfully raising the (single egg) offspring of the little auk (Kidawa et al., 2012). However, this species is known for the female deserting the brood during the last week of the chick rearing period, with the male parent staying in the nest to continue the chick's care (Harding et al., 2004; Wojczulanis-Jakubas and Jakubas, 2012). This is an unusual trait of these birds, as for most bird species, the male parent deserts the brood earlier than the mother. The time at which each female desserts the brood – although constrained to the very last week of the chick rearing period - seems to be flexible; sometimes females desert the brood a week before chick fledgling, sometimes they stay until the end of the fledgling period (Wojczulanis-Jakubas and Jakubas, 2012). There are premises that in less favourable environmental conditions the female stays longer (possibly bi-parental care is still necessary to provision the chick adequately). Why it is the female and not the male that deserts the brood is not clear. Body condition does not seem to be the main trigger (Wojczulanis-Jakubas and Jakubas, 2012; Wojczulanis-Jakubas et al., 2014). Nevertheless females usually (but not always) have lower body mass than males, so may be more prone to body reserve depletion, which could be the trigger for leaving the brood first.

In this chapter we analyse two different capture-recapture data sets for female auks breeding in two different colonies which differ in terms of oceanographic conditions. The first data set consits of capture-recapture data for which sex and site covariates are recorded for 950 individuals. The second data set consits of capture-recapture data for 56 female little

auks for which site and presence covariates are recorded. The presence covariates contain information about the female's length of stay in the brood.

In order to understand the relationship between female little auks brood desertion and their survival, in this chapter we analyse the capture-recapture data. We use covariates to study if survival rates are affected by sex, or by the environmental conditions in which these birds breed. Additionally, we use presence data, in the form of continuous covariates, to assess if a longer presence in the brood has an impact on female survival.

In Section 3.2 we describe the characteristics of the data, giving some background on how the capture-recapture and female presence data are collected, and what these comprise. In Section 3.3 we describe the models implemented, and capture-recapture models in the presence of categorical and continuous covariates. In Section 3.4 we provide a simulation study to check the adequacy of our models. In Section 3.5 we discuss the results obtained for the little auk data. Finally, in Section 3.6 we provide an overview of the work carried out in this chapter.

3.2 Data

For the purpose of this study, data were collected in two breeding colonies in the Norwegian island of Spitsbergen, Hornsund (77°00'N, 15°33'E) and Magdalenefjorden (77°00'N, 15°33'E). These sites were selected they are considered the two largest breeding aggregations of the little auk on this island (Isaksen and Gavrilo, 2000; Keslinka et al., 2019). Figure 3.1 shows a map of Spitsbergen indicating the location of both colonies.

The oceanographic conditions in the foraging grounds are different for the two colonies. In Hornsund, birds utilise profitable, cold water masses (Jakubas and Wojczulanis-Jakubas, 2013; Jakubas et al., 2014). In Magdalenefjorden, birds forage in an area that is dominated by less profitable warm water masses. However, they have also been reported to utilise more distant foraging areas, at the edge of the sea ice (Jakubas et al., 2012; Jakubas and Wojczulanis-Jakubas, 2013). Specific information regarding the conditions of both sites can be found in Wojczulanis-Jakubas et al. (2019)

Across the two colonies capture-recapture data were collected on 950 individuals of both sexes. Additionally, capture-recapture data on another 56 female little auks were also collected. For these data rather than considering randomly sampled individuals, nests were randomly selected and monitored. That is, occupied nests were chosen at random and presence covariates for the females found breeding in them were recorded. The studies were made at different times at the two sites. While some of the data for Magdalenefjorden have already been used in Wojczulanis-Jakubas and Jakubas (2012), the data from Hornsund are

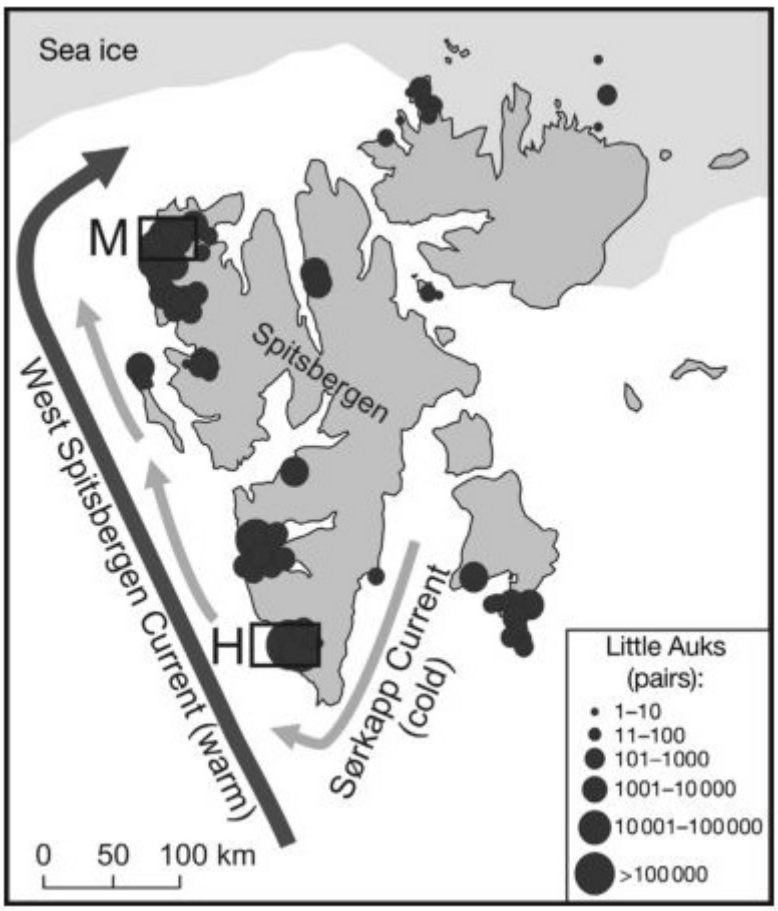

Fig. 3.1 Map of the little auk colonies discussed in this chapter. Here, H stands for Hornsund and M for Magdalenefjorden. The map is taken with permission from Jakubas et al. (2011).

considered here for the first time. The next sections explain the characteristics of these data: the capture recapture data for all individuals studied and the capture-recapture and presence data collected on the 56 females.

3.2.1 Capture-Recapture Data

Capture-recapture data were collected during the seasons 2001-2017 in Hornsund and in 2007-2011 in Magdalenefjorden. We consider birds marked between 2001 and 2016 in Hornsund, and between 2007 and 2010 in Magdalenefjorden. These birds are recaptured between 2002 and 2017 in Hornsund, and between 2009 and 2011 in Magdalenefjorden. The birds considered in this study were captured by hand while incubating and/or brooding in the nests. Each newly caught bird was ringed with a unique number and a small blood or feather sample was taken for purposes of molecular sexing, following the methods described in Jakubas and Wojczulanis (2007). Table 3.1 shows the total number of birds marked in each site during the study. From Table 3.1 we can observe that more birds were ringed in Hornsund than in Magdalenefjorden. This is due to the number of years in which data were collected in both sites, with 15 years of capture-recapture data collection in Hornsund, and five in Magdalenefjorden. Moreover, roughy the same number of female and male birds have been ringed within each site.

Table 3.1 Total number of individuals marked in each site between 2001 and 2016 for both sexes.

Site	Female	Male	Total
Hornsund	337	375	712
Magdalenefjorden	107	131	238
Total	444	506	950

Table 3.2 shows the total number of birds captured each year from 2001 to 2017 in Hornsund for each sex. The years 2003, and 2013 are not included in Table 3.2, as Hornsund was not visited. Table 3.2 also discloses the total of birds captured, the number of birds that were captured for the first time each year and the number of birds that were recaptured. In Table 3.2 we can see that the number of first captures increases from 2001 to 2006, and the number of recaptures are low until 2006. Between 2007 and 2009 both first captures and recaptures are very low. The numbers of first captures and recaptures are highest between 2011 and 2017.

Table 3.2 Total number of individuals captured and recaptured in Hornsund per sex in every year of the study. The first column (S) indicates the sex of the individuals, with F for female and M for male birds. The rows in black indicate the total number of birds that were captured. The rows in grey indicate the number of birds that were captured for the first time (First) and the number of birds that were recaptured (Recap).

S	Cap	Year														
		01	02	04	05	06	07	08	09	10	11	12	14	15	16	17
F	Total	17	18	0	32	63	7	2	12	8	85	105	93	40	43	37
	First	17	15	0	32	46	1	1	11	5	71	54	50	19	15	-
	Recap	0	3	0	0	17	6	1	1	3	14	51	43	21	28	37
M	Total	18	20	1	36	60	9	2	14	10	92	120	104	45	65	51
	First	18	15	0	34	40	0	2	9	9	81	57	59	26	25	-
	Recap	0	5	1	2	20	9	0	5	1	11	63	45	19	40	51

Similarly, Table 3.3 shows the total number of birds captured each year from 2007 to 2011 in Magdalenefjorden for each sex. Table 3.3 shows that although in Magdalenefjorden in 2008 some individuals were captured and marked for the first time, none of the birds marked in 2007 were recaptured in 2008, for either sex.

Table 3.3 Total number of individuals captured and recaptured in Magdalenefjorden per sex in every year of the study. The first column (S) indicates the sex of the individuals, with F for female and M for male birds. The rows in black indicate the total number of birds that were captured. The rows in grey indicate the number of birds that were captured for the first time (First) and the number of birds that were recaptured (Recap).

Sex	Cap	Year				
		07	08	09	10	11
F	Total	33	26	46	38	9
	First	33	26	36	12	-
	Recap	0	0	10	26	9
M	Total	29	36	58	64	26
	First	29	36	36	30	-
	Recap	0	0	22	34	26

3.2.2 Capture-Recapture and Presence Data—Female Nest Data

Across both sites, for 56 females capture-recapture data and presence data were collected, with 25 females in Hornsund and 31 in Magdalenefjorden. In this section we explain the

details for both the capture-recapture and the presence data for these individuals. The capture-recapture encounters for these females are analysed separately from the larger capture-recapture data set explained in Section 3.2.1, for this reason we refer to the data collected for these female birds as the female nest data.

Capture-Recapture Data

The number of birds within the female nest data captured for each year of study are shown in Table 3.4 for Hornsund, and in Table 3.5 for Magdalenefjorden. For each site both the number of birds first captured and the number of birds recaptured are very low for every year of study.

Table 3.4 shows that in Hornsund capture-recapture data were collected for 11 years during the years 2001-2017. At this site there were eight years of marking (as no marking took place in 2005 or 2006) and 9 years of recaptures, as there were no recaptures in 2002). Table 3.4 does not contain information for the years 2003, 2007, 2008, 2009, 2010 and 2013 as the female individuals considered for this study were not captured or recaptured during these years. The lack of information for these years does not necessarily mean that there were no attempted recaptures in these given years. Instead, this means that no individuals were observed. As a result, the parameter estimates for the capture probability will be 0 for these years.

Table 3.4 Total number of female birds in the female nest data captured and recaptured in Hornsund in every year of the study. The rows in black indicate the total number of females that were captured. The rows in grey indicate the number of female birds that were captured for the first time (First) and the number of female birds that were recaptured (Recap).

Cap	Year										
	01	02	04	05	06	11	12	14	15	16	17
Total	1	3	1	5	4	4	6	9	9	17	10
First	1	3	0	3	0	3	2	3	4	6	-
Recap	0	0	1	2	4	1	4	6	5	11	10

Table 3.5 shows that for Magdalenefjorden there are only three years of marking (2008-2010), and three years of recaptures (2009-2011). Although more females were marked in Magdalenefjorden, the number of captures and recaptures are very low. For example, Table 3.5 shows that in total there were 31 individuals marked, and for all these there were 37 recaptures during the study period.

Table 3.5 Total number of female birds in the female nest data captured and recaptured in Magdalenefjorden in every year of the study. The rows in black indicate the total number of females that were captured. The rows in grey indicate the number of female birds that were captured for the first time (First) and the number of female birds that were recaptured (Recap).

Cap	Year			
	08	09	10	11
Total	7	20	26	15
First	7	13	11	-
Recap	0	7	15	15

Presence Data

To track colony presence of females, direct observations were carried out in Hornsund and Magdalenefjorden for some females. Additionally in some cases video recording was also carried out in Hornsund. Presence data were collected in 2009 and 2010 in Magdalenefjorden and in 2004, 2016 and 2017 in Hornsund.

Direct observations were performed 2-3 times per season on marked individuals, during the time of the chick rearing period. Each observation lasted uninterruptedly for either 24h or 48h. Each focal individual was monitored continuously, and its presence status was noted every 10 min.

For the video recorded individuals, a video camera filmed continuously for more than 24 hours all the individuals present in a 3 m radius of focal nest entrance. There were 2-4 cameras operating simultaneously, with changing position according to the birds phenology, aiming to register the birds presence pattern mainly at the fourth week of the chick rearing period.

For both sites most individuals in the female nest data were only observed once while nesting. Table 3.6 shows that only for three females presence data were collected in two different years, and for 22 females presence data were collected in one year of the study. In Magdalenefjorden presence data for six females were collected in two different years, and presence data for 25 females were collected only in one year of the study.

For those female birds that were observed, the following information was recorded:

- The number of days that a chick took to fledge. This information was always observed precisely. Therefore there is perfect detection for the fledging day. We refer to the number of days that a chick took to fledge as “fledge”.

Table 3.6 The number of females for which presence data were collected on either one or two occasions, for each site.

Presence occasions	Hornsund	Magdalenefjorden
1	22	25
2	3	6
Total	25	31

- Female presence in the nest. When a nest was observed if the female was there, a 1 was recorded. The female was observed precisely before the chick fledged. However, from the day of chick fledging there was imperfect detection for females in the nest. In addition, some nests were observed after the chick fledged, but some others were not. We refer to the last day in which a female was recorded as "last1".

- First day the female was not seen. If the nest was observed throughout the whole period, the day that the female left was perfectly detected. However some nests were not observed on some particular days, therefore, the record for the first day of not seeing a female might be an over (or under) estimate of the actual day of departure. We refer to the first day in which the female was not observed in the nest as "first0".

- The index of departure day. For some females the specific day in which they left the nest is not known precisely. For this reason we estimate the departure day from the colony, using the arithmetic mean:

$$\text{Index of departure day} = \frac{\text{first0} + \text{last1}}{2}.$$

  We refer to this as "index".

Table 3.7 shows the summary statistics for the presence data. We use the three different days recorded and the index of departure day as an indicator of female presence in our analysis, including them as individual covariates. Specific details on the modelling can be found in Section 3.3.

Table 3.7 Summary statistics for the presence data. The first column specifies the type of statistic, with Min. short for minimum value, 1st Qu. short for first quartile, 3rd Qu. short for third quartile, and Max. short for maximum value. The remaining columns specify the type of information that was recorded for those female birds that were observed.

Stat	fledge	last1	first0	index
Min.	21	11	18	14.5
1st Qu.	26	21	25	23
Median	27	24	26	25
Mean	26.94	22.82	26.33	24.58
3rd Qu.	28	26	28	27
Max.	31	29	32	30.5

Capture-Recapture and Presence Data

We use the presence data as continuous individual time-varying covariates. However the size of the female nest data is small, and the existing presence data contain many missing values.

It is common when using time-varying covariates in capture-recapture or mark-recapture-recovery studies that many missing values arise. This is because usually for the years in which the individuals are not captured, the covariate data available are not observed. Moreover, missing data can also arise if the individual is captured in a particular year, but its corresponding covariate is not observed (see for example, Bonner et al., 2010, Langrock and King, 2013, and Worthington et al., 2015).

For our female nest data set the information available is limited. This data set consists of 56 marked female little auks, which were encountered on 136 occasions. Of these encounters, covariate data were recorded only for 65 capture and recapture encounters. That is, 47% of the encounters for the female nest data contain covariate information. However, we must bear in mind that, even considering both sites together, only approximately five birds were being marked each year in the female nest data (see Tables 3.4 and 3.5 for details on the capture-recapture histories of the female nest data). Moreover, covariate data were recorded on two occasions for only 9 of the 56 females. For the remaining females covariate data were recorded only on one occasion each.

Thus, given the limitations of our data, we perform a simple deterministic imputation approach and we proceed with the capture-recapture analysis as if the missing values had been observed. For the individuals for which we have only one presence observation, we use the same value from the first year of capture, until the end of the capture-recapture study, regardless of the year in which this covariate observation was made. For those individuals for

which we have two different values in two different years, we keep those values in the specific years in which they were recorded, and for the remaining years we impute using the average between the two observed values. Tables 3.8, shows an example of capture-recapture and presence histories for two individuals, and the imputation of the missing covariate data for the Magdalenefjorden site. In Table 3.8 we observe that female 41163 was first captured in 2008 and that no presence information was recorded for her. This female was also recaptured in 2009 when it was recorded that its chick took 26 days to fledge, and also in 2010 when it was recorded that its chick took 28 days to fledge. We impute presence data with the average, 27 days, for the years 2008, when this female was first captured, and in 2011, the last year of the capture-recapture study in Magdalenefjorden, in which this female was not recaptured. Equally, Table 3.8 contains information regarding the last day in which the female was seen in the brood (last1), and the first day in which she was noticed missing.

Table 3.8 Example of two capture-recapture histories with presence covariate data for two females in Magdalenefjorden. The first column indicates the individual identification number given at marking. The rows labelled as Encounter contain the corresponding individual's capture-recapture history. The covariate data recorded can be found in the rows labelled as fledge, last1 and first0. In these rows, ? denotes that no presence information was recorded. Immediately after these rows, the rows in grey rows labelled as Impute, contain the imputed covariate information for the particular covariate.

Indiv	Year captured					Data
no	2007	2008	2009	2010	2011	
41163	0	1	1	1	0	Encounter
	-	?	26	28	?	fledge
	-	27	26	28	27	Impute
	-	?	25	26	?	last1
	-	25.5	25.5	25.5	25.5	Impute
	-	?	27	28	?	first0
	-	27.5	27.5	27.5	27.5	Impute
41185	0	0	1	0	0	Encounter
	-	-	26	?	?	fledge
	-	-	26	26	26	Impute
	-	-	26	?	?	last1
	-	-	26	26	26	Impute
	-	-	27	?	?	first0
	-	-	27	27	27	Impute

3.3 Capture-Recapture Models

The objective of this study is to establish if the survival of the little auk is affected by its sex and/or the site where it breeds. Moreover, we are interested in understanding if the females' efforts in raising their chicks have an effect on survival.

As explained in Section 3.2, two capture-recapture data sets are available, we refer to them as the capture-recapture data set and the female nest data set. The former contains information about the sex and the site in which each individual was captured while breeding. The model for these data is described in Section 3.3.1. The latter contains capture-recapture information on female birds, as well as additional covariate information regarding the length of the female stay in the brood. The model for these data is described in Section 3.3.2.

We use an extension of the Cormack-Jolly-Seber (CJS) Cormack (1964), Jolly (1965) and Seber (1965) model to fit the capture-recapture data by adding sex, site and presence data as covariates. The CJS model specifications can be found in Chapter 1, in Section 1.2.1.

Covariates are added through the use of logistic regression.

3.3.1 Capture-Recapture Data

For the capture-recapture we use the individual's sex and the individual's breeding site as covariates. Both are categorical covariates with two levels that do not change with time.

These covariates can be added to the survival or to the capture probability using logistic regression (Lebreton et al., 1992). Different combinations are possible, for example, survival can depend only on the site covariate, or only on the sex covariate, or it can depend both on site and sex. The capture probability can also adopt similar dependencies, and these dependencies can be added in one or both parameters at the same time. Equation 3.1 shows the logistic regression model to estimate survival with site and sex as covariates

$$\phi_{site,sex} = \frac{1}{1+e^{-(\alpha+\beta_{site}x_{1,i}+\beta_{sex}x_{2,i})}}, \tag{3.1}$$

where $x_{1,i}$ is an indicator covariate which represents the site in which individual i was captured breeding, with $x_{1,i} = 1$ if individual i breeds at Hornsund and $x_{1,i} = 0$ if it breeds at Magdalenefjorden. Similarly, $x_{2,i}$ is the indicator covariate that represents the sex of the individual i, with $x_{2,i} = 1$ if individual i is female and $x_{2,i} = 0$ if individual i is male.

As the discrete covariates are known for each individual observed in the study, the likelihood function follows immediately by specifying the parameter dependencies given in the standard CJS likelihood. The data likelihood corresponds to the joint distribution of the encounter histories and all covariate values.

3.3.2 Female Nest Data

For the female nest data we use two types of covariates. The first is the individual's breeding site which does not change with time. The second utilises the presence data, which is a time-varying covariate with missing values.

These covariates can be added to the survival or to the capture probability using logistic regression. Different combinations are possible, for example, survival can depend only on the site covariate, or only on presence covariate, or it can depend both on site and presence covariates. The capture probability can also adopt site dependencies however, we do not add presence covariates to this parameter. These dependencies can be added in one or both parameters at the same time. Equation 3.2 shows the logistic model to estimate survival with site and presence data as covariates

$$\phi_{site,presence} = \frac{1}{1+e^{-(\alpha+\beta_{site}x_{1,i}+\beta_{presence}x_{2,i,t})}}, \tag{3.2}$$

where $x_{1,i}$ is the indicator covariate that represents the site in which individual i was captured breeding, with $x_{1,i} = 1$ if individual i breeds at Hornsund and $x_{1,i} = 0$ if it breeds at Magdalenefjorden. The covariate $x_{2,i,j}$ represents the number of presence days for female i in year j. The presence data can be measured by the number of days that the chick took to fledge, the number of days that the female stayed in the nest, or by the day number in which the female was last seen in the nest.

The missing values for the covariate $x_{2,i,j}$, are imputed as explained in Section 3.2.2.Thus, the likelihood expression for this model is equally obtained by multiplying the contributions for each individual.

3.4 Simulation Study

We perform a simulation study to: 1. assess how the number of individuals marked affects the precision of the parameter estimation when we include categorical and continuous covariates, and 2. examine the accuracy of our imputation method for the female nest data. For each simulation, 100 capture-recapture data sets were simulated, and we provide the average parameter estimate, the average standard error and the mean squared error. Further details are given in the following two sections, 3.4.1 and 3.4.2.

3.4.1 Assessing the Effect of Sample Size on Parameter Estimation

The data described in this chapter, and particularly the female nest data, have some limitations in terms of sample size. For this reason the aim of this simulation study is to validate the accuracy of the results obtained depending on the number of individuals marked in each sample and for different parameter values. We consider four capture-recapture studies with $T = 11$ capture-recapture events, 10 first capture occasions in years $T = 1\ldots,10$, and 10 recapture occasions in years $T = 2\ldots,11$. We create four simulation sets, with either 100, 50, 10 or five individuals marked on each occasion, so that there are 1000, 500, 100 or 50 individuals in total. We examine the effect of adding categorical covariates with two levels such as site or sex, and continuous covariates, such as presence, to the survival parameter ϕ and the capture parameter p.

The parameter values when kept constant are fixed at 0.80, 0.40 or 0.20, for both survival and capture probabilities. The simulation study was motivated by the real data. Thus, in the cases in which survival or capture probabilities have any dependency, we use the parameter estimates obtained in Results section, 3.5. When we add categorical covariates, if the model has one categorical covariate, we name the slope parameter β_{site}. If the model has two categorical covariates we call the slopes β_{site} and β_{sex} respectively. If we have continuous covariates, we refer to the slope parameter as $\beta_{presence}$.

Table 3.9 shows the simulation results for a capture-recapture study with survival depending on a categorical covariate with two levels, i.e.site, and constant capture probability fixed at 0.40. Simulation results for different parameter values and different categorical and continuous covariate combinations can be found in Appendix B.

In Table 3.9 we observe that the MSE increases as the sample size decreases. The estimate of β_{site} is biased when the sample size is five, but this also has a much larger average standard error.

Further results in Appendix B show that in the cases in which the number of individuals marked is equal to five or 10 per year of study, the bias in estimation can be large, particularly when the survival or capture probabilities have more than one dependency, regardless of the type. For this reason, if data are limited caution must be taken when interpreting the results. Standard errors and evaluating standardised eigenvalues (see Section 1.2.4), can help to validate the significance of our results.

Table 3.9 Simulation study for 11-year of capture-recapture studies with survival as a function of a categorical covariate with two levels and capture probability fixed at 0.40. The first row specifies the model parameters and the values used to generate the simulated data. The first column (size) specifies the number of individuals marked every year of the study. The remaining columns contain the average parameter estimate (par est) and the average standard error, given in parentheses, along with the mean square error (MSE).

	ϕ				p	
	$\alpha = 1.10$		$\beta_{site} = -1.35$		$p = 0.40$	
size	par est	MSE	par est	MSE	par est	MSE
100	1.11(0.09)	0.0090	-1.38(0.13)	0.0149	0.40(0.01)	0.0004
50	1.10(0.13)	0.0169	-1.37(0.18)	0.0308	0.40(0.03)	0.0011
10	1.07(0.29)	0.0833	-1.38(0.42)	0.1709	0.41(0.04)	0.0042
5	1.13(0.43)	0.1960	-1.83(42.68)	6.0043	0.40(0.06)	0.0080

3.4.2 Examining the Deterministic Imputation Method

In this simulation study we include continuous covariates in the survival parameter and compare the results obtained with different levels of missing data. We provide two different simulation studies, A and B. Simulation study A considers what happens when capture histories are omitted due to no covariates being observed. In simulation study B we compare the imputation method described in this chapter with an alternative imputation method.

We consider three capture-recapture studies with $T = 11$ capture-recapture events, 10 first capture occasions in years $T = 1\ldots,10$, and 10 recapture occasions in years $T = 2\ldots,11$. The parameter estimates used are based on those obtained for the real data in Section 3.5.2. Thus, survival is a function of the continuous covariate, with $\alpha = 1.20$ and $\beta_{presence} = 0.25$, and capture probability is constant and fixed at 0.60.

We generate simulated covariate data so that it changes per individual and year of study. To do so, for every individual i, we simulate the mean individual covariate value, $m_i \sim N(20,5)$. Using the individual covariate mean, we simulate a covariate value for each individual for each year of study t, so $x_{i,t} \sim N(m_i,1)$, where $x_{i,t}$ is the yearly individual continuous covariate value.

Simulation Study A

We create four simulation sets, with either 100, 50, or 10 individuals marked on each occassion, so that there are 1000, 500, or 100 individuals in total. As in our female nest data, the years in which covariate data were recorded are specified. Thus we do not simulate

missing data at random. For each of these samples, we generate continuous covariate data for five scenarios:

- S1 covariate data were recorded in every year of the study for every individual even if the individual was not captured;
- S2 covariate data were recorded for each individual only if the individual was captured;
- S3 covariate data were recorded only in 6 specific years of the capture-recapture study (years 1, 2, 4, 6, 8 and 10) for those individuals that were captured;
- S4 covariate data were recorded only in 4 specific years of the capture-recapture study (years 2, 4, 6 and 8) for those individuals that were captured;
- S5 covariate data were recorded only in 2 specific years or the capture-recapture study (years 2 and 8) for those individuals that were captured.

We start by simulating data for the first scenario, when there is no missing covariate information. For comparison with later results, we retain these data and remove data as necessary to obtain scenarios S2-S5. In scenario S2 we remove the covariate data for years in which an individual was not captured. However, no capture-recapture histories are removed, as every individual has covariate data recorded for at least one year, the year in which they were captured. To obtain scenarios S3-S5, when the covariate data are recorded only in specific years and if the individuals are recaptured, we remove the presence data for the years with no covariate data records from scenario S2. For example, to obtain S3, we take the covariate data in S2, and remove all the covariate information for the years 3, 5, 7, and 9. In scenarios S3-S5, the number of individuals considered differs from the initial total number of individuals marked (given in S1 and S2). This is because if a particular individual was not observed during at least one of the specified years in which the covariate data were recorded, the capture-recapture history for this individual is removed, as no covariate data for this individual were recorded. For the individuals for which covariate data were recorded in at least one of the selected years, we use the same deterministic imputation method described in Section 3.2.2, for the remaining years in which covariate data were missing.

Table 3.10 shows the simulation results for 11-year long capture-recapture studies, when 100 (rows 3-8), 50 (rows 9-13) or 10 (rows 14-18) were marked each year of the study, giving a total sample size of 1000, 500 or 100 individuals, respectively. We do not use a sample size of five individuals marked per year of capture-recapture study, as in the cases in which we have many years of covariate data missing, we would run out of data.

Table 3.10 shows that as the amount of missing data increases, the parameter estimation accuracy decreases. This is particularly true for the case in which the continuous covariate was recorded only in two years. The MSE error increases as sample size decreases or as the amount of missing data increases.

With our imputation method the more missing covariate data we have, the more capture-recapture histories we remove. Usually those individuals that are removed are those with less captures. Thus removing these individuals would result in an increased survival probability. In Table 3.10 we observe that as the number of individuals decreases for each of the three sample sizes, the parameter estimates for survival, particularly the intercept, increase. For scenarios S2-S5 there is bias in the estimation of the intercept.

Table 3.10 Simulation study A for 11-year long capture-recapture studies with survival as a function of a continuous covariate and capture probability fixed at 0.60. The first row specifies the model parameters and the values used to generate the simulated data. The first column (Scenario) specifies the missing data scenario S1-S5. The second column specifies the mean number of individuals marked throughout the study. The remaining columns contain the average parameter estimate (par est) and the average standard error, given in parentheses, along with the mean square error (MSE).

		ϕ				p	
Scenario	no.	$\alpha = 1.20$		$\beta_{presence} = 0.25$		$p = 0.60$	
	ind.	par est	MSE	par est	MSE	par est	MSE
S1	1000	1.20(0.05)	0.0027	0.25(0.05)	0.0022	0.60(0.01)	0.0002
S2	1000	1.20(0.05)	0.0027	0.25(0.05)	0.0022	0.60(0.01)	0.0002
S2	821	1.37(0.06)	0.0303	0.23(0.05)	0.0028	0.63(0.01)	0.0012
S4	621	1.38(0.06)	0.0367	0.23(0.06)	0.0034	0.64(0.01)	0.0016
S5	394	1.63(0.08)	0.1946	0.24(0.08)	0.0050	0.66(0.02)	0.0035
S1	500	1.19(0.07)	0.0043	0.25(0.07)	0.0060	0.60(0.02)	0.0003
S2	500	1.19(0.07)	0.0043	0.24(0.07)	0.0060	0.60(0.02)	0.0003
S3	412	1.35(0.08)	0.0278	0.23(0.08)	0.0064	0.63(0.02)	0.0014
S4	312	1.38(0.08)	0.0363	0.23(0.08)	0.0067	0.64(0.02)	0.0018
S5	198	1.64(0.11)	0.2019	0.26(0.11)	0.0103	0.65(0.02)	0.0035
S1	100	1.20(0.16)	0.0214	0.26(0.16)	0.0264	0.59(0.04)	0.0020
S2	100	1.20(0.16)	0.0214	0.26(0.16)	0.0263	0.59(0.04)	0.0021
S3	83	1.37(0.18)	0.0564	0.26(0.18)	0.0314	0.62(0.04)	0.0025
S4	62	1.38(0.19)	0.0603	0.24(0.19)	0.0301	0.64(0.05)	0.0032
S5	39	1.63(0.26)	0.2327	0.30(0.26)	0.0602	0.65(0.05)	0.0056

Simulation Study B

We create four simulation sets, with either 50, 10 or five individuals marked on each occasion, so that there are 500, 100 or 50 individuals in total. For each of these samples, we generate continuous covariate data for four scenarios:

S1 covariate data were recorded in every year of the study for every individual even if the individual was not captured;

S2 covariate data were recorded for each individual only if the individual was captured;

S3 15 % of the covariate data were not recorded and covariate data could only be recorded if an individual was observed;

S4 30 % of the covariate data were not recorded and covariate data could only be recorded if an individual was observed.

We compare two different imputation methods:

a For each individual missing covariates are imputed using the average of the covariate data available for this individual.

b For each individual missing covariates are imputed using a normal distribution with mean equal to the average of the covariate data available for the individual and variance equal to 1. Note that for many individuals only one covariate value is available for the capture history. If we were to use the standard deviation of the covariate data available for each individual in these cases, the standard deviation would be equal to 0. For this reason, we set the variance equal to 1, which turns out to be the same variance that we used for the simulated data. The reader should note, that we choose a value of 1 because a higher value would just add more noise to the imputed data and as a result the parameter estimates and the MSE would worsen.

Table 3.11 shows the simulation results for 11-year long capture-recapture studies with survival as a function of a continuous covariate and capture probability fixed at 0.60. In this simulation result we compare two imputation methods: method a, in which the missing covariate data are imputed based on the mean individual covariate values available and method b, in which each missing covariate value is imputed using a normal distribution. In Table 3.11 we can see that imputation method a (the one implemented for our data in this chapter) performs similar in terms of bias to the imputation method b. However, imputation method a results in lower MSEs for all three parameter estimates at all three sample sizes. This is likely due to the extra variation introduced in method b. Moreover, unlike in simulation study A, where capture histories were removed, we observe no systematic positive bias resulting from the removal of those individuals with fewer captures.

Table 3.11 Comparison between imputation methods: Simulation study B for 11-year long capture-recapture studies with survival as a function of a continuous covariate and capture probability fixed at 0.60. The first row specifies the model parameters and the values used to generate the simulated data. The first column (Scenario) specifies the missing data scenario, S1-S4, and the imputation method a or b. The second column specifies the mean number of individuals marked throughout the study. The remaining columns contain the average parameter estimate (par est) and the average standard error, given in parentheses, along with the mean square error (MSE).

		ϕ				p	
Scenario	no.	$\alpha = 1.20$		$\beta_{presence} = 0.25$		$p = 0.60$	
	ind.	par est	MSE	par est	MSE	par est	MSE
S1	50	1.17(0.23)	0.0502	0.23(0.23)	0.0485	0.61(0.06)	0.0036
S2a	50	1.17(0.23)	0.0502	0.22(0.23)	0.0489	0.61(0.06)	0.0036
S2b	50	1.18(0.25)	0.0887	0.18(0.24)	0.1163	0.61(0.06)	0.0044
S3a	50	1.17(0.23)	0.0501	0.23(0.23)	0.0472	0.61(0.06)	0.0036
S3b	50	1.19(0.26)	0.0898	0.18(0.25)	0.0946	0.61(0.06)	0.0044
S4a	50	1.17(0.23)	0.0502	0.22(0.23)	0.0472	0.61(0.06)	0.0036
S4b	50	1.19(0.25)	0.2229	0.18(0.25)	0.7100	0.61(0.06)	0.0044
S1	100	1.20(0.16)	0.0331	0.24(0.16)	0.0304	0.60(0.04)	0.0013
S2a	100	1.19(0.16)	0.0331	0.24(0.16)	0.0295	0.60(0.04)	0.0013
S2b	100	1.24(0.18)	0.0609	0.20(0.12)	0.1123	0.60(0.04)	0.0018
S3a	100	1.19(0.16)	0.0331	0.25(0.16)	0.0296	0.60(0.04)	0.0013
S3b	100	1.25(0.18)	0.0579	0.19(0.12)	0.0932	0.60(0.04)	0.0018
S4a	100	1.19(0.18)	0.0331	0.24(0.17)	0.0297	0.60(0.04)	0.0013
S4b	100	1.24(0.17)	0.0587	0.19(0.12)	0.1004	0.60(0.04)	0.0018
S1	500	1.19(0.07)	0.0045	0.25(0.07)	0.0045	0.60(0.02)	0.0003
S2a	500	1.19(0.07)	0.0046	0.24(0.07)	0.0043	0.60(0.02)	0.0003
S2b	500	1.22(0.08)	0.0183	0.24(0.07)	0.0067	0.59(0.02)	0.0007
S3a	500	1.19(0.07)	0.0046	0.24(0.07)	0.0044	0.60(0.02)	0.0003
S3b	500	1.22(0.08)	0.0185	0.24(0.07)	0.0083	0.60(0.02)	0.0007
S4a	500	1.19(0.07)	0.0046	0.24(0.07)	0.0043	0.60(0.02)	0.0003
S4b	500	1.22(0.08)	0.0186	0.25(0.07)	0.098	0.60(0.02)	0.0007

3.5 Results

In this section we present the results obtained from fitting the capture-recapture models described above. In Section 3.5.1 we present the results obtained when fitting the CJS models to all the individuals captured, we use covariates to study the effects of site and sex in survival. In Section 3.5.2 we use the subsample of the data for which both capture-recapture and presence information was registered for female birds.

3.5.1 Capture-Recapture Data

We analyse data for the 950 individuals that comprise the capture-recapture data. We fit all possible models, which include all combinations in terms of site and sex covariates in the survival parameter ϕ and the capture parameter p.

Table 3.12 shows a comparison of all the models fitted. The best models have a site dependency in both parameters. Sex appears to be an important covariate as well for both the survival and the capture probabilities.

Table 3.13 shows the parameter estimates for the three best models in terms of AIC. For the best model, both survival and capture probabilities depend on the site covariate. Additionally, for this model the capture probability depends on the sex covariate. The corresponding survival probabilities are estimated as 0.74 (0.09) for Hornsund and 0.43 (0.11) for Magdalenefjorden. The capture probabilities are estimated as 0.30 (0.11) for females in Hornsund and 0.36(0.11) for males in Hornsund; 0.65(0.27) for females in Magdalenefjorden and 0.71 (0.27) for males in the same site. In the second best model, both survival and capture probabilities depend on sex and site covariates. Survival probabilities are estimated as 0.74 (0.09) for females in Hornsund and 0.75(0.09) for males in Hornsund; 0.42 (0.11) for females in Magdalenefjorden and 0.43(0.11) for males in the same site. Capture probabilies are estimated as 0.30(0.11) and 0.36(0.11) for females and males in Hornsund respectively; 0.66(0.27) for females in Magdalenefjorden and 0.71(0.27) in the same site. In contrast, in the third best model both survival and capture probabilities only depend on the site covariate. For this model the corresponding survival probabilities are estimated as 0.74 (0.09) in Hornsund and 0.43(0.11) in Magdalenefjorden. Capture probabilities are estimated at 0.33(0.07) for Hornsund and 0.69(0.24) for Magdalenefjorden.

These results show that for the analysed data on the little auk the probability of survival is much higher in Hornsund than in Magdalenefjorden, however the capture probability is much lower in Hornsund. Additionally, capture probabilities are slightly higher for males than females across both sites. These results are in line with the ecologist's expectations. The higher survival in Hornsund is justified by the overall better foraging conditions in this

Table 3.12 Fitted models compared in terms of AIC for all data.

Model	No. parameters	Δ AIC
$\phi_{site}, p_{sex,site}$	5	0.00
$\phi_{sex,site}, p_{sex,site}$	6	1.70
ϕ_{site}, p_{site}	4	3.13
$\phi_{sex,site}, p_{site}$	5	4.73
$\phi_{site}, p_{sex,site,sex*site}$	6	5.21
$\phi_{sex,site,sex*site}, p_{sex,site}$	7	6.24
$\phi_{sex,site,sex*site}, p_{site}$	6	6.58
$\phi_{sex,site,sex*site}, p_{sex,site,sex,site}$	8	6.99
ϕ_{site}, p_{sex}	4	36.56
$\phi_{sex,site}, p_{sex}$	5	38.43
$\phi_{sex,site}, p$	4	40.80
ϕ_{site}, p	3	40.99
$\phi_{sex,site,sex*site}, p$	5	41.17
$\phi_{sex,site,sex*site}, p_{sex}$	6	42.31
$\phi_{sex,site}, p_{sex,site,sex*site}$	7	66.70
$\phi_{sex}, p_{sex,site,sex*site}$	6	88.50
ϕ, p_{sex}	3	90.13
$\phi, p_{sex,site}$	4	91.84
$\phi, p_{sex,site,sex*site}$	5	90.88
ϕ_{sex}, p_{sex}	4	92.13
$\phi_{sex}, p_{sex,site}$	5	93.84
ϕ, p	2	94.15
ϕ_{sex}, p	3	94.70
ϕ, p_{site}	3	95.74
ϕ_{sex}, p_{site}	4	96.32

site. Similarly, the interannual variation in the fieldwork efforts in Hornsund may result in lower capture probabilities.

Table 3.13 Parameter estimates with standard errors in parentheses obtained by the top three models in terms of AIC value, as identified in Table 3.12.

$\phi_{sex,site}$			$p_{sex,site}$		
α	β_{sex}	β_{site}	α	β_{sex}	β_{site}
1.05(0.07)	-	-1.35(0.14)	-0.86(0.10)	0.29(0.13)	1.49(0.17)
1.01(0.09)	0.07(0.12)	-1.35(0.13)	-0.84(0.11)	0.25(0.15)	1.49(0.27)
1.04(0.07)	-	-1.35(0.14)	-0.70(0.08)	-	1.52(0.27)

3.5.2 Female Nest Data

We fit all the possible combinations in which the survival probability depends on presence, site or presence, and site covariates, and the capture probability depends on site or is constant. We also fit the constant model, in which the survival and the capture probability do not have any covariates.

Table 3.14 shows the best models in terms of AIC. Table 3.14 shows that all top models include site as a covariate in the survival probability. Note that in Table 3.14 we have not included any models that contained site dependencies for the capture probability, as these models presented signs of near-parameter redundancy, having very large standard errors and one or more zero standardised eigenvalue. The reason for this is that for Magdalenefjorden the capture histories do not contain any zeroes occurring between the first capture and last recapture, which means that the capture probability parameter cannot be estimated for this site.

Table 3.15 shows the parameter estimates for the two top models in terms of AIC for the female nest data of the capture-recapture data. For the first model the survival probability is dependent on the site covariate and the capture probability is constant. The corresponding survival probabilities are estimated as 0.92 (0.42) for female birds in Hornsund and 0.60 (0.25) for females in Magdalenefjorden. The capture probability is estimated as 0.61 (0.05). These results agree with those from fitting the largest capture-recapture data set with 950 individuals in the fact that the survival probability is higher in Hornsund than in Magdalenefjorden. However, the survival probabilities and the standard errors are much higher than those in the capture-recapture model for the capture-recapture sample in which site is also used as a covariate. Thus, caution should be taken if making ecological conclusions based on these results. For the second best model survival probability is dependent on the site and fledge covariates, and the capture probability is constant. The corresponding survival parameters for this model can be seen in Figure 3.2.

Table 3.14 Fitted models compared in terms of AIC for the female data. The subscripts refer to site and presence covariates. The label fledge refers to the number of days that a chick took to fledge; index refers to the index departure data; first0 to the first day the female was not seen and last1 to the last day in which the female was recorded in the nest.

Model	No. pars	Δ AIC
ϕ_{site}, p	3	0.00
$\phi_{site,fledge}, p$	4	0.13
$\phi_{site,index}, p$	4	1.01
$\phi_{site,first0}, p$	4	1.13
$\phi_{site,last1}, p$	4	1.23
ϕ, p	2	19.97
ϕ_{index}, p	3	20.23
ϕ_{last1}, p	3	20.26
ϕ_{fledge}, p	3	20.49
ϕ_{first0}, p	3	20.63

Table 3.15 Parameter estimates with standard errors in parentheses obtained by the top two models in terms of AIC value, as identified in Table 3.14.

α	β_{site}	β_{fledge}	p
2.39(0.43)	-1.98(0.49)	-	0.60(0.05)
2.40(0.44)	-2.04 (0.50)	0.32(0.24)	0.60(0.05)

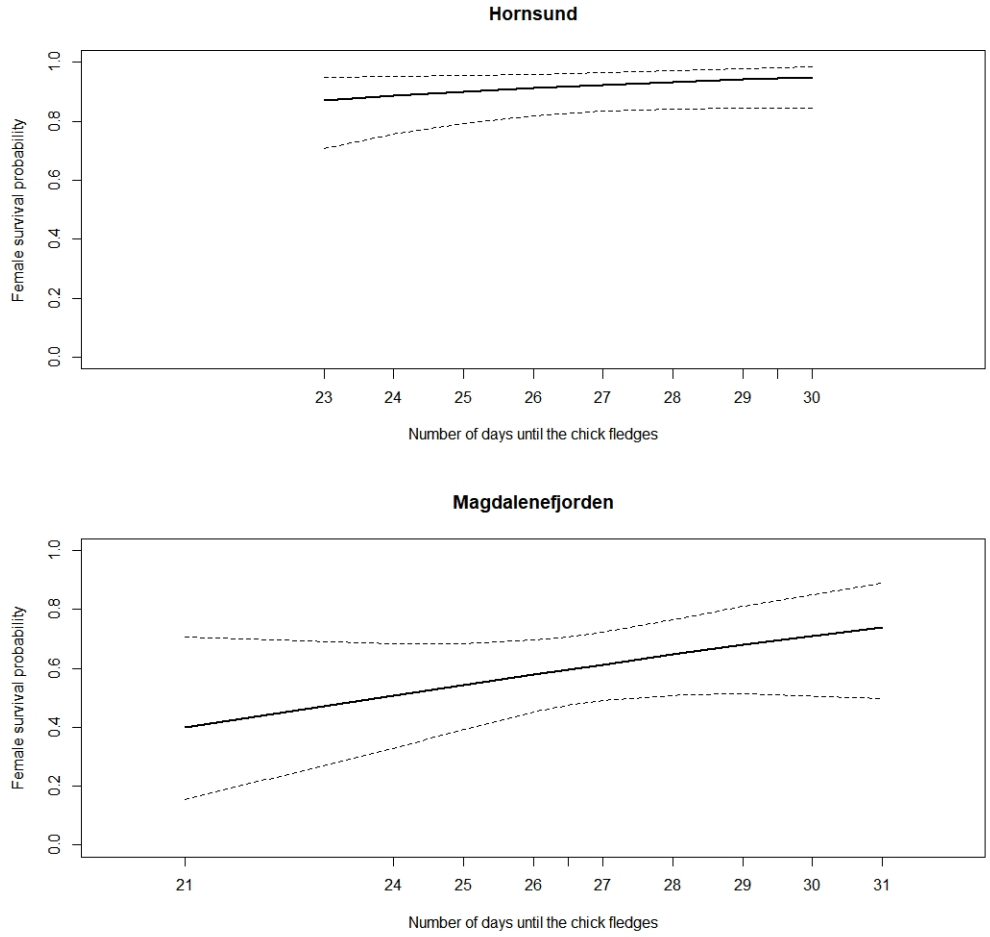

Fig. 3.2 Estimated survival probability with fledged chick as a covariate for each site. The dashed lines represent the 95 % confidence interval.

3.6 Discussion

In this chapter we have analysed capture-recapture data in the presence of categorical and continuous covariates for the little auk. This species is known for the female parent leaving the brood earlier than its male counterpart. The aim of this study was to examine if the survival of the little auk was affected by its sex and/or by the site in which it breeds. Additionally we were interested in understanding if the length of stay of the female birds in the nest during breeding affects their survival.

To answer these questions we analysed two capture-recapture data sets for birds breeding in two sites with different environmental conditions. The first capture-recapture data set, which we refer to as the capture-recapture data set, contains 950 individuals for which

information about their sex and the site in which they were breeding was available. This data set was used to answer questions about the effects of sex and site on survival. The second data set, which we refer to as the female nest data, contains 56 female birds for which, in addition to site (and sex), information was available on the length of stay while breeding.

Extensions to the Cormack-Jolly-Seber model were used to analyse the capture-recapture data by adding covariates through the use of logistic regression. We add two types of covariates, categorical (sex, site), and continuous covariates (female presence data). For the former model, adding covariates is straightforward as the covariates are constant throughout all the years of study and are known regardless of encounter. For the latter, challenges regarding the presence of missing values in the years in which the information was not observed arise.

To validate our models we performed a simulation study, and we found that the models perform better when used to analyse large data sets. Moreover, results also improve when the survival and capture probabilities are higher. This is true, specially in the cases in which several dependencies are added to either one or both parameters. Additionally, we perform a simulation study to examine the accuracy of our deterministic imputation method. We find that as sample size decreases, the MSE increases, and that survival parameters get overestimated in the presence of abundant missing data. This bias is particularly noticeable in the last two rows of Table 3.10, in which the number of individuals are 62 and 39.

From analysing the capture-recapture data we find that, as expected by the field experts, survival is higher in Hornsund than in Magdalenefjorden, and that the capture probabilities are higher in Magdalenefjorden than in Hornsund. The difference in survival amongst sites might be justified by the difference in environmental conditions between the two sites (Jakubas et al., 2011). Birds breeding in Magdalenefjorden are exposed to less favourable environmental conditions than those breeding in Hornsund, and this could be one of the reasons impacting their survival.

Moreover, no differences in the survival probabilities arise between sexes. Previous studies have shown that the female little auk's body conditions during the chick rearing period are similar to those of males (Wojczulanis-Jakubas et al., 2012, 2014, 2015). This could explain the similarities in survival between both sexes. If the female little auk does not deteriorate from breeding more than its male counterpart does, similar survival for both parents appears to be a reasonable result.

The results from analysing the female nest data set also show differences in survival between sites. Moreover, the models show that survival increases as the length of stay of the mother in the brood increases. However the standard errors for these parameters are large, so caution should be taken when interpreting these results.

Inferences about survival in terms of the sex and site can be made from the capture-recapture data set. In terms of the female length of stay, ecologists are suggesting that a longer stay could be explained by the female's good body conditions. Thus, the better body conditions, the longer they would stay in the brood, and their survival would be higher in the following year. However, to make strong conclusions about female survival and her length of stay in the brood, larger data sets would be needed.

There are now many methods for fitting capture-recapture and more generally mark-recapture-recovery data in the presence of continuous covariates. There are several alternatives which range from imputing data (see for example Little and Rubin, 2002), to data augmentation methods. We refer the reader to Bonner et al. (2010), Langrock and King (2013), and Worthington et al. (2015) where comparisons of existing methods can be found.

Bonner et al. (2010) examine three methods to incorporate time varying, individual covariates of the survival probabilities into the analysis of data from mark-recapture-recovery experiments. These methods are: deterministic imputation by linear interpolation between an individual's first and last capture and by last observation carried forward after the last recapture; the Bayesian imputation approach described in Bonner and Schwarz (2006), and King et al. (2008a); and the trinomial model described in Catchpole et al. (2008).

The simplest method for analysing data with missing covariates is deterministic imputation. This consists of generating and imputing values for the missing covariates based on some deterministic algorithm, and analysing the data as if these values were observed. For several strategies on imputing missing values in longitudinal data we refer the reader to Little and Rubin (2002).

Bonner and Schwarz (2006) and King et al. (2008a) propose a Bayesian approach in which missing values are treated as auxiliary variables. These methods perform well, even if survival and capture probabilities are low, but only if a reasonable model for the covariate is available.

Using a conditional likelihood approach for those covariates observed, the trinomial model results in a simple closed likelihood expression. This process is easy to implement, and computationally fast. However, in this process individuals for which there are missing covariate values are removed (Catchpole et al., 2008). Which means that, when simulation studies have been performed the number of individuals marked in each year of the study was much bigger than the number of individuals marked yearly in our data. For example, in the simulation study of Catchpole et al. (2008) 100 animals were marked in each year of study. Moreover, this model is not recommended when capture probabilities are low (Bonner et al., 2010).

Langrock and King (2013) provide a novel HMM-based approach based on a fine discretisation of the space of covariate values as an alternative method for dealing with missing covariates and through a simulation study they compare results to the trinomial model developed by Catchpole et al. (2008). The simulation study shows that if the modelling of the covariate process is done adequately, and even if there is some degree of misspecification, this approach leads to more precise results than the trinomial method.

Worthington et al. (2015) propose a two-step multiple imputation approach to obtain estimates of the demographic parameters in mark-recapture-recovery studies. In their simulation study they show that this two-step approach performs well when covariate values are always observed (or at least observed once for each individual). However, they warn that if a significant proportion of individuals are observed with no recorded covariate values, demographic estimates could be biased. In their simulation study they generate large capture-recapture samples, with 10 capture-recapture events and 100 individuals marked during each capture occasion, which results in a sample of 900 individuals.

All the methods described in these papers consider missing covariate data at random, and in general the sample sizes used in the simulation studies are large.

To address the problem of missing data in specific years of the capture-recapture study for the female nest data set, we used a deterministic imputing approach. We used a more simplistic approach as the existing data were very limited and the covariate data were not missing at random. However, we believe that for larger data sets with lower proportions of missing data, and if these data were missing at random, the analysis could benefit from using the aforementioned methodologies.

Chapter 4

State-Space Models for Population Census Data

4.1 Introduction

In this chapter we review and implement different model fitting methodologies for discrete state-space models (SSMs). The motivation behind this work is closely related to the development of the spatially-explicit integrated population (SE-IPMs) presented in Chapter 5.

SSMs have been widely used to obtain vital rates, such as survival and productivity, from census data. A popular approach for fitting state-space models for bird census data is the use of Poisson, or binomial-Poisson non-stationary processes, or appropriate approximations to normal processes, (see for example, Besbeas et al., 2002, King et al., 2008b, and Abadi et al., 2010).

Rather than one single nation-wide time-series of counts, spatial census data consist of multiple time-series associated to specific locations. These data can be particularly challenging to model because of the very small counts at some locations. We find that if these discrete non-stationary time processes are used to model census data that include small counts, the Poisson parameter is systematically negatively biased. To show this, we use a single-state state-space model which describes the population dynamics of starlings (*Sturnus vulgaris*), the illustrative species that we use in Chapter 5. The model is described in Section 4.2.

We consider using the Kalman filter (KF) and hidden Markov models (HMMs) to fit the state-space models. The KF is an algorithm allowing exact inference in a linear dynamical system. In the KF, the state space of the latent variables is continuous and all latent and

observed variables have a Gaussian distribution—usually a multivariate Gaussian distribution (Faragher, 2012). The KF has been successfully used to fit the state-space model of integrated population models (IPMs) that contained time-series data with large counts. However, due to the normality assumption required for the implementation of the KF, in the presence of time-series with small counts alternative methods that do not require normal approximations are needed. The KF is described in Section 4.3.

HMMs can be used as an alternative method to the KF to fit the state-space model. HMMs are a type of dependent mixture model that can be used to infer unobservable states (see for example Zucchini et al., 2016). Besbeas and Morgan (2019) show how HMMs can be used to fit state-space models. The HMM method is described in Section 4.4.

As explained in Section 1.2.2, the SSM is parameter redundant. In Section 1.2.2 we described that to solve this issue, Besbeas et al. (2002) combined the SSM with a ring-recovery model into an IPM. Thus, to examine the suitability of the two methods proposed here to fit the SMM, we use an IPM that combines ring-recovery and census data. We describe the two joint likelihoods—one that uses the KF and one that uses HMMs to fit the SSM in Section 4.5.

In Section 4.6.1 we perform a simulation study where we compare the suitability of KF and HMMs to fit SSMs containing census data under different circumstances. We first use IPMs, and find that if the counts in the time-series census data are small, the productivity parameter, ρ, is systematically negatively biased. We review the literature and we find that this systematic underestimation was also shown in Abadi et al. (2010), although this was not reported as larger data sets were used and the bias was small. Moreover, we highlight that Brooks et al. (2004) already pointed out that although the normal approximation of the KF was robust, in the presence of observations below 10, this started to break down.

To understand the reason for this bias, in Section 4.6.2 we perform a second simulation study in which we use a non-stationary Poisson process to fit time-series count data. We find that due to the skewness of the distribution, and to the Markov property, in the presence of small valued time-series data a negative bias appears in the estimation of the Poisson mean.

Additionally, in Section 4.6.4 we provide a third simulation study in which we examine the effect of jointly analysing several census data sets that vary in average count size. We find that the bias issue in the estimation of the productivity parameter ρ is mitigated with the addition of multiple time-series data sets.

4.2 Single-state State-Space Model for Census Data

In this section we describe the single-state SSM used to model starling populations. We assume that breeding starts at age 1, that only breeding birds are censused, that there is no sex information, and that there is no migration.

Suppose N_t is the number of individuals in the population at time t. The number of observed individuals in year t is y_t, the time-invariant, i.e. constant survival probabilities are ϕ_a and ϕ_1 for adult and first-year birds respectively. The parameter ρ represents the mean number of young per individual recruited into the adult population. The state process is given by

$$N_{t+1}|N_t \sim \text{Bin}(N_t, \phi_a) + \text{Pois}(N_t \phi_1 \rho_t). \tag{4.1}$$

We define the observation process to follow a Poisson distribution, with

$$y_t|N_t \sim \text{Pois}(N_t). \tag{4.2}$$

The SSM presented in equations 4.1 and 4.2 is graphically reproduced in Figure 4.1. This SSM has a single-state as starlings are able to breed from their first year of life. Thus, in the underlying population process, the age differences are only accounted for in the survival parameters, ϕ_1 and ϕ_a.

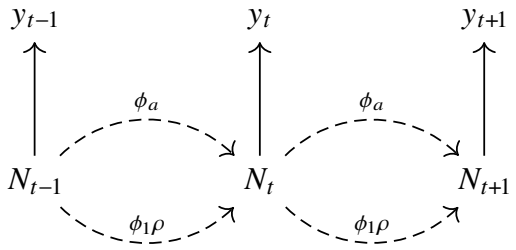

Fig. 4.1 Diagram of the single-state SSM representing the life cycle of the population, and the relationship between the underlying population size N_t and the number of individuals observed at time y, y_t.

4.3 Kalman Filter

The Kalman filter is a recursive algorithm developed by Kalman (1960), permitting the exact inference of the hidden or latent state of a linear dynamic system affected by Gaussian white

noise. To do so, it uses measurements (observations) that are linear functions of the system state but corrupted by additive Gaussian white noise (Grewal and Andrews, 2001).

The KF is widely applied in complex dynamical systems as it provides a means for inferring the missing information from indirect and noisy measurements. In this section, we refer to the original KF formulation (Kalman, 1960) where the measurements occur and the state is estimated at discrete points in time.

4.3.1 General Setting—The Discrete Kalman Filter

We first introduce the KF in a general setting, following Bishop and Welch (2001).

The KF model assumes that the state of a system at a time $t+1$ evolved from the prior state at time t according to the state process,

$$\mathbf{N}_{t+1}|\mathbf{N}_t = \mathbf{G}_t\mathbf{N}_t + \mathbf{B}_t\mathbf{u}_t + \boldsymbol{\epsilon}_t, \tag{4.3}$$

where $\mathbf{N}_t$ is the state vector containing the terms of interest for the system (e.g. the underlying population size) at time t, $\mathbf{G}_t$ is the state transition matrix (matrix containing the demographic parameters, e.g. survival, reproduction rates), $\mathbf{B}_t$ is the control input matrix which applies the effect of each control parameter on the optional control input vector $\mathbf{u}_t$. The vector $\boldsymbol{\epsilon}_t$ contains the process noise terms for each parameter in the state vector. The process noise is assumed to be drawn from a zero mean multivariate normal distribution with covariance matrix $\mathbf{Q}_t$. The control terms are optional, and we do not use them when applying the KF to our models, for this reason, we simplify equation (4.3) to

$$\mathbf{N}_{t+1}|\mathbf{N}_t = \mathbf{G}_t\mathbf{N}_t + \boldsymbol{\epsilon}_t. \tag{4.4}$$

Let us assume that the signal $\mathbf{N}_t$ is not directly measured, but instead we have some measurements given by the linear observation equation,

$$\mathbf{y}_t = \mathbf{Z}_t\mathbf{N}_t + \boldsymbol{\eta}_t, \tag{4.5}$$

where $\mathbf{y}_t$ is a vector containing measurements at time t, $\mathbf{Z}_t$ is the transformation matrix that maps the state vector parameters into the measurement domain, and $\boldsymbol{\eta}_t$ is the vector containing the measurement noise terms for each parameter in the measurement vector. The measurement noise is assumed to be drawn from a zero mean multivariate normal distribution with covariance matrix $\mathbf{H}_t$.

The initial state vector, at time $t = 0$, has a normal distribution with mean $\hat{\boldsymbol{N}}_0 = E(\boldsymbol{N}_0)$ and covariance $\boldsymbol{P}_0 = \text{cov}(\boldsymbol{N}_0)$. The two error terms, $\boldsymbol{\epsilon}_t$ and $\boldsymbol{\eta}_t$ are assumed to be mutually independent from each other and mutually independent of $\boldsymbol{N}_0$.

We can think of the KF as a two step feedback process: 1. the filter estimates the process state at some time; 2. feedback is obtained in the form of (noisy) measurements. Thus, the equations needed to build the KF algorithm can be categorised in two groups: **time update equations**, or prediction equations, and **measurement update equations**, or correction equations. The former take the current state and its error covariance and project them forward in time so that *a priori* estimates for the next time step can be obtained. The latter provides feedback, in the form of noisy measurements, to these "*a priori* estimates" so that improved *a posteriori* estimates can be obtained. This two step process is then iterated.

Time Update Equations

The time update equations are

$$\hat{\boldsymbol{N}}_{t+1}^{-} = \mathbf{G}_t \hat{\boldsymbol{N}}_t, \tag{4.6}$$

$$\hat{\boldsymbol{P}}_{t+1}^{-} = \mathbf{G}_t \boldsymbol{P}_t \mathbf{G}_t' + \mathbf{Q}_t, \tag{4.7}$$

where, $\hat{\boldsymbol{N}}_t$ is the posterior state estimate at time t, $\hat{\boldsymbol{N}}_{t+1}^{-}$ is the prior estimate, i.e. the estimate before the measurement update correction at time $t+1$, and $\hat{\boldsymbol{P}}_{t+1}^{-}$ is the prior error covariance at time $t+1$. We use these prior values in the measurement update equations.

Measurement Update Equations

The measurement update equations are

$$\boldsymbol{K}_t = \boldsymbol{P}_t^{-} \mathbf{Z}_t' (\mathbf{Z}_t \boldsymbol{P}_t^{-} \mathbf{Z}_t' + \boldsymbol{H}_t)^{-1}, \tag{4.8}$$

where $\boldsymbol{K}_t$ is the KF gain at time t.

$$\hat{\boldsymbol{N}}_t = \hat{\boldsymbol{N}}_t^{-} + \boldsymbol{K}_t (\mathbf{y}_t - \mathbf{Z}_t \hat{\boldsymbol{N}}_t^{-}) \tag{4.9}$$

$$\boldsymbol{P}_t = (\boldsymbol{I} - \boldsymbol{K}_t \mathbf{Z}_t) \boldsymbol{P}_t^{-}, \tag{4.10}$$

In the measurement update, the first step is to compute the KF gain, $\boldsymbol{K}_t$, equation (4.8). The next step is to measure $\mathbf{y}_t$ so that we can obtain an *a posteriori* state estimate, $\hat{\boldsymbol{N}}_t$,

equation (4.9). Finally, in the last step we obtain an *a posteriori* error covariance estimate, equation (4.10).

Figure 4.2 shows a graphical representation of the steps of the KF algorithm.

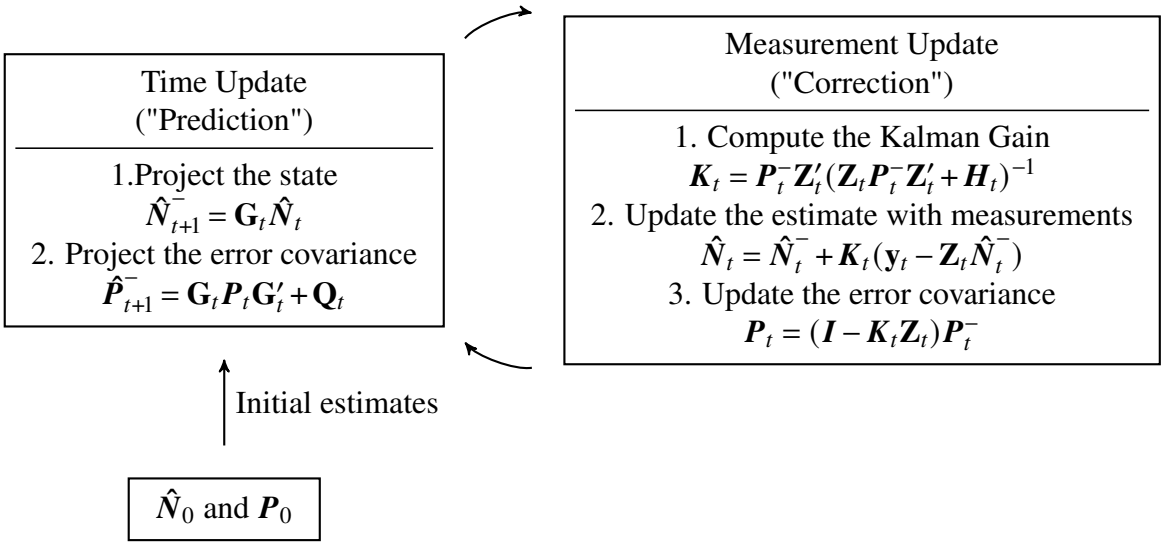

Fig. 4.2 Graphical representation of the KF algorithm.

The log-likelihood function for the state-space model can be written as

$$\log\{L_{KF}(\Psi)\} = C - \frac{1}{2}\sum_{t=1}^{T}[\log|(\mathbf{Z}_t P_t^{-} \mathbf{Z}_t')| + (\mathbf{y}_t - \mathbf{Z}_t \hat{N}_t^{-})^T (\mathbf{Z}_t P_t^{-} \mathbf{Z}_t')^{-1} (\mathbf{y}_t - \mathbf{Z}_t \hat{N}_t^{-})], \quad (4.11)$$

where C is a constant and Ψ represents the unknown parameters (see for example Besbeas and Morgan, 2012).

For more details on the computational and probabilistic origins of the filter, as well as for information on how to apply the KF to non-linear systems, we refer the reader to Chapter 4 of Bishop and Welch (2001).

4.3.2 Application of the Kalman Filter to the Census Data

We follow Besbeas and Morgan (2012) and provide the normal approximations required to apply the KF to the SSM presented in Section 4.2. The expectation and the variance of N_t is just the sum of the expectations and the variances respectively of the binomial and Poisson distributions. The state process is given by the normal approximation,

$$N_{t+1}|N_t = (\phi_a + \phi_1 \rho) N_t + \epsilon_t, \quad (4.12)$$

where $\epsilon_t \sim \mathcal{N}(0, \sigma^2_{\epsilon_t})$, and $\sigma^2_{\epsilon_t} = [\phi_a(1-\phi_a) + \phi_1\rho]N_{t-1}$, the sum of the respective variances of the binomial and Poisson distributions.

The observation equation is given by

$$y_t|N_t = N_t + \eta_t, \tag{4.13}$$

where $\eta_t \sim \mathcal{N}(0, \sigma^2_\eta)$ for all t.

The reader should note that the observation equation (4.13) is not the strict analogue of equation 4.2. If it were, then the mean and the variance of the normal distribution would be the same, as in equation 4.2 the observation process follows a Poisson distribution. Besbeas and Morgan (2019) described the form of the observation equation for the KF that would equate to that in equation 4.2. In this $y_t|N_t \approx \mathcal{N}(\hat{N}_t, \hat{N}_t^-)$, where $\hat{N}_t^-$ is the one-step-ahead prediction from the KF. However, traditionally in many studies σ^2_η has been estimated. Using simulation, for a stable population we compare both approaches for three different population sizes in Section C.1. We find no differences in the parameter estimate results obtained when using either approach. In this thesis we estimate σ^2_η.

There are several methods for initialising the KF, such as the approximate diffuse initialisation (AD). For this particular method, arbitrary decisions on the starting parameters that determine the starting variance-covariance matrix, or subjective criteria on the number of initial terms in the time series to initialise the KF are needed. The stable age initialisation (SA) method proposed in Besbeas and Morgan (2012) and Besbeas et al. (2009) incorporates information from the transition Leslie matrix. Then initialisation of the KF algorithm is based on the asymptotic growth rate of the population. We implement this initialisation method in our analyses.

We refer to the KF's likelihood as

$$L_{KF}(\phi_1, \phi_a, \rho, \sigma_\eta),$$

and the log-likelihood can be maximised following equation (4.11).

4.4 Hidden Markov Models

HMMs are probabilistic models in which it is assumed that the distribution that generates an observation depends on the state of a latent underlying and unobserved Markov process (Zucchini et al., 2016).

In a typical Markov model, the system can be directly observed, thus the only parameters in the model are the transition probabilities between states. However, in a hidden Markov

model, the states are not directly observed—instead some variables that are influenced by the states are observed.

In this section we provide a general setting to fitting one dimensional state-space models for discrete time-series data using HMMs.

4.4.1 General Setting—The Discrete Hidden Markov Model

We first introduce HMMs in a general setting in which the observed values are discrete, following Zucchini et al. (2016).

A HMM consists of two parts: an unobserved parameter process $\{C_t : t = 1, 2, \dots\}$, and a state-dependent process $\{Y_t : t = 1, 2, \dots\}$. The unobserved (latent) process satisfies the Markov property, given in equation (4.14), and the state-dependent process, given in equation (4.15), is conditional on the current state of C_t. Thus, the observation Y_t does not depend on previous observations Y_{t-1}. A HMM is a particular dependent mixture with the following form,

$$\Pr(C_t|\mathbf{C}^{(t-1)}) = \Pr(C_t|C_{t-1}), \quad t = 2, 3 \dots \tag{4.14}$$

$$\Pr(Y_t|\mathbf{Y}^{(t-1)}, \mathbf{C}^{(t)}) = \Pr(Y_t|C_t), \quad t \in \mathbb{N}, \tag{4.15}$$

where $\mathbf{C}^{(t)}$, represents the underlying latent process, and $\mathbf{Y}^{(t)}$ represents the observation from time 1 to time t.

If the Markov chain is in state i at time t, the probability mass function of Y_t conditional on state i is

$$p_i(y) = \Pr(Y_t = y|C_t = i),$$

for $i = 1, 2 \dots, m$, where m is the number of states of the Markov chain.

The unconditional probability mass function of Y_t is

$$\Pr(Y_t = y) = \sum_{i=1}^{m} \Pr(C_t = i) \Pr(Y_t = y|C_t = i) = \sum_{i=1}^{m} u_i(t) p_i(y), \tag{4.16}$$

where, $u_i(t) = \Pr(C_t = i)$ for $i = 1, \dots, T$.

We can rewrite this probability in matrix form

$$\Pr(Y_t = y) = (u_1(t), \ldots, u_m(t)) \begin{pmatrix} p_1(y) & & 0 \\ & \ddots & \\ 0 & & p_m(y) \end{pmatrix} \begin{pmatrix} 1 \\ \vdots \\ 1 \end{pmatrix} = \mathbf{u}(t)\mathbf{P}(y)1^\top,$$

where $\mathbf{P}$ is the diagonal matrix with ith diagonal element $p_i(x)$, $x^\top$ represents the transpose of x, and where 1 is a vector of ones.

The transition between states is represented by the square matrix $\mathbf{\Gamma}$, which has row sums equal to 1. The transition probabilities are denoted by

$$\gamma_{i,j}(t) = \Pr(C_{t+1} = j | C_t = i),$$

and thus,

$$\mathbf{\Gamma} = \begin{pmatrix} \gamma_{11} & \cdots & \gamma_{1m} \\ \vdots & \ddots & \vdots \\ \gamma_{m1} & \cdots & \gamma_{mm} \end{pmatrix}.$$

Zucchini et al. (2016) provide the general likelihood expression for an observation sequence $y_1, y_2, \ldots, y_T$ generated by a HMM,

$$\begin{aligned} L_{HMM_T} &= \boldsymbol{\delta}\mathbf{P}(y_1)\mathbf{\Gamma}\mathbf{P}(y_2)\ldots\mathbf{\Gamma}\mathbf{P}(y_T)1^\top \\ &= \boldsymbol{\delta}\mathbf{P}(y_1)\prod_{i=2}^{n}\mathbf{\Gamma}\mathbf{P}(y_i)1^\top. \end{aligned} \tag{4.17}$$

where $\boldsymbol{\delta}$ is a vector of size m that represents the initial distribution (that for C_1) for the Markov chain.

We could calculate the likelihood recursively, starting at

$$\boldsymbol{\alpha}_1 = \boldsymbol{\delta}\mathbf{P}(y_1),$$

then continuing with

$$\boldsymbol{\alpha}_t = \boldsymbol{\alpha}_{t-1}\mathbf{\Gamma}\mathbf{P}(y_t), \text{ for } i = 2, 3, \ldots, T.$$

Then

$$L_{HMM} = \boldsymbol{\alpha}_{\boldsymbol{T}}1^\top.$$

However, $\boldsymbol{\alpha}_t$ becomes progressively smaller as t increases, since $\boldsymbol{\alpha}_t$ is the product of discrete probabilities. As a result, the likelihood approaches 0 exponentially fast with

probability 1. We refer to this event as underflow. Zucchini et al. (2016) provide a scaling mechanism to solve the underflow issue. We give an overview of the solution below, further details can be found in Chapter 3 of Zucchini et al. (2016). Let $\boldsymbol{S}_t$ be the scaling vector for $t = 0,1,\ldots,T$,

$$\boldsymbol{S}_t = \boldsymbol{\alpha}_t / w_t,$$

with

$$w_t = \sum_i \alpha_t(i) = \boldsymbol{\alpha}_t 1^\top.$$

Thus, if $w_0 = \boldsymbol{\alpha}_0 1^\top = \boldsymbol{\delta} 1^\top = 1$, and $\boldsymbol{S}_0 = \boldsymbol{\delta}$,

$$\begin{aligned} w_t \boldsymbol{S}_t &= w_{t-1} \boldsymbol{S}_{t-1} \boldsymbol{\Gamma} \mathbf{P}(y_t) \\ L_{HMM} = \boldsymbol{\alpha}_T 1^\top &= w_T \left(\boldsymbol{S}_T 1^\top \right) = w_T. \end{aligned} \tag{4.18}$$

Thus, $L_{HMM} = w_T = \prod_{t=1}^{T} (w_t / w_{t-1})$, and $w_t = w_{t-1} \left(\boldsymbol{S}_{t-1} \boldsymbol{\Gamma} \mathbf{P}(y_t) 1^\top \right)$ follows from equation (4.18). Following this, the log-likelihood is given by,

$$\log\{L_{HMM}(\boldsymbol{\Psi})\} = \sum_{t=1}^{T} \log\left(w_t / w_{t-1}\right) = \sum_{t=1}^{T} \log\left(\boldsymbol{S}_{t-1} \boldsymbol{\Gamma} \mathbf{P}(y_t) 1^\top \right), \tag{4.19}$$

where $\boldsymbol{\Psi}$ is the vector of unknown parameters that we wish to estimate.

4.4.2 Application of the Hidden Markov Model to the Census Data

In Section 1.2.3 we described that Besbeas and Morgan (2019) developed the methodology to use HMMs to fit discrete SSMs within the IPM context. We apply the methods described in 1.2.3 to implement the HMMs describe in 4.4.1.

The hidden Markov model for the state-space model described in Section 4.2, has a state process given by

$$N_{t+1} | N_t \sim \text{Bin}(N_t, \phi_a) + \text{Pois}(\phi_1 \rho N_t),$$

and an observation process given by,

$$Y_t \sim \text{Pois}(N_t).$$

The random variable N_{t+1} is given by a binomial-Poisson convolution.

$$X_1 \sim \text{Bin}(N_t, \phi_a), \quad N_t \geqslant 0, \quad 0 < \phi_a < 1,$$

independently of N_t,

$$X_2 \sim \text{Pois}(\phi_1 \rho N_t), \quad \phi_1 \rho \geqslant 0.$$

The probability mass function of $N_{t+1}|N_t$ is given by

$$\Pr(N_{t+1} = z|N_t) = \sum_{k=0}^{min(N_t,z)} \Pr(X_1 = k) \times \Pr(X_2 = z-k) = \tag{4.20}$$

$$= \sum_{k=0}^{min(N_t,z)} \binom{N_t}{k} \phi_a^k (1-\phi_a)^{(N_t-k)} \times \frac{e^{-\phi_1 \rho N_t} (\phi_1 \rho N_t)^{(z-k)}}{(z-k)!}. \tag{4.21}$$

Let N be a vector of length $m+1$ describing the possible values of the transition equation, i.e., $N = (0,1,\ldots,m)$ represents the possible underlying number of individuals in the population. We consider every single individual in the population, from 0 individuals to a previously set upper bound $m = N_{max}$, where N_{max} is the highest considered number of individuals in the population (for computational reasons—in the theoretical model we do not require an upper bound). We specify $N_{max} = Y_{max} + (Y_{max} - Y_{min})$, where Y_{max} and Y_{min} are the highest and lowest number of individuals observed respectively in the observation vector. For modelling purposes we shall assume that $N_t \leq N_{max}$ for every t. In such a way, we consider every "underlying" possible number of individuals to be a state of the HHM.

Let Γ be the $(m+1) \times (m+1)$ transition matrix which represents the probabilities of the state process of the SSM, with $\Gamma_{i,j} = P(N_j|N_i)$ and each entry is the result of the binomial-Poisson convolution given in equation (4.20). Similarly, the matrix form of the transition matrix is given by,

$$\mathbf{\Gamma} = \begin{pmatrix} P(N_0|N_0) & \cdots & P(N_{max}|N_0) \\ \vdots & \ddots & \vdots \\ P(N_0|N_{max}) & \cdots & P(N_{max}|N_{max}) \end{pmatrix}.$$

The observation matrix $\Pr(Y_t = y)$ is the $(m+1)$ diagonal matrix with entry (i,i) given by $P(Y_t|N_i) \sim \text{Pois}(N_i)$, with matrix form given by,

$$\Pr(Y_t = y) = \begin{pmatrix} P(Y_t|N_0) & & 0 \\ & \ddots & \\ 0 & & P(Y_t|N_{max}) \end{pmatrix}$$

Finally, δ is a vector of length $(m+1)$ representing the initial distribution of the SSM with $\delta_i = P(Y = N_i) \sim \text{Pois}(\mu)$, where μ is a parameter to be estimated which represents the mean of the initial state.

We refer to the HMM's likelihood as

$$L_{HMM}(\phi_1, \phi_a, \rho, \mu),$$

and the log-likelihood can be maximised following equation (4.19).

4.5 Integrated Population Model

As mentioned in Section 1.2.2, the SSM on its own is parameter redundant (see for example Cole and McCrea, 2016). Besbeas *et al.* (2002), approached this issue by fitting this model jointly with a ring-recovery model. In order to compare the suitability of the two different algorithms considered in this thesis—the KF, and HMMs, we will examine the parameter estimates obtained from an IPM in which we combine census and ring-recovery data. We consider two different joint likelihood functions for the IPM: one that uses a KF to fit the census data and one that uses a HMM to fit the state-space model. We refer to them as:

$$L_{IPM,KF} = L_{RR}(\phi_1, \phi_a, \lambda) \times L_{KF}(\rho, \phi_1, \phi_a, \sigma_\eta),$$

$$L_{IPM,HMM} = L_{RR}(\phi_1, \phi_a, \lambda) \times L_{HMM}(\rho, \phi_1, \phi_a, \mu),$$

where L_{RR} is the likelihood function for the ring-recovery model described in equation 2.1, L_{KF} is the likelihood function for the SSM using the KF algorithm described in Section 4.3.2, and L_{HMM} is the likelihood function for the SSM using the HMM algorithm described in Section 4.4.2.

In Section 4.6 we perform a simulation study for the two different IPMs separately and we compare the results.

4.6 Simulation Study

In this section we discuss the suitability of the SSM described in this chapter and implemented in Chapter 5 to model census data sets of different sizes. To do this, in Section 4.6.1 we use the IPMs described in Section 4.5, which fit the SSM using the KF and HMMs and we compare the results. We find that in the presence of small data sets, the estimation of the productivity parameter, ρ, is systematically negatively biased. We explain the source of this bias through the use of a Poisson non-stationary process in Section 4.6.2. In Section 4.6.4 we assess if combining the likelihood functions of several census data sets aids the bias issue.

4.6.1 Performance of the IPM under Different Scenarios

We conduct a simulation study for the IPMs, in which we generate 150 data sets in each simulation. To do so, for the SSM we simulate time-series data from the HMM described in Section 4.4.2 and for the ring-recovery model we simulate data from the standard model described in Section 1.2.1. In each simulation of the ring-recovery model, 1000 birds are ringed in each year of study and for each age category: first-year and adult. We keep all the parameters constant and focus particularly on the estimations of the productivity parameter ρ, as the survival and recovery parameters can be estimated without bias from the ring-recovery data alone. We use the census and ring-recovery data sets simulated to fit two IPMs that differ in the modelling methodology used for the SSM, with one using the KF and the other a HMM.

We investigate the performance of both model fitting methodologies under different scenarios: 1. different population trajectories; 2. different population sizes; 3. different parameter values; 4. different lengths of study. These scenarios are closely related to each other. A stable population is one which does not fluctuate with time, i.e. every year, the number of individuals gained in the population is (on average) equal to the number of individuals lost. In an increasing, or decreasing population, the number of individuals increases or decreases respectively with time. The trajectory of the population is defined as: stable, increasing, or decreasing. To describe the different population sizes, we use the value of N_0, the starting population size, as an indication. Thus, if we have a stable population, in theory the expected value of N_t over time does not change. However, if we had a decreasing or increasing population we would expect to gain or lose individuals every year of study. The parameter values chosen to affect the trajectory of the population might have an impact in the performance of our model, as might the number of years of study, especially when sample sizes are small. Small sample sizes are of particular interest in this thesis as these models are intended for spatial data, which at higher resolutions have smaller counts, as we shall see in Chapter 5.

The trajectory of the population is given by the demographic parameters, ϕ_1, ϕ_a, and ρ, contained in the transition matrix of the state process in the SSM. For our model, as we have only one single-state, the trajectory of the population is given by $\theta = (\phi_a + \phi_1\rho)$. Thus a stable population will have $\theta = 1$, an increasing (decreasing) population will have $\theta > 1$ ($\theta < 1$).

Figures 4.3, 4.4, and Table 4.1 show the simulation results in terms of bias for a stable population, where $\phi_1 = 0.30$, $\phi_a = 0.70$ and $\rho = 1$ for a 10 years simulation study. Figures 4.3, 4.4 and Table 4.1 compare the results obtained for the KF on the left, and the HMM on the right, for several population sizes.

Table 4.1 Median relative bias for an stable population, with $\phi_1 = 0.30$, $\phi_a = 0.70$ and $\rho = 1$, for different population sizes, for 10 years of census and ring-recovery study.

	$\phi_1 = 0.30$		$\phi_a = 0.70$		$\rho = 1.00$	
N_0	KF	HMM	KF	HMM	KF	HMM
5	-	0.0003	-	0.0022	-	-0.1664
10	-0.0042	-0.0042	0.0006	0.0010	-0.1030	-0.0838
20	0.0011	0.0022	0.0026	0.0014	-0.0839	-0.0591
40	0.0020	0.0022	0.0011	0.0013	-0.0407	-0.0290

Figures 4.3 and 4.4 contain boxplots with simulation results for the productivity parameter, ρ, for a stable population. The first row shows a population with $N_0 = 5$, then the following rows show results for simulations in which the starting value of the populations are 10, 20 and 40.

Figure 4.3 shows that the estimate of ρ is systematically negatively biased for both the KF and the HMM when $N_0 \leq 40$. If the population size is on average smaller than 10, the KF fails to work for some of the results generated. For this reason we do not present here a boxplot for the KF when $N_0 = 5$. If the number of counts per year is 40 or bigger, both methods return similar results for all the shared parameters (ρ, ϕ_1, ϕ_a). Table 4.1 shows that the bias in estimating ρ is slightly bigger when fitting the SSM using the KF rather than a HMM.

Figure 4.4 shows the results for the same simulation study as in Figure 4.3 and Table 4.1. However, in Figure 4.4 we plot each estimate of ρ obtained against the sum of the counts of each time-series generated. For example, here, as the population is stable if the starting value of our time-series is 20, i.e. $N_0 = 20$, the sum of the counts after 10 years is expected to be 200. Figure 4.4 shows that if we have a larger initial population size, for example that with $N_0 = 40$, the data simulations are approximately symmetric, in the sense that roughly the same number of time series with the sum of the counts below 400 are generated as with the sum of the total number of counts above 400. As the population size becomes smaller many more data sets are generated below the expected sum of the time series.

Additional results for different parameter values, for populations with different trajectories and for a longer period of study can be found in Appendix C. These results are in line with the results shown here for a 10 year simulation study for a stable population with parameters $\phi_1 = 0.30$, $\phi_a = 0.70$ and $\rho = 1$. Moreover, in Appendix C, we find that in the case in which we consider the population to be decreasing, with $\phi_1 = 0.30$, $\phi_a = 0.70$, and $\rho = 0.90$ the KF stops working when $N_0 = 10$ as well as when $N_0 = 5$ (see Table C.3). This is a reasonable result—if a decreasing population starts initially at size 10, then there is a good chance that it

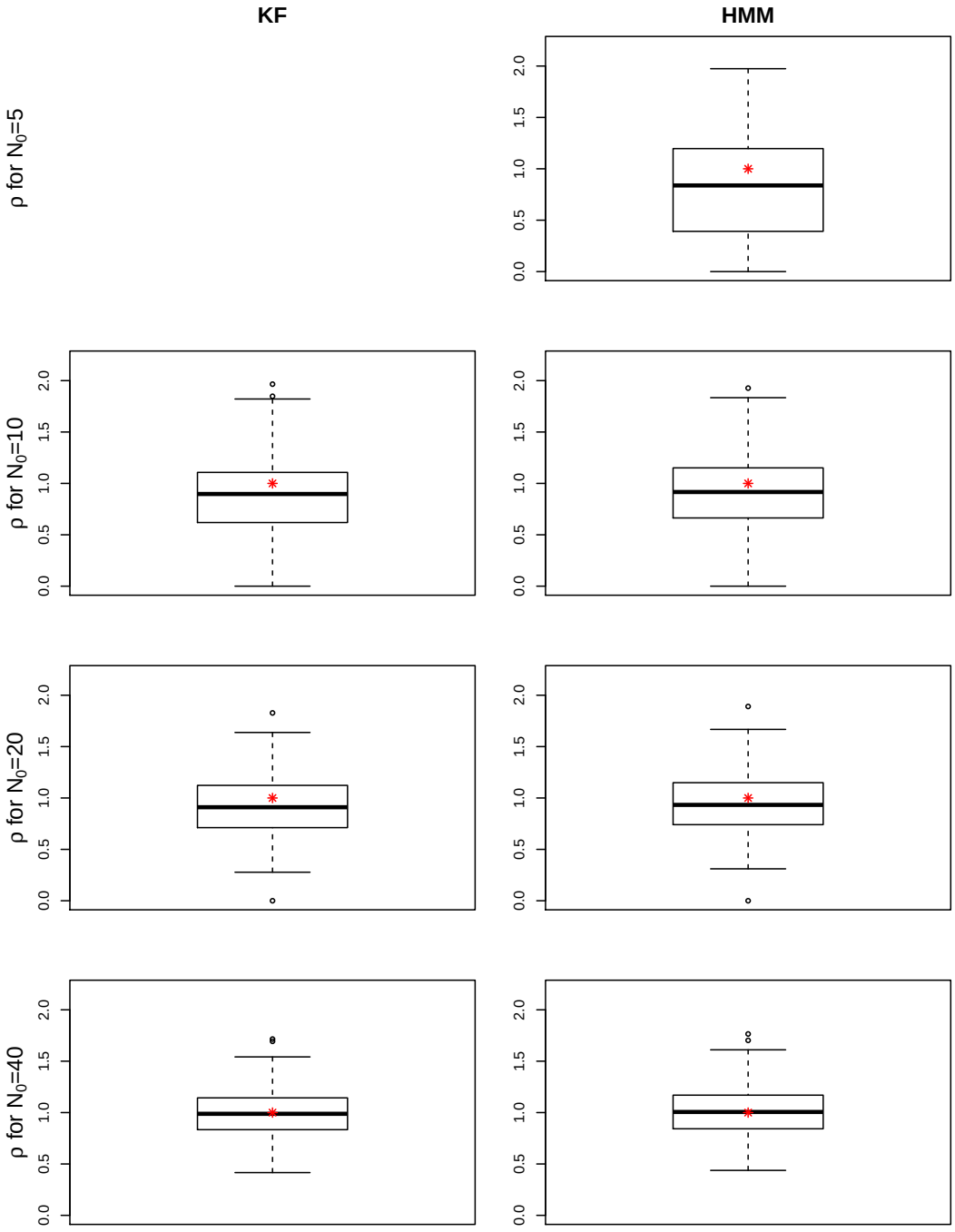

Fig. 4.3 Boxplots containing the simulation results for the productivity parameter, ρ, for 10 years of study for a stable population, with $\phi_1 = 0.30$, $\phi_a = 0.70$ and $\rho = 1$, for different population sizes. The thick middle black line represents the median estimated value, and the red star the real value of ρ.

dies completely after a few years. Additionally, in Appendix C we also show results for a 20 years of simulation study for a stable population with parameter: $\phi_1 = 0.30$, $\phi_a = 0.70$, and $\rho = 1$. Table C.4 shows these results, and here we can see that although the bias decreases slightly in comparison with the 10 years study for the larger data sets, for $N_0 = 5$ both the KF and the HMM stop working, and for $N_0 = 10$ only the KF stops working. If we generate data for a stable population with an average size of five for a period of 20 years, we are more likely to produce smaller values that might lead to zeroes in the time series than when we generate the same process for a 10 year period.

Given this realisation, we examine other simulation studies in the literature, and we find similar patterns in Abadi et al. (2010) and Brooks et al. (2004). Both of these papers use a Bayesian approach to fit IPMs similar to the ones considered in this thesis. The main difference is that the SSMs fitted in these papers have two states (see the state-space model in Section 1.2.2).

Abadi et al. (2010) performed a simulation study (the results can be found in Appendix B of their paper) using an IPM containing census, capture-recapture and reproductive success data, in which the state-process of the SSM did not depend on normal approximations. The results showed, that the productivity parameter, ρ, was always systematically underestimated, at every sample size and regardless of the level of dependence between data sets. Moreover, one can observe that the negative bias persisted in the results of this paper, even when an additional data set containing reproductive success information was incorporated. Further, the bias decreased as the sample size increased and also decreased with the addition of the reproductive success data set. These patterns agree with our findings, however the bias issue in the productivity parameter was not reported in the paper. This is because the bias was small, as larger data sets were used, still, it is important to highlight that ρ was systematically negatively biased.

Brooks et al. (2004) used a Bayesian approach to compare the results from fitting binomial-Poisson distributions directly to those from normal approximations. They found, as we do, that the normal approximations are incredibly robust, however in the presence of many observations below 10 in a 26-year the time-series, the normal approximations started to break down. Hence, they already stated that the ability of fitting the binomial-Poisson model would be crucial if data at local levels (small counts) were modelled.

As these different model fitting methodologies—the KF, the HMM, and the Bayesian approaches in Abadi et al. (2010) and Brooks et al. (2004)—show a systematic negative bias in the estimation of the productivity parameter ρ, one might question the suitability of discrete non-stationary distributions (or in the case of the KF its approximations to a normal distribution) in the presence of small counts.

In the next section we investigate the effect of the sample size when fitting non-stationary Poisson processes to time-series count data.

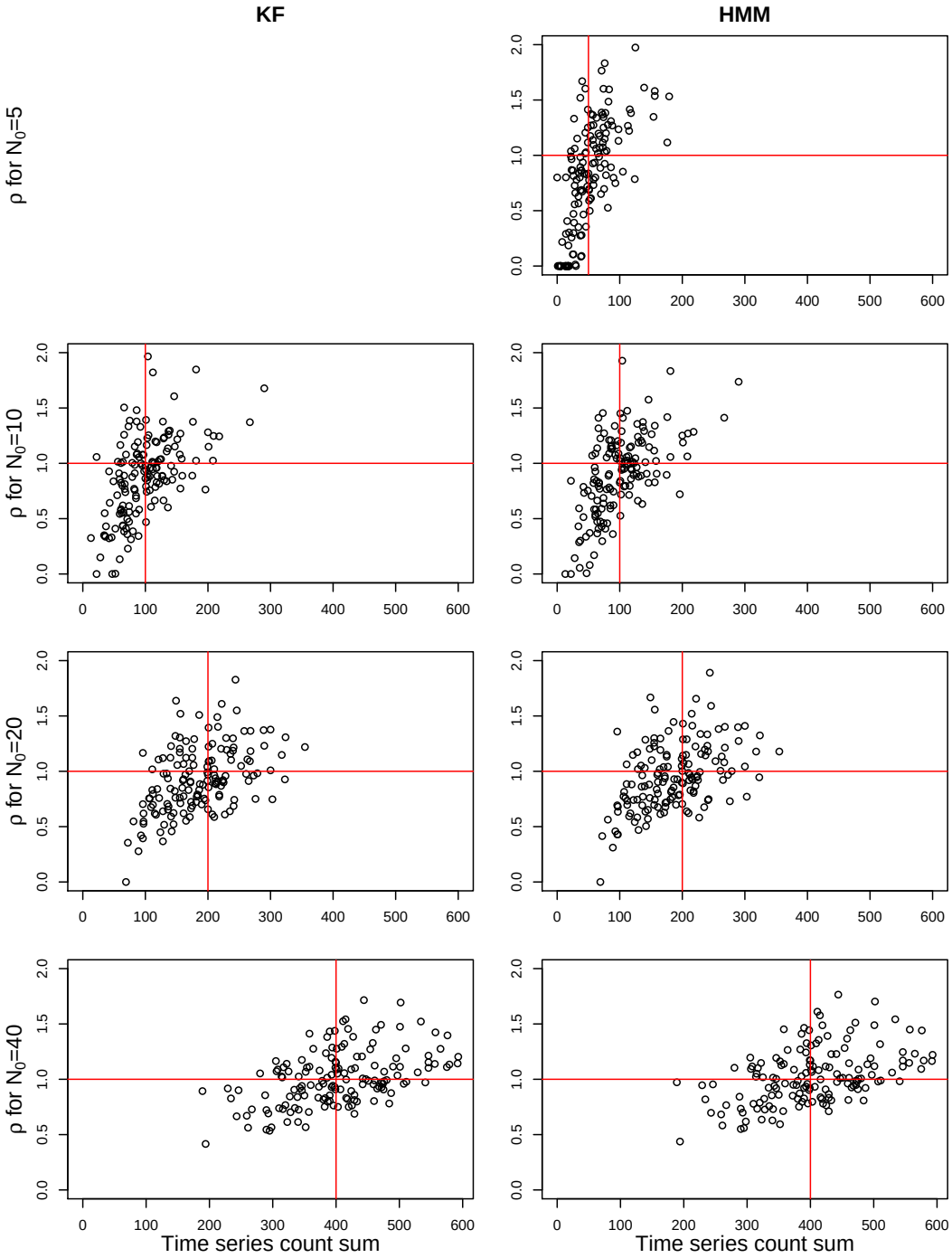

Fig. 4.4 Simulation results for the productivity parameter, ρ, against the time series count sum for different population sizes for 10 years of study for a stable population, with $\phi_1 = 0.30$, $\phi_a = 0.70$ and $\rho = 1$, for different population sizes. The horizontal red lines in each plot represent the true value of ρ, and the vertical red lines represent the expected sum of the counts of the time-series observed in the 10 years of study.

4.6.2 The Non-Stationary Poisson Process for Time-Series SSMs.

The aim of this study is to investigate if a systematic negative bias is also present when fitting a non-stationary Poisson process outside the state-space model framework. We conduct a simulation study for a Poisson non-stationary process, in which we generate 150 data sets in each simulation. The Poisson process replicates the state process described above by the binomial and Poisson convolution for a stable population. For this reason, we keep the mean parameter of the Poisson distribution, $\theta = 1$.

In Appendix C.2.1 we show the shape of the binomial-Poisson convolution and we compare this to binomial and Poisson distributions alone. Using a stable population, we compare the shape of these distributions in the case when the mean population value is 10, i.e. $N_0 = 10$ and $N_0 = 100$. We find that these distributions are heavily skewed when the sample size is small and small values are chosen.

Figure 4.5 and Table 4.2 show the simulation results in terms of relative bias for the mean parameter of a Poisson non-stationary process with mean, $\theta = 1$, at different sample sizes for a 10 years study.

Table 4.2 and the left hand side of Figure 4.5 show that for the Poisson non-stationary process there is also a systematic negative bias, which decreases as sample size increases. Additionally, on the right side of Figure 4.5 we can observe the estimate of θ obtained against the sum of the counts of each time-series generated. The findings are again similar to those obtained when fitting the IPMs: for smaller data sets, more data are being generated below the average sample size when the value of N_0 is small. Further, the bias for the Poisson non-stationary process is smaller than that obtained from fitting the IPMs. However, in the IPMs' state-space model several discrete non-stationary processes are used: the combination of two discrete non-stationary distributions (the binomial-Poisson convolution) in the state process, and an additional Poisson non-stationary process in the observation process. This may explain the larger negative bias.

Table 4.2 Median relative bias for a non-stationary Poisson distribution with mean, $\theta = 1$ for a time series of 10 years.

N_0	$\theta = 1.00$
5	-0.0733
10	-0.0394
20	-0.0251
40	-0.0129

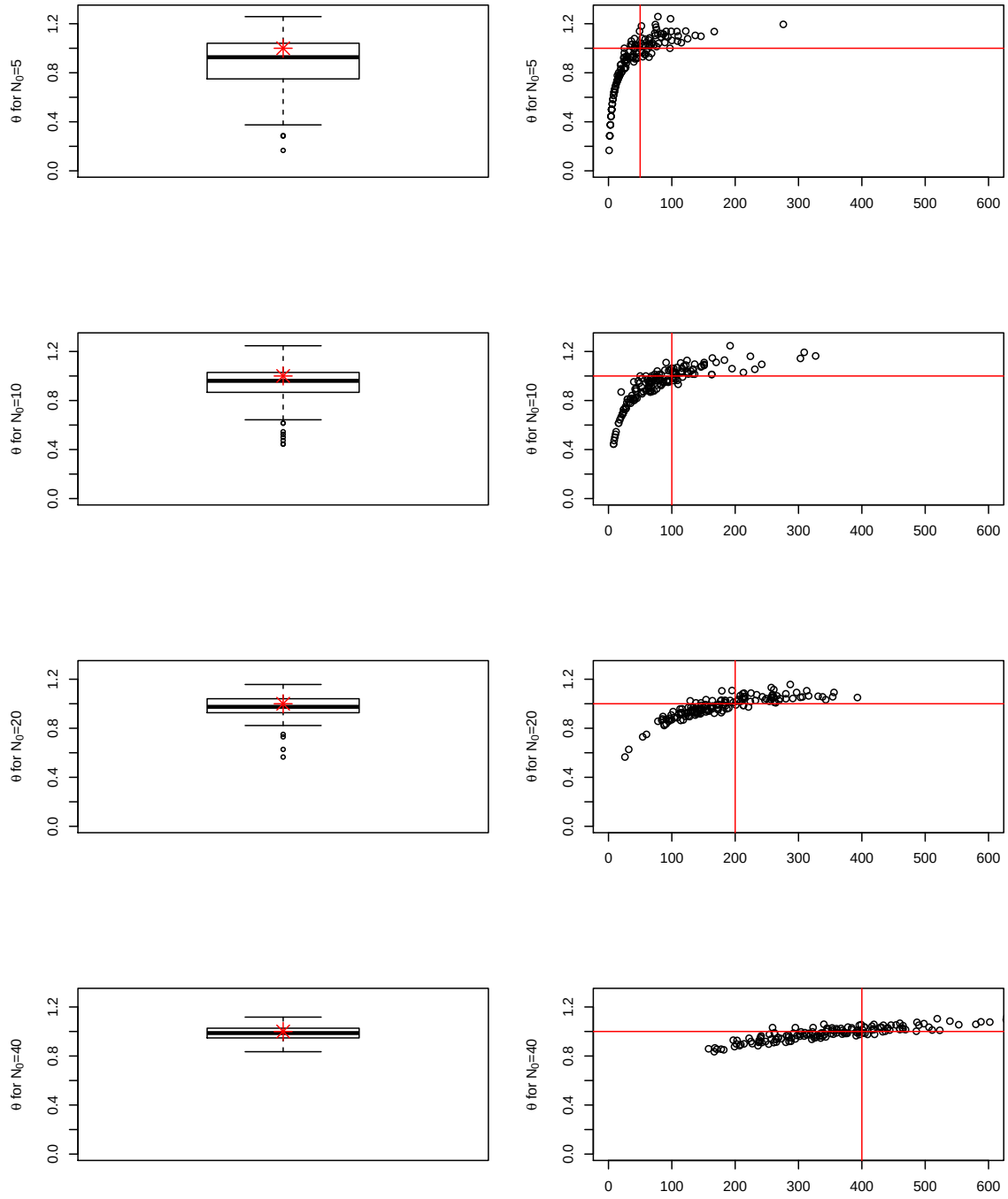

Fig. 4.5 Simulation results for a non-stationary Poisson process with 10 years of data. On the left we present the boxplots containing the simulation results for the mean parameter, θ. The thick middle black line represents the median estimated value, and the red star the real value of θ. On the right we can observe the results for the mean parameter, θ, against the time series count sum for different population sizes for 10 years of study. The horizontal red lines in each plot represent the true value of θ, and the vertical red lines represent the expected sum of the counts of the time-series observed in the 10 years of study.

Additional results for a 20 years simulation study can be found in Appendix C. These results are similar to those described here. We find that there is also a systematic negative bias, which is actually bigger than that obtained for a 10 years period, especially for smaller data sets. This can be explained as for a period of 20 years, for smaller data sets, we are more likely to produce smaller values that might lead to zeroes in the time series than when we generate the same process for a 10 years period.

The skewness of the distribution and the dependence on previous values in the time-series appears to be the cause of the bias, rather than the set up of the SSM or the method used to implement it.

Usually for many species different demographic data are available, and it is often the case that these data are collected for small populations. Thus, the combination of data from different sources adds extra information and helps to estimate the parameters in the model. Whilst IPMs are particularly valuable for small populations (Schaub and Abadi, 2011), when non-stationary discrete distributions are used to model population counts, the use of "small" data sets has to be carefully considered, as a systematic bias might be introduced. In the next section we consider whether combining big and small count data sets will correct this bias.

4.6.3 Computational Time

In this section we compare the computational times for the KF and the HMM. For this we conduct a simulation study in which we generate 100 data sets in each simulation. To do so, we simulate time-series data from the HMM described in Section 4.4.2 for a stable population with parameter values: $\phi_1 = 0.30$, $\phi_a = 0.70$ and $\rho = 1.00$. Then we fit the KF and HMM algorithms to the data and record the time the likelihood function takes to compute in seconds. We do this for three population sizes of $N_0 = 20$, 40 and 60.

Table 4.3 shows the computational times for the KF and the HMM for three population sizes. Here, we observe that the computational time of the KF does not change regardless of the population size. Additionally, the KF timings are always considerably smaller than the HMM's ones. The HMM timings increase considerably as the population size increases.

Table 4.3 Median computational time (in seconds) to calculate the likelihood function of the SSM using the KF and HMM. We perform 100 simulations for a stable population with parameter values: $\phi_1 = 0.30$, $\phi_a = 0.70$ and $\rho = 1.00$, for 10 years of census study. The first column specifies the sample size, the second the SSM algorithm used and the third the time in seconds they took to compute, with the standard deviation in parentheses.

N_0	Method	Time
20	KF	0.02(0.01)
20	HMM	58.10(121.64)
40	KF	0.02(0.01)
40	HMM	258.75(382.07)
60	KF	0.02(0.01)
60	HMM	499.24(549.27)

4.6.4 Combining Multiple Time-Series Data Sets—Effect on Bias

In Chapter 5 we will construct a spatially-explicit IPM which will contain spatially-explicit ring-recovery data and spatially-explicit count time-series data of different sizes. We will illustrate this model using starling data. For the starling time-series data there are five data sets that contain large counts, and 10 data sets that contain small counts. The detailed number of counts per year for these data sets are shown in Table 5.5. Thus, we are interested in assessing the bias in the productivity parameter when several time-series data sets of different sizes are combined. We generate 100 data sets in each simulation—for this we consider a 10 year period in which 1000 birds were ringed in the adult age class in each year of study, and 1000 birds were ringed in the first-year age class in each year of study. We combine the ring-recovery data with several time-series data sets which are fitted using HMMs, the KF, or both methodologies. Although the HMM generally provides estimates with smaller bias than the KF, the HMM is considerably computationally more expensive than the KF. We found that for $N_0 \geq 40$ the KF and the HMM provide similar unbiased estimates. For this reason, for time-series with $N_0 \geq 40$ we fit the SSM using the KF and for those with $N_0 < 40$ we use HMMs. We simulate 40 time-series data sets from which 20 data sets start at $N_0 = 40$ and are fitted using the KF, and 20 data sets start at $N_0 = 10$ and are fitted using HMMs. We use IPMs containing the ring-recovery data and the time-series data sets fitted using both the KF models and HMMs, the ring-recovery data and the time-series data sets fitted using only the KF, and the ring-recovery models and the time-series data sets fitted using only HMMs. We also change the number of time-series data sets used for each methodology in each combination. The parameter values are similar to those used for the simulation study in Table 4.1 where we considered a stable population with $\phi_1 = 0.30$, $\phi_a = 0.70$, and $\rho = 1$.

Table 4.4 shows the simulation results for ρ. We first show the effect on the bias, if we only use one time-series data set with small counts (row 3), one with large counts (row 4), or one with small counts and another with big counts in combination (row 5). In the following rows we compare the results of combining: five data sets with small counts with 0, 5, 10 or 20 data sets with big counts (rows 6-9 respectively); 10 data sets with small counts with 0, 5, 10 or 20 data sets with big counts (rows 10-13 respectively); and 20 small data sets with 0, 5, 10 or 20 data sets with big counts (rows 14-17 respectively). Finally in rows 18-20 we compare the results of combining 5,10 and 20 data sets with big counts with no data sets with small counts. Overall, in Table 4.4 we can see that in the presence of data sets with small counts, the bias reduces as the number of data sets with big counts incorporated in the IPM increases. This is also true for the data sets with big counts, the bias also reduces if we increase the number of them in the IPM. Additionally in Appendix C we provide more results for a simulation study in which we compare combining data sets of size $N_0 = 60$ and $N_0 = 10$. The results are similar to those described here, and the decrease in the bias is slightly higher with the incorporation of the larger data sets, as there are more data.

From Table 4.4 we conclude that the negative systematic bias from ρ decreases as the number of time-series data sets used increases. We observe that bias decreases as time-series data sets containing larger counts are used. Thus, in this case, using the KF provides better results in terms of bias not because this method works better than HMMs, but because the counts in these data sets are larger. If we compare the results obtained when combining multiple data sets in Table 4.4 with those obtained when fitting only 1 time-series data set in Table 4.1 we observe that the estimation of the productivity parameter ρ naturally improves with the addition of multiple time-series data sets. Additionally, it is worth noting that the bias of many small (rows with 0/10 0/20) is less pronounced than few small (5/0). So arguably, if there was limited effort/resources, combining time-series data sets with small counts would also improve the results. The simulation study results are key to the development of the spatially-explicit IPM in Chapter 5 in which ring-recovery data is combined with several time-series containing both small and large counts.

Table 4.4 Median relative bias for a stable population in the productivity parameter, ρ for IPMs that combine ring-recovery data with several time-series data sets which contain large and small counts. The time-series with large counts have $N_0 = 40$ and are fitted using the KF. The time-series with small counts have $N_0 = 10$ and are fitted using HMMs. Column 1 indicates the number of large data sets used and column 2 the number of small data sets used, and column 3 the bias for ρ. The first row indicates the data used and the combinations fitted.

large KF	small HMM	RR+large+small RR+KF+HMM
0	1	-0.1403
1	0	-0.0782
1	1	-0.0802
0	5	-0.0630
5	5	-0.0343
10	5	-0.0375
20	5	-0.0277
0	10	-0.0562
5	10	-0.0476
10	10	-0.0327
20	10	-0.0164
0	20	-0.0364
10	20	-0.0143
20	20	-0.0100
5	0	-0.0618
10	0	-0.0265
20	0	-0.0212

4.7 Discussion

In this chapter we have studied different methodologies for fitting discrete SSMs. Particularly we have reviewed and described how to implement the KF and HMMs for time-series count data which are modelled with Poisson or binomial-Poisson non-stationary processes, or appropriate normal approximations.

The motivation for this work lays in the development of SE-IPMs, which will be the subject of Chapter 5, for which the combination of several count time-series of different sizes will be combined. For this reason we evaluate the performance of the KF and the HMMs when the counts in the time-series have different sizes, and are particularly small. To do this, we first introduce the general characteristics of the state-space model in Section 4.2, and we describe the model fitting methodologies using the KF in Section 4.3 and using HMMs in Section 4.4. Moreover, as the SSM is parameter redundant, in Section 4.5 we introduce a

general form of the IPM needed to solve the identifiability issues. We then, in Section 4.6, perform a simulation study to show how these methods work in practice.

In the simulation study in Section 4.6.1 we find that in the presence of small data sets, within the IPM context, the estimation of the productivity parameter, ρ, is systematically negatively biased. This bias appears regardless of whether we employ the KF or HMMs, although for the latter the bias is slightly smaller. Moreover, although we do not fit these models using a Bayesian approach, we find that in the simulation study of Abadi et al. (2010), a systematic negative bias also occurs for similar models.

We examine the shape of the discrete non-stationary distributions, and we find that these are heavily skewed when time-series that contain small values are fitted. Thus, in Section 4.6.2 we investigate if there is bias when a single non-stationary Poisson process is fitted to a time-series. The results are very similar to those obtained when fitting the IPM, although now the bias is slightly smaller as there is only one non-stationary process in contrast with the IPM, where there were three.

Finally, as we would be combining different size time-series data sets for the spatially-explicit IPM in Chapter 6, we investigate if combining several time-series data sets help to aid the issue of the bias in Section 4.6.4. We conclude that the estimation of the productivity parameter ρ improves with the addition of multiple time-series data sets.

Overall from our simulation results we found that for time-series with counts on average greater than 40, i.e. $N_0 \geq 40$ the KF and HMMs provide similar results—the estimate for the productivity parameter is not biased. We recommend that, within the frequentist approach, the KF should be used when $N_0 \geq 40$, as HMMs are computationally more expensive to fit. One could argue that this is an arbitrary value, however it would be difficult to provide a precise cut off value, for example 38, or 39 instead of 40, as this value would slightly vary depending on the specific data. Nevertheless, at $N_0 \geq 40$ we are confident that using the KF is not going to bias the results. Moreover, for some data sets the KF could perform similarly well at slightly smaller values like 38 or 39, however using a HMM instead of a KF in those cases will not change the results. Instead, it would only make the algorithm slower. In Section 4.6.3 we saw that using HMMs increase computational times, this is particularly noticeable with large data sets, i.e. those with $N_0 \geq 40$. We also recommend that time-series with counts on average equal or smaller than five should not be used, as the bias when fitting these is large. Moreover, for time-series of 20 years, such as that presented in Figure C.1, and Table C.4 we showed that the KF and HMMs stop working when $N_0 = 5$. Additionally, we recommend that if time-series data sets with small counts are analysed, i.e. if the counts are on average smaller than 40, $N_0 < 40$, these should be combined with larger data sets so the bias issue is mitigated. If this is not possible, because additional larger data sets are

not available, caution should be taken in the interpretation of the productivity parameter. Moreover, it should be clearly stated that these estimates could be negatively biased.

Chapter 5

Spatially-Explicit Integrated Population Modelling

5.1 Introduction

In order to monitor population dynamics, the British Trust for Ornithology (BTO) has developed an Integrated Population Monitoring programme to monitor the numbers, breeding performance and survival rates of a wide range of bird species breeding in the UK, by combining data from different monitoring schemes (Baillie, 1990; Werham et al., 1998). Many wildlife species are currently in decline, an example of this, is the Starling (*Sturnus vulgaris*) a species on the UK Red List – of highest conservation priority. Such declines can be explained by changes in vital rates, such as annual survival probability and productivity, which are in turn related to environmental factors. Integrated population models (IPMs) combine different types of data into one analysis and provide reliable means for estimating these vital rates for a species across a population. However, traditionally, for the analysis of census, ring-recovery data, or the combination of both into an IPM, spatial information has only been considered at large population scales; for example Freeman et al. (2007b) used IPMs to study demographics of starlings at national and regional levels. Robinson et al. (2012) used IPMs to study the demographic processes driving the populations of blackbirds *Turdus merula* in the east, the west, and the whole of Britain. Morrison et al. (2016) constructed a regional IPM for Afro-Palaearctic migratory bird species that are declining in the southeast of Britain but increasing in the northwest. They showed that the differences in regional trajectories were a consequence of differences in productivity. Besbeas et al. (2005) showed demographic differences for the northern lapwings *Vanellus vanellus* in arable and pastoral regions of Britain.

Recently, the joint analysis of spatial capture-recapture and census data in an IPM has been considered (Chandler and Clark, 2014; Chandler et al., 2018). Moreover, Sun et al. (2019) introduced a spatially-explicit integrated model that combines presence-absence data, commonly collected in citizen science efforts, with systematically collected spatial capture-recapture data. Yet, spatially-explicit IPMs still appear to be a relatively novel idea. In this chapter we present a spatially-explicit integrated population model (SE-IPM) by combining ring-recovery and census data and adding spatial information in the form of geographical coordinates and/or land cover type to the parameters of the ring-recovery and state-space models (SSMs).

Spatial ecological data present many challenges, such as the differences in the scales at which the data are recorded, the existence of small or missing values, or spatio-temporal variation for the spatial information collected, which require careful examination and the implementation of appropriate methods that can accommodate data heterogeneity and sparseness. Integrating different models for separate data sets for the same population into one single analysis can help to compensate for data sparseness, as well as strengthen the results (Besbeas et al., 2005, 2002).

Our models are able to reconcile spatial data at different resolutions. While for ring-recovery data approximate geographical points in terms of latitude and longitude are available, for census data the finest observations are geographically registered in terms of 1 km by 1km squares. Unlike most conventional IPMs, the spatially-explicit ring-recovery models presented here are parameterised entirely in terms of individuals.

Generally, bird count data are typically modelled at large scales using SSMs. In classical analysis, the time-series likelihood component has traditionally been approximated using Kalman filter (KF) methodology, which is computationally efficient but relies on the assumption of Gaussian data. However, in the case of spatially-explicit census data, which consist of multiple time-series associated to specific locations, it is common to find areas in which the numbers of observed birds are low. In Chapter 4 we addressed the challenge of modelling time-series containing very small counts. In this chapter, to model the time-series count data, we combine the KF and hidden Markov models (HMMs) in a flexible algorithm which adapts to the varying sample sizes at different locations, being able to accommodate varied data sets for many bird species.

Through the use of IPMs incorporating detailed spatial information, we can cover wider areas of the country, and obtain robust spatial results that can explain demographic changes in populations across the UK.

In this chapter we examine the characteristics of the data collected by the BTO, we describe the independent spatially-explicit ring-recovery and census models implemented,

we present an SE-IPM (SE-IPM), and use starling data to illustrate how the model works in practice. We start with an introduction to the types of spatial data used for our analysis in Sections 5.1.1 and 5.1.2. We continue by introducing the starling data in Section 5.2, describing the characteristics of the ring-recovery and census data in Sections 5.2.1 and 5.2.2. In Section 5.3 we introduce the spatially-explicit models developed and combine them into an SE-IPM. In Section 5.4 we present the results obtained when fitting such models to the starling data provided by the BTO. We conclude this chapter in Section 5.5 with a discussion on the work developed and the possible future extensions for these models.

5.1.1 Geographic Coordinate and Grid Reference Systems

The BTO data include information on location and time. The two coordinate systems used to map data by the BTO are: the World Geodetic System (WGS-84) and the Ordnance Survey National Grid reference system (OSGB36).

The World Geodetic System (WGS-84) is the standard international method used in cartography, geodesy, and satellite navigation. This system uses two coordinates, latitude and longitude, to locate any point on the surface of the Earth. Both latitude and longitude are angles. Latitude ranges from 0° at the Equator to ±90° at the Poles (North or South). Longitude defines how far east or west a point is from the Prime Meridian at Greenwich, London, this is the position of 0° longitude. Longitude ranges from 0° to ±180°. Latitude and longitude can be easily transformed into the decimal system. Thus, latitude and longitude can be expressed in degrees-minutes-seconds or decimal degrees. In this chapter, and throughout this thesis when we refer to the WGS-84 system, we always express the coordinates in decimal degrees. Decimal degrees can be positive or negative, with negative values used for positions West of the Greenwich Meridian or South of the Equator (Evans, 1998).

The Ordnance Survey National Grid reference system (OSGB36) or British National Grid (BNG) is an extensively used geographical reference system for registering survey data in Great Britain at all scales. The OSGB36 is designed to cover the whole of Great Britain and extends 700 km to the east and 1300 km to the north of the false origin (Ordnance Survey Guide, 2016). The OSGB36 consists of a series of 25, 500×500 km squares, each labelled with a letter of the alphabet from A-Z (excluding I). These 500 km squares can be then subdivided into a series of 25, 100×100km squares, and these are each labelled with a letter of the alphabet A-Z (excluding I). As a result, a series of 100 km squares are obtained with references such as TQ. These 100 km squares can be subdivided further into 100, 10 km×10 km squares. These are each labelled with a number from 00 to 99. Finally, these 10 km squares can be subdivided into one of two ways: either into 5 km by 5 km squares or

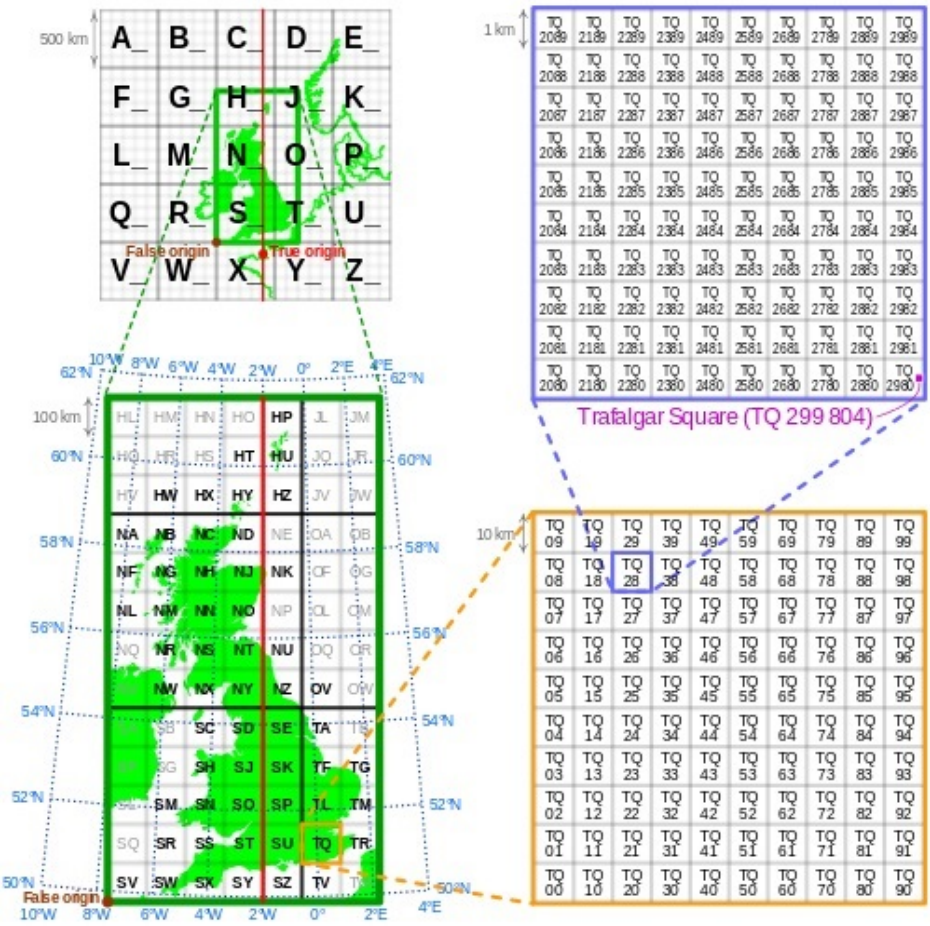

Fig. 5.1 Illustration of the Ordnance Survey National Grid coordinate system (OSGB36), with Trafalgar Square as an example, from Wikipedia contributors (2019).

into 1 km by 1 km squares. These squares can be easily transformed into various coordinate systems, such as WGS-84, using latitude and longitude (Ordnance-Survey, 2011).

Transformations between both systems are possible and the calculations required for this can be found at the Ordnance Survey Guide (2016) website. Moreover, the Grid Reference Finder (2019) and Where's the Path (2019) websites can be used to obtain these conversions.

Figure 5.1 shows graphically an example of the different grid dimensions of the OSGB36. It uses as an example Trafalgar Square, in London, with grid reference TQ299 804. The corresponding WGS-84 coordinates for this location correspond to latitude 51.51 and longitude -0.13, or (51.51,-0.13). Note that throughout the thesis we give the coordinates to 2 decimal places, however when included in our calculations we use a precision of 6 decimal places.

5.1.2 Land Cover Data

As the data for starlings that we will analyse is for the time period of 1990 to 1999, we use the National-Scale Land Cover Map of Great Britain (1990), LCM1990. This is a digital data set which provides classification of land cover into 25 classes available at different spatial resolutions. The data were derived using a supervised maximum likelihood classification of data collected by the satellite Landsat 5 Thematic Mapper, which combined winter and summer data (Fuller et al., 1994a,b).

The Land Cover Map of Great Britain is available as a standard digital product: as either the full set of 25 "target" cover-types, or as an aggregation of these into 17 "key" cover-types. We use the 25-class data set at a 1km resolution. For this data set there are 25 layers, one for each "target" class. The values for each 1 km grid cell represent the percentage of that cell that has been designated as being of a particular "target" cover-type.

We group the full set of the 25 "target" cover-types into six categories: farm, grass, urban, water, wood and unclassified. We choose these six land-cover categories, to describe the preferred habitats of various British birds at a large scale (cf. Gregory and Baillie, 1998). Table 5.1 shows the grouping of the "target" data into six categories. Among these six categories, we have the unclassified category, which represents the land cover data that did not belong to any of the 25 "target" cover-types, usually due to the presence of clouds on every occasion that the satellite recorded data (which happens often at sea). For our illustrative example we need to use the land cover data at a 100 km square resolution. At this resolution, some squares contain a high proportion of unclassified land cover data (see Table 5.6), however these squares also contain a larger proportion of sea water than land. For example, in Table 5.6 we can observe that the TR and TM squares which have a high percentage of unclassified land, mostly contain sea. In contrast, the inland squares SO, SP, SU, TL (which are later used for our analysis) have quite a low proportion of unclassified land ($\% < 5$). Thus, removing the unclassified category from our analysis is unlikely to substantially bias the proportional coverage of the other land cover types. Additionally, for other species, or other time periods, the census data are less sparse and thus, it is possible to use data at a higher resolution (i.e. 10 km or 1 km squares). This means that we would be less likely to have large amounts of unclassified land for the squares in which sampling took place, as these squares would be inland and not in the sea. Therefore we use the remaining land cover five categories for our analysis. The description of the "target" variables can be found in the documentation of the Land Cover Map of Great Britain (1990), LCM1990.

Table 5.1 Land cover "target" cover-types grouping into six land cover categories.

Land cover type	"targets"
Farm	tilled land
Grass	grass heath, pasture, meadows SNG, rough/marsh grass, bracken, dwarf shrub and grass, dense shrub heath, dense shrub moor, mountain grass, lowland heath, weeds, dwarf shrub grass heath, inland bare ground
Urban	suburban, urban development
Water	sea/estuary, inland water, beach and coastal bare, saltmarsh, upland bog, lowland bog
Wood	scrub/orchard, deciduous woodland, coniferous woodland, felled forest
Unclassified	Unclassified

5.2 Data

The starling (*Sturnus vulgaris*), or common starling is an endemic bird of Europe and Western Asia (Robinson et al., 2006). Due to its continuous decline in the last four decades it has been categorised as a species of highest conservation concern in Britain (Gregory et al., 2002).

There are two main populations of starlings in the UK: the native and the migrant starling populations. The native starlings breed in the country and are considered sedentary birds—with an estimated mean natal dispersal of 9.5 km, and a breeding dispersal of 3.4 km (Paradis et al., 1998). The migrant starlings arrive during the months of October and November and leave in March to breed mainly in Sweden and the Baltic States (Wernham et al., 2002).

The British Trust for Ornithology has monitored the breeding population of starlings since 1962. Robinson et al. (2002) estimated that the population size of starlings during the breeding season was 8,860,000 (averaged during the years 1994-2000). The densities of starlings change significantly with location. Most starlings occur in Southern Britain, with 36% of the population found in the south of England and 21% in Scotland. The differences in abundances are mostly due to land cover changes, with 73% of starlings occurring in gardens and areas of unimproved grass. Particularly, densities of starlings are greatest in suburban habitats, followed by farmland areas. Nevertheless, starling populations in suburban areas and the wider countryside have declined by over 50% (Robinson et al., 2002). For further information on starling habitat preferences see Gregory and Baillie (1998).

Figure 5.2, from Robinson et al. (2002), shows the population decline of starling in Britain between 1962 and 2000. The starling population is represented in terms of an index calculated from the Common Birds Census Data (CBC). For further information on how the CBC index is derived, we refer the reader to Marchant (1983).

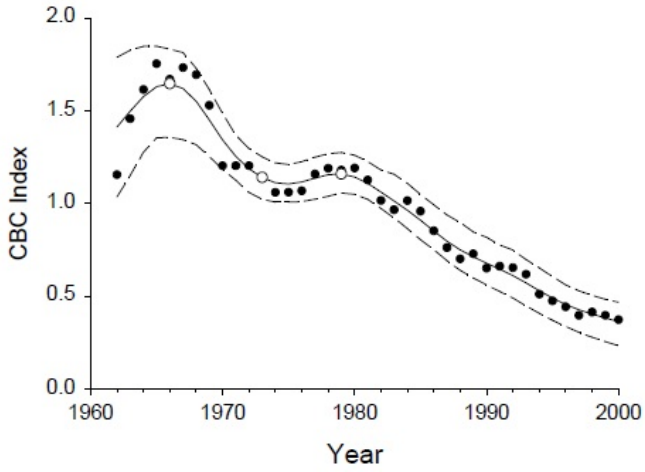

Fig. 5.2 Population index of starlings in Britain 1962-2000 from Robinson et al. (2012). The Solid line represents a smoothed GAM trend, and the dashed lines the 95% confidence limits. The filled circles show the annual indices without any smoothing, and the empty circles represent significant turning points in the GAM trend.

Starlings have experienced a decline of 68% since 1962, though this decline is more abrupt in woodland areas (92% since 1965) (Robinson et al., 2006). In addition, a rapid population decline between the years 1966 to 1980 can be observed in Figure 5.2. In this chapter, to illustrate our methods, we consider the ring-recovery and census data for years 1990-1999 and analyse them using an SE-IPM. We chose this period of time for several reasons: 1. these data contained both small and large counts, 2. Additional data from the BBS are available for these years in case we want to incorporate these in future work, and 3. In terms of spatial information, we can use the Land Cover map of Great Britain (1990) for this decade, if we assume that the types of land remain unchanged during this decade, which according to our BTO collaborators is a sensible assumption. In Section 5.2.1 we describe the spatial ring-recovery data and in 5.2.2 we describe the spatial census data for starlings.

5.2.1 Spatial Ring-Recovery Data

Starlings are ringed at different age categories throughout Great Britain. We consider two age categories: birds in their first year of life, which we refer to as first-year birds, and older birds ($\geq$ 1 year old), which we refer to as adult birds. For the years 1990-1999 there were a total of 60,815 starlings ringed. Out of these, 45,181 birds were ringed as first-year birds and 15,634 as adults. Starlings were ringed between April and September, and recoveries happened throughout the year. The number of birds recovered dead during this time period

was relatively small, with only 601 of the birds ringed in their first year of life recovered, and 217 of the birds ringed in the adult category recovered.

The data provided contain detailed information on each individual ringed, including spatial information. For those individuals recovered there is also corresponding spatial information available. Table 5.2 shows an extract of these data. These data can be read as follows: for example taking the first row, in 1990 an adult bird was ringed and identified with the number CJ17509, at latitude 52.20 and longitude 0.08, but this individual was never found dead. Also in 1990 (row 2), another adult bird, with the identification number CP58083 was ringed but at latitude 51.35 and longitude -0.333. This bird was recovered dead in 1992 at the same latitude and longitude where it was ringed. Additionally, ring-recovery m-arrays for starlings ringed as first-year birds and as adults are provided in Appendix D, in Tables D.1 and D.2.

Table 5.2 Extract of starling ring-recovery data with available geographical coordinates for the years 1990-1999. The first column contains the identification number for each individual. The second column specifies the age at ringing. The next three columns contain the year and the geographical location, in terms of latitude and longitude expressed in decimal degrees, at which each individual was ringed. The last three columns provide information on recoveries, that is, if a ringed individual was found dead and reported, the year and the coordinates at which this particular bird was found dead.

Ring number	Age ringing	Year ringed	Lat ringing	Long ringing	Year recovered	Lat recovered	Long recovered
CJ17509	Adult	1990	52.20	0.08	-	-	-
CP58083	Adult	1990	51.35	-0.33	1992	51.35	-0.33
RR54191	Adult	1995	55.00	-1.58	-	-	-
XJ32066	1-year	1998	50.91	0.95	-	-	-
RE44087	1-year	1990	53.33	-2.80	1990	53.35	-2.76
RP73583	1-year	1998	52.77	-2.37	-	-	-

Figure 5.3 shows the distribution of ringed, map (a), and recovered birds, map (b), throughout Great Britain during the years 1990-1999. These maps show the contrast between ringing and recoveries. While ringings are abundant and spread out through the country, recoveries represent a small percentage of the sample. Recovery reporting rates are likely to be lower in areas with lower human population densities. Furthermore, a larger proportion of ringings occur in the south-east, as a result, proportionally, there are fewer recoveries in the north of Britain, as we can see in Figure 5.3 (b). This figure presents an overall summary for these 10 years of ringing.

For both age categories more birds were ringed in the South East of England than in any other region. Also, from the data we can observe that, while a significant number of

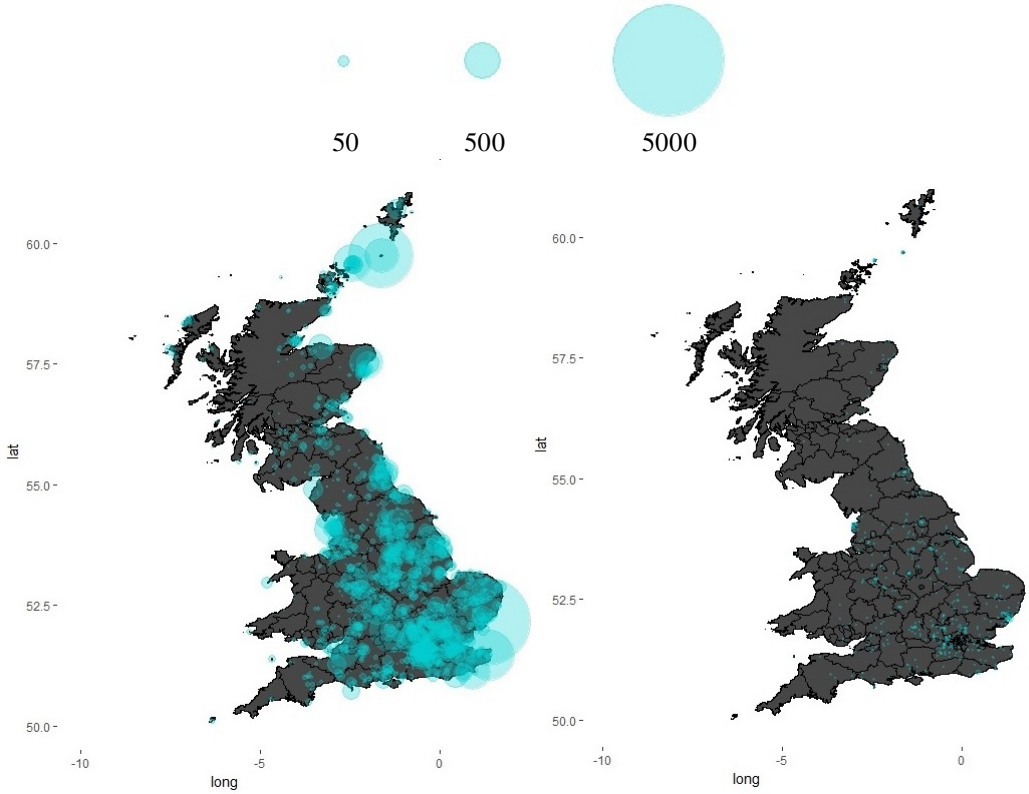

(a) Ringed birds (b) Recovered birds

Fig. 5.3 Ringed and recovered starlings, 1990-1999. The size of circle represents the number of birds ringed (or recovered) at a single site. The legend above shows circles for counts of size 50, 500, and 5000.

Table 5.3 Relative distance in km between ringing and recovery for birds ringed as first-year. The first column specifies the age of the birds at ringing. Columns 2-6 contain the frequency (with corresponding proportion shown in brackets) of birds recovered within 25 km of the place of ringing, 26 to 50, 51 to 75, 76 to 100 km of ringing and recovered more than 101 km away from the place of ringing.

Age	0-25	26-50	51-75	76-100	101+
First-year	598(86.8%)	45(6.5%)	16(2.3%)	4(0.6%)	26(3.8%)
Adult	236(94.8%)	4(1.6%)	2(0.8%)	3(1.2%)	4(1.6%)

birds were ringed in Orkney and Shetland, the two northernmost islands in Scotland, the South of Scotland, the North and West of England, and Wales have few ringings. Besides the spatial difference in the number of birds ringed across Great Britain, Figure 5.4 shows that the proportion of birds recovered is reasonably spatially homogeneous.

For those birds that were recovered dead, we know the exact coordinates at ringing and at recovery. In order to understand how starlings behave spatially we measure the distance between the locations where a bird was ringed and recovered. To do so, we use the Haversine formula, which determines the great-circle distance between two points on a sphere given their longitudes and latitudes (Van Brummelen, 2012). This can be easily implemented in R, using the package 'fossil' (Vavrek, 2011). Table 5.3 shows this distance for those birds that were recovered dead. We observe from Table 5.3 that most starlings recovered dead were found within 25 km from the place where they were ringed.

The land cover data are matched to the geographical coordinates of the location in which a bird is ringed. The land cover are available at a 100×100 km squares scale. Every 100×100 km squared is formed of different types of land that are expressed as a percentage. Table 5.4 shows an extract of the spatial land cover data for starlings for the years 1990-1999 at a 100x100 km resolution.

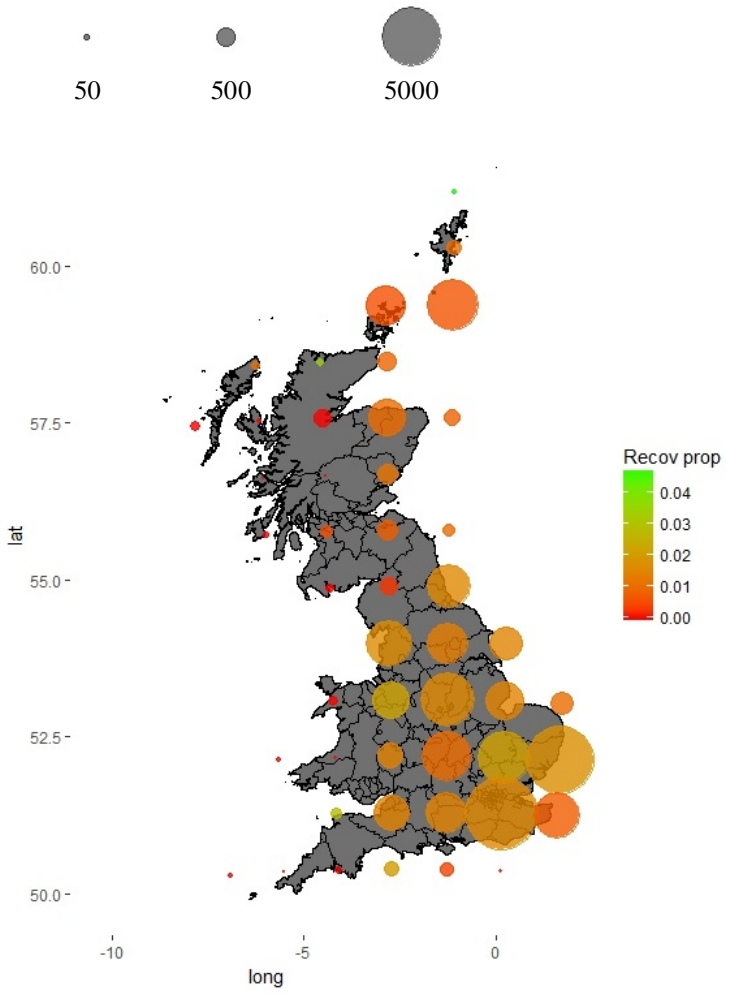

Fig. 5.4 Proportion of ringed and recovered starlings at a 100 km square resolution, 1990-1999. The proportion is given by the colour of the circle. The size of the circle represents the number of starlings ringed. The legend above shows circles for counts of size 50, 500, and 5000.

Table 5.4 Extract of starling ring-recovery data with available spatial location in terms of geographical coordinates and land cover for the years 1990-1999. The first column contains the identification number for each individual. The second column specifies the 100 km square in which the individual was ringed. The third and fourth columns contain a more precise location in which each individual was ringed, giving the approximate geographic coordinates. The remaining six columns contain the percentage of the specified type of land contained in the 100 km square.

Ring	Grid ref	Lat	Long	Farm	Grass	Urban	Water	Wood	Unclassified
CJ17509	TL	52.20	0.08	61.9481	22.7809	9.5649	0.4632	4.6118	0.6311
CP58083	TQ	51.35	51.35	18.0957	41.7325	19.4911	1.5373	9.8263	9.3171
RR54191	NZ	55.00	-1.58	18.3133	22.1068	6.9576	0.7213	2.3753	49.5257
XJ32066	TR	50.91	0.95	6.0528	5.1078	1.2055	0.4045	0.9185	86.3109
RE44087	SJ	53.33	-2.76	17.7371	54.0629	11.4581	0.8519	7.5941	8.2959
RP73583	SJ	52.7 7	-2.37	17.7371	54.0629	11.4581	0.8519	7.5941	8.2959

5.2.2 Spatial Census Data

Terrestrial bird monitoring was operated mainly by the CBC scheme until the introduction of the BBS in 1994 (Marchant et al., 1990). Census data were collected on farmland, woodland, or 'special' (the latter consisting of areas dominated by wetlands, lakes, coastal habitat etc.) plots, with a much higher coverage in the first two types of land (Robinson et al., 2002). The data were collected by volunteers with survey sites not chosen at random, as plots were selected by the observers. The average cover of farmland plots was around 70 hectares (0.7 square km) in extent, whilst woodland plots covered just over 20 hectares (0.2 square km). A territory-mapping approach was used to estimate the number and positions of territories of each species present on a each survey plot during the breeding season (Marchant, 1983). The detailed survey design is described in (Marchant et al., 1990). The CBC was broadly representative of agricultural practices (Fuller et al., 1985). In addition, the number of volunteers was higher in the south and east of the UK, thus more information was collected in these areas (Gregory et al., 2000).

Observations of birds were made either by sight or sound, and they were registered as an estimated count of birds seen in a specific location, for which a 1×1 km grid reference was given. From 1962 to 2000 starlings were recorded during the breeding season on 146 plots, however, not all the survey plots were visited every year (Robinson et al., 2002). Moreover, the number of counts of starlings per 1 km square tended to be small, and excluded many areas of the country. We group the 1 km grid squares into 100 km squares, by merging smaller squares together so we can make use of data that would otherwise be too sparse to be modelled. However, even then, many areas of the country are not represented, and some of the areas visited vary through the years.

Figure 5.5 shows the 100 km by 100 km squares in which counts were registered for starlings between 1962 and 2000. The red dots represent those squares in which at least one bird was seen and registered between 1962 and 2000. The blue dots represent those squares with at least one count between 1990 and 1999. Finally, the yellow squares represent those squares with an average count of at least 40 birds for the years 1990 to 1999, and the green squares represent those squares with an average count of more than five birds but fewer than 40 for the same period. In our analysis, we use the yellow and green squares; none of these contain a value of 0 for any of the years in the time series. Table 5.5, provides the specific count of birds for the yellow and green squares in Figure 5.5. Additionally, in Table 5.6 we show the percentage of each type land contained in each 100 km square. In Chapter 4 we considered and compared two different methods, namely the KF and HMMs, that could be used to fit time-series data depending on the size of the counts.

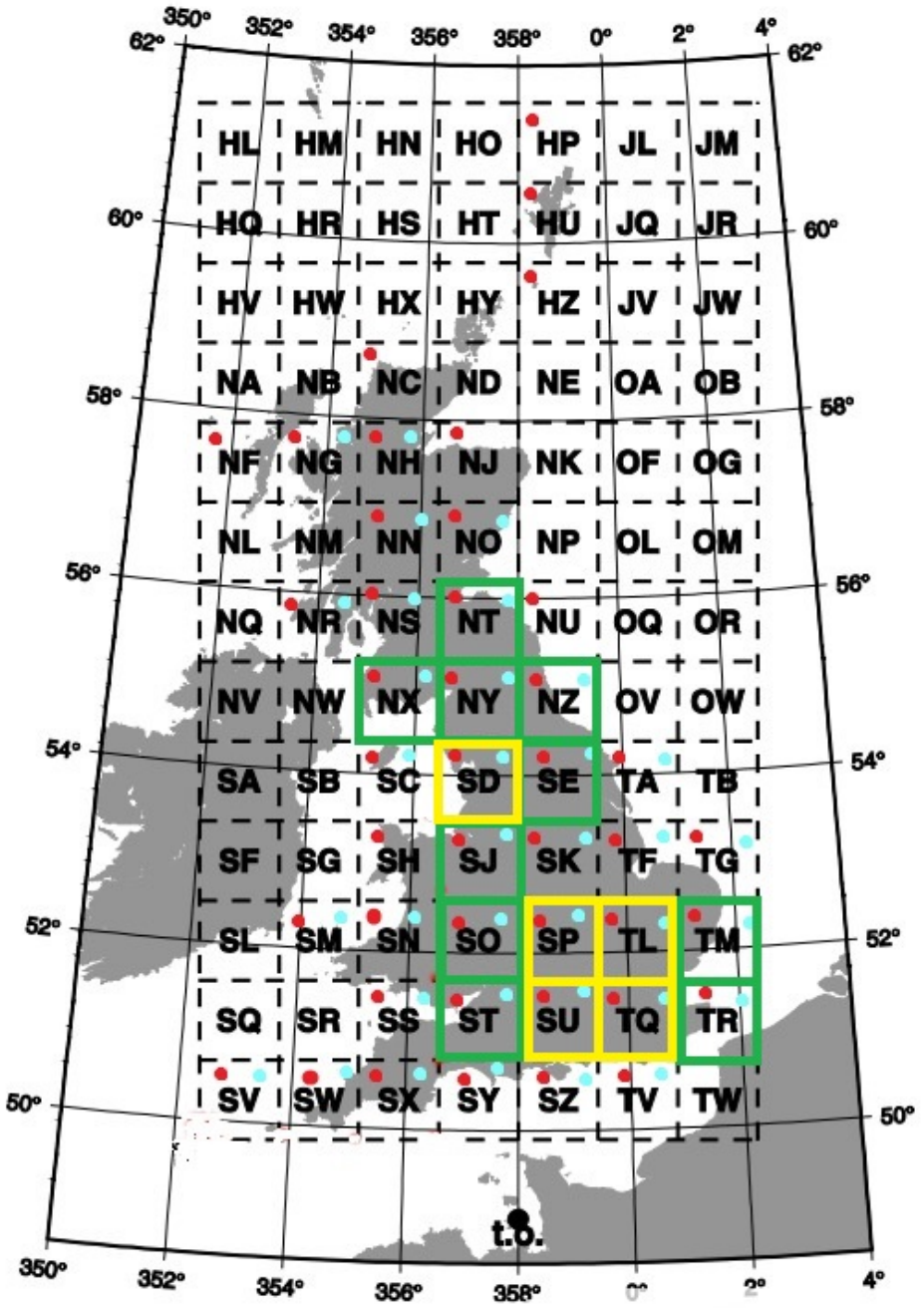

Fig. 5.5 Squares containing at least one count for the CBC starling data from 1962-1999. The red dots represent those squares in which at least one bird was seen between 1962 and 2000. The blue dots represent those squares with at least one count between 1990 and 1999. Finally, the yellow squares represent those squares with at least 40 counts on average for each year between 1990 and 1999 and the green squares represent those squares with more than five birds but fewer than 40 on average for each year from 1990 to 1999.

Table 5.5 CBC Spatial counts for starling per 100 km by 100 km squares for the years 1990-1999. The letters in green represent those squares with small counts, the letters in yellow represent those squares with large counts.

Year/Square	NT	NX	NY	NZ	SE	SJ	SO	ST	TM	TR	SD	SP	SU	TL	TQ
1990	10	10	11	18	23	9	26	31	10	2	22	58	66	69	125
1991	4	14	11	18	17	8	30	25	11	14	92	67	100	95	95
1992	7	17	11	25	18	4	20	34	21	10	105	48	72	80	132
1993	11	28	10	15	15	5	22	17	36	2	96	54	85	70	84
1994	8	8	8	8	17	3	19	35	36	2	85	47	85	52	72
1995	6	3	6	18	12	2	19	20	21	2	68	58	90	48	45
1996	5	12	8	28	14	3	13	25	16	4	23	53	86	40	41
1997	6	10	9	28	9	5	10	18	17	2	57	29	67	36	31
1998	11	21	9	49	7	2	4	7	2	1	74	28	70	20	44
1999	8	45	13	33	18	4	8	8	4	6	88	25	44	28	30

Table 5.6 Percentage of each land cover type per 100 km square.

Square /land	Unclassified	Water	Grass	Wood	Farm	Urban
NT	22.7945	1.3919	43.8950	6.6763	22.9810	2.2613
NX	51.4347	2.1074	35.0696	9.3083	1.7696	0.3104
NY	5.1149	2.1437	77.1602	8.4553	5.7731	1.3528
NZ	49.5257	0.7213	22.1068	2.3753	18.3133	6.9576
SE	1.7335	0.7830	39.4151	5.9919	42.2678	9.8087
SJ	8.2959	0.8519	54.0629	7.5941	17.7371	11.4581
SO	3.9441	0.3801	54.1667	12.1185	21.8844	7.5062
ST	13.4033	0.7643	52.5053	7.5818	19.2613	6.4840
TM	64.8435	0.7117	9.4289	0.9989	21.4129	2.6041
TR	86.3109	0.4045	5.1078	0.9185	6.0528	1.2055
SD	28.8674	1.8312	51.2835	3.9791	7.8963	6.1425
SU	2.7645	0.5357	39.6705	14.6676	31.7188	10.6429
SP	0.7463	0.1908	33.8646	4.5394	46.2877	14.3712
TL	0.6311	0.4632	22.7809	4.6118	61.9481	9.5649
TQ	9.3171	1.5373	41.7325	9.8263	18.0957	19.4911

5.3 Spatially-Explicit Integrated Population Model

5.3.1 Spatially-Explicit Ring-Recovery Model

Standard ring-recovery models (see Section 1.2.1) provide information on an overall population, but do not account for spatial differences in survival or recovery probabilities. We propose adding spatial information in the form of geographical coordinates and/or land cover type as covariates. The covariates are latitude and longitude in decimal degrees and/or type of land cover as the percentage of a specific type of land type within each 100 km square.

In general the survival and recovery rates of birds can be greatly affected by location. However, Table 5.3 in Section 5.2.1 showed that in general, the distance between ringing and recovery is very small for starlings. There is no evidence that starlings travel more than just a few kilometres from their ringing location. Additionally, Figure 5.4 showed that while the proportion of recoveries is very small, it does not change substantially with space. Thus, in our model, for simplicity, we only use the ringing location.

The spatial covariates are contained in the design matrix X and we use the standard logistic regression form to express how we model survival. For example in Equation 5.1 we express the probability of survival for the ith bird in the age class h, $h = \{1, a\}$, as

$$\phi_{h,i} = \frac{1}{1+e^{-(\alpha_h+\beta_{lat,h}x_{1,i}+\beta_{long,h}x_{2,i}+\beta_{land,h}x_{3,i})}}, \tag{5.1}$$

where $x_{1,i}$ is the latitude, $x_{2,i}$ is the longitude, $x_{3,i}$ is the percentage of a specific type of land cover in the 100 km square in which the individual was ringed. The regression parameters are α_h, $\beta_{lat,h}$, $\beta_{long,h}$, and $\beta_{land,h}$.

Thus, we allow the probability of survival for adults and first-year birds to vary continuously with geographical coordinates, and type of land, but we consider the effect of these covariates does not change over the years.

This model can be extended by adding covariates with different polynomial terms. For example, the probability of survival for the ith bird in the age class h using quadratic terms, can be equally expressed as

$$\phi_{h,i} = \frac{1}{1+e^{-(\alpha_h+\beta_{lat,h}x_{1,i}+\beta_{long,h}x_{2,j}+\beta_{lat^2,h}x_{1,i}^2+\beta_{long^2,h}x_{2,j}^2)}}.$$

5.3.2 Spatially-Explicit Census Model

To model census data we extend the single-state SSM presented in Section 4.2 to include spatial information at a 100 km square resolution.

Traditionally, as explained in Section 1.2.3, the population counts were transformed into an index, y_t, derived from a Poisson generalised linear model that took into account site and year effects (Ter Braak et al., 1994). Instead of using this index, and in order to be able to add spatial information on the same scale as the ring-recovery model, we use the count of birds for each 100 km square. For starlings, we actually know the counts for each 1 km square, but for most of these squares, the counts are too low and include many zeros across the time series. Therefore we aggregate them into 100 km squares. The number of birds observed in the 100 km square s, in the year t, is given by

$$y_{s,t} = \sum_{i=1}^{100} G_{i,s,t}\,, \tag{5.2}$$

where $G_{i,s,t}$ represents each 1 km square i, within a 100 km square s for the year t.

For other species, where data are less sparse aggregation may be possible at a higher resolution (i.e. 10 km squares). Moreover note that for our data, the average collection plot sizes were of 70 hectares (0.7 square km) and 20 hectares (0.2 square km) for farmland and woodland respectively, which makes the use of a 1 km resolution appropriate if there were enough count data.

We use the centre of each of the 100 km by 100 km square s, to obtain a geographical location, in terms of latitude and longitude. We can also include the percentage of a specific type of land cover in each 100 km square as another covariate. The spatial covariates are contained in the design matrix X and we use the standard logistic regression form to express how we model survival, for each each class h, $h = \{1, a\}$. For example in Equation 5.3 we express the probability of survival for those birds in the square s,

$$\phi_{h,s} = \frac{1}{1+e^{-(\alpha_h+\beta_{lat,h}x_{1,s}+\beta_{long,h}x_{2,s}+\beta_{land,h}x_{3,s})}}\,, \tag{5.3}$$

where $x_{1,s}$ is the latitude at the centre of the 100 km square s, $x_{2,s}$ is the longitude at the centre of the square s, $x_{3,s}$ is the percentage of a specific type of land cover in the 100 km square s, and α_h, $\beta_{lat,h}$, $\beta_{long,h}$, and $\beta_{land,h}$ are the regression parameters. Thus, the probability of survival for the census model, for adults and first-year birds varies discretely within 100 km squares.

Similarly to the ring-recovery spatial model, the spatial census model can be extended by adding covariates with different polynomial terms.

Traditionally, an index derived on bird counts has been considered at large scales and, when using classical statistics, the KF has been used to fit the SSM. The KF is an algorithm

that relies on Gaussian approximations, but the Gaussian approximation may not be valid for smaller counts.

The simulation study in Section 4.6.4 showed that the KF can be used for squares that have on average more than 40 birds recorded each year (the yellow squares in Figure 5.5). Additionally, in Section 4.6.4 we discussed that HMMs should be used to fit time-series data which contain counts that are on average smaller than 40. Thus, we use HMMs to fit those squares with small counts, between five and 39 birds per year, (the green squares in Figure 5.5).

The joint likelihood for the census model consists of the following components:

The Kalman Filter

For large counts the contribution to the likelihood involves using the KF (Meinhold and Singpurwalla, 1983) for each of the chosen 100 by 100 km squares for our analysis. The joint likelihood for the census data in this case is given by,

$$L_{J,KF}(\phi_{1,s}, \phi_{a,s}, \rho, \sigma_\eta) = \prod_{s_K \in S_K} L_{s_K}(\phi_{1,s}, \phi_{a,s}, \rho, \sigma_\eta), \tag{5.4}$$

where L_{s_K} is the likelihood of each of the squares contained in the set of all the 100×100 km squares, S_K with an average count of at least 40. For the starling data set that is the five yellow squares in Figure 5.5.

Hidden Markov Model

For small counts the contribution to the likelihood involves using HMMs for each of the chosen 100 km squares for our analysis. The joint likelihood for the census data in this case is given by,

$$L_{J,H}(\phi_{1,s}, \phi_{a,s}, \rho, \mu) = \prod_{s_H \in S_H} L_{s_H}(\phi_{1,s}, \phi_{a,s}, \rho, \mu), \tag{5.5}$$

where L_{s_H} is the likelihood of each of the squares contained in the set of all the 100×100 km squares, S_H with an average count between five and 39. For the starling data set that is the 10 green squares in Figure 5.5.

5.3.3 Spatially-Explicit Integrated Population Model

The likelihood of an IPM is formed as the product of all components. In Section 1.2.3 we showed the expression for a traditional IPM consisting of a ring-recovery and a SSM.

Similarly, for the SE-IPM, the joint likelihood is then given by the product of the likelihoods of the ring-recovery and the SSMs,

$$L_{SEIPM}(\phi_{1,s}, \phi_{a,s}, \lambda, \rho, \sigma_\eta) = L_{RRSM}(\phi_{1,i}, \phi_{a,i}, \lambda) \times L_{J,KF}(\phi_{1,s}, \phi_{a,s}\rho, \sigma_\eta), \times L_{J,HMM}(\phi_{1,s}, \phi_{a,s}\rho, \mu)$$

where $SEIPM$ stands for spatially-explicit integrated population model, and $RRSM$ stands for ring-recovery spatial model.

5.4 Results

In this section we fit the SE-IPM described in Section 5.3.3 to the starling data for the years 1990-1999. For the SE-IPMs we add geographical coordinates and/or the percentage of type of land as a covariate to the adult and first-year survival probabilities.

When using spatial data, we need to consider spatial autocorrelation, which occurs when the values of variables sampled at nearby locations are not independent from each other (Dormann et al., 2007). Several methods have been developed to correct the effects of spatial autocorrelation, however, before applying any of these correction methods, it is reasonable to check if our data is affected by this phenomenon. To do so, we can check if the assumption of independence in the spatial data is violated by looking at the distribution of the residuals (Dormann et al., 2007). In the context of the SE-IPM described here, it is not straight forward to check for spatial autocorrelation. In Section 5.2 we discussed that the starling mean dispersal is on average below 10 km (Paradis et al., 1998). Moreover, in Section 5.2.1 we showed that within our ring-recovery data most starlings recovered dead were found within 25 km from where they were ringed. Based on this, for starlings we should not expect to encounter spatial autocorrelation. Thus in this section, rather than an in-depth examination, we briefly explore some indicators of spatial autocorrelation, however due to the complexity of the data and the models, we do not provide any formal means for the analysis or the correction of spatial autocorrelation. For the ring-recovery component, we examine the residuals of the ring-recovery model by binning the spatial ring-recovery data into 100 km squares. In Figure D.13 of Appendix D we present a map of residuals for the starling ring-recovery data, which does not present any obvious pattern. For the state-space component, it is more challenging to obtain residuals or estimate results per square as the model is parameter redundant, and for many of the squares we have very small counts. As a result, we do not present here any results or residuals for the SSM. The ring-recovery data dominates the data in the IPM, thus based on the preliminary observation of the ring-recovery estimates and residuals, we are going to make the assumption that the starling data are not

spatially correlated. However, future work should focus on providing methods for analysing and correcting (if needed) spatial autocorrelation in SE-IPMs.

There are many possible combinations of covariates that can be fitted. We start by fitting the constant model, and then we add covariates in a "forward selection" fashion, starting with the adult survival probability ϕ_a. Here we include five "forward selection" steps, in each step the best model is highlighted in bold. In step 1, we add one spatial covariate, either in terms of coordinates or type of land, to the adult survival probability and we keep the first-year survival constant. We choose the model with the lowest AIC and we use this as the starting model for step 2. In step 2, we add one spatial covariate to the first-year survival probability and for the adult survival probability we use the best model in terms of AIC selected in step 1. In step 3, we use the best model selected in step 2 and we add an additional covariate to the adult survival probability. We proceed similarly in steps 4 and 5. We stop in step 5, as the best model in this step is not better than the best model in step 4. Moreover by adding more covariates than those in step 5 the model becomes overparameterised and starts showing signs of near-parameter redundancy caused by the lack of data.

Table 5.7 shows the model comparison for the models fitted following the "forward selection" approach starting with the adult survival probability ϕ_a. Additional fitted models to those resulting from the "forward selection" procedure with additional covariates can be found in Appendix D TableD.8.

Table 5.7 shows five "forward selection" steps starting with ϕ_a. In Table 5.7 we find that the best model in terms of AIC is that which depends quadratically on the latitude for adult survival, and on urban and farm covariates for the first-year survival. Followed by the second and third best models in terms of AIC which are similar to the best model, but in the second best, first-year survival on urban and latitude and in the third best,first-year survival only depends on urban information.

Table 5.7 Model comparison for the constant and SE-IPMs fitted for the starling data for the years 1990-1999. We start with a constant model, and then add covariates, starting with the adult survival probability ϕ_a in a forward selection fashion.

Model	No. pars	AIC	Δ AIC
ϕ_a, ϕ_1	6	11,918.44	65.57
$\phi_{a,(lat)}, \phi_1$	7	**11,891.83**	38.96
$\phi_{a,(long)}, \phi_1$	7	11,907.28	54.41
$\phi_{a,(farm)}, \phi_1$	7	11,910.23	57.36
$\phi_{a,(grass)}, \phi_1$	7	11,918.19	65.32
$\phi_{a,(urban)}, \phi_1$	7	11,909.99	57.12
$\phi_{a,(water)}, \phi_1$	7	11,913.66	60.79

Table 5.7 – continued from previous page

Model	No. pars	AIC	Δ AIC
$\phi_{a,(wood)}, \phi_1$	7	11,917.48	64.61
$\phi_{a,(lat)}, \phi_{1,(lat)}$	8	11,883.78	30.91
$\phi_{a,(lat)}, \phi_{1,(long)}$	8	11,895.05	42.18
$\phi_{a,(lat)}, \phi_{1,(farm)}$	8	11,886.05	33.18
$\phi_{a,(lat)}, \phi_{1,(grass)}$	8	11,890.01	37.14
$\phi_{a,(lat)}, \phi_{1,(urban)}$	8	**11,864.56**	11.69
$\phi_{a,(lat)}, \phi_{1,(wood)}$	8	11,891.29	38.42
$\phi_{a,(lat)}, \phi_{1,(water)}$	8	11,897.54	44.67
$\phi_{a,(lat+long)}, \phi_{1,(urban)}$	9	11,866.17	13.30
$\phi_{a,(lat+lat^2)}, \phi_{1,(urban)}$	9	**11,856.94**	4.07(3)
$\phi_{a,(lat+farm)}, \phi_{1,(urban)}$	9	11,865.20	12.33
$\phi_{a,(lat+grass)}, \phi_{1,(urban)}$	9	11,866.36	13.49
$\phi_{a,(lat+urban)}, \phi_{1,(urban)}$	9	11,866.46	13.59
$\phi_{a,(lat+water)}, \phi_{1,(urban)}$	9	11,866.28	13.41
$\phi_{a,(lat+wood)}, \phi_{1,(urban)}$	9	11,864.78	11.91
$\phi_{a,(lat+lat^2)}, \phi_{1,(urban+lat)}$	10	11,854.98	2.11(2)
$\phi_{a,(lat+lat^2)}, \phi_{1,(urban+long)}$	10	11,858.73	5.86(4)
$\phi_{a,(lat+lat^2)}, \phi_{1,(urban+farm)}$	10	**11,852.87**	0.00 (1)
$\phi_{a,(lat+lat^2)}, \phi_{1,(urban+grass)}$	10	11,858.74	5.87(5)
$\phi_{a,(lat+lat^2)}, \phi_{1,(urban+water)}$	10	11,859.24	6.37
$\phi_{a,(lat+lat^2+long)}, \phi_{1,(urban+farm)}$	11	11,899.04	46.17
$\phi_{a,(lat+lat^2+farm)}, \phi_{1,(urban+farm)}$	11	11,898.62	45.75
$\phi_{a,(lat+lat^2+grass)}, \phi_{1,(urban+farm)}$	11	11,899.66	46.79
$\phi_{a,(lat+lat^2+urban)}, \phi_{1,(urban+farm)}$	11	11,898.84	45.97
$\phi_{a,(lat+lat^2+water)}, \phi_{1,(urban+farm)}$	11	**11,889.20**	36.33
$\phi_{a,(lat+lat^2+wood)}, \phi_{1,(urban+farm)}$	11	11,899.97	47.10

The parameter estimates for the constant model and the best model in term of AIC are shown in Table 5.8. The spatially-explicit survival probabilities for the best model are presented in Figures 5.6 - 5.8. Moreover, Figures D.1-D.6 show the spatially-explicit survival probabilities for the second and third models in terms of AIC. These figures are heat maps obtained from extending by region the point estimates from our models. The heat maps were created by calculating the minimal distance between the estimated points and each of the geographical points of the polygons that define each region. We present the heat maps to

highlight the spatial patterns. However, the specific spatial point estimates obtained from the models can be found in Figures D.7-D.12. For all the models the survival probabilities and the confidence intervals are between 0.3 and 0.9, so in order to compare the survival probabilities between models and the two age categories we provide this scale in our figures. However, for the adult survival probability providing this scale means that no spatial pattern can be appreciated, as adult survival changes with space between 0.69 and 0.75. For this reason, we provide additional close up maps for the adult survival probabilities.

Our results confirm that starlings are affected by location. The three best models have the same covariates for the adult survival probability, in Figure D.6 we can appreciate that the adult survival probabilities for starlings change with latitude, increasing as we approach North. For the first-year starlings, our results do not change much between models. For these, survival is lower in the south east and centre of Great Britain, particularly for first-year starlings, where there are more urban areas.

Additionally, in Appendix D.2 we provide a comparison between the IPMs and the separate models (i.e. SSMs and ring-recovery models). To do this we compare the results obtained from the best models in terms of AIC presented in Table 5.7 for each step of the "forward selection" procedure with the results obtained from fitting ring-recovery and state-space models with similar parameterisations. We find that for our data, for the constant models there is little improvement from fitting an IPM instead of a ring-recovery model. Still, the IPM is able to estimate productivity parameters, which we cannot obtain from any of the other models, as the SSM is parameter redundant. Moreover, for the spatially-explicit data the standard errors decrease when using SE-IPMs to fit the data instead of ring-recovery models. Using a SE-IPM is an improvement over separate models, because it allows the estimation of the productivity parameter, as well as improving precision of other parameters.

Table 5.8 Parameter estimates, with standard errors given in parentheses, for the constant IPM, and the best SE-IPM in terms of AIC.

Pars		Constant Model	Best Model
ϕ_a	α_1	0.660(0.101)	0.669(0.101)
	β_{lat_1}	-	0.160(0.083)
	$\beta_{lat_1^2}$	-	0.170(0.048)
ϕ_1	α_1	0.546(0.021)	1.041(0.151)
	β_{urban}	-	-0.057(0.011)
	β_{farm}	-	- 0.011(0.004)
ρ		0.550(0.050)	0.535(0.050)
σ_η		15.523(1.55)	16.520(2.037)
μ		17.838(2.263)	14.941(1.517)
λ		0.016(0.001)	0.017(0.001)

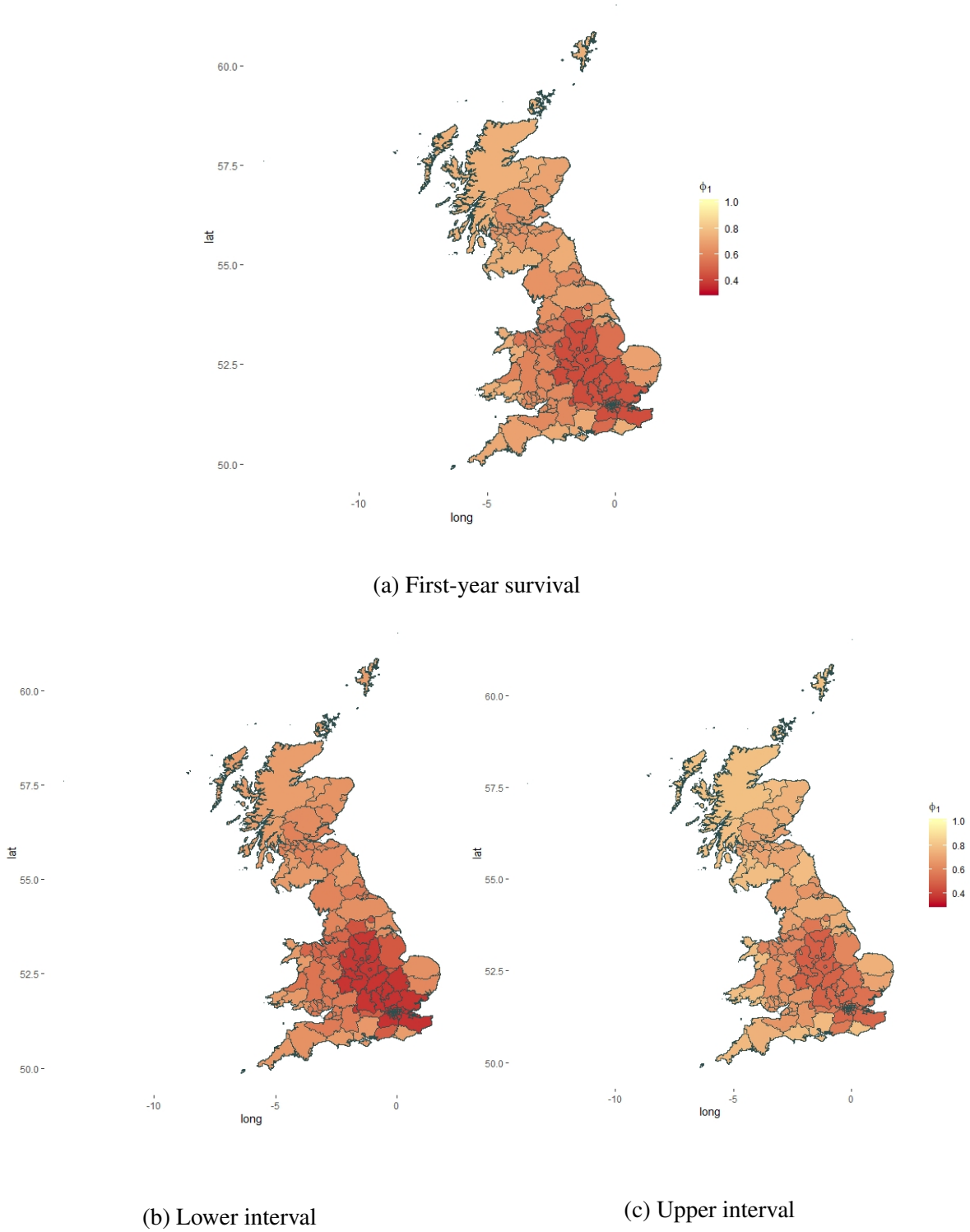

(a) First-year survival

(b) Lower interval

(c) Upper interval

Fig. 5.6 Heat maps for best model in terms of AIC: Survival probability and 95% confidence intervals for first-year starlings for the years 1990-1999.

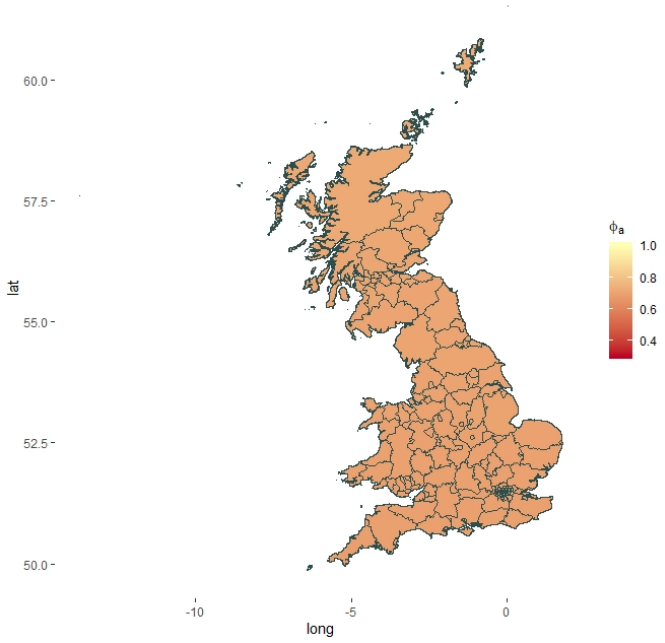

(a) Adult survival

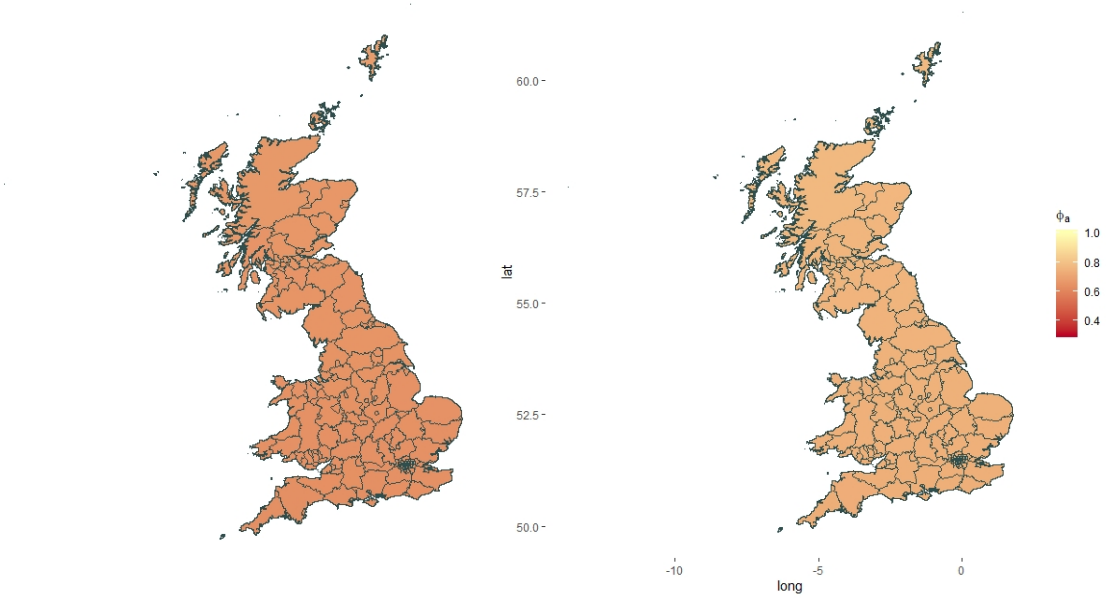

(b) Lower interval

(c) Upper interval

Fig. 5.7 Heat maps for best model in terms of AIC: Survival probability and 95% confidence intervals for adult starlings for the years 1990-1999.

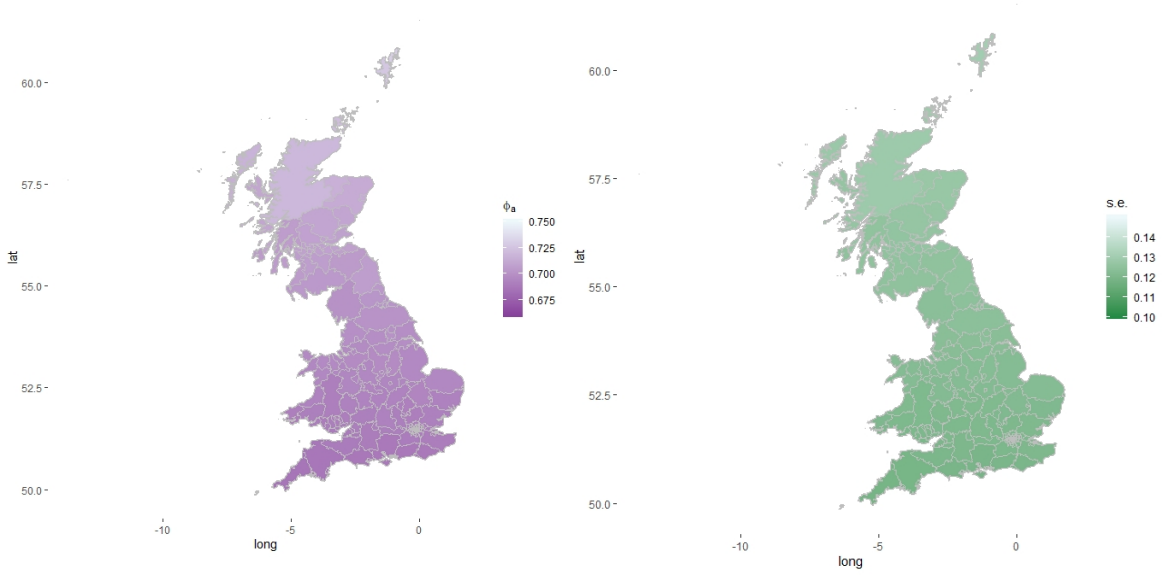

(a) Adult survival

(b) Standard errors

Fig. 5.8 Adult survival probability and standard errors for the best model in terms of AIC for starlings for the years 1990-1999.

5.5 Discussion

In this chapter we have assembled a spatially-explicit integrated population model which jointly analyses spatial ring-recovery and census data. The SE-IPM proposed here allows for the combination of spatial data at different spatial resolutions, enabling us to cover wider areas of the country than in using either type of data on their own. The models developed here include spatial data in the form of geographical coordinates and land cover covariates.

We illustrated our models using starling data. The best model in terms of AIC depended quadratically on latitude for adult survival, and additionally on latitude and urban information for the first-year survival. Urban areas may offer more limited invertebrate food for young starlings which may explain reduced survival there. The latitude relationships are likely linked to damper, cooler conditions with more grassland in northern and western areas, leading to higher abundance of soil invertebrates on which starlings feed (Dunnet, 1955). Additionally, we compared the results obtained from our data from fitting IPMs and separate models. We found that when spatial information is available the SE-IPMS provide more precise results which can be appreciated by a decrease in the standard errors.

The models presented here can be easily extended through the addition of other types of spatial/geographical information such as altitude, or weather. Brown (2010) describes how to add weather covariates for animal survival modelling. Moreover, these models can be also extended through the incorporation of other demographic data, such as nest data, which would help our understanding regarding productivity estimates, and would enable the addition of spatial components, not just to the survival probabilities, but also to the productivity rates.

Additionally, spatial information could be added to the productivity parameter, ρ, in the same way that it was added for the survival parameters. We built models in which we added the spatial information to the productivity parameter and we tried to fit the starling data. However, given the limited information, i.e. for the census spatial data, which provides information on productivity, we only consider 15 squares, and with 10 of these squares containing small counts, when fitting these models, the likelihood could not be optimised. It would be interesting to run similar models for other species for which more spatial census data are available. Nonetheless, if this extension of the model is considered, the bias issue in the estimation of the productivity parameter, ρ, should be investigated further.

An important aspect of this model is that it allows the use of spatially-explicit small valued time-series census data sets in combination with other census data sets which contain larger values, and spatially-explicit ring-recory data sets. Additionally, the SE-IPMs could be enhanced by adding temporal components, such as temporal trends. Along this line, we could also look at the analysis of longer time periods, which would allow us to understand the

population dynamics of different species. For more recent periods, it would be advantageous to incorporate BBS data, which is a more recent version of the CBC data collected by the BTO, for which small changes in the observation process of the SSM would be needed. Joint trends based on CBC and BBS data are now widely reported by the BTO. Robinson et al. (2014) used joint CBC/BBS trends for a range of species within IPMs.

Although for starlings, we assume that there is no spatial autocorrelation, future work in this area should prioritise the development of methods to analyse and correct spatial autocorrelation which might be present in the data of many species. By doing so, the SE-IPM should be transferable to species characterised for their small dispersal. Additionally, by incorporating parameters that account for bird migration in this model, we would allow the use of the SE-IPM to model the spatial survival within a country for a wider range of species.

Furthermore if the data are available, it is possible to add land cover data for both the ring-recovery and the census data at smaller spatial resolutions, such as 10 by 10 km squares. This can be computationally expensive, and as such avenues for optimising the computational times shall be explored. If this is done, not only the precision of the model would increase but also more specific land cover categories could be added.

We note that for the census data we made the assumption that all squares have the same initial state distribution. We did this, in order to limit the number of parameters in the model. However, extensions to this work can be considered where for example a distribution for μ can be assumed, so the flexibility of the modelling framework increases.

The spatially-explicit IPMs presented here allow for individual heterogeneity in the survival probabilities, however this heterogeneity is only considered in terms of location. Other sources of variations such as sex or additional age classes for the individuals can be easily added.

Some of the extensions discussed here consist of the introduction of covariates and/or parameter dependencies. As a result the number of possible models to fit increases substantially. Thus, it would be advantageous to develop additional model selection and goodness of fit methods. Besbeas and Morgan (2014) and Besbeas et al. (in prep.) developed model selection and goodness of fit methodology for IPMs. These could be extended to incorporate spatial information.

We have fitted the SE-IPMs using a frequentist approach, however this model could be adapted to a Bayesian approach and it would be interesting to compare the benefits of using each method.

Chapter 6

Discussion

In this thesis we have examined and further developed a number of statistical methods to address different ecological data challenges. As a result, this thesis consists of three main projects that combine different types of data together. The data sets that motivated the work in this thesis, or that were used to illustrate our methods, were characterised by the presence of missing, sparse and/or spatial information.

In Chapter 1 we introduced the reader to the statistical and ecological topics that are covered and extended throughout the thesis. In this chapter, we defined the general forms of marking, and census data, as well as, statistical models for marking data, discrete state-space models (SSMs), and integrated population models. Additionally, we defined parameter redundancy and provided details for the model fitting and model comparison methods implemented throughout the thesis.

In Chapter 2 we presented our work on analysing historical age-aggregated ring-recovery data sets to estimate age-dependent survival (Jiménez-Muñoz et al., 2019). Here, we described a new model to estimate age-dependent survival probabilities from historical data when information on age at ringing is missing. Using simulation and a data set where the ringing numbers are known by age category, we demonstrated that the historical data model gave almost identical parameter estimates as the standard ring-recovery model. In this chapter we estimated probabilities for two age categories: first year and adult birds. However, with the addition of an age-mixture model (McCrea et al., 2013) the historical model could be extended to incorporate other age dependencies that accommodate for differences in breeding age between species. Data from the British Trust for Ornithology (BTO) on sandwich terns and blackbirds were used to illustrate these methods. Although this work was motivated based on data from the BTO, many national ringing schemes, in Europe and North America (Tautin, 2008), face a similar challenge. Thus, rather than fully computerising historical data, by implementing these models, many organisations could save on human and time resources.

In Chapter 3 we used capture-recapture models to examine the timing of female brood desertion and the survival of the little auk *Alle alle*. To that effect, we considered extensions to the Cormack-Jolly-Seber capture-recapture models through the addition of categorical (sex, site) and continuous covariates (the time at which the female deserted the brood, i.e. presence data). The categorical covariates were easily included in the model, as they were constant throughout all the years of study and were known regardless of encounter. To validate the models we performed a simulation study, and we found that the models performed better when used to analyse large data sets. Moreover, results also improved when the survival and capture probabilities were fixed higher. This was true particularly in the cases in which several dependencies were added. The continuous covariates for the little auk data were very sparse, with missing values in the years in which individuals were not observed. Thus, although several methods for fitting capture-recapture and more generally mark-recapture-recovery data in the presence of continuous covariates were available (see for example, Bonner et al., 2010; Langrock and King, 2013; Worthington et al., 2015) a deterministic imputation method was used. We performed a simulation study to examine the accuracy of our deterministic imputation method. We found that when the sample size decreased, the MSE increased, and that the survival parameters were overestimated when the data sets contained abundant missing data.

From analysing the little auk data in Chapter 3, we found that the survival probability was lower in the site with more extreme weather conditions. However, the survival probability did not appear to be affected by the sex of the individuals analysed. This could mean that the female little auk does not deteriorate more when breeding than its male counterpart. Additionally, our results also showed that the survival of female little auks increased as the length of stay of the mother in the brood increased. However the standard errors for these parameters were large, meaning that these results were not really conclusive. We recommended that further data should be collected in order to make conclusions regarding the effect of the length of stay of the female in the brood on survival probability.

Chapters 4 and 5 were closely related and focused on the development of a spatially-explicit integrated population (SE-IPM) model for spatial ring-recovery and spatial census data. The complementary schemes through which the British Trust for Ornithology collect data motivated this work.

Chapter 4 described and implemented the methodology needed to fit discrete SSMs for population census data of different sizes. We directly compared two model fitting methodologies for discrete SSMs—the Kalman filter (KF) and hidden Markov models (HMMs). These were implemented within a frequentist framework. Additionally we investigated the results of King et al. (2008b), and Abadi et al. (2010), who used a Bayesian approach to fit similar

SSMs. All the methods were revised in the context of an integrated population model (IPM), as the SSMs model when fitted alone is parameter redundant. We compared our methods using simulations for different sample sizes and found that if time-series containing small counts are used, a systematic negative bias appears in the estimation of the productivity parameter, ρ. Moreover, we found that this bias also appeared in the results of Abadi et al. (2010), albeit to a lesser degree due to the larger data sizes considered in that case. We used a non-stationary Poisson process to investigate the reason for this bias. We found that the dependence on previous values in the time-series when small counts were used resulted in the skewness of the distribution to the left. We concluded that this was the cause of the bias, rather than the set up of the SSMs or the methods used to implement it. Additionally, the bias was more pronounced when the KF was used to fit time-series data sets. The KF is computationally faster than using HMMs. As the bias reduced when we increased the sample size, we recommended to use the KF to fit time-series data when the average count size is at least 40, and HMMs otherwise. However we warned that caution should be taken when dealing with really small counts.

In the future, it would be advantageous to compare our results directly to those obtained from fitting the same models using a Bayesian approach. Additionally, the effect on the bias of adding additional data, such as nest data, should be further investigated. Finally, theoretical methods that would allow to identify potential bias from time-series data sets could be developed.

The SE-IPM presented in Chapter 5 combined several time-series data sets, of different sizes. Thus, in Chapter 4 we also performed a simulation study to examine the effect on the bias if several time-series data sets were combined, and these contained counts of different sizes. We recommended that if time-series data sets with small counts are analysed, i.e. if the counts are on average smaller than 40, these should be combined with larger data sets so the bias issue is mitigated. The development of methods that can improve the bias issue is a topic of future work.

In Chapter 5 we assembled an SE-IPM, which was formed from the combination of spatially explicit ring-recovery and census data. To do this, we added spatial information in the form of geographical coordinates and/or land cover data to the survival parameters of the ring-recovery and the SSMs. To make the model more efficient and accurate, we combined both HMMs and the KF to fit the several time-series data sets available for the spatial data. We were able to do this following the recommendations of Chapter 4. To show how our methods performed in practice we used data for starlings.

SE-IPMs are a relatively novel idea. The work of Chapter 5 focused on accommodating spatially-explicit ring-recovery and census data at different spatial resolutions and for extreme

cases when the time-series data were very sparse. Thus, we built the foundations for these models, and several extensions are possible. In Chapter 5 we introduced the spatially-explicit information in IPMs through the survival probabilities. Hence, one natural extension would be to investigate the effect of adding spatial information to different parameters such as productivity. Moreover for the census data we assumed that for each of the squares that were fitted using HMMs, the initial distribution followed a Poisson distribution with mean μ. To avoid overparameterisation the estimate of μ was shared for all the squares. In the future, alternatives to this limitation should be studies. For example, a distribution for μ could be assumed, so the flexibility of the modelling framework increases.

For the SE-IPMs presented in Chapter 5 we included spatial information in the form of geographical coordinates and land cover types. Further work should consider the addition of alternative spatial/geographical information such as altitude or weather. Additionally, besides ring-recovery and census data other demographic data, such as nest data, could be incorporated to the models. This would not only improve our understanding of productivity estimates, but also would enable the addition of spatial information to productivity rates.

SE-IPMs would really benefit from the addition of temporal components. These would allow to identify time-trends in demographic parameters and would help us understand better the demographic processes affecting animal populations. However, an in depth investigation on the effects of using spatio-temporal components to analyse these types of data would be needed. If the data are insufficient it might not be possible to describe both spatial and temporal effects. Moreover, spatio-temporal correlation issues would need to be investigated and dealt with.

These models are applicable to many bird species. Thus, it would be beneficial to develop open access computer software which would make the implementation of SE-IPMs easier. These models could impact conservation policies by helping experts better identify the particular areas of a country where specific species are declining.

References

Abadi, F., Gimenez, O., Arlettaz, R., and Schaub, M. (2010). An assessment of integrated population models: Bias, accuracy, and violation of the assumption of independence. *Ecology*, 91(1):7–14.

Akaike, H. (1974). A new look at the statistical model identification. In *Selected Papers of Hirotugu Akaike*, pages 215–222. Springer.

Anderson, D. and Burnham, K. (2004). Model selection and multi-model inference. *Second. NY: Springer-Verlag*, 63.

Baillie, S. R. (1990). Integrated population monitoring of breeding birds in Britain and Ireland. *Ibis*, 132(2):151–166.

Baillie, S. R., Brooks, S. P., King, R., and Thomas, L. (2009). Using a state-space model of the British song thrush *Turdus philomelos* population to diagnose the causes of a population decline. In *Modeling Demographic Processes in Marked Populations*, pages 541–561. Springer.

Besbeas, P., Borysiewicz, R. S., and Morgan, B. J. T. (2009). Completing the ecological jigsaw. In *Modeling Demographic Processes in Marked Populations*, pages 513–539. Springer.

Besbeas, P. and Freeman, S. N. (2006). Methods for joint inference from panel survey and demographic data. *Ecology*, 87(5):1138–1145.

Besbeas, P., Freeman, S. N., and Morgan, B. J. T. (2005). The potential of integrated population modelling. *Australian & New Zealand Journal of Statistics*, 47(1):35–48.

Besbeas, P., Freeman, S. N., Morgan, B. J. T., and Catchpole, E. A. (2002). Integrating mark–recapture–recovery and census data to estimate animal abundance and demographic parameters. *Biometrics*, 58(3):540–547.

Besbeas, P., McCrea, R. S., and Morgan, B. J. T. (in prep.). Integrated population model selection in ecology. *Manuscript in preparation*.

Besbeas, P. and Morgan, B. J. T. (2012). Kalman filter initialization for integrated population modelling. *Journal of the Royal Statistical Society: Series C (Applied Statistics)*, 61(1):151–162.

Besbeas, P. and Morgan, B. J. T. (2014). Goodness-of-fit of integrated population models using calibrated simulation. *Methods in Ecology and Evolution*, 5(12):1373–1382.

Besbeas, P. and Morgan, B. J. T. (2018). A general framework for modelling population survey data. *Technical report, University of Kent, Canterbury CT2 7FS, England*.

Besbeas, P. and Morgan, B. J. T. (2019). Exact inference for integrated population modelling. *Biometrics* advanced online publication:https://doi.org/10.1111/biom.13045.

Bishop, G. and Welch, G. (2001). An introduction to the Kalman filter. *Proc of SIGGRAPH, Course*, 8(41):27599–23175.

Bonner, S. J., Morgan, B. J. T., and King, R. (2010). Continuous covariates in mark-recapture-recovery analysis: A comparison of methods. *Biometrics*, 66(4):1256–1265.

Bonner, S. J. and Schwarz, C. J. (2006). An extension of the Cormack–Jolly–Seber model for continuous covariates with application to microtus pennsylvanicus. *Biometrics*, 62(1):142–149.

Brooks, S. P., King, R., and Morgan, B. J. T. (2004). A Bayesian approach to combining animal abundance and demographic data. *Animal Biodiversity and Conservation*, 27(1):515–529.

Brown, D. I. (2010). *Climate Modelling for Animal Survival*. PhD thesis, University of Kent.

Brownie, C., Anderson, D. R., Burnham, K. P., and Robson, D. S. (1985). *Statistical Inference from Band Recovery Data - A Handbook*. Resource Publication (No. 156). United States Department of the Interior, Fish and Wildlife Service, Washington, DC.

BTO-Website (2017). British Trust for Ornithology Website: Ringing scheme. http://www.bto.org/volunteer-surveys/ringing/about. [Online; accessed 15-04-2018].

Buckland, S. T., Newman, K. B., Thomas, L., and Kösters, N. (2004). State-space models for the dynamics of wild populations. *Ecological Modelling*, 171(1–2):157–175.

Caswell, H. (2001). *Matrix Population Models: Construction, Analysis, and Interpretation (2nd edn.)*. Sinauer Associates Incorporated, U.S.

Catchpole, E. A., Freeman, S. N., Morgan, B. J. T., and Harris, M. P. (1998). Integrated recovery/recapture data analysis. *Biometrics*, 54(1):33–46.

Catchpole, E. A., Kgosi, P. M., and Morgan, B. J. T. (2001). On the near-singularity of models for animal recovery data. *Biometrics*, 57(3):720–726.

Catchpole, E. A. and Morgan, B. J. T. (1996). Model selection in ring-recovery models using score tests. *Biometrics*, 52(2):664–672.

Catchpole, E. A. and Morgan, B. J. T. (1997). Detecting parameter redundancy. *Biometrika*, 84(1):187–196.

Catchpole, E. A., Morgan, B. J. T., and Tavecchia, G. (2008). A new method for analysing discrete life history data with missing covariate values. *Journal of the Royal Statistical Society: Series B (Statistical Methodology)*, 70(2):445–460.

Chandler, R. B. and Clark, J. D. (2014). Spatially explicit integrated population models. *Methods in Ecology and Evolution*, 5(12):1351–1360.

Chandler, R. B., Hepinstall-Cymerman, J., Merker, S., Abernathy-Conners, H., and Cooper, R. J. (2018). Characterizing spatio-temporal variation in survival and recruitment with integrated population models. *The Auk*, 135(3):409–426.

Chis, O.-T., Villaverde, A. F., Banga, J. R., and Balsa-Canto, E. (2016). On the relationship between sloppiness and identifiability. *Mathematical Biosciences*, 282:147–161.

Choquet, R. and Cole, D. J. (2012). A hybrid symbolic-numerical method for determining model structure. *Mathematical Biosciences*, 236(2):117–125.

Choquet, R., Reboulet, A. M., Pradel, R., Gimenez, O., and Lebreton, J.-D. (2004). M–SURGE: New software specifically designed for multistate capture–recapture models. *Animal Biodiversity and Conservation*, 27(1):207–215.

Choquet, R., Rouan, L., and Pradel, R. (2009). Program E-SURGE: A software application for fitting multievent models. In *Modeling Demographic Processes in Marked Populations*, pages 845–865. Springer.

Cole, D. J. (2019). Parameter redundancy and identifiability in hidden Markov models. *Metron*, 77:105–118.

Cole, D. J. and McCrea, R. S. (2016). Parameter redundancy in discrete state-space and integrated models. *Biometrical Journal*, 58(5):1071–1090.

Cole, D. J., Morgan, B. J. T., Catchpole, E. A., and Hubbard, B. A. (2012). Parameter redundancy in mark-recovery models. *Biometrical Journal*, 54(4):507–523.

Cole, D. J., Morgan, B. J. T., and Titterington, D. (2010). Determining the parametric structure of models. *Mathematical Biosciences*, 228(1):16–30.

Cormack, R. M. (1964). Estimates of survival from the sighting of marked animals. *Biometrika*, 51(3–4):429–438.

Coulson, J. (1961). The post-fledging mortality of the blackbird in Great Britain. *Bird Study*, 8(2):89–97.

Cowen, L. and Schwarz, C. J. (2006). The Jolly–Seber model with tag loss. *Biometrics*, 62(3):699–705.

Dormann, C. F., McPherson, J. M., Araújo, M. B., Bivand, R., Bolliger, J., Carl, G., Davies, R. G., Hirzel, A., Jetz, W., Kissling, W. D., Kühn, I., Ohlemüller, R., Peres-Neto, P. R., Reineking, B., Schröder, B., Schurr, F. M., and Wilson, R. (2007). Methods to account for spatial autocorrelation in the analysis of species distributional data: A review. *Ecography*, 30(5):609–628.

Du Feu, C. R., Clark, J. A., Schaub, M., Fiedler, W., and Baillie, S. R. (2016). The EURING Data Bank—a critical tool for continental-scale studies of marked birds. *Ringing & Migration*, 31(1):1–18.

Dunnet, G. M. (1955). The breeding of the Starling *Sturnus vulgaris* in relation to its food supply. *Ibis*, 97(4):620–662.

Eaton, M., Aebischer, N., Brown, A., Hearn, R., Lock, L., Musgrove, A., Noble, D., Stroud, D., and Gregory, R. (2015). Birds of conservation concern 4: the population status of birds in the UK, Channel Islands and Isle of Man. *British Birds*, 108:708–746.

Evans, J. (1998). *The History and Practice of Ancient Astronomy*. Oxford University Press.

Faragher, R. (2012). Understanding the basis of the Kalman filter via a simple and intuitive derivation. *IEEE Signal Processing Magazine*, 29(5):128–132.

Finke, A., King, R., Beskos, A., and Dellaportas, P. (2019). Efficient sequential Monte Carlo algorithms for integrated population models. *Journal of Agricultural, Biological and Environmental Statistics*, 24(2):204–224.

Freeman, S. N. and Morgan, B. J. T. (1992). A modelling strategy for recovery data from birds ringed as nestlings. *Biometrics*, 48(1):217–235.

Freeman, S. N., Noble, D. G., Newson, S. E., and Baillie, S. R. (2007a). Modelling population changes using data from two different surveys: the Common Birds Census and the Breeding Bird Survey. *Bird Study*, 54:61–72.

Freeman, S. N., Robinson, R. A., Clark, J. A., Griffin, B. M., and Adams, S. Y. (2007b). Changing demography and population decline in the common Starling *Sturnus vulgaris*: A multisite approach to integrated population monitoring. *Ibis*, 149(3):587–596.

Fuller, R. J., Marchant, J. H., and Morgan, R. A. (1985). How representative of agricultural practice in Britain are Common Birds Census farmland plots? *Bird Study*, 32(56-70).

Fuller, R. M., Groom, G. B., and Jones, A. R. (1994a). The land-cover map of Great Britain: An automated classification of Landsat Thematic Mapper data. *Photogrammetric Engineering and Remote Sensing*, 60(5):553–562.

Fuller, R. M., Groom, G. B., and Wallis, S. M. (1994b). The availability of Landsat TM images of Great Britain. *International Journal of Remote Sensing*, 15(6):1357–1362.

Gauthier, G. and Lebreton, J. D. (2008). Analysis of band-recovery data in a multistate capture-recapture framework. *Canadian Journal of Statistics*, 36(1):59–73.

Gimenez, O., Viallefont, A., Catchpole, E. A., Choquet, R., and Morgan, B. J. T. (2004). Methods for investigating parameter redundancy. *Animal Biodiversity and Conservation*, 27(1):561–572.

Greenwood, J. J. (2009). 100 years of ringing in Britain and Ireland. *Ringing & Migration*, 24(3):147–153.

Gregory, R. D. and Baillie, S. R. (1998). Large-scale habitat use of some declining British birds. *Journal of Applied Ecology*, 35(5):785–799.

Gregory, R. D., Baillie, S. R., and Bashford, R. I. (2000). Monitoring breeding birds in the United Kingdom. *Bird Census News*, 13:101–112.

Gregory, R. D., Wilkinson, N. I., Noble, D. G., Robinson, J. A., Brown, A. F., Hughes, J., Procter, D., Gibbons, D. W., and Galbraith, C. A. (2002). The population status of birds in the United Kingdom, Channel Islands and Isle of Man. *British Birds*, 95:410–448.

Grewal, M. S. and Andrews, A. P. (2001). *Kalman Filtering: Theory and Practice Using Matlab*. Wiley.

Grid Reference Finder (2019). Grid reference finder. https://gridreferencefinder.com/. [Online; accessed 22-01-2019].

Haldane, J. (1955). The calculation of mortality rates from ringing data. In *Proc. Int. Ornithol. Congr.*, volume 11, pages 454–458.

Harding, A. M., Van Pelt, T. I., Lifjeld, J. T., and Mehlum, F. (2004). Sex differences in Little auk *Alle alle* parental care: Transition from biparental to paternal-only care. *Ibis*, 146(4):642–651.

Hoenig, J. M., Pollock, K. H., and Hearn, W. (2005). Tag-recovery models. In Amstrup, S. C., Mcdonald, T. L., and Manly, B. F. J., editors, *Handbook of Capture-Recapture Analysis*, pages 124–141. Princeton University Press, New Jersey, USA.

Hubbard, B. A., Cole, D. J., and Morgan, B. J. T. (2014). Parameter redundancy in capture-recapture-recovery models. *Statistical Methodology*, 17:17–29.

Isaksen, K. and Gavrilo, M. (2000). Little auk *Alle alle*. *The status of marine birds breeding in the Barents Sea Region. Tromso: Norsk Polarinstitutt, Rapportserie*, 113:131–136.

Jackson, C. H. (2011). Multi-state models for panel data: The msm package for R. *Journal of Statistical Software*, 38(8):1–29.

Jakubas, D., Głuchowska, M., Wojczulanis-Jakubas, K., Karnovsky, N. J., Keslinka, L., Kidawa, D., Walkusz, W., Boehnke, R., Cisek, M., Kwaśiewski, S., et al. (2011). Foraging effort does not influence body condition and stress level in little auks. *Marine Ecology Progress Series*, 432:277–290.

Jakubas, D., Iliszko, L., Wojczulanis-Jakubas, K., and Stempniewicz, L. (2012). Foraging by little auks in the distant marginal sea ice zone during the chick-rearing period. *Polar Biology*, 35(1):73–81.

Jakubas, D. and Wojczulanis, K. (2007). Predicting the sex of dovekies by discriminant analysis. *Waterbirds*, 30(1):92–97.

Jakubas, D. and Wojczulanis-Jakubas, K. (2013). Rates and consequences of relaying in little auks *Alle alle* breeding in the High Arctic an experimental study with egg removal. *Journal of Avian Biology*, 44(1):062–068.

Jakubas, D., Wojczulanis-Jakubas, K., Iliszko, L., Darecki, M., and Stempniewicz, L. (2014). Foraging strategy of the little auk Alle alle throughout breeding season–switch from unimodal to bimodal pattern. *Journal of Avian Biology*, 45(6):551–560.

Jiménez-Muñoz, M., Cole, D. J., Freeman, S. N., Robinson, R. A., Baillie, S. R., and Matechou, E. (2019). Estimating age-dependent survival from age-aggregated ringing data—extending the use of historical records. *Ecology and Evolution*, 9(2):769–779.

Jolly, G. M. (1965). Explicit estimates from capture-recapture data with both death and immigration-stochastic model. *Biometrika*, 52(1-2):225–247.

Kalman, R. E. (1960). A new approach to linear filtering and prediction problems. *Journal of Basic Engineering*, 82(1):35–45.

Keslinka, L. K., Wojczulanis-Jakubas, K., Jakubas, D., and Neubauer, G. (2019). Determinants of the little auk *(Alle alle)* breeding colony location and size in W and NW coast of Spitsbergen. *PloS One*, 14(3):e0212668.

Kidawa, D., Jakubas, D., Wojczulanis-Jakubas, K., Iliszko, L., and Stempniewicz, L. (2012). The effects of loggers on the foraging effort and chick-rearing ability of parent little auks. *Polar Biology*, 35(6):909–917.

King, R. and Brooks, S. (2002a). Model selection for integrated recovery/recapture data. *Biometrics*, 58(4):841–851.

King, R. and Brooks, S. (2002b). Bayesian model discrimination for multiple strata capture-recapture data. *Biometrika*, 89(4):785–806.

King, R. and Brooks, S. P. (2003). Survival and spatial fidelity of mouflons: The effect of location, age, and sex. *Journal of Agricultural, Biological, and Environmental Statistics*, 8(4):486.

King, R., Brooks, S. P., and Coulson, T. (2008a). Analyzing complex capture–recapture data in the presence of individual and temporal covariates and model uncertainty. *Biometrics*, 64(4):1187–1195.

King, R., Brooks, S. P., Mazzetta, C., Freeman, S. N., and Morgan, B. J. T. (2008b). Identifying and diagnosing population declines: a Bayesian assessment of lapwings in the UK. *Journal of the Royal Statistical Society: Series C (Applied Statistics)*, 57(5):609–632.

King, R., Morgan, B. J. T., Gimenez, O., and Brooks, S. (2009). *Bayesian Analysis for Population Ecology*. Chapman and Hall/CRC.

Knape, J., Jonzén, N., and Sköld, M. (2011). On observation distributions for state space models of population survey data. *Journal of Animal Ecology*, 80(6):1269–1277.

Langrock, R. and King, R. (2013). Maximum likelihood estimation of mark–recapture–recovery models in the presence of continuous covariates. *The Annals of Applied Statistics*, 7(3):1709–1732.

Lebreton, J.-D., Burnham, K. P., Clobert, J., and Anderson, D. R. (1992). Modeling survival and testing biological hypotheses using marked animals: A unified approach with case studies. *Ecological Monographs*, 62(1):67–118.

Leslie, P. H. (1945). On the use of matrices in certain population mathematics. *Biometrika*, 33(3):183–212.

Little, R. J. A. and Rubin, D. B. (2002). Bayes and multiple imputation. *Statistical Analysis with Missing Data*, pages 200–220.

Marchant, J. (1983). BTO Common Bird Census instructions. *British Trust for Ornithology, Tring*.

Marchant, J., Hudson, R., Carter, S. P., and Whittington, P. (1990). Population trends in British breeding birds. *British Trust for Ornithology, Tring*.

Martin, K. (1995). Patterns and mechanisms for age-dependent reproduction and survival in birds. *American Zoologist*, 35(4):340–348.

McCrea, R. S. and Morgan, B. J. T. (2015). *Analysis of Capture-Recapture Data*. Chapman & Hall, London.

McCrea, R. S., Morgan, B. J. T., Brown, D. I., and Robinson, R. A. (2012). Conditional modelling of ring-recovery data. *Methods in Ecology and Evolution*, 3(5):823–831.

McCrea, R. S., Morgan, B. J. T., and Cole, D. J. (2013). Age-dependent mixture models for recovery data on animals marked at unknown age. *Journal of the Royal Statistical Society: Series C (Applied Statistics)*, 62(1):101–113.

McCrea, R. S., Morgan, Morgan, B. J. T., Gimenez, O., Besbeas, P., Lebreton, J. D., and Bregnballe, T. (2010). Multi-site integrated population modelling. *Journal of Agricultural, Biological and Environmental Statistics*, 15(4):539–561.

Meinhold, R. J. and Singpurwalla, N. D. (1983). Understanding the Kalman filter. *The American Statistician*, 37(2):123–127.

Morgan, B. J. T. (2008). *Applied Stochastic Modelling*. Chapman and Hall/CRC.

Morrison, C. A., Robinson, R. A., Butler, S. J., Clark, J. A., and Gill, J. A. (2016). Demographic drivers of decline and recovery in an afro-palaearctic migratory bird population. *Proceedings of the Royal Society B: Biological Sciences*, 283(1842):20161387.

Newman, K. B., Buckland, S. T., Morgan, B. J. T., King, R., Borchers, D. L., Cole, D. J., Besbeas, P., Gimenez, O., and Thomas, L. (2014). *Modelling Population Dynamics: Model Formulation, Fitting and Assessment using State-Space Models*. Methods in Statistical Ecology, Springer Science and Business Media New York.

Ordnance-Survey (2011). National grid script. https://www.ordnancesurvey.co.uk/docs/support/national-grid.pdf. [Online; accessed 22-01-2019].

Ordnance Survey Guide (2016). A guide to coordinate systems in Great Britain. https://www.ordnancesurvey.co.uk/docs/support/guide-coordinate-systems-great-britain.pdf. [Online; accessed 22-01-2019].

Paradis, E., Baillie, S. R., Sutherland, W. J., and Gregory, R. D. (1998). Patterns of natal and breeding dispersal in birds. *Journal of Animal Ecology*, 67(4):518–536.

Péron, G., Gaillard, J.-M., Barbraud, C., Bonenfant, C., Charmantier, A., Choquet, R., Coulson, T., Grosbois, V., Loison, A., Marzolin, G., et al. (2016). Evidence of reduced individual heterogeneity in adult survival of long-lived species. *Evolution*, 70(12):2909–2914.

Plard, F., Turek, D., Grüebler, M. U., and Schaub, M. (2019). Ipm^2: Toward better understanding and forecasting of population dynamics. pages 1–18. *Ecological Monographs* advanced online publication: https: https://doi.org/10.1002/ecm.1364.

Pledger, S., Efford, M., Pollock, K., Collazo, J., and Lyons, J. (2009). Stopover duration analysis with departure probability dependent on unknown time since arrival. In *Modeling Demographic Processes in Marked Populations*, pages 349–363. Springer.

Pledger, S. and Schwarz, C. J. (2002). Modelling heterogeneity of survival in band-recovery data using mixtures. *Journal of Applied Statistics*, 29(1-4):315–327.

Pollock, K. H. (1981). Capture-recapture models allowing for age-dependent survival and capture rates. *Biometrics*, 37(3):521–529.

Pradel, R. (2005). Multievent: An extension of multistate capture–recapture models to uncertain states. *Biometrics*, 61(2):442–447.

Pradel, R. (2009). The stakes of capture–recapture models with state uncertainty. In *Modeling Demographic Processes in Marked Populations*, pages 781–795. Springer.

R Core Team (2018). *R: A Language and Environment for Statistical Computing*. R Foundation for Statistical Computing, Vienna, Austria.

Riecke, T. V., Williams, P. J., Behnke, T. L., Gibson, D., Leach, A. G., Sedinger, B. S., Street, P. A., and Sedinger, J. S. (2019). Integrated population models: Model assumptions and inference. *Methods in Ecology and Evolution*, 10(7).

Robinson, R. A. (2010). Estimating age-specific survival rates from historical ringing data. *Ibis*, 152(3):651–663.

Robinson, R. A., Baillie, S. R., and King, R. (2012). Population processes in European blackbirds *Turdus merula*: A state–space approach. *Journal of Ornithology*, 152(2):419–433.

Robinson, R. A., Morrison, C. A., and Baillie, S. R. (2014). Integrating demographic data: Towards a framework for monitoring wildlife populations at large spatial scales. *Methods in Ecology and Evolution*, 5(12):1361–1372.

Robinson, R. A., Siriwardena, G. M., and Crick, H. Q. P. (2002). Status and population trends of the starling *Sturnus vulgaris* in Great Britain. *BTO Research Report*, pages 11–32.

Robinson, R. A., Siriwardena, G. M., and Crick, H. Q. P. (2006). The population decline of the starling, *Sturnus vulgaris* in Great Britain: Patterns and causes. *Acta Zoologica Sinica*, 52(sup):550–553.

Rydzewski, W. (1962). Longevity of ringed birds. *Ring*, 33(96-97):147–152.

Schaub, M. and Abadi, F. (2011). Integrated population models: A novel analysis framework for deeper insights into population dynamics. *Journal of Ornithology*, 152(1):227–237.

Schaub, M., Gimenez, O., Sierro, A., and Arlettaz, R. (2007). Use of integrated modeling to enhance estimates of population dynamics obtained from limited data. *Conservation Biology*, 21(4):945–955.

Seber, G. A. F. (1965). A note on the multiple-recapture census. *Biometrika*, 52(1-2):249–259.

Seber, G. A. F. (1971). Estimating age-specific survival rates from bird-band returns when the reporting rate is constant. *Biometrika*, 58(3):491–497.

Sun, C. C., Fuller, A. K., and Royle, J. A. (2019). Incorporating citizen science data in spatially explicit integrated population models. *Ecology* advanced online publication: https://doi.org/10.1002/ecy.2777.

Tautin, J. (2008). A history of the bird banding lab: 1920-2002. *Memoirs of the Nuttall Ornithological Club*, 15:65–92.

Ter Braak, C. J. F., Van Strien, A. J., Meijer, R., and Verstrael, T. J. (1994). Analysis of monitoring data with many missing values: which method? In Hagemeijer, E. and Verstrael, T., editors, *Bird Numbers 1992. Distribution, Monitoring and Ecological Aspects*, pages 663–673. Sovon, Proceedings of the 12th International Conference, International Bird Census Council and European Ornithological Atlas Committee. Beek-Ubbergen, The Netherlands.

Thomson, D. L., Baillie, S. R., and Peach, W. J. (1999). A method for studying post-fledging survival rates using data from ringing recoveries. *Bird Study*, 46(sup1):S104–S111.

Van Brummelen, G. (2012). *Heavenly Mathematics: The Forgotten Art of Spherical Trigonometry*. Princeton University Press.

Vavrek, M. J. (2011). fossil: Palaeoecological and palaeogeographical analysis tools. *Palaeontologia Electronica*, 14(1). R package version 0.3.0.

Werham, C. V., Baillie, S. R., Clark, J. A., Crick, H. Q. P., and Siriwardena, G. M. (1998). The BTO integrated population monitoring programme: The contributions of ringing. *Acta Zoologica Lituanica*, 8(sup1):93–105.

Wernham, C., Toms, M., Marchant, J., Clark, J., Siriwardena, G., and Baillie, S. (2002). The migration atlas: Movements of the birds of Britain and Ireland.

Where's the Path (2019). Where's the path. https://wtp2.appspot.com/wheresthepath.htm/. [Online; accessed 22-01-2019].

Wikipedia contributors (2019). Ordnance survey national grid—Wikipedia, the free encyclopedia. [Online; accessed 21-January-2019].

Williams, B. K., Nichols, J. D., and Conroy, M. J. (2002). *Analysis and Management of Animal Populations*. Academic Press, New York.

Wojczulanis-Jakubas, K. and Jakubas, D. (2012). When and why does my mother leave me? The question of brood desertion in the dovekie (*Alle alle*). *The Auk*, 129(4):632–637.

Wojczulanis-Jakubas, K., Jakubas, D., Kulaszewicz, I., Kidawa, D., and Taylor, J. R. (2014). Influence of primary reproductive investments on blood biochemistry, leukocyte profile, and body mass in a small arctic seabird. *The Auk: Ornithological Advances*, 131(4):743–755.

Wojczulanis-Jakubas, K., Jiménez-Muñoz, M., Jakubas, D., Kidawa, D., Karnovsky, N., Cole, D. J., and Matechou, E. (2019). Timing of female brood desertion and survival in the little auk—are these traits linked? *Manuscript sumbitted for publication.*

Worthington, H., King, R., and Buckland, S. T. (2015). Analysing mark-recapture-recovery data in the presence of missing covariate data via multiple imputation. *Journal of Agricultural, Biological, and Environmental Statistics*, 20(1):28–46.

Zhou, M., McCrea, R. S., Matechou, E., Cole, D. J., and Griffths, R. A. (2019). Removal models accounting for temporary emigration. *Biometrics*, 75:24–35.

Zucchini, W., MacDonald, I. L., and Langrock, R. (2016). *Hidden Markov Models for Time Series: An Introduction Using R*. Chapman and Hall/CRC.

Appendix A

Supporting Information for Chapter 2

This appendix provides data, and additional results to support the findings in Chapter 2.

A.1 Blackbird Data

Ring-recovery m-arrays for the blackbird data taken from Robinson et al. (2012). These data are part of the BTO Ringing Scheme, which is funded by a partnership of the British Trust for Ornithology, the Joint Nature Conservation Committee (on behalf of: Natural England, Natural Resources Wales and Scottish Natural Heritage and the Department of Agriculture, Environment and Rural Affairs (Northern Ireland)), The National Parks and Wildlife Service (Ireland) and the ringers themselves. Table A.1 contains the ringing and recovery totals for the birds ringed as pulli. Table A.2 contains the ringing and recovery totals for birds ringed as juveniles and adults respectively.

Table A.1 Ring-recovery data for pulli blackbirds for the years 1964-1983.

Year of ringing	Year of recovery																				Total ringed
	1	2	3	4	5	6	7	8	9	10	11	12	13	14	15	16	17	18	19	20	
Ringed as pulli																					
1964	52	15	10	2	8	5	3	1	0	1	0	0	0	0	0	0	0	0	0	0	2488
1965		74	30	14	18	7	12	2	1	3	1	1	0	0	0	0	0	0	0	0	3583
1966			78	29	20	11	4	4	2	0	2	1	0	1	0	0	0	0	0	0	4518
1967				67	22	12	4	7	4	2	2	1	4	1	2	0	0	0	0	0	4315
1968					101	30	10	8	8	6	3	6	1	1	1	0	0	0	0	0	4347
1969						81	27	10	11	10	4	1	3	1	3	1	0	0	1	0	4517
1970							58	15	8	5	4	4	3	2	0	0	1	1	0	0	3448
1971								55	19	11	10	6	6	5	3	0	1	1	0	0	3461
1972									67	21	14	6	7	6	1	0	2	2	0	1	3745
1973										54	26	6	8	2	4	2	1	0	1	1	3139
1974											42	17	5	9	3	1	1	3	0	0	2811
1975												57	12	8	4	2	5	0	0	1	3166
1976													58	15	10	5	8	2	3	2	3141
1977														64	13	7	7	4	3	1	3535
1978															60	21	8	10	9	1	3646
1979																62	15	11	4	9	3918
1980																	54	15	8	9	3403
1981																		57	18	8	3510
1982																			41	14	2927
1983																				70	4150

Table A.2 Ring-recovery data for fledged blackbirds for the years 1964-1983.

Year of ringing	Year of recovery 1	2	3	4	5	6	7	8	9	10	11	12	13	14	15	16	17	18	19	20	Total ringed
Ringed as juveniles																					
1964	114	39	17	12	10	12	8	5	3	3	0	0	0	0	0	0	0	0	0	0	4408
1965		93	26	31	19	16	6	7	3	6	1	1	0	0	0	1	0	0	0	0	4621
1966			70	32	19	20	8	5	4	4	2	1	1	1	0	0	0	0	0	0	4121
1967				85	34	21	25	13	11	4	2	4	3	0	2	0	0	0	0	0	5069
1968					75	30	34	18	16	8	11	5	6	2	1	0	0	0	0	0	5438
1969						76	30	28	25	20	9	7	5	5	2	2	0	0	0	0	5127
1970							61	27	23	21	13	6	7	4	3	2	0	0	0	0	4281
1971								53	34	15	14	11	10	4	8	1	1	0	0	0	3866
1972									74	21	17	14	11	8	9	6	3	1	1	0	4108
1973										81	28	25	19	14	13	9	6	5	2	2	4275
1974											67	16	11	11	11	10	2	1	0	0	3429
1975												71	33	17	15	7	6	1	5	0	4175
1976													68	28	17	11	13	5	8	4	4652
1977														82	34	23	13	9	7	3	5202
1978															74	30	13	15	8	7	4762
1979																75	29	17	17	13	5148
1980																	61	35	24	13	5669
1981																		62	31	22	5532
1982																			59	36	5566
1983																				99	6942
Ringed as adults																					
1964	39	18	19	8	9	3	0	2	5	0	0	0	0	0	0	0	0	0	0	0	1994
1965		44	23	16	15	16	4	6	1	1	0	0	1	0	0	0	0	0	0	0	2471
1966			32	27	10	11	10	6	3	4	1	1	0	0	0	0	0	0	0	0	2459
1967				42	29	24	12	10	6	4	4	4	3	0	0	0	0	0	0	0	3131
1968					38	31	15	14	11	4	6	5	1	0	0	0	0	0	0	0	2991
1969						62	29	18	20	15	12	8	4	2	2	0	0	0	0	0	3069
1970							47	25	21	20	18	7	3	3	0	2	0	0	0	0	3202
1971								32	39	20	15	11	13	3	2	4	0	0	0	0	3450
1972									38	28	25	20	14	9	3	3	0	0	1	0	3784
1973										42	33	24	17	10	7	5	1	1	0	0	3903
1974											35	28	26	16	11	3	6	2	0	0	3795
1975												37	25	15	10	9	10	4	4	0	5045
1976													36	31	19	12	8	6	1	2	4432
1977														41	23	17	15	11	2	2	4181
1978															38	16	18	13	10	8	4156
1979																41	31	28	7	9	4052
1980																	50	38	23	16	4632
1981																		48	26	30	4924
1982																			25	21	4126
1983																				41	4670

A.2 Sandwich Tern Data

In this section we provide the ring-recovery m-arrays for sandwich tern data. These data are part of the BTO Ringing Scheme, which is funded by a partnership of the British Trust for Ornithology, the Joint Nature Conservation Committee (on behalf of: Natural England, Natural Resources Wales and Scottish Natural Heritage and the Department of Agriculture, Environment and Rural Affairs (Northern Ireland)), The National Parks and Wildlife Service (Ireland) and the ringers themselves. Table A.3 contains the ringing and recovery totals for birds ringed as pulli. Table A.4 contains the recovery totals for birds ringed as juveniles and adults respectively. The total number of birds ringed in each age category are not known, and are represented with a dash (-). Table A.5 contains the total number of birds ringed as fledged birds (juveniles and adults).

Table A.3 Ring-recovery data for pulli sandwich terns for the years 1970-1990.

Year of	Year of recovery																				Total
ringing	1	2	3	4	5	6	7	8	9	10	11	12	13	14	15	16	17	18	19	20	21	ringed
Ringed as pulli																						
1970	23	17	1	1	4	7		1	1	2	1	2	3		1	1	1	2		2	2	4021
1971		17	7	7	5	6	4	3	1	2	2	4	1	0	0	0	1	1	2	3	4	3780
1972			24	10	4	1	2	1	0	0	1	0	2	2	0	1	0	1	0	1	2	3583
1973				18	15	1	4	4	2	3	4	4	1	2	0	1	3	0	0	2	1	3903
1974					17	6	2	1	3	4	3	4	3	0	2	1	0	0	2	2	5	3561
1975						24	10	5	3	4	0	3	2	1	0	2	2	2	2	1	4	3532
1976							15	10	2	4	2	0	1	0	1	1	0	1	1	0	0	2378
1977								18	3	7	1	1	0	1	1	0	0	0	0	0	1	2286
1978									10	12	4	4	2	5	2	2	0	2	2	1	4	3239
1979										14	2	0	1	1	0	1	1	1	1	0	2	2429
1980											18	6	4	7	6	5	3	2	0	3	6	4550
1981												17	13	4	3	3	2	3	0	2	2	4083
1982													17	7	6	2	1	2	1	3	2	4464
1983														19	10	2	2	3	2	1	4	3723
1984															8	7	3	5	2	3	6	3378
1985																4	6	4	1	1	6	2373
1986																	6	7	3	3	6	3378
1987																		5	5	4	4	1799
1988																			7	4	3	1848
1989																				4	5	2542
1990																					12	2158

Table A.4 Number of fledged sandwich terns recovered dead from 1970-1990. The number of birds ringed for each category is not known. The total amount of birds ringed for the fledged birds is given in Table A.5.

Year of	Year of recovery																				Total
ringing	1	2	3	4	5	6	7	8	9	10	11	12	13	14	15	16	17	18	19	20	21	ringed
Ringed as juveniles																						
1970	0	0	0	0	0	0	0	0	0	0	0	0	0	0	0	0	0	0	0	0	0	-
1971		0	0	0	0	0	1	0	0	0	0	0	0	0	0	0	0	0	0	0	0	-
1972			0	0	0	0	0	0	0	0	0	0	0	0	0	0	0	0	0	0	0	-
1973				0	0	0	0	0	0	0	0	0	0	0	0	0	0	0	0	0	0	-
1974					0	0	0	0	0	0	0	0	0	0	0	0	0	0	0	0	0	-
1975						0	0	0	0	0	0	0	0	0	0	0	0	0	0	0	0	-
1976							0	0	0	0	0	0	0	0	0	0	0	0	0	0	0	-
1977								0	0	0	0	0	0	0	0	0	0	0	0	0	0	-
1978									0	0	0	0	0	0	0	0	0	0	0	0	0	-
1979										0	0	0	0	0	1	0	0	0	0	0	0	-
1980											0	0	0	0	0	0	0	0	0	0	0	-
1981												0	0	0	0	0	0	0	0	0	0	-
1982													0	0	0	0	0	0	0	0	1	-
1983														0	0	0	0	0	0	0	0	-
1984															0	2	0	0	0	0	0	-
1985																0	0	0	0	0	0	-
1986																	2	2	0	0	1	-
1987																		0	1	0	0	-
1988																			0	0	0	-
1989																				0	0	-
1990																					1	-
Ringed as adults																						
1970	1	0	0	0	0	0	0	0	0	0	0	0	0	0	0	0	0	0	0	0	0	-
1971		0	0	0	0	0	0	0	0	0	0	0	0	0	0	0	0	0	0	0	0	-
1972			0	0	0	0	0	0	0	0	0	0	0	0	0	0	0	0	0	0	0	-
1973				0	0	0	0	0	0	0	0	0	0	0	0	0	0	0	0	0	0	-
1974					0	0	0	0	0	0	0	0	0	0	0	0	0	0	0	0	0	-
1975						0	0	0	0	0	0	0	0	0	0	0	0	0	0	0	0	-
1976							0	0	0	0	0	0	0	0	0	0	0	0	0	0	0	-
1977								0	0	0	0	0	0	0	0	0	0	0	0	0	0	-
1978									0	0	0	0	0	0	0	0	0	0	0	0	0	-
1979										0	0	1	0	0	0	0	0	0	0	0	0	-
1980											0	0	0	1	0	0	1	0	0	0	0	-
1981												1	0	0	0	0	0	0	1	0	0	-
1982													0	0	0	0	1	0	2	0	0	-
1983														0	1	0	1	0	0	0	0	-
1984															1	0	0	0	0	0	0	-
1985																0	0	0	0	0	0	-
1986																	8	1	0	0	1	-
1987																		0	2	0	0	-
1988																			0	0	0	-
1989																				0	0	-
1990																					1	-

Table A.5 Total number of fledged sandwich terns ringed from 1970-1990.

Year	1970	1971	1972	1973	1974	1975	1976	1977	1978	1979	1980	1981	1982	1983	1984	1985	1986	1987	1988	1989	1990
	19	11	2	3	10	7	10	32	16	86	19	95	75	87	45	34	301	108	13	97	174

A.3 Simulation Study for Populations with Homogeneous Survival Probabilities

Simulation results for five, and 20 years of ring-recovery study for an homogeneous population. Results for 10 years of simulation study are presented in the results section of the main thesis. We also explain in this section how the length of the study affects the estimation of the parameters for each of the models. In each simulation 100 data sets with constant probabilities ϕ_1, ϕ_a, and λ are simulated from the standard combined model with a total of 1000 birds ringed, with a constant proportion π of these birds ringed as young and $(1-\pi)$ of the birds ringed as adults. We fit a model with separate constant survival probabilities for first year and adult birds, ϕ_1, and ϕ_a respectively, and a constant reporting probability, λ.

Table A.6 Simulation study for 20 years of ring-recovery study. The first column specifies the type of model fitted, with Stand. Comb. short for standard combined, and Hist. short for historical. In this first column, the last two rows contain information for the models in which the proportion parameter was fixed and the values used. The remaining columns contain the average parameter estimate (par est) and the average standard error, given in parentheses, along with the mean squared error (MSE).

	ϕ_1		ϕ_a		λ		π	
	par est	MSE	par est	MSE	par est	MSE	par est	MSE
True Value	0.50	-	0.60	-	0.05	-	0.40	-
Stand. Comb.	0.50(0.03)	0.0006	0.60(0.01)	0.0002	0.05(0.002)	0.0000	-	-
Hist.	0.50(0.03)	0.0006	0.60(0.01)	0.0002	0.05(0.002)	0.0000	0.40(0.02)	0.0002
Hist. $\pi = 0.40$	0.50(0.03)	0.0006	0.60(0.01)	0.0002	0.05(0.002)	0.0000	-	-
Hist. $\pi = 0.20$	0.48(0.04)	0.0008	0.61(0.02)	0.0002	0.05(0.003)	0.0000	-	-

Table A.7 Simulation study for five years of ring-recovery study. The first column specifies the type of model fitted, with Stand. Comb. short for standard combined, and Hist. short for historical. In this first column, the last two rows contain information for the models in which the proportion parameter was fixed and the values used. The remaining columns contain the average parameter estimate (par est) and the average standard error, given in parentheses, along with the mean squared error (MSE).

	ϕ_1		ϕ_a		λ		π	
	par est	MSE	par est	MSE	par est	MSE	par est	MSE
True Value	0.50	-	0.60	-	0.05	-	0.40	-
Stand. Comb.	0.50(0.06)	0.0041	0.60(0.05)	0.0029	0.05(0.001)	0.0000	-	-
Hist.	0.50(0.06)	0.0039	0.60(0.05)	0.0030	0.05(0.005)	0.0000	0.40(0.02)	0.0006
Hist. $\pi = 0.40$	0.50(0.06)	0.0041	0.60(0.06)	0.0030	0.05(0.005)	0.0000	-	-
Hist. $\pi = 0.20$	0.63(0.11)	0.0541	0.81(0.07)	0.0673	0.05(0.200)	0.1432	-	-

A.4 Simulation Study for Populations with Heterogeneous Adult Survival Probability

Simulation results for five, 10, and 20 years of ring-recovery study for heterogeneous populations in terms of adult survival. For these studies, we fit a model with separate constant survival probabilities for first year and adult birds, ϕ_1, and ϕ_a respectively, and a constant reporting probability, λ.

We provide two different types of heterogeneous populations, first we look at a population in which adult survival $\phi_{a,i}$, varies individually, where i denotes a logit-normal individual random effect. We also simulate data for a population formed by two different sub-populations with two different adult survival probabilities $\phi_{a,A}$, and $\phi_{a,B}$.

A.4.1 Simulation Study with Individual Variation in the Adult Survival Probability

In each simulation 100 data sets are simulated from the standard combined model with 1000 birds ringed, with a constant proportion π of these birds ringed as young and $(1-\pi)$ of the birds ringed as adults. To simulate these data, we keep the first year survival probability, ϕ_1, and the reporting probability, λ constant. The adult survival probability, $\phi_{a,i}$, varies according to a logit-normal individual random effect i; $\text{logit}(\phi_{a,i}) = \alpha + \epsilon_i$, with $\epsilon_i \sim N(0, \sigma^2)$. The true value of alpha is set to 0.405, and the mean value of $\phi_{a,i}$ is 0.60. We also set σ^2 to two different values. In Tables (A.8, A.10, A.12) we show the results of using a logit-normal individual random effect with $\sigma^2 = 0.50$, and in Tables (A.9, A.11, A.13) we show the results of setting σ^2 to 1.

Table A.8 Simulation study for 20 years of ring-recovery study for a population with heterogeneous adult survival, where the adult survival probability, $\phi_{a,i}$ changes per individual and $\sigma^2 = 0.50$. The first column specifies the type of model fitted, with Stand. Comb. short for standard combined, and Hist. short for historical. In this first column, the last two rows contain information for the models in which the proportion parameter was fixed and the values used. The remaining columns contain the average parameter estimate (par est) and the average standard error, given in parentheses, along with the mean squared error (MSE).

	ϕ_1		$\phi_{a,i}$		λ		π	
	par est	MSE	par est	MSE	par est	MSE	par est	MSE
True Value	0.50	-	0.60	-	0.05	-	0.40	-
Stand. Comb.	0.50(0.06)	0.0006	0.60(0.01)	0.0002	0.05(0.002)	0.0000	-	-
Hist.	0.50(0.06)	0.0006	0.60(0.01)	0.0002	0.05(0.002)	0.0000	0.40(0.02)	0.0002
Hist. $\pi = 0.40$	0.50(0.06)	0.0006	0.60(0.01)	0.0002	0.05(0.002)	0.0000	-	-
Hist. $\pi = 0.20$	0.48(0.09)	0.0010	0.61(0.01)	0.0003	0.05(0.002)	0.0000	-	-

Table A.9 Simulation study for 20 years of ring-recovery study for a population with heterogeneous adult survival, where the adult survival probability, $\phi_{a,i}$ changes per individual and $\sigma^2 = 1$. The first column specifies the type of model fitted, with Stand. Comb. short for standard combined, and Hist. short for historical. In this first column, the last two rows contain information for the models in which the proportion parameter was fixed and the values used. The remaining columns contain the average parameter estimate (par est) and the average standard error, given in parentheses, along with the mean squared error (MSE).

	ϕ_1		$\phi_{a,i}$		λ		π	
	par est	MSE	par est	MSE	par est	MSE	par est	MSE
True Value	0.50	-	0.60	-	0.05	-	0.40	-
Stand. Comb.	0.49(0.03)	0.0009	0.62(0.01)	0.0008	0.05(0.002)	0.0000	-	-
Hist.	0.49(0.03)	0.0009	0.62(0.01)	0.0008	0.05(0.002)	0.0000	0.40(0.02)	0.0003
Hist. $\pi = 0.40$	0.49(0.03)	0.0009	0.62(0.01)	0.0008	0.05(0.002)	0.0000	-	-
Hist. $\pi = 0.20$	0.48(0.03)	0.0014	0.63(0.01)	0.0011	0.05(0.002)	0.0000	-	-

Table A.10 Simulation study for 10 years of ring-recovery study for a population with heterogeneous adult survival, where the adult survival probability, $\phi_{a,i}$ changes per individual and $\sigma^2 = 0.50$. The first column specifies the type of model fitted, with Stand. Comb. short for standard combined, and Hist. short for historical. In this first column, the last two rows contain information for the models in which the proportion parameter was fixed and the values used. The remaining columns contain the average parameter estimate (par est) and the average standard error, given in parentheses, along with the mean squared error (MSE).

	ϕ_1		$\phi_{a,i}$		λ		π	
	par est	MSE	par est	MSE	par est	MSE	par est	MSE
True Value	0.50	-	0.60	-	0.05	-	0.40	-
Stand. Comb.	0.49(0.04)	0.0015	0.60(0.02)	0.0004	0.05(0.002)	0.0000	-	-
Hist.	0.49(0.04)	0.0015	0.60(0.02)	0.0004	0.05(0.002)	0.0000	0.40(0.02)	0.0006
Hist. $\pi = 0.40$	0.49(0.04)	0.0016	0.60(0.02)	0.0004	0.05(0.002)	0.0000	-	-
Hist. $\pi = 0.20$	0.46(0.04)	0.0032	0.62(0.03)	0.0011	0.05(0.003)	0.0000	-	-

Table A.11 Simulation study for 10 years of ring-recovery study for a population with heterogeneous adult survival, where the adult survival probability, $\phi_{a,i}$ changes per individual and $\sigma^2 = 1$. The first column specifies the type of model fitted, with Stand. Comb. short for standard combined, and Hist. short for historical. In this first column, the last two rows contain information for the models in which the proportion parameter was fixed and the values used. The remaining columns contain the average parameter estimate (par est) and the average standard error, given in parentheses, along with the mean squared error (MSE).

	ϕ_1		$\phi_{a,i}$		λ		π	
	par est	MSE	par est	MSE	par est	MSE	par est	MSE
True Value	0.50	-	0.60	-	0.05	-	0.40	-
Stand. Comb.	0.48(0.04)	0.0024	0.58(0.03)	0.0011	0.05(0.002)	0.0000	-	-
Hist.	0.48(0.04)	0.0023	0.58(0.03)	0.0011	0.05(0.002)	0.0000	0.40(0.02)	0.0006
Hist. $\pi = 0.40$	0.48(0.04)	0.0024	0.58(0.03)	0.0011	0.05(0.002)	0.0000	-	-
Hist. $\pi = 0.20$	0.45(0.04)	0.0048	0.61(0.03)	0.0009	0.05(0.002)	0.0000	-	-

Table A.12 Simulation study for five years of ring-recovery study for a population with heterogeneous adult survival, where the adult survival probability, $\phi_{a,i}$ changes per individual and $\sigma^2 = 0.50$. The first column specifies the type of model fitted, with Stand. Comb. short for standard combined, and Hist. short for historical. In this first column, the last two rows contain information for the models in which the proportion parameter was fixed and the values used. The remaining columns contain the average parameter estimate (par est) and the average standard error, given in parentheses, along with the mean squared error (MSE).

	ϕ_1		$\phi_{a,i}$		λ		π	
	par est	MSE	par est	MSE	par est	MSE	par est	MSE
True Value	0.50	-	0.60	-	0.05	-	0.40	-
Stand. Comb.	0.48(0.06)	0.0040	0.58(0.06)	0.0038	0.05(0.005)	0.0000	-	-
Hist.	0.48(0.06)	0.0041	0.58(0.06)	0.0037	0.05(0.005)	0.0000	0.40(0.04)	0.0012
Hist. $\pi = 0.40$	0.49(0.06)	0.0040	0.58(0.06)	0.0037	0.05(0.005)	0.0000	-	-
Hist. $\pi = 0.20$	0.55(0.10)	0.0319	0.75(0.07)	0.0468	0.16(0.089)	0.0780	-	-

Table A.13 Simulation study for five years of ring-recovery study for a population with heterogeneous adult survival, where the adult survival probability, $\phi_{a,i}$ changes per individual and $\sigma^2 = 1$. The first column specifies the type of model fitted, with Stand. Comb. short for standard combined, and Hist. short for historical. In this first column, the last two rows contain information for the models in which the proportion parameter was fixed and the values used. The remaining columns contain the average parameter estimate (par est) and the average standard error, given in parentheses, along with the mean squared error (MSE).

	ϕ_1		$\phi_{a,i}$		λ		π	
	par est	MSE	par est	MSE	par est	MSE	par est	MSE
True Value	0.50	-	0.60	-	0.05	-	0.40	-
Stand. Comb.	0.46(0.06)	0.0046	0.53(0.05)	0.0086	0.05(0.004)	0.0000	-	-
Hist.	0.46(0.06)	0.0048	0.53(0.05)	0.0090	0.05(0.004)	0.0000	0.41(0.04)	0.0018
Hist. $\pi = 0.40$	0.46(0.06)	0.0046	0.53(0.05)	0.0086	0.05(0.004)	0.0000	-	-
Hist. $\pi = 0.20$	0.51(0.09)	0.0328	0.68(0.07)	0.0388	0.05(0.099)	0.0068	-	-

A.4.2 Simulation Study for two Populations with Different Constant Adult Survival Probabilities

For each study we generate data for two sub-populations that have the same constant first year probability ϕ_1, and reporting probability λ, but a different constant adult survival probability. Then we merge these data together into a data set of 2000 ringed birds with heterogeneous adult survival. We simulate two sets of 100 data sets from the standard combined model with 1000 birds ringed in each set, with a similar constant proportion π of these birds ringed as young and $(1-\pi)$ of the birds ringed as adults. Each of these two sets of 100 data sets, have the same constant first year survival probability, and the same reporting probability, but each of them have a different constant adult survival probability ϕ_a.

We provide results for five, 10 and 20 years of ring-recovery studies, and three case scenarios in which the two sub-populations have different adult survival probabilities. The first population is formed by two sub-populations with adult survival probabilities of 0.4 and 0.7 respectively, the second has two adult survival probabilities of 0.4 and 0.8, and finally the last heterogeneous population has adult survival probabilities of 0.3 and 0.8 for each sub-population.

Table A.14 Simulation study for 20 years of ring-recovery study for a population with heterogeneous adult survival, where there are two different adult survival probabilities, $\phi_{a,A} = 0.40$ and $\phi_{a,B} = 0.70$. The first column specifies the type of model fitted, The first column specifies the type of model, with Stand. Comb. short for standard combined, and Hist. short for historical. In this first column, the last two rows contain information for the models in which the proportion parameter was fixed and the values used. The remaining columns contain the average parameter estimate (par est) and the average standard error, given in parentheses, along with the mean squared error (MSE).

	ϕ_1		$\phi_{a,A}, \phi_{a,B}$	λ		π	
	par est	MSE	par est	par est	MSE	par est	MSE
True Value	0.50	-	0.40, 0.70	0.05	-	0.40	-
Stand. Comb.	0.50(0.02)	0.0003	0.58(0.01)	0.05(0.001)	0.0000	-	-
Hist.	0.50(0.02)	0.0003	0.58(0.01)	0.05(0.001)	0.0000	0.40(0.01)	0.0001
Hist. $\pi = 0.40$	0.50(0.02)	0.0004	0.58(0.01)	0.05(0.001)	0.0000	-	-
Hist. $\pi = 0.20$	0.49(0.02)	0.0006	0.59(0.01)	0.05(0.001)	0.0000	-	-

Table A.15 Simulation study for 20 years of ring-recovery study for a population with heterogeneous adult survival, where there are two different adult survival probabilities, $\phi_{a,A} = 0.40$ and $\phi_{a,B} = 0.80$. The first column specifies the type of model fitted, with Stand. Comb. short for standard combined, and Hist. short for historical. In this first column, the last two rows contain information for the models in which the proportion parameter was fixed and the values used. The remaining columns contain the average parameter estimate (par est) and the average standard error, given in parentheses, along with the mean squared error (MSE).

	ϕ_1		$\phi_{a,A}, \phi_{a,B}$	λ		π	
	par est	MSE	par est	par est	MSE	par est	MSE
True Value	0.50	-	0.40, 0.80	0.05	-	0.40	-
Stand. Comb.	0.49(0.02)	0.0004	0.66(0.01)	0.05(0.001)	0.0000	-	-
Hist.	0.49(0.02)	0.0004	0.66(0.01)	0.05(0.001)	0.0000	0.40(0.01)	0.0001
Hist. $\pi = 0.40$	0.49(0.02)	0.0004	0.66(0.01)	0.05(0.001)	0.0000	-	-
Hist. $\pi = 0.20$	0.47(0.02)	0.0010	0.66(0.01)	0.05(0.001)	0.0000	-	-

Table A.16 Simulation study for 20 years of ring-recovery study for a population with heterogeneous adult survival, where there are two different adult survival probabilities, $\phi_{a,A} = 0.30$ and $\phi_{a,B} = 0.80$. The first column specifies the type of model fitted, with Stand. Comb. short for standard combined, and Hist. short for historical. In this first column, the last two rows contain information for the models in which the proportion parameter was fixed and the values used. The remaining columns contain the average parameter estimate (par est) and the average standard error, given in parentheses, along with the mean squared error (MSE).

	ϕ_1		$\phi_{a,A}, \phi_{a,B}$	λ		π	
	par est	MSE	par est	par est	MSE	par est	MSE
True Value	0.50	-	0.30, 0.80	0.05	-	0.40	-
Stand. Comb.	0.49(0.02)	0.0004	0.64(0.01)	0.05(0.001)	0.0000	-	-
Hist.	0.49(0.02)	0.0004	0.64(0.01)	0.05(0.001)	0.0000	0.40(0.01)	0.0001
Hist. $\pi = 0.40$	0.49(0.02)	0.0004	0.64(0.01)	0.05(0.001)	0.0000	-	-
Hist. $\pi = 0.20$	0.48(0.02)	0.0008	0.64(0.01)	0.05(0.001)	0.0000	-	-

Table A.17 Simulation study for 10 years of ring-recovery study study for a population with heterogeneous adult survival, where there are two different adult survival probabilities, $\phi_{a,A} = 0.40$ and $\phi_{a,B} = 0.70$. The first column specifies the type of model fitted, with Stand. Comb. short for standard combined, and Hist. short for historical. In this first column, the last two rows contain information for the models in which the proportion parameter was fixed and the values used. The remaining columns contain the average parameter estimate (par est) and the average standard error, given in parentheses, along with the mean squared error (MSE).

	ϕ_1		$\phi_{a,A}, \phi_{a,B}$	λ		π	
	par est	MSE	par est	par est	MSE	par est	MSE
True Value	0.50	-	0.40,0.70	0.05	-	0.40	-
Stand. Comb.	0.50(0.03)	0.0008	0.56(0.02)	0.05(0.002)	0.0000	-	-
Hist.	0.50(0.03)	0.0008	0.56(0.02)	0.05(0.002)	0.0000	0.40(0.02)	0.0004
Hist. $\pi = 0.40$	0.50(0.03)	0.0007	0.56(0.02)	0.05(0.002)	0.0000	-	-
Hist. $\pi = 0.20$	0.47(0.03)	0.0007	0.58(0.02)	0.05(0.002)	0.0000	-	-

Table A.18 Simulation study for 10 years of ring-recovery study for a population with heterogeneous adult survival, where there are two different adult survival probabilities, $\phi_{a,A} = 0.40$ and $\phi_{a,B} = 0.80$. The first column specifies the type of model fitted, with Stand. Comb. short for standard combined, and Hist. short for historical. In this first column, the last two rows contain information for the models in which the proportion parameter was fixed and the values used. The remaining columns contain the average parameter estimate (par est) and the average standard error, given in parentheses, along with the mean squared error (MSE).

	ϕ_1		$\phi_{a,A}, \phi_{a,B}$	λ		π	
	par est	MSE	par est	par est	MSE	par est	MSE
True Value	0.50	-	0.40,0.80	0.05	-	0.40	-
Stand. Comb.	0.48(0.03)	0.0010	0.60(0.02)	0.05(0.002)	0.0000	-	-
Hist.	0.48(0.03)	0.0010	0.60(0.02)	0.05(0.002)	0.0000	0.41(0.02)	0.0005
Hist. $\pi = 0.40$	0.48(0.03)	0.0010	0.61(0.02)	0.05(0.002)	0.0000	-	-
Hist. $\pi = 0.20$	0.45(0.03)	0.0033	0.63(0.02)	0.05(0.002)	0.0000	-	-

Table A.19 Simulation study for 10 years of ring-recovery study for a population with heterogeneous adult survival, where there are two different adult survival probabilities, $\phi_{a,A} = 0.30$ and $\phi_{a,B} = 0.80$. The first column specifies the type of model fitted, with Stand. Comb. short for standard combined, and Hist. short for historical. In this first column, the last two rows contain information for the models in which the proportion parameter was fixed and the values used. The remaining columns contain the average parameter estimate (par est) and the average standard error, given in parentheses, along with the mean squared error (MSE).

	ϕ_1		$\phi_{a,A}, \phi_{a,B}$	λ		π	
	par est	MSE	par est	par est	MSE	par est	MSE
True Value	0.50	-	0.30,0.80	0.05	-	0.40	-
Stand. Comb.	0.48(0.03)	0.0013	0.57(0.02)	0.05(0.002)	0.0000	-	-
Hist.	0.48(0.03)	0.0013	0.57(0.02)	0.05(0.002)	0.0000	0.41(0.02)	0.0004
Hist. $\pi = 0.40$	0.48(0.03)	0.0014	0.57(0.02)	0.05(0.002)	0.0000	-	-
Hist. $\pi = 0.20$	0.44(0.03)	0.0039	0.58(0.02)	0.05(0.002)	0.0000	-	-

Table A.20 Simulation study for five years of ring-recovery study for a population with heterogeneous adult survival, where there are two different adult survival probabilities, $\phi_{a,A} = 0.40$ and $\phi_{a,B} = 0.70$. The first column specifies the type of model fitted, with Stand. Comb. short for standard combined, and Hist. short for historical. In this first column, the last two rows contain information for the models in which the proportion parameter was fixed and the values used. The remaining columns contain the average parameter estimate (par est) and the average standard error, given in parentheses, along with the mean squared error (MSE).

	ϕ_1		$\phi_{a,A}, \phi_{a,B}$	λ		π	
	par est	MSE	par est	par est	MSE	par est	MSE
True Value	0.50	-	0.40,0.70	0.05	-	0.40	-
Stand. Comb.	0.48(0.04)	0.0021	0.53(0.04)	0.05(0.003)	0.0000	-	-
Hist.	0.48(0.04)	0.0021	0.53(0.04)	0.05(0.003)	0.0000	0.40(0.02)	0.0008
Hist. $\pi = 0.40$	0.48(0.04)	0.0021	0.53(0.04)	0.05(0.003)	0.0000	-	-
Hist. $\pi = 0.20$	0.45(0.05)	0.0077	0.63(0.05)	0.06(0.017)	0.0031	-	-

Table A.21 Simulation study for five years of ring-recovery study study for a population with heterogeneous adult survival, where there are two different adult survival probabilities, $\phi_{a,A}$ and $\phi_{a,B}$. The first column specifies the type of model fitted, with Stand. Comb. short for standard combined, and Hist. short for historical. In this first column, the last two rows contain information for the models in which the proportion parameter was fixed and the values used. The remaining columns contain the average parameter estimate (par est) and the average standard error, given in parentheses, along with the mean squared error (MSE).

	ϕ_1		$\phi_{a,A}, \phi_{a,B}$	λ		π	
	par est	MSE	par est	par est	MSE	par est	MSE
True Value	0.50	-	0.40,0.80	0.05	-	0.40	-
Stand. Comb.	0.46(0.04)	0.0031	0.55(0.04)	0.05(0.003)	0.0000	-	-
Hist.	0.47(0.04)	0.0028	0.54(0.04)	0.05(0.003)	0.0000	0.42(0.03)	0.0011
Hist. $\pi = 0.40$	0.46(0.04)	0.0030	0.55(0.04)	0.05(0.003)	0.0000	-	-
Hist. $\pi = 0.20$	0.50(0.08)	0.0237	0.70(0.07)	0.11(0.06)	0.0385	-	-

Table A.22 Simulation study for five years of ring-recovery study for a population with heterogeneous adult survival, where there are two different adult survival probabilities, $\phi_{a,A}$ and $\phi_{a,B}$. The first column specifies the type of model fitted, with Stand. Comb. short for standard combined, and Hist. short for historical. In this first column, the last two rows contain information for the models in which the proportion parameter was fixed and the values used. The remaining columns contain the average parameter estimate (par est) and the average standard error, given in parentheses, along with the mean squared error (MSE).

	ϕ_1		$\phi_{a,A}, \phi_{a,B}$	λ		π	
	par est	MSE	par est	par est	MSE	par est	MSE
True Value	0.50	-	0.30,0.80	0.05	-	0.40	-
Stand. Comb.	0.45(0.04)	0.0046	0.49(0.04)	0.04(0.003)	0.0000	-	-
Hist.	0.46(0.04)	0.0042	0.49(0.04)	0.04(0.003)	0.0000	0.42(0.03)	0.0010
Hist. $\pi = 0.40$	0.45(0.04)	0.0046	0.49(0.05)	0.04(0.003)	0.0000	-	-
Hist. $\pi = 0.20$	0.42(0.05)	0.0139	0.58(0.05)	0.06(0.017)	0.0120	-	-

A.5 Blackbird Results

Here, we provide the parameter estimates results for the models selected in Tables 2.5 and 2.6 where the historical and the historical combined models were compared (in terms of the ranking obtaining when model selection was performed) to their equivalent standard models.

A.5.1 Results from Table 2.5

Tables A.23-A.25 present the results for the standard combined models, and Tables A.26-A.31 present the results for the historical models for the blackbird data.

The results in Table A.23 compare to those in Tables A.26 and A.28. In these, both survival parameters are kept constant, and the reporting probability has a time dependency. The results provided by the standard combined and the historical models are identical in this case.

The results in Table A.24 compare to those in Tables A.27 and A.29. In these, first-year survival is kept constant, and both the adult survival and the reporting probabilities have time dependencies. The results provided by the standard combined and the historical models are fairly similar. However, in the case of the historical model $\phi_{a,1}$ gets slightly underestimated when the proportion parameter is time dependent. This is happening as π_1 is being overestimated in this case, with its real value fixed at 0.72.

The results in Table A.25 compare to those in Tables A.30 and A.31. In these, adult survival is kept constant, and both the first-year survival and the reporting probabilities have time dependencies. Here the results for the historical models show some evidence of near-parameter redundancy which can be noticed by the large standard errors obtained for $\phi_{1,1}$ in both Tables A.30 and A.31, and the large standard error obtained for π_1 in Table A.31. Moreover, in Table A.31, the parameter π_1 is underestimated compared to its real value of 0.72.

The bias in the estimation of the survival parameters and the large standard errors are not surprising since the blackbird data contains a lot of $R_{i,t} = 0$. In Section 1.2.4, we described that having several $R_{i,t} = 0$ can cause near-redundancy issues.

Standard Combined Model

Table A.23 Estimates of survival and reporting probabilities for the blackbird data for the standard combined model with juvenile and adult data for the model with parameters: ϕ_1, ϕ_a, λ_t. Standard errors are provided in parentheses.

year	ϕ_1	ϕ_a	λ_t
1	0.6055(0.0087)	0.7043(0.0051)	0.0656(0.0054)
2			0.0517(0.0037)
3			0.0412(0.0030)
4			0.0442(0.0028)
5			0.0393(0.0025)
6			0.0460(0.0026)
7			0.0410(0.0024)
8			0.0379(0.0023)
9			0.0458(0.0025)
10			0.0422(0.0023)
11			0.0422(0.0024)
12			0.0381(0.0022)
13			0.0377(0.0021)
14			0.0350(0.0020)
15			0.0347(0.0020)
16			0.0324(0.0019)
17			0.0305(0.0018)
18			0.0312(0.0018)
19			0.0269(0.0017)
20			0.0316(0.0017)

Table A.24 Estimates of survival and reporting probabilities for the blackbird data for the standard combined model with juvenile and adult data for the model with parameters: ϕ_1, $\phi_{a,t}$, λ_t. Standard errors are provided in parentheses.

year	ϕ_1	$\phi_{a,t}$	λ_t
1	0.6073(0.0092)	0.7059(0.0468)	0.0659(0.0060)
2		0.7094(0.0330)	0.0522(0.0048)
3		0.7352(0.0307)	0.0440(0.0046)
4		0.7058(0.0291)	0.0437(0.0041)
5		0.6671(0.0300)	0.0359(0.0033)
6		0.6766(0.0267)	0.0439(0.0038)
7		0.7153(0.0262)	0.0434(0.0041)
8		0.7202(0.0274)	0.0401(0.0041)
9		0.7152(0.0270)	0.047(0.0046)
10		0.7444(0.0267)	0.0467(0.0047)
11		0.7803(0.0246)	0.0515(0.0055)
12		0.7149(0.0344)	0.0361(0.0043)
13		0.6271(0.0372)	0.0293(0.0033)
14		0.6891(0.0343)	0.0343(0.0038)
15		0.6641(0.0370)	0.0322(0.0037)
16		0.7064(0.0330)	0.0342(0.0038)
17		0.6715(0.0334)	0.029(0.0031)
18		0.6827(0.0346)	0.0309(0.0033)
19		0.6828(0.0437)	0.0268(0.0033)
20		0.7408(0.0358)	0.0363(0.0037)

Table A.25 Estimates of survival and reporting probabilities for the blackbird data for the standard combined model with juvenile and adult data for the model with parameters: $\phi_{1,t}$, ϕ_a, λ_t. Standard errors are provided in parentheses.

year	$\phi_{1,t}$	ϕ_a	λ_t
1	0.6102(0.0719)	0.7046(0.0052)	0.0662(0.0106)
2	0.6056(0.0425)		0.0517(0.0042)
3	0.5442(0.0690)		0.0402(0.0030)
4	0.6165(0.0367)		0.0444(0.0029)
5	0.6367(0.0365)		0.0397(0.0025)
6	0.6307(0.0352)		0.0462(0.0026)
7	0.6395(0.0366)		0.0410(0.0024)
8	0.6323(0.0391)		0.0379(0.0023)
9	0.6107(0.0350)		0.0458(0.0025)
10	0.5608(0.0364)		0.0422(0.0023)
11	0.5427(0.0391)		0.0425(0.0024)
12	0.5705(0.0387)		0.0380(0.0022)
13	0.6400(0.0356)		0.0378(0.0021)
14	0.5815(0.0365)		0.0349(0.0020)
15	0.6191(0.0350)		0.0347(0.0020)
16	0.6008(0.0363)		0.0324(0.0019)
17	0.6299(0.0388)		0.0306(0.0018)
18	0.6147(0.0390)		0.0312(0.0018)
19	0.6503(0.0370)		0.0270(0.0017)
20	0.5665(0.0346)		0.0314(0.0017)

Historical Model

Table A.26 Estimates of survival and reporting probabilities for the blackbird data for the historical model with data for fledged birds for the model with parameters: ϕ_1, ϕ_a, λ_t, π_t. Standard errors are provided in parentheses.

year	ϕ_1	ϕ_a	λ_t	π_t
1	0.6107(0.0087)	0.7022(0.0052)	0.0661(0.0054)	0.6909(0.0400)
2			0.0516(0.0037)	0.6519(0.0351)
3			0.0411(0.0030)	0.5890(0.0362)
4			0.0441(0.0028)	0.6180(0.0308)
5			0.0394(0.0025)	0.5987(0.0307)
6			0.0460(0.0026)	0.5377(0.0278)
7			0.0406(0.0024)	0.5935(0.0289)
8			0.0376(0.0023)	0.5792(0.0301)
9			0.0454(0.0025)	0.5704(0.0270)
10			0.0420(0.0023)	0.5678(0.0277)
11			0.0419(0.0024)	0.5251(0.0282)
12			0.0377(0.0022)	0.5212(0.0286)
13			0.0377(0.0021)	0.5460(0.0280)
14			0.0351(0.0020)	0.5725(0.0283)
15			0.0347(0.0020)	0.6211(0.0278)
16			0.0325(0.0019)	0.6114(0.0287)
17			0.0306(0.0018)	0.5105(0.0296)
18			0.0312(0.0018)	0.4973(0.0288)
19			0.0270(0.0017)	0.6205(0.0300)
20			0.0317(0.0017)	0.6026(0.0271)

Table A.27 Estimates of survival and reporting probabilities for the blackbird data for the historical model with data for fledged birds for the model with parameters: ϕ_1, $\phi_{a,t}$, λ_t, π_t. Standard errors are provided in parentheses.

year	ϕ_1	$\phi_{a,t}$	λ_t	π_t
1	0.6146(0.0093)	0.5385(0.0760)	0.0594(0.0053)	0.7778(0.0431)
2		0.6989(0.0421)	0.0533(0.0059)	0.6331(0.0449)
3		0.7663(0.0357)	0.0496(0.0065)	0.5425(0.0449)
4		0.6960(0.0345)	0.0427(0.0044)	0.6204(0.0344)
5		0.6413(0.0354)	0.0342(0.0035)	0.6183(0.0324)
6		0.7010(0.0308)	0.0476(0.0049)	0.5306(0.0309)
7		0.7102(0.0289)	0.0425(0.0043)	0.5856(0.0313)
8		0.7153(0.0291)	0.0393(0.0042)	0.5720(0.0324)
9		0.7066(0.0289)	0.0459(0.0046)	0.5683(0.0292)
10		0.7378(0.0294)	0.0460(0.0050)	0.5546(0.0308)
11		0.7877(0.0259)	0.0530(0.0061)	0.4942(0.0318)
12		0.7208(0.0335)	0.0366(0.0042)	0.5244(0.0316)
13		0.6369(0.0369)	0.0301(0.0033)	0.5725(0.0294)
14		0.7016(0.0366)	0.0352(0.0042)	0.5719(0.0315)
15		0.6324(0.0380)	0.0297(0.0033)	0.6385(0.0290)
16		0.6803(0.0366)	0.0326(0.0037)	0.6110(0.0312)
17		0.6953(0.0362)	0.0317(0.0037)	0.5059(0.0328)
18		0.7220(0.0358)	0.0343(0.0041)	0.4844(0.0324)
19		0.6666(0.0482)	0.0251(0.0032)	0.6288(0.0323)
20		0.7618(0.0387)	0.0386(0.0046)	0.5729(0.0328)

Table A.28 Estimates of survival and reporting probabilities for the blackbird data for the historical model with data for fledged birds for the model with parameters: ϕ_1, ϕ_a, λ_t, π. Standard errors are provided in parentheses.

year	ϕ_1	ϕ_a	λ_t	π
1	0.6066(0.0086)	0.7040(0.0051)	0.0678(0.0055)	0.5750(0.0067)
2			0.0521(0.0038)	
3			0.0412(0.0030)	
4			0.0443(0.0028)	
5			0.0395(0.0025)	
6			0.0460(0.0026)	
7			0.0407(0.0024)	
8			0.0376(0.0023)	
9			0.0455(0.0025)	
10			0.0420(0.0023)	
11			0.0419(0.0024)	
12			0.0377(0.0021)	
13			0.0377(0.0021)	
14			0.0351(0.0020)	
15			0.0347(0.0020)	
16			0.0325(0.0019)	
17			0.0305(0.0018)	
18			0.0312(0.0018)	
19			0.0270(0.0017)	
20			0.0317(0.0017)	

Table A.29 Estimates of survival and reporting probabilities for the blackbird data for the historical model with data for fledged birds for the model with parameters: ϕ_1, $\phi_{a,t}$, λ_t, π. Standard errors are provided in parentheses.

year	ϕ_1	$\phi_{a,t}$	λ_t	π
1	0.6103(0.0092)	0.7580(0.0451)	0.0729(0.0074)	0.5733(0.0068)
2		0.7209(0.0356)	0.0534(0.0055)	
3		0.7366(0.0311)	0.0439(0.0049)	
4		0.7083(0.0330)	0.0436(0.0043)	
5		0.6615(0.0281)	0.0352(0.0036)	
6		0.6810(0.0263)	0.0443(0.0041)	
7		0.7167(0.0263)	0.0433(0.0042)	
8		0.7197(0.0265)	0.0396(0.0040)	
9		0.7133(0.0257)	0.0464(0.0043)	
10		0.7415(0.0254)	0.0460(0.0044)	
11		0.7643(0.0236)	0.0481(0.0047)	
12		0.7017(0.0294)	0.0351(0.0035)	
13		0.6386(0.0332)	0.0309(0.0031)	
14		0.6909(0.0329)	0.0347(0.0037)	
15		0.6628(0.0351)	0.0322(0.0035)	
16		0.7069(0.0324)	0.0344(0.0037)	
17		0.6716(0.0327)	0.0291(0.0030)	
18		0.6755(0.0337)	0.0304(0.0031)	
19		0.6879(0.0428)	0.0273(0.0033)	
20		0.7562(0.0339)	0.0382(0.0039)	

Table A.30 Estimates of survival and reporting probabilities for the blackbird data for the historical model with data for fledged birds for the model with parameters: $\phi_{1,t}$, ϕ_a, λ_t, π. Standard errors are provided in parentheses.

year	$\phi_{1,t}$	ϕ_a	λ_t	π
1	0.3474(0.1231)	0.7027(0.0052)	0.0477(0.0077)	0.5716(0.0068)
2	0.5732(0.0443)		0.0507(0.0040)	
3	0.5388(0.0472)		0.0400(0.0030)	
4	0.6125(0.0371)		0.0443(0.0029)	
5	0.6215(0.0373)		0.0395(0.0025)	
6	0.6278(0.0354)		0.0461(0.0026)	
7	0.6619(0.0356)		0.0408(0.0024)	
8	0.6674(0.0374)		0.0376(0.0023)	
9	0.6399(0.0340)		0.0456(0.0025)	
10	0.5821(0.0361)		0.0419(0.0023)	
11	0.5786(0.0386)		0.0419(0.0024)	
12	0.6153(0.0373)		0.0377(0.0022)	
13	0.6401(0.0357)		0.0378(0.0021)	
14	0.5635(0.0370)		0.0350(0.0020)	
15	0.6149(0.0352)		0.0347(0.0020)	
16	0.5874(0.0368)		0.0325(0.0019)	
17	0.6246(0.0391)		0.0306(0.0018)	
18	0.6217(0.0388)		0.0312(0.0018)	
19	0.6372(0.0377)		0.0270(0.0017)	
20	0.5465(0.0350)		0.0315(0.0017)	

Table A.31 Estimates of survival and reporting probabilities for the blackbird data for the historical model with data for fledged birds for the model with parameters: $\phi_{1,t}$, ϕ_a, λ_t, π_t. Standard errors are provided in parentheses.

year	$\phi_{1,t}$	ϕ_a	λ_t	π_t
1	0.3724(3.1190)	0.7023(0.0052)	0.0488(0.1408)	0.5810(1.2104)
2	0.6085(0.0454)		0.0516(0.0042)	0.6512(0.0375)
3	0.5404(0.0481)		0.0400(0.0030)	0.5778(0.0373)
4	0.6230(0.0372)		0.0443(0.0029)	0.6199(0.0313)
5	0.6258(0.0374)		0.0395(0.0025)	0.6003(0.0309)
6	0.6245(0.0357)		0.0461(0.0026)	0.5386(0.0279)
7	0.6625(0.0356)		0.0407(0.0024)	0.5944(0.0289)
8	0.6672(0.0374)		0.0376(0.0023)	0.5796(0.0301)
9	0.6400(0.0340)		0.0456(0.0025)	0.5712(0.0270)
10	0.5821(0.0361)		0.0419(0.0023)	0.5671(0.0277)
11	0.5795(0.0386)		0.0419(0.0024)	0.5255(0.0281)
12	0.6105(0.0376)		0.0377(0.0022)	0.5211(0.0286)
13	0.6389(0.0357)		0.0378(0.0021)	0.5469(0.0279)
14	0.5635(0.0371)		0.0350(0.0020)	0.5711(0.0283)
15	0.6157(0.0352)		0.0347(0.0020)	0.6211(0.0278)
16	0.5883(0.0367)		0.0325(0.0019)	0.6111(0.0287)
17	0.6203(0.0393)		0.0306(0.0018)	0.5109(0.0296)
18	0.6175(0.0390)		0.0312(0.0018)	0.4975(0.0288)
19	0.6373(0.0377)		0.0270(0.0017)	0.6206(0.0300)
20	0.5487(0.0350)		0.0315(0.0017)	0.5998(0.0272)

A.5.2 Results from Table 2.6

Tables A.32-A.35 present the results for the standard combined models, and Tables A.37-A.41 present the results for the historical combined models for the blackbird data.

The results in Table A.32 compare to those in Tables A.37 and A.39. In these, both survival parameters are kept constant, and the reporting probability has a time and and age dependency. The results provided by the standard combined and the historical models are similar in this case. However, the parameter estimate for $\phi_{1,1}$ is lower in both historical combined models. For the model in Table A.39, where the proportion parameter is time-dependent, the standard error for $\lambda_{a,1}$ is very high. Moreover ϕ_1 is also overestimated. This is caused by the sparse blackbird data.

The results in Table A.33 compare to those in Table A.36. In these, adult survival is kept constant, and the first-year survival and reporting probabilities have time dependencies. Again, for the historical model the survival parameter $\phi_{1,1}$ is underestimated and it has a large standard error.

The results in Table A.34 compare to those in A.38 and A.40. In these, both survival parameters are kept constant, and the reporting probability has a time dependency. The results provided by the standard combined and the historical combined models are identical in this case. These models do not show any sign of near-redundancy and that is probably because there are less parameters in these models compared to those described above.

The results in Table A.35 compare to those in Table A.41. In these, first-year survival is kept constant, and the adult survival and reporting probabilities have time dependencies. The results provided by the standard combined and the historical combined models are fairly similar. However, in the case of the historical combined model $\phi_{a,1}$ gets underestimated. This is happening as π_1 is being slightly overestimated, with its real value fixed at 0.72.

Standard Combined Model

Table A.32 Estimates of survival and reporting probabilities for the blackbird data for the standard combined model with data for pulli, juvenille and adult birds for the model with parameters: ϕ_1, ϕ_a, $\lambda_{1,t}$, $\lambda_{a,t}$. Standard errors are provided in parentheses.

year	ϕ_1	ϕ_a	$\lambda_{1,t}$	$\lambda_{a,t}$
1	0.5335(0.0150)	0.7013(0.0047))	0.0515(0.0043)	0.0655(0.0104)
2			0.0437(0.0036)	0.0515(0.0049)
3			0.0366(0.0032)	0.0434(0.0036)
4			0.0346(0.0030)	0.0439(0.0031)
5			0.0385(0.0031)	0.0433(0.0028)
6			0.0349(0.0030)	0.0476(0.0028)
7			0.033(0.0032)	0.0408(0.0025)
8			0.0316(0.0032)	0.0364(0.0023)
9			0.0385(0.0034)	0.0429(0.0025)
10			0.0392(0.0036)	0.0395(0.0024)
11			0.0374(0.0037)	0.0409(0.0024)
12			0.0373(0.0035)	0.0361(0.0022)
13			0.0347(0.0033)	0.0372(0.0022)
14			0.0358(0.0032)	0.0339(0.0021)
15			0.0342(0.0031)	0.0329(0.0020)
16			0.0324(0.0029)	0.0302(0.0019)
17			0.0272(0.0027)	0.0315(0.0020)
18			0.0282(0.0027)	0.0320(0.0019)
19			0.0253(0.0026)	0.0277(0.0018)
20			0.0327(0.0027)	0.0305(0.0019)

Table A.33 Estimates of survival and reporting probabilities for the blackbird data for the standard combined model with data for pulli, juvenille and adult birds for the model with parameters: $\phi_{1,t}$, ϕ_a, λ_t. Standard errors are provided in parentheses.

year	$\phi_{1,t}$	ϕ_a	λ_t
1	0.6321(0.0650)	0.6998(0.0047)	0.0653(0.0104)
2	0.5721(0.0361)		0.0484(0.0034)
3	0.5646(0.0330)		0.0405(0.0025)
4	0.5880(0.0292)		0.0404(0.0022)
5	0.5614(0.0272)		0.0415(0.0020)
6	0.5797(0.0270)		0.0428(0.0020)
7	0.5759(0.0290)		0.0380(0.0019)
8	0.5574(0.0310)		0.0348(0.0018)
9	0.5506(0.0279)		0.0414(0.0019)
10	0.5289(0.0289)		0.0394(0.0019)
11	0.5468(0.0304)		0.0398(0.0019)
12	0.5236(0.0304)		0.0364(0.0018)
13	0.5672(0.0293)		0.0364(0.0018)
14	0.5366(0.0290)		0.0345(0.0017)
15	0.5583(0.0288)		0.0333(0.0016)
16	0.5365(0.0297)		0.0309(0.0016)
17	0.5624(0.0311)		0.0301(0.0015)
18	0.5518(0.0308)		0.0308(0.0015)
19	0.5944(0.0311)		0.0269(0.0014)
20	0.5257(0.0279)		0.0312(0.0015)

Table A.34 Estimates of survival and reporting probabilities for the blackbird data for the standard combined model with data for pulli, juvenille and adult birds for the model with parameters: ϕ_1, ϕ_a, λ_t. Standard errors are provided in parentheses.

year	ϕ_1	ϕ_a	λ_t
1	0.5566(0.0069)	0.6982(0.0046)	0.0560(0.0039)
2			0.0476(0.0028)
3			0.0403(0.0023)
4			0.0398(0.0021)
5			0.0414(0.0020)
6			0.0425(0.0020)
7			0.0380(0.0019)
8			0.0348(0.0018)
9			0.0414(0.0019)
10			0.0393(0.0019)
11			0.0398(0.0019)
12			0.0364(0.0018)
13			0.0364(0.0018)
14			0.0346(0.0017)
15			0.0333(0.0016)
16			0.0310(0.0016)
17			0.0301(0.0015)
18			0.0308(0.0015)
19			0.0269(0.0014)
20			0.0314(0.0015)

Table A.35 Estimates of survival and reporting probabilities for the blackbird data for the standard combined model with data for pulli, juvenille and adult birds for the model with parameters: ϕ_1, $\phi_{a,t}$, λ_t. Standard errors are provided in parentheses.

year	ϕ_1	$\phi_{a,t}$	λ_t
1	0.5568(0.0073)	0.6763(0.0472)	0.0553(0.0041)
2		0.7002(0.0285)	0.0478(0.0033)
3		0.7214(0.0239)	0.0419(0.0030)
4		0.6882(0.0236)	0.0387(0.0026)
5		0.6891(0.0231)	0.0406(0.0027)
6		0.6699(0.0219)	0.0404(0.0026)
7		0.7056(0.0217)	0.0394(0.0029)
8		0.7129(0.0225)	0.0363(0.0028)
9		0.7110(0.0216)	0.0425(0.0031)
10		0.7274(0.0220)	0.0417(0.0032)
11		0.7331(0.0220)	0.0422(0.0034)
12		0.7127(0.0256)	0.0362(0.0030)
13		0.6469(0.0289)	0.0312(0.0026)
14		0.6877(0.0268)	0.0341(0.0028)
15		0.6624(0.0292)	0.0312(0.0027)
16		0.7054(0.0262)	0.0325(0.0027)
17		0.6743(0.0278)	0.0291(0.0024)
18		0.6842(0.0288)	0.0307(0.0025)
19		0.6754(0.0368)	0.0263(0.0025)
20		0.7245(0.0314)	0.0344(0.0027)

Historical Model

Table A.36 Estimates of survival and reporting probabilities for the blackbird data for the historical combined model with data for pulli and fledged birds for the model with parameters: $\phi_{1,t}$, ϕ_a, λ_t, π. Standard errors are provided in parentheses.

year	$\phi_{1,t}$	ϕ_a	λ_t	π
1	0.4312(0.1021)	0.6982(0.0047)	0.0473(0.0076)	0.5716(0.0067)
2	0.5519(0.0368)		0.0477(0.0033)	
3	0.5622(0.0331)		0.0404(0.0025)	
4	0.5855(0.0293)		0.0403(0.0022)	
5	0.5526(0.0273)		0.0415(0.0020)	
6	0.5781(0.0271)		0.0427(0.0020)	
7	0.5891(0.0288)		0.0378(0.0019)	
8	0.578(0.0307)		0.0345(0.0018)	
9	0.5675(0.0278)		0.0411(0.0019)	
10	0.5415(0.0288)		0.0391(0.0019)	
11	0.5674(0.0302)		0.0394(0.0019)	
12	0.5505(0.0302)		0.0361(0.0018)	
13	0.5671(0.0293)		0.0364(0.0018)	
14	0.5254(0.0291)		0.0347(0.0017)	
15	0.5556(0.0288)		0.0334(0.0016)	
16	0.5281(0.0298)		0.0310(0.0016)	
17	0.5589(0.0312)		0.0301(0.0015)	
18	0.5561(0.0308)		0.0308(0.0015)	
19	0.5853(0.0312)		0.0270(0.0014)	
20	0.5129(0.0281)		0.0314(0.0015)	

Table A.37 Estimates of survival and reporting probabilities for the blackbird data for the historical combined model with data for pulli and fledged birds for the model with parameters: ϕ_1, ϕ_a, $\lambda_{1,t}$, $\lambda_{a,t}$, π. Standard errors are provided in parentheses.

year	ϕ_1	ϕ_a	$\lambda_{1,t}$	$\lambda_{a,t}$	π
1	0.4019(0.0290)	0.6983(0.0047)	0.0417(0.0042)	0.0576(0.0097)	0.6483(0.0177)
2			0.0342(0.0034)	0.0572(0.0061)	
3			0.0281(0.0029)	0.0506(0.0048)	
4			0.0263(0.0027)	0.0519(0.0045)	
5			0.0300(0.0029)	0.0509(0.0042)	
6			0.0268(0.0027)	0.0565(0.0044)	
7			0.0240(0.0027)	0.0495(0.0039)	
8			0.0220(0.0025)	0.0450(0.0037)	
9			0.0266(0.0028)	0.0534(0.0041)	
10			0.0268(0.0029)	0.0493(0.0039)	
11			0.0243(0.0028)	0.0518(0.0040)	
12			0.0233(0.0026)	0.0465(0.0037)	
13			0.0233(0.0026)	0.0470(0.0037)	
14			0.0253(0.0027)	0.0422(0.0034)	
15			0.0238(0.0025)	0.0411(0.0033)	
16			0.0232(0.0025)	0.0373(0.0030)	
17			0.0191(0.0022)	0.039(0.0031)	
18			0.0194(0.0022)	0.040(0.0031)	
19			0.0181(0.0022)	0.034(0.0028)	
20			0.0242(0.0024)	0.0370(0.0029)	

Table A.38 Estimates of survival and reporting probabilities for the blackbird data for the historical combined model with data for pulli and fledged birds for the model with parameters: ϕ_1, ϕ_a, λ_t, π_t. Standard errors are provided in parentheses.

year	ϕ_1	ϕ_a	λ_t	π_t
1	0.5590(0.0069)	0.6968(0.0046)	0.0563(0.0040)	0.6739(0.0408)
2			0.0476(0.0028)	0.6406(0.0355)
3			0.0402(0.0023)	0.5820(0.0364)
4			0.0397(0.0021)	0.6130(0.0309)
5			0.0415(0.0020)	0.5931(0.0308)
6			0.0425(0.0020)	0.5358(0.0278)
7			0.0377(0.0019)	0.5930(0.0289)
8			0.0345(0.0018)	0.5791(0.0301)
9			0.0411(0.0019)	0.5696(0.0270)
10			0.0391(0.0019)	0.5670(0.0277)
11			0.0394(0.0019)	0.5256(0.0282)
12			0.0361(0.0018)	0.5190(0.0286)
13			0.0364(0.0018)	0.5446(0.0280)
14			0.0347(0.0017)	0.5712(0.0283)
15			0.0334(0.0016)	0.6208(0.0278)
16			0.0311(0.0016)	0.6109(0.0287)
17			0.0302(0.0015)	0.5089(0.0296)
18			0.0308(0.0015)	0.4959(0.0288)
19			0.0270(0.0014)	0.6204(0.0300)
20			0.0315(0.0015)	0.6005(0.0271)

Table A.39 Estimates of survival and reporting probabilities for the blackbird data for the historical combined model with data for pulli and fledged birds for the model with parameters: ϕ_1, ϕ_a, $\lambda_{1,t}$, $\lambda_{a,t}$, π_t. Standard errors are provided in parentheses.

year	ϕ_1	ϕ_a	$\lambda_{1,t}$	$\lambda_{a,t}$	π_t
1	0.4126(0.0296)	0.6987(0.0047)	0.0354(0.0052)	0.1400(0.1389)	0.8557(0.1415)
2			0.0331(0.0034)	0.0615(0.0075)	0.7100(0.0415)
3			0.0285(0.0030)	0.0501(0.0051)	0.6518(0.0424)
4			0.0258(0.0027)	0.0535(0.0050)	0.6958(0.0341)
5			0.0302(0.0031)	0.0507(0.0045)	0.6605(0.0373)
6			0.0280(0.0029)	0.0544(0.0043)	0.6167(0.0335)
7			0.0238(0.0027)	0.0497(0.0041)	0.6757(0.023)
8			0.0223(0.0026)	0.0447(0.0038)	0.6581(0.0339)
9			0.0272(0.0029)	0.0525(0.0042)	0.6451(0.0316)
10			0.0277(0.0031)	0.0480(0.0038)	0.6329(0.0331)
11			0.0258(0.0031)	0.0495(0.0039)	0.6050(0.0341)
12			0.0252(0.0029)	0.0438(0.0035)	0.5886(0.0358)
13			0.0244(0.0028)	0.0454(0.0036)	0.6220(0.0341)
14			0.0263(0.0029)	0.0409(0.0034)	0.6274(0.0349)
15			0.0233(0.0026)	0.0418(0.0035)	0.6879(0.0317)
16			0.0232(0.0026)	0.0374(0.0032)	0.6675(0.0334)
17			0.0209(0.0025)	0.0366(0.0030)	0.5823(0.0372)
18			0.0215(0.0026)	0.0371(0.0029)	0.5679(0.0368)
19			0.0175(0.0022)	0.0349(0.0030)	0.6998(0.0332)
20			0.0246(0.0026)	0.0365(0.0030)	0.6489(0.0336)

Table A.40 Estimates of survival and reporting probabilities for the blackbird data for the historical combined model with data for pulli and fledged birds for the model with parameters: ϕ_1, ϕ_a, λ_t, π. Standard errors are provided in parentheses.

year	ϕ_1	ϕ_a	λ_t	π
1	0.5573(0.0069)	0.6979(0.0046)	0.0577(0.0040)	0.5728(0.0067)
2			0.0480(0.0029)	
3			0.0403(0.0023)	
4			0.0398(0.0021)	
5			0.0415(0.0020)	
6			0.0425(0.0020)	
7			0.0378(0.0019)	
8			0.0345(0.0018)	
9			0.0411(0.0019)	
10			0.0391(0.0019)	
11			0.0395(0.0019)	
12			0.0361(0.0018)	
13			0.0364(0.0018)	
14			0.0347(0.0017)	
15			0.0334(0.0016)	
16			0.0311(0.0016)	
17			0.0301(0.0015)	
18			0.0308(0.0015)	
19			0.0270(0.0014)	
20			0.0316(0.0015)	

Table A.41 Estimates of survival and reporting probabilities for the blackbird data for the historical combined model with data for pulli and fledged birds for the model with parameters: ϕ_1, $\phi_{a,t}$, λ_t, π_t. Standard errors are provided in parentheses.

year	ϕ_1	$\phi_{a,t}$	λ_t	π_t
1	0.5604(0.0074)	0.5607(0.0708)	0.0525(0.0040)	0.7451(0.0461)
2		0.6931(0.0330)	0.0483(0.0037)	0.6257(0.0414)
3		0.7333(0.0257)	0.0435(0.0033)	0.5534(0.0401)
4		0.6777(0.0260)	0.0380(0.0027)	0.6193(0.0327)
5		0.6848(0.0262)	0.0407(0.0030)	0.5949(0.0333)
6		0.6825(0.0238)	0.0417(0.0030)	0.5375(0.0294)
7		0.7010(0.0232)	0.0387(0.0029)	0.5877(0.0305)
8		0.7089(0.0236)	0.0357(0.0029)	0.5728(0.0316)
9		0.7063(0.0226)	0.0419(0.0031)	0.5662(0.0285)
10		0.7230(0.0233)	0.0412(0.0032)	0.5581(0.0296)
11		0.7358(0.0225)	0.0425(0.0035)	0.5149(0.0299)
12		0.7183(0.0257)	0.0364(0.0031)	0.5167(0.0308)
13		0.6530(0.0293)	0.0317(0.0027)	0.5655(0.0294)
14		0.6956(0.0281)	0.0347(0.0029)	0.5712(0.0306)
15		0.6388(0.0303)	0.0297(0.0025)	0.6372(0.0288)
16		0.6882(0.0284)	0.0317(0.0027)	0.6074(0.0307)
17		0.6917(0.0293)	0.0308(0.0027)	0.5053(0.0320)
18		0.7120(0.0293)	0.0328(0.0029)	0.4855(0.0314)
19		0.6604(0.0401)	0.0251(0.0025)	0.6309(0.0319)
20		0.7346(0.0338)	0.0353(0.0030)	0.5797(0.0309)

A.6 Sandwich Tern Results

Figures A.1 and A.2 show the time dependent parameters for two of the best historical combined data models fitted to the sandwich tern data. Figure A.1 shows the time dependency

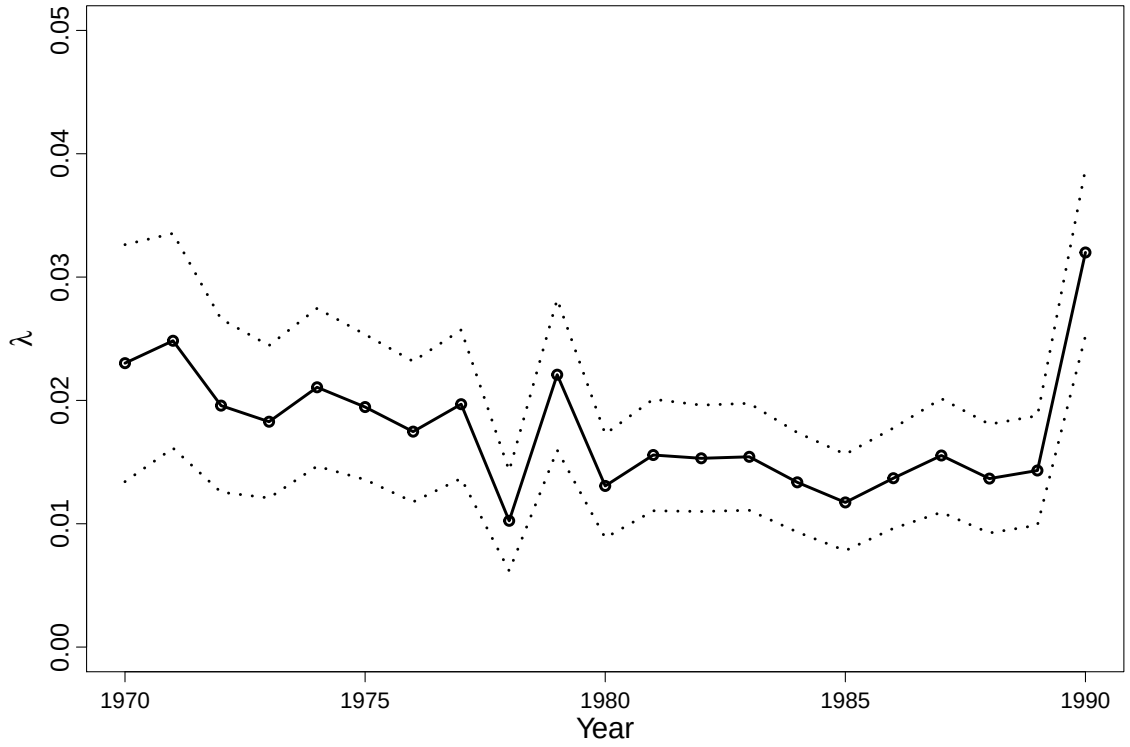

Fig. A.1 Estimated recovery probability, λ_t, for the historical combined data model with parameters (ϕ_1, ϕ_a, λ_t, π) for sandwich tern data for the years 1970-1990. The continuous line represent the estimated recovery probability, and the dotted lines represent 95 % confidence interval.

Fig. A.2 Estimated first-year survival probability, $\phi_{1,t}$, for the historical combined data model with parameters ($\phi_{1,t}$, ϕ_a, λ, π) for sandwich tern data for the years 1970-1990. The continuous line represent the estimated survival probability, and the dotted lines represent 95 % confindece interval.

Appendix B

Supporting Information for Chapter 3

This appendix provides additional simulation results to support the findings in Chapter 3. We present simulation studies for capture-recapture models in the presence of categorical, and continuous covariates.

B.1 Simulation Study in the Presence of Categorical Covariates

In this section we present simulation studies for most of the models fitted for the entire sample, and some of the models fitted for the female subsample. To generate the categorical covariates we simulate data from an uniform distribution with probability 0.50 and size 1. The models explained in Section 3.3.1, with either one or two categorical covariates, are used to fit each simulated dataset.

The parameter values chosen for the categorical covariates for our simulation study are selected so they are close to those obtained for our data in the results Section 3.5. When the parameters are kept constant, we choose from values that represent high survival or capture probabilities i.e 0.80, to values that represent low survival or capture probability, i.e. 0.20.

Survival depends on one categorical covariate and recapture is constant

This section shows results for capture-recapture models with the survival probability depending on a categorical covariate with two levels, i.e. site, and the capture probability kept constant. We examine how the estimates change with sample size and for different values for the capture parameter p. Tables B.1, 3.9, and B.2 show results for the capture probability fixed at 0.80, and 0.20. For all the two simulation studies, we keep $\alpha = 1.10$ and $\beta_{site} = -1.35$, these values give survival probabilities of 0.44 when $x_{1,i} = 1$, and 0.75 when $x_{1,i} = 0$.

Table B.1 Simulation study for 11-year of capture-recapture studies with survival as a function of a categorical covariate with two levels and capture probability fixed at 0.80. The first row specifies the model parameters and the values used to generate the simulated data. The first column (size) specifies the number of individuals marked every year of the study. The remaining columns contain the average parameter estimate (par est) and the average standard error, given in parentheses, along with the mean square error (MSE).

	ϕ				p	
	$\alpha = 1.10$		$\beta_{site} = -1.35$		$p = 0.80$	
size	par est	MSE	par est	MSE	par est	MSE
100	1.10(0.07)	0.0053	-1.35(0.11)	0.0103	0.80(0.01)	0.0003
50	1.09(0.10)	0.0093	-1.34(0.15)	0.0206	0.80(0.02)	0.0004
10	1.09(0.22)	0.0517	-1.35(0.34)	0.1192	0.80(0.05)	0.0024
5	1.04(0.31)	0.1145	-1.38(0.48)	0.2973	0.82(0.07)	0.0049

Tables B.1 and B.2 show that MSE increases when the sample size (the number of individuals marked each year) decreases. The best results are obtained when 100 individuals are marked. Additionally, a higher capture probability improves the results, with lower MSE when the capture probability is 0.80. Moreover, in Table B.2, the results for the sample size of five show a small bias in the estimation of all parameter estimates as well as large standard errors for the intercept and slope parameters. These results suggest that this model could be suffering from parameter redundancy issues caused by the limited data. This is, for a sample size of five, there is a probability of 0.03 that no individuals are simulated in one site.

Table B.2 Simulation study for 11-year of capture-recapture studies with survival as a function of a categorical covariate with two levels and capture probability fixed at 0.20. The first row specifies the model parameters and the values used to generate the simulated data. The first column (size) specifies the number of individuals marked every year of the study. The remaining columns contain the average parameter estimate (par est) and the average standard error, given in parentheses, along with the mean square error (MSE).

	ϕ				p	
	$\alpha = 1.10$		$\beta_{site} = -1.35$		$p = 0.20$	
size	par est	MSE	par est	MSE	par est	MSE
100	1.08(0.13)	0.0170	-1.33(0.16)	0.0257	0.20(0.02)	0.0003
50	1.12(0.20)	0.0336	-1.39(0.24)	0.0650	0.20(0.03)	0.0007
10	1.11(0.47)	0.2437	-1.45(0.57)	0.4570	0.21(0.06)	0.0035
5	1.25(7.78)	1.9522	-2.59(159.47)	21.9878	0.22(0.09)	0.0073

Survival is constant and recapture depends on one categorical covariate

This section shows results for capture-recapture models with the capture probability depending on a categorical covariate, i.e. sex, and the survival probability kept constant. We examine how the estimates change with sample size and for different values for the survival parameter. Tables B.3, B.4, and B.5 show results for the survival probability fixed at 0.80, 0.40 and 0.20. For all the three simulation studies, we keep $\alpha = 1.10$ and $\beta_{site} = -1.35$, these values give capture probabilities of 0.44 when $x_{1,i} = 1$, and 0.75 when $x_{1,i} = 0$.

Tables B.3, B.4, and B.5 show that the MSE increases when the sample size (the number of individuals marked each year) decreases. The best results are obtained when 100 individuals are marked. Additionally, a higher capture probability improves the results, with lower MSE when the survival probability is 0.80. Moreover, in Table B.4, the results for the sample size of five show a large bias in the estimation of all parameter estimates as well as large standard errors for the intercept and slope parameters. These results suggest that this model could be suffering from parameter redundancy issues caused by the limited data. This is, for a sample size of five, there is a probability of 0.03 that no individuals are simulated in one site.

Finally in this particular simulation we observe that when survival is set at 0.20 (Table B.5), there is a large bias in the estimation of all the parameters related to the capture probability. Note that, when the data sample is 10 or five individuals marked per year, we do not show results, as in some simulations there were problems when optimising the likelihood and simulations stopped.

Table B.3 Simulation study for 11-year of capture-recapture studies with survival probability fixed at 0.80 and capture probability as a function of a categorical covariate with two levels. The first row specifies the model parameters and the values used to generate the simulated data. The first column (size) specifies the number of individuals marked every year of the study. The remaining columns contain the average parameter estimate (par est) and the average standard error, given in parentheses, along with the mean square error (MSE).

	ϕ		p			
	$\phi = 0.80$		$\alpha = 1.10$		$\beta_{site} = -1.35$	
size	par est	MSE	par est	MSE	par est	MSE
100	0.80(0.01)	0.0001	1.10(0.09)	0.0074	-1.35(0.11)	0.0117
50	0.80(0.01)	0.0002	1.10(0.12)	0.0144	-1.36(0.16)	0.0226
10	0.80(0.03)	0.0007	1.10(0.27)	0.0640	-1.35(0.36)	0.1131
5	0.80(0.04)	0.0021	1.18(0.40)	0.2226	-1.45(0.53)	0.2804

Table B.4 Simulation study for 11-year of capture-recapture studies with survival probability fixed at 0.40 and capture probability as a function of a categorical covariate with two levels. The first row specifies the model parameters and the values used to generate the simulated data. The first column (size) specifies the number of individuals marked every year of the study. The remaining columns contain the average parameter estimate (par est) and the average standard error, given in parentheses, along with the mean square error (MSE).

	ϕ		p			
	$\phi = 0.40$		$\alpha = 1.10$		$\beta_{site} = -1.35$	
size	par est	MSE	par est	MSE	par est	MSE
100	0.40(0.02)	0.0003	1.13(0.24)	0.0672	-1.39(0.28)	0.1015
50	0.40(0.03)	0.0006	1.13(0.34)	0.1004	-1.38(0.39)	0.1429
10	0.38(0.06)	0.0036	2.73(163.69)	23.0983	-2.67(170.34)	24.7866
5	0.40(0.08)	0.0084	5.68(853.73)	73.7301	-4.39(1012.39)	70.6918

Table B.5 Simulation study for 11-year of capture-recapture studies with survival probability fixed at 0.20 and capture probability as a function of a categorical covariate with two levels. The first row specifies the model parameters and the values used to generate the simulated data. The first column (size) specifies the number of individuals marked every year of the study. The remaining columns contain the average parameter estimate (par est) and the average standard error, given in parentheses, along with the mean square error (MSE).

	ϕ		p			
	$\phi = 0.20$		$\alpha = 1.10$		$\beta_{site} = -1.35$	
size	par est	MSE	par est	MSE	par est	MSE
100	0.20(0.02)	0.0005	1.67(14.02)	5.8808	-1.85(14.00)	5.5339
50	0.20(0.03)	0.0013	2.64(114.97)	22.0384	-2.77(114.95)	19.8712
10	-	-	-	-	-	-
5	-	-	-	-	-	-

Both survival and recapture depend on one categorical covariate with two levels

This section shows results for capture-recapture models with both the survival and the capture probability depending on one categorical covariate with two levels, i.e. sex. We examine how the estimates change with sample size and for different values for the survival and capture parameters in Tables B.6, B.7, B.8, and B.9. We now choose two different values for α and β_{site}, and we use these two combinations to account for survival or for the capture probability. We either set $\alpha = 1.10$ and $\beta_{site} = -1.35$, these values give survival or capture probabilities of 0.44 when $x_{1,i} = 1$, and 0.75 when $x_{1,i} = 0$. Alternatively we set $\alpha = -0.70$ and $\beta_{site} = 1.85$ these values give survival or capture probabilities of 0.76 when $x_{1,i} = 1$, and 0.33 when $x_{1,i} = 0$.

Tables B.6, B.7, B.8, and B.9 show that MSE increases when the sample size (the number of individuals marked each year) decreases. Moreover, in Tables B.7, B.8, and B.9 the results for the sample sizes of five and 10 show a large bias in the estimation of all parameter estimates as well as large standard errors for the intercept and slope parameters. These results suggest that this model could be suffering from parameter redundancy issues caused by the limited data. This is, for a sample size of five, there is a probability of 0.03 that no individuals are simulated in one site.

Table B.6 Simulation study for 11-year of capture-recapture studies with both survival and capture probabilities as a function of a categorical covariate with two levels. The first row specifies the model parameters and the values used to generate the simulated data. The first column (size) specifies the number of individuals marked every year of the study. The remaining columns contain the average parameter estimate (par est) and the average standard error, given in parentheses, along with the mean square error (MSE).

	ϕ				p			
	$\alpha = 1.10$		$\beta_{site} = -1.35$		$\alpha = 1.10$		$\beta_{site} = -1.35$	
size	par est	MSE	par est	MSE	par est	MSE	par est	MSE
100	1.09(0.07)	0.0046	-1.38(0.15)	0.0190	1.10(0.10)	0.0090	-1.32(0.23)	0.0612
50	1.11(0.10)	0.0110	-1.37(0.21)	0.0531	1.10(0.13)	0.0167	-1.35(0.32)	0.1058
10	1.10(0.22)	0.0469	-1.42(0.49)	0.1995	1.12(0.30)	0.0638	-0.85(51.80)	8.1302
5	1.13(0.37)	0.1555	-1.61(0.68)	0.6474	1.19(0.52)	0.2362	1.88(633.78)	55.6706

Table B.7 Simulation study for 11-year of capture-recapture studies with both survival and capture probabilities as a function of a categorical covariate with two levels. The first row specifies the model parameters and the values used to generate the simulated data. The first column (size) specifies the number of individuals marked every year of the study. The remaining columns contain the average parameter estimate (par est) and the average standard error, given in parentheses, along with the mean square error (MSE).

	ϕ				p			
	$\alpha = -0.70$		$\beta_{site} = 1.85$		$\alpha = -0.70$		$\beta_{site} = 1.85$	
size	par est	MSE	par est	MSE	par est	MSE	par est	MSE
100	-0.72(0.21)	0.0663	1.87(0.22)	0.0727	-0.69(0.31)	0.1185	1.85(0.33)	0.1164
50	-0.74(0.27)	0.0688	1.89(0.29)	0.0727	-0.61(0.42)	0.1488	1.78(0.44)	0.1622
10	-0.89(0.59)	0.6635	2.02(0.64)	0.6935	2.45(377.62)	48.1398	-1.27(377.67)	48.1351
5	-1.67(54.18)	9.0680	2.82(54.23)	9.3771	5.40(1221.29)	98.5901	-4.19(1221.33)	98.2563

Table B.8 Simulation study for 11-year of capture-recapture studies with both survival and capture probabilities as a function of a categorical covariate with two levels. The first row specifies the model parameters and the values used to generate the simulated data. The first column (size) specifies the number of individuals marked every year of the study. The remaining columns contain the average parameter estimate (par est) and the average standard error, given in parentheses, along with the mean square error (MSE).

	ϕ				p			
	$\alpha = 1.10$		$\beta_{site} = -1.35$		$\alpha = -0.70$		$\beta_{site} = 1.85$	
size	par est	MSE	par est	MSE	par est	MSE	par est	MSE
100	1.09(0.10)	0.0111	-1.34(0.14)	0.0161	-0.69(0.10)	0.0105	1.86(0.25)	0.0646
50	1.10(0.16)	0.0217	-1.34(0.20)	0.0415	-0.70(0.15)	0.0181	1.90(0.34)	0.0968
10	1.06(0.33)	0.0850	-1.34(0.44)	0.1642	-0.65(0.33)	0.1021	3.64(256.70)	29.9263
5	1.13(0.53)	0.3186	-1.41(0.66)	0.4767	-0.69(0.50)	0.3171	5.89(652.10)	64.6317

Table B.9 Simulation study for 11-year of capture-recapture studies with both survival and capture probabilities as a function of a categorical covariate with two levels. The first row specifies the model parameters and the values used to generate the simulated data. The first column (size) specifies the number of individuals marked every year of the study. The remaining columns contain the average parameter estimate (par est) and the average standard error, given in parentheses, along with the mean square error (MSE).

	ϕ				p			
	$\alpha = -0.70$		$\beta_{site} = 1.85$		$\alpha = 1.10$		$\beta_{site} - 1.35$	
size	par est	MSE	par est	MSE	par est	MSE	par est	MSE
100	-0.71(0.10)	0.0111	1.87(0.14)	0.0224	1.14(0.30)	0.0871	-1.38(0.32)	0.1056
50	-0.73(0.16)	0.0309	1.89(0.20)	0.0519	1.30(0.52)	0.5018	-1.57(0.53)	0.5310
10	-0.77(0.36)	0.1716	1.96(0.46)	0.2055	5.15(492.33)	60.9590	-5.39(492.36)	60.9079
5	-0.85(0.46)	0.3233	1.92(0.65)	0.5620	8.77(1209.51)	115.3935	-8.71(1259.01)	115.5446

Survival depends on two categorical covariates with two levels and recapture is constant

This section shows results for capture-recapture models with the survival probability depending on two categorical covariates with two levels, i.e. sex and site, and the capture probability kept constant. We examine how the estimates change with sample size and for different values for the capture parameter. Tables B.10, B.11, and B.12 show results for the capture probability fixed at 0.80, 0.40 and 0.20. For all the three simulation studies, we keep $\alpha = 1.10$, $\beta_{sex} = 0.05$, and $\beta_{site} = -1.35$. The intercept and the slope value corresponding to the site covariate are kept at the same value than for the simulation in which we use one categorical covariate only. These values give survival probabilities of 0.75 when $x_{1,i} = 0$, and $x_{2,i} = 0$, 0.76 when $x_{1,i} = 0$, and $x_{2,i} = 1$, 0.44 when $x_{1,i} = 1$, and $x_{2,i} = 0$ and 0.45 when when $x_{1,i} = 1$, and $x_{2,i} = 1$.

If we compare these results to those obtained when survival only depends on one covariate Tables, B.1, 3.9, and B.2, for the shared parameters the MSE increases slightly. Moreover, the results presented for two categorical covariates also show that MSE increases when the sample size (the number of individuals marked each year) decreases, with the best results obtained when 100 individuals are marked. Additionally, in Table B.12, the results for the sample size of five show a large bias in the estimation of all parameter estimates as well as large standard errors for the intercept and slope parameters. These results suggest that this model could be suffering from parameter redundancy issues caused by the limited data. This is, for a sample size of five, there is a probability of 0.03 that no individuals are simulated in one site.

Table B.10 Simulation study for 11-year of capture-recapture studies with survival as a function of two categorical covariates with two levels and capture probability fixed at 0.80. The first row specifies the model parameters and the values used to generate the simulated data. The first column (size) specifies the number of individuals marked every year of the study. The remaining columns contain the average parameter estimate (par est) and the average standard error, given in parentheses, along with the mean square error (MSE).

	ϕ						p	
	$\alpha = 1.10$		$\beta_{sex} = 0.05$		$\beta_{site} = -1.35$		$p = 0.80$	
size	par est	MSE	par est	MSE	par est	MSE	par est	MSE
100	1.11(0.09)	0.0066	0.04(0.10)	0.0079	-1.35(0.15)	0.0101	0.80(0.02)	0.0002
50	1.09(0.13)	0.0133	0.07(0.15)	0.037	-1.35(0.15)	0.0225	0.80(0.02)	0.0004
10	1.12(0.27)	0.0911	0.01(0.33)	0.1140	-1.33(0.33)	0.0889	0.81(0.04)	0.0020
5	1.00(0.45)	0.2112	0.15(0.49)	0.2546	-1.33(0.48)	0.1656	0.81(0.07)	0.0045

Table B.11 Simulation study for 11-year of capture-recapture studies with survival as a function of two categorical covariates with two levels and capture probability fixed at 0.40. The first row specifies the model parameters and the values used to generate the simulated data. The first column (size) specifies the number of individuals marked every year of the study. The remaining columns contain the average parameter estimate (par est) and the average standard error, given in parentheses, along with the mean square error (MSE).

	ϕ						p	
	$\alpha = 1.10$		$\beta_{sex} = 0.05$		$\beta_{site} = -1.35$		$p = 0.40$	
size	par est	MSE	par est	MSE	par est	MSE	par est	MSE
100	1.10(0.11)	0.0132	0.05(0.13)	0.0146	-1.37(0.13)	0.0163	0.40(0.02)	0.0004
50	1.08(0.17)	0.0346	0.09(0.18)	0.0365	-1.38(0.18)	0.0267	0.40(0.03)	0.0010
10	1.03(0.35)	0.1302	0.06(0.41)	0.1480	-1.38(0.42)	0.1736	0.42(0.07)	0.0037
5	1.02(0.51)	0.2235	0.04(0.60)	0.3702	-1.47(0.63)	0.4050	0.42(0.09)	0.0082

Table B.12 Simulation study for 11-year of capture-recapture studies with survival as a function of two categorical covariates with two levels and capture probability fixed at 0.20. The first row specifies the model parameters and the values used to generate the simulated data. The first column (size) specifies the number of individuals marked every year of the study. The remaining columns contain the average parameter estimate (par est) and the average standard error, given in parentheses, along with the mean square error (MSE).

	ϕ						p	
	$\alpha = 1.10$		$\beta_{sex} = 0.05$		$\beta_{site} = -1.35$		$p = 0.20$	
size	par est	MSE	par est	MSE	par est	MSE	par est	MSE
100	1.11(0.16)	0.0291	0.06(0.16)	0.0304	-1.37(0.17)	0.0251	0.20(0.02)	0.0003
50	1.10(0.23)	0.0408	0.05(0.23)	0.0489	-1.38(0.24)	0.0547	0.20(0.03)	0.0007
10	1.04(0.52)	0.3113	0.12(0.55)	0.3835	-1.37(0.58)	0.3565	0.20(0.06)	0.0027
5	1.58(132.29)	30. 6801	0.15(217.27)	31.6926	-3.07(307.43)	54.6110	0.23(0.09)	0.0094

Survival is constant and recapture depends on two two categorical covariates with two levels

This section shows results for capture-recapture models with the capture probability depending on two categorical covariates with two levels, i.e. sex, and site, and the survival probability kept constant. We examine how the estimates change with sample size and for different values for the survival parameter. Tables B.13, B.14, and B.15 show results for the survival probability fixed at 0.80, 0.40 and 0.20. For all the three simulation studies, we keep $\alpha = 1.10$, $\beta_{sex} = 0.05$, and $\beta_{site} = -1.35$. The intercept and the slope value corresponding to the site covariate are kept at the same value than for the simulation in which we use one categorical covariate only. These values give capture probabilities of 0.75 when $x_{1,i} = 0$, and $x_{2,i} = 0$, 0.76 when $x_{1,i} = 0$, and $x_{2,i} = 1$, 0.44 when $x_{1,i} = 1$, and $x_{2,i} = 0$ and 0.45 when when $x_{1,i} = 1$, and $x_{2,i} = 1$.

If we compare these results to those obtained when recapture only depends on one covariate Tables, (see B.3, B.4, and B.5), for the MSE increases slightly for the shared parameters. Moreover, the results presented for two categorical covariates also show that the MSE increases when the sample size (the number of individuals marked each year) decreases, with the best results obtained when 100 individuals are marked. Moreover, in Table B.14, the results for the sample sizes of five and 10 show a large bias in the estimation of all parameter estimates as well as large standard errors for the intercept and slope parameters. These results suggest that this model could be suffering from parameter redundancy issues caused by the limited data. This is, for a sample size of five, there is a probability of 0.03 that no individuals are simulated in one site.

Finally in this particular simulation we observe that when survival is set at 0.20 (Table B.15), there is a large bias in the estimation of all the parameters related to the capture probability. Note that, when the data sample is 10 or five individuals marked per year, we do not show results, as in some simulations there were problems when optimising the likelihood and simulations stopped.

Table B.13 Simulation study for 11-year of capture-recapture studies with constant survival probability fixed at 0.80 and capture probability as a function of two categorical covariates with two levels. The first row specifies the model parameters and the values used to generate the simulated data. The first column (size) specifies the number of individuals marked every year of the study. The remaining columns contain the average parameter estimate (par est) and the average standard error, given in parentheses, along with the mean square error (MSE).

	ϕ		p					
	$\phi = 0.80$		$\alpha = 1.10$		$\beta_{sex} = 0.05$		$\beta_{site} = -1.35$	
size	par est	MSE	par est	MSE	par est	MSE	par est	MSE
100	0.80(0.01)	0.0001	1.11(0.10)	0.0108	0.05(0.11)	0.0119	-1.36(0.11)	0.0145
50	0.80(0.01)	0.0001	1.06(0.15)	0.0225	0.09(0.16)	0.0261	-1.35(0.80)	0.0287
10	0.81(0.03)	0.0008	1.09(0.36)	0.1229	0.04(0.37)	0.1081	-1.37(0.36)	0.1409
5	0.81(0.04)	0.0018	1.29(28.10)	2.8947	0.08(0.52)	0.3158	-1.67(28.15)	3.0204

Table B.14 Simulation study for 11-year of capture-recapture studies with constant survival probability fixed at 0.40 and capture probability as a function of two categorical covariates with two levels. The first row specifies the model parameters and the values used to generate the simulated data. The first column (size) specifies the number of individuals marked every year of the study. The remaining columns contain the average parameter estimate (par est) and the average standard error, given in parentheses, along with the mean square error (MSE).

	ϕ		p					
	$\phi = 0.40$		$\alpha = 1.10$		$\beta_{sex} = 0.05$		$\beta_{site} = -1.35$	
size	par est	MSE	par est	MSE	par est	MSE	par est	MSE
100	0.40(0.02)	0.0004	1.11(0.27)	0.0650	0.06(0.26)	0.0735	-1.38(0.27)	0.0631
50	0.39(0.03)	0.0007	1.22(0.40)	0.2017	0.02(0.39)	0.1482	-1.45(0.40)	0.2252
10	0.40(0.06)	0.0036	3.41(321.37)	38.1956	0.29(42.86)	10.0349	-3.25(310.08)	34.0445
5	0.41(0.08)	0.0060	5.53(989.19)	84.7461	0.42(644.76)	55.7477	-4.80(1178.88)	110.5444

Table B.15 Simulation study for 11-year of capture-recapture studies with constant survival probability fixed at 0.20 and capture probability as a function two categorical covariates with two levels. The first row specifies the model parameters and the values used to generate the simulated data. The first column (size) specifies the number of individuals marked every year of the study. The remaining columns contain the average parameter estimate (par est) and the average standard error, given in parentheses, along with the mean square error (MSE).

	ϕ		p					
	$\phi = 0.20$		$\alpha = 1.10$		$\beta_{sex} = 0.05$		$\beta_{site} = -1.35$	
size	par est	MSE	par est	MSE	par est	MSE	par est	MSE
100	0.20(0.02)	0.0004	1.39(13.48)	3.9703	0.16(9.66)	1.7158	-1.64(13.42)	3.8040
50	0.20(0.03)	0.0012	3.19(186.87)	29.7226	0.25(8.28)	3.9943	-3.38(18604)	28.4985
10	-	-	-	-	-	-	-	-
5	-	-	-	-	-	-	-	-

Survival Parameter with One Continuous Covariates

Simulation results for capture-recapture models with survival depending on a continuous covariates. The capture probability is kept constant at 0.80, 0.40 and 0.20. For all the three simulation studies, we keep $\alpha = 1.20$, and $\beta_{presence} = 0.25$. Tables B.16, B.17, B.18 show that the MSE increases when the sample size (the number of individuals marked each year) decreases, with the best results obtained when 100 individuals are marked.

Table B.16 Simulation study for 11-year of capture-recapture studies with survival as a function of a continuous covariate and capture probability fixed at 0.80. The first row specifies the model parameters and the values used to generate the simulated data. The first column (size) specifies the number of individuals marked every year of the study. The remaining columns contain the average parameter estimate (par est) and the average standard error, given in parentheses, along with the mean square error (MSE).

	ϕ				p	
	$\alpha = 1.20$		$\beta_{presence} = 0.25$		$p = 0.80$	
size	par est	MSE	par est	MSE	par est	MSE
100	1.20(0.05)	0.0023	0.25(0.05)	0.0024	0.80(0.01)	0.0001
50	1.20(0.07)	0.0051	0.25(0.07)	0.0043	0.80(0.02)	0.0002
10	1.21(0.16)	0.0260	0.26(0.16)	0.025	0.80(0.04)	0.0012
5	1.21(0.23)	0.0481	0.27(0.23)	0.0580	0.80(0.05)	0.0025

Table B.17 Simulation study for 11-year of capture-recapture studies with survival as a function of a continuous covariate and capture probability fixed at 0.40. The first row specifies the model parameters and the values used to generate the simulated data. The first column (size) specifies the number of individuals marked every year of the study. The remaining columns contain the average parameter estimate (par est) and the average standard error, given in parentheses, along with the mean square error (MSE).

	ϕ				p	
	$\alpha = 1.20$		$\beta_{presence} = 0.25$		$p = 0.40$	
size	par est	MSE	par est	MSE	par est	MSE
100	1.20(0.07)	0.0040	0.26(0.06)	0.0033	0.40(0.02)	0.0003
50	1.21(0.10)	0.0098	0.24(0.09)	0.0065	0.40(0.02)	0.0004
10	1.19(0.22)	0.0486	0.27(0.20)	0.0352	0.40(0.05)	0.0023
5	1.20(0.32)	0.1051	0.26(0.28)	0.0816	0.40(0.07)	0.0047

Table B.18 Simulation study for 11-year of capture-recapture studies with survival as a function of a continuous covariate and capture probability fixed at 0.20. The first row specifies the model parameters and the values used to generate the simulated data. The first column (size) specifies the number of individuals marked every year of the study. The remaining columns contain the average parameter estimate (par est) and the average standard error, given in parentheses, along with the mean square error (MSE).

	ϕ				p	
	$\alpha = 1.20$		$\beta_{presence} = 0.25$		$p = 0.20$	
size	par est	MSE	par est	MSE	par est	MSE
100	1.21(0.10)	0.0117	0.25(0.08)	0.0063	0.20(0.01)	0.0002
50	1.18(0.15)	0.0222	0.27(0.11)	0.0162	0.20(0.02)	0.0004
10	1.19(0.34)	0.1110	0.33(0.31)	0.1366	0.21(0.04)	0.0018
5	1.23(0.56)	0.3443	0.41(0.51)	0.5212	0.22(0.06)	0.0046

B.2 Simulation Study for Categorical and Continuous Covariates

Survival depends on one continuous covariate and recapture on one categorical covariate

Simulation results for capture-recapture models with survival depending on a continuous covariates, and recapture depending on a categorical covariate with two levels. For the survival probability we keep $\alpha = 1.20$, and $\beta_{presence} = 0.25$, and for the capture probability we keep $\alpha = 1.10$, and $\beta_{site} = -1.35$. Table B.19 shows that the MSE increases when the sample size (the number of individuals marked each year) decreases, with the best results obtained when 100 individuals are marked.

Table B.19 Simulation study for 11-year of capture-recapture studies with survival probability as a function of a continuous covariate and capture probability as a function of a categorical covariate with two levels. The first row specifies the model parameters and the values used to generate the simulated data. The first column (size) specifies the number of individuals marked every year of the study. The remaining columns contain the average parameter estimate (par est) and the average standard error, given in parentheses, along with the mean square error (MSE).

	ϕ				p			
	$\alpha = 1.20$		$\beta_{presence} = 0.25$		$\alpha = 1.10$		$\beta_{site} = -1.35$	
size	par est	MSE	par est	MSE	par est	MSE	par est	MSE
100	1.21(0.06)	0.0033	0.25(0.06)	0.0036	1.10(0.09)	1.0270	-1.35(0.12)	0.0114
50	1.21(0.08)	0.0069	0.24(0.08)	0.0062	1.11(0.13)	0.0182	-1.38(0.17)	0.0288
10	1.19(0.19)	0.0278	0.25(0.18)	0.0421	1.12(0.32)	0.1186	-1.35(0.40)	0.1310
5	1.23(0.27)	0.0607	0.28(0.26)	0.0831	1.11(0.42)	0.1754	-1.39(0.55)	0.3281

Survival depends on one continuous covariate and one categorical covariate and recapture is constant

Simulation results for capture-recapture models with survival probability depending on a categorical covariate with two levels and a continuous covariate. The capture probability is fixed at 0.80, 0.40 and 0.20. For the survival probability we keep $\alpha = 2.40$, $\beta_{presence} = 0.30$, and $\beta_{site} = -2.05$. Tables B.20, B.21, B.22 show that the MSE increases when the sample size (the number of individuals marked each year) decreases, with the best results obtained when 100 individuals are marked, and when the capture probability decreases, with better results when the capture probability is 0.80. Moreover, in Tables B.21, and B.22 the results for the sample sizes of five and 10 show a large bias in the estimation of all parameter estimates as well as large standard errors for the intercept and slope parameters. These results suggest that this model could be suffering from parameter redundancy issues caused by the limited data. This is, for a sample size of five, there is a probability of 0.03 that no individuals are simulated in one site.

Table B.20 Simulation study for 11-year of capture-recapture studies with survival as a function of a continuous and a categorical covariate with two levels and capture probability fixed at 0.80. The first column (size) specifies the number of individuals marked every year of the study. The remaining columns contain the average parameter estimate (par est) and the average standard error, given in parentheses, along with the mean square error (MSE).

	ϕ						p	
	$\alpha = 2.40$		$\beta_{site} = -2.05$		$\beta_{presence} = 0.30$		$p = 0.80$	
size	par est	MSE	par est	MSE	par est	MSE	par est	MSE
100	2.41(0.10)	0.0104	-2.06(0.12)	0.0174	0.30(0.06)	0.0039	0.80(0.01)	0.0001
50	2.41(0.14)	0.0183	-2.07(0.17)	0.0322	0.31(0.08)	0.0074	0.80(0.01)	0.0002
10	2.43(0.33)	0.1141	-2.11(0.40)	0.1448	0.30(0.19)	0.0261	0.80(0.03)	0.0010
5	2.45(0.44)	0.2377	-2.16(0.56)	0.4459	0.38(0.33)	0.1291	0.80(0.04)	0.0022

Table B.21 Simulation study for 11-year of capture-recapture studies with survival as a function of a continuous and a categorical covariate with two levels and capture probability fixed at 0.40. The first column (size) specifies the number of individuals marked every year of the study. The remaining columns contain the average parameter estimate (par est) and the average standard error, given in parentheses, along with the mean square error (MSE).

	ϕ						p	
	$\alpha = 2.40$		$\beta_{site} = -2.05$		$\beta_{presence} = 0.30$		$p = 0.40$	
size	par est	MSE	par est	MSE	par est	MSE	par est	MSE
100	2.39(0.13)	0.0148	-2.06(0.15)	0.0211	0.29(0.07)	0.0065	0.40(0.01)	0.0002
50	2.40(0.19)	0.0340	-2.07(0.21)	0.0396	0.30(0.10)	0.0095	0.40(0.02)	0.0004
10	2.43(0.45)	0.2204	-2.13(0.52)	0.2969	0.35(0.25)	0.0692	0.40(0.04)	0.0019
5	2.87(17.15)	5.3972	-2.85(17.25)	11.6433	0.44(0.50)	1.4108	0.40(0.07)	0.00435

Table B.22 Simulation study for 11-year of capture-recapture studies with survival as a function of a continuous and a categorical covariate with two levels and capture probability fixed at 0.20. The first column (size) specifies the number of individuals marked every year of the study. The remaining columns contain the average parameter estimate (par est) and the average standard error, given in parentheses, along with the mean square error (MSE).

	ϕ						p	
	$\alpha = 2.40$		$\beta_{site} = -2.05$		$\beta_{presence} = 0.30$		$p = 0.20$	
size	par est	MSE	par est	MSE	par est	MSE	par est	MSE
100	2.42(0.21)	0.0581	-2.11(0.22)	0.0575	0.30(0.10)	0.0106	0.20(0.01)	0.0002
50	2.47(0.32)	0.1084	-2.12(0.33)	0.1260	0.31(0.14)	0.0185	0.20(0.02)	0.0003
10	3.12(90.42)	10.5316	-2.84(90.44)	10.6138	0.34(0.35)	0.1430	0.21(0.04)	0.0017
5	9.12(214.89)	1122.8116	-12.12(319.60)	2693.0096	0.55(83.16)	607.7539	0.21(0.05)	0.0037

Survival depends on one continuous covariate and one categorical covariate and recapture depends on one categorical covariate

Simulation results for capture-recapture models with survival probability depending on a categorical covariate with two levels and a continuous covariates, and capture probability depending on a categorical covariate with two levels. For the survival probability we keep $\alpha = 2.40$, $\beta_{presence} = 0.30$, and $\beta_{site} = -2.05$. For the capture probability we choose two alternative scenarios, one when $\alpha = 1.10$, and $\beta_{site} = -1.35$, and the other when $\alpha = -0.70$, and $\beta_{site} = 1.85$.

Tables B.23 and B.24, show that the MSE increases when the sample size (the number of individuals marked each year) decreases, with the best results obtained when 100 individuals are marked, and when the capture probability decreases. Moreover, in Table B.24 the results for the sample sizes of five and 10 show a large bias in the estimation of all parameter estimates as well as large standard errors for the intercept and slope parameters. These results suggest that this model could be suffering from parameter redundancy issues caused by the limited data. This is, for a sample size of five, there is a probability of 0.03 that no individuals are simulated in one site. Additionally, for the case in which the capture parameters $\alpha = 1.10$, and $\beta_{site} = -1.35$, when the data sample is of five individuals marked per year of study, we do not show results, as in some simulations there were problems when optimising the likelihood and simulations stopped.

Table B.23 Simulation study for 11-year of capture-recapture studies with survival as a function of a continuous and a categorical covariate with two levels and capture probability as a function of site. The first column (size) specifies the number of individuals marked every year of the study. The remaining columns contain the average parameter estimate (par est) and the average standard error, given in parentheses, along with the mean square error (MSE).

	ϕ						p			
	$\alpha = 2.40$		$\beta_{site} = -2.05$		$\beta_{presence} = 0.30$		$\alpha = 1.10$		$\beta_{site} = -1.35$	
size	par est	MSE	par est	MSE	par est	MSE	par est	MSE	par est	MSE
100	2.41(0.10)	0.0105	-2.08(0.14)	0.0203	0.31(0.06)	0.0039	1.10(0.07)	0.0035	-1.33(0.15)	0.0232
50	2.41(0.15)	0.0192	-2.09(0.20)	0.0421	0.30(0.09)	0.0088	1.10(0.09)	0.0110	-1.33(0.21)	0.0471
10	2.48(0.34)	0.1312	-2.21(0.48)	0.2999	0.31(0.22)	0.0523	1.12(0.21)	0.0365	-1.18(19.76)	2.9298
5	-	-	-	-	-	-	-	-	-	-

Table B.24 Simulation study for 11-year of capture-recapture studies with survival as a function of a continuous and a categorical covariate with two levels and capture probability as a function of site. The first column (size) specifies the number of individuals marked every year of the study. The remaining columns contain the average parameter estimate (par est) and the average standard error, given in parentheses, along with the mean square error (MSE).

	ϕ						p			
	$\alpha = 2.40$		$\beta_{site} = -2.05$		$\beta_{presence} = 0.30$		$\alpha = -0.70$		$\beta_{site} = 1.85$	
size	par est	MSE	par est	MSE	par est	MSE	par est	MSE	par est	MSE
100	2.40(0.15)	0.0238	-2.07(0.17)	0.0293	0.29(0.07)	0.0054	-0.69(0.07)	0.0036	1.85(0.16)	0.0230
50	2.40(0.21)	0.0548	-2.04(0.24)	0.0691	0.31(0.09)	0.0086	-0.69(0.10)	0.0100	1.87(0.22)	0.0451
10	2.69(17.80)	2.4815	-2.35(17.85)	2.5554	0.32(0.23)	0.0596	-0.71(0.23)	0.0551	2.28(20.82)	5.0845
5	4.34(240.93)	26.1501	-4.06(241.00)	26.2814	0.27(0.35)	0.0855	-0.73(0.31)	0.1076	3.62(370.54)	29.6803

Appendix C

Simulation Study for Chapter 4

This appendix provides additional simulation results to support the findings in Chapter 4.

C.1 Comparison for Kalman Filter with Different Observation Errors

This section provides simulation results to compare the KF's results for two approaches which differ in the way the observation error was calculated. In the first one, the observation error is estimated as a parameter of the model. In the second one, the observation error is equal to the mean of the normal distribution. Further information about these two approaches can be found in Section 4.3.2. We conduct a simulation study for the IPMs, in which we generate 150 data sets in each simulation. To do so, for the SSM we simulate time-series data from the HMM described in Section 4.4.2 and for the ring-recovery model we simulate data from the standard model described in Section 1.2.1. In each simulation of the ring-recovery model 1000 birds are ringed in each year of study and for each age category: first-year and adult. Our simulations are for a stable population with parameter values: $\phi_1 = 0.30$, $\phi_a = 0.70$, $\rho = 1.00$, and $\lambda = 0.02$. We do this for three population sizes of $N_0 = 20$, 40 and 60.

Table C.1 shows the simulation results for this comparison. Here, we can observe that the parameter estimate results and the MSE are the same for both approaches. Meaning that, choosing one approach over the other does not seem to have an impact in the parameter estimates that we obtain. This probably results from the KF estimating the value of σ^2_η very close to the value of N_0. This is true for all the different population sizes that we compare. The reader should note that as we are simulating the data for the observation process from a Poisson distribution for a stable population, $\hat{N}_t \approx N_0$ for all t. Therefore, as in the Poisson

distribution the mean and the variance are the same, when we estimate σ_η^2 its value is very close to N_0. In the future we suggest the study of non-stable populations.

Table C.1 Simulation study to compare the KF results for two approaches that use different observation errors. The first column (N_0) specifies the average population size for a stable population with parameters $\phi_1 = 0.30$, $\phi_a = 0.70$, $\rho = 1.00$, and $\lambda = 0.02$. The second column method specifies which observation error was used: KF_1 means that σ_η was estimated and KF_2 that σ_η was equal to the mean of the normal distribution as in Besbeas and Morgan (2019). The remaining columns contain the average parameter estimate (par est) and the average standard error, given in parentheses, along with the mean square error (MSE). We do not provide the MSE for σ_η^2 as the data are simulated directly from the HMM, and therefore this parameter is not specified.

		$\phi_1 = 0.30$		$\phi_a = 0.70$		$\rho = 1.00$		$\lambda = 0.02$		σ_η
N_0	method	par est	MSE	par est	MSE	par est	MSE	par est	MSE	par est
20	KF_1	0.30(0.04)	0.0013	0.70(0.03)	0.0010	0.95(0.26)	0.0733	0.02(0.001)	0.0000	15.65(10.91)
20	KF_2	0.30(0.04)	0.0013	0.70(0.03)	0.0010	0.95(0.26)	0.0784	0.02(0.001)	0.0000	-
40	KF_1	0.30(0.04)	0.0015	0.70(0.03)	0.0009	0.96(0.22)	0.0588	0.02(0.001)	0.0000	31.32(20.13)
40	KF_2	0.30(0.04)	0.0015	0.70(0.03)	0.0008	0.95(0.22)	0.0546	0.02(0.001)	0.0000	-
60	KF_1	0.30(0.04)	0.0014	0.70(0.03)	0.0008	0.97(0.21)	0.0459	0.02(0.001)	0.0000	51.04(33.23)
60	KF_2	0.30(0.04)	0.0014	0.70(0.03)	0.0008	0.97(0.21)	0.0464	0.02(0.001)	0.0000	-

C.2 Performance of the IPM Under Different Scenarios

This section provides further simulation results to support the findings described in 4.6.1. Table C.2 shows the simulation results for 10 years of simulation study for an increasing population with $\phi_1 = 0.30$, $\phi_a = 0.70$ and $\rho = 1.10$. In Table C.2 we observe that the bias in estimating the productivity parameter ρ progressively decreases as size increases. Simulation results are not shown for the KF when $N_0 = 5$ as the algorithm stops working early in the simulation.

Table C.2 Median relative bias for an increasing population, with $\phi_1 = 0.30$, $\phi_a = 0.70$ and $\rho = 1.10$, for different population sizes, for 10 years of census and ring-recovery study.

	$\phi_1 = 0.30$		$\phi_a = 0.70$		$\rho = 1.10$	
N_0	KF	HMM	KF	HMM	KF	HMM
5	-	0.0008	-	0.0002	-	-0.1505
10	0.0047	0.0051	-0.0006	0.0006	-0.1530	-0.1089
20	0.0001	0.0002	-0.0018	-0.0019	-0.0480	-0.0289
40	-0.0014	-0.0010	-0.0059	-0.0062	-0.0196	-0.0023

Table C.3 shows the simulation results for 10 years of simulation study for a decrease population with $\phi_1 = 0.30$, $\phi_a = 0.70$ and $\rho = 0.90$. In Table C.3 we observe that the bias in estimating the productivity parameter ρ progressively decreases as size increases. Simulation results are not shown for the KF when $N_0 = 5$, and $N_0 = 10$ as the algorithm stops working early in the simulation.

Table C.3 Median relative bias for a decreasing population, with $\phi_1 = 0.30$, $\phi_a = 0.70$ and $\rho = 0.90$, for different population sizes, for 10 years of census and ring-recovery study.

	$\phi_1 = 0.30$		$\phi_a = 0.70$		$\rho = 0.90$	
N_0	KF	HMM	KF	HMM	KF	HMM
5	-	0.0075	-	0.0002	-	-0.2879
10	-	-0.0015	-	0.0031	-	-0.0730
20	0.0034	0.0037	-0.0021	-0.0018	-0.0836	-0.0443
40	-0.0008	-0.0005	0.0024	0.0023	-0.0680	-0.0515

Table C.4 shows the simulation results for 20 years of simulation study for stable population with $\phi_1 = 0.30$, $\phi_a = 0.70$ and $\rho = 1$. In Table C.4 we observe that the bias in estimating the productivity parameter ρ progressively decreases as size increases. Simulation results are not shown for the KF or the HMM when $N_0 = 5$, as the algorithms stop working early in the simulation. Moreover simulation results are not shown for the KF when $N_0 = 10$ for similar

reasons. Additionally, Figures C.1 and C.2 show boxplots and data plots which reflect the bias of the productivity parameter, ρ, presented in Table C.4.

Table C.4 Median relative bias for an stable population, with $\phi_1 = 0.30$, $\phi_a = 0.70$ and $\rho = 1$, for different population sizes, for 20 years of census and ring-recovery study.

	$\phi_1 = 0.30$		$\phi_a = 0.70$		$\rho = 1$	
N_0	KF	HMM	KF	HMM	KF	HMM
5	-	-	-	-	-	-
10	-	0.0003	-	-0.0016	-	-0.0748
20	0.0030	0.0030	0.0002	0.0003	-0.0406	-0.0259
40	-0.0006	-0.0006	0.0007	0.0007	-0.0030	0.0003

Table C.5 shows the simulation results for 10 years of simulation study for a stable population with $\phi_1 = 0.40$, $\phi_a = 0.60$ and $\rho = 1$. In Table C.5 we observe that the bias in estimating the productivity parameter ρ progressively decreases as size increases. Simulation results are not shown for the KF when $N_0 = 5$ as the algorithm stops working early in the simulation.

Table C.5 Median relative bias for a stable population, with $\phi_1 = 0.40$, $\phi_a = 0.60$ and $\rho = 1$, for different population sizes for 10 years of census and ring-recovery study.

	$\phi_1 = 0.40$		$\phi_a = 0.60$		$\rho = 1$	
N_0	KF	HMM	KF	HMM	KF	HMM
5	-	-0.0055	-	-0.0013	-	-0.0543
10	-0.0073	-0.0071	-0.0063	-0.0058	-0.0979	-0.0688
20	-0.0005	-0.0007	-0.0050	-0.0049	-0.0813	-0.0611
40	0.0038	0.0037	0.0004	0.0002	-0.0398	-0.0242

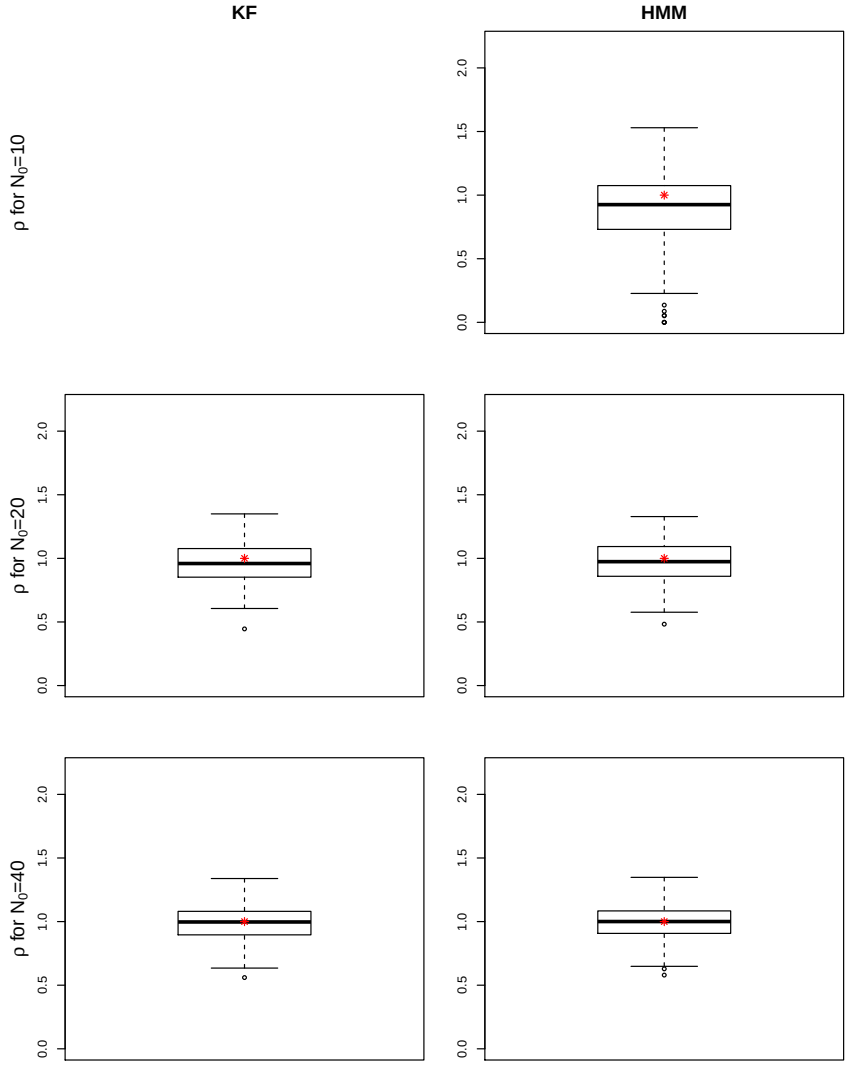

Fig. C.1 Boxplots containing the simulation results for the productivity parameter, ρ, for 20 years of study for a stable population, with $\phi_1 = 0.30$, $\phi_a = 0.70$ and $\rho = 1$, for different population sizes. The thick middle black line represents the median estimated value, and the red star the real value of ρ.

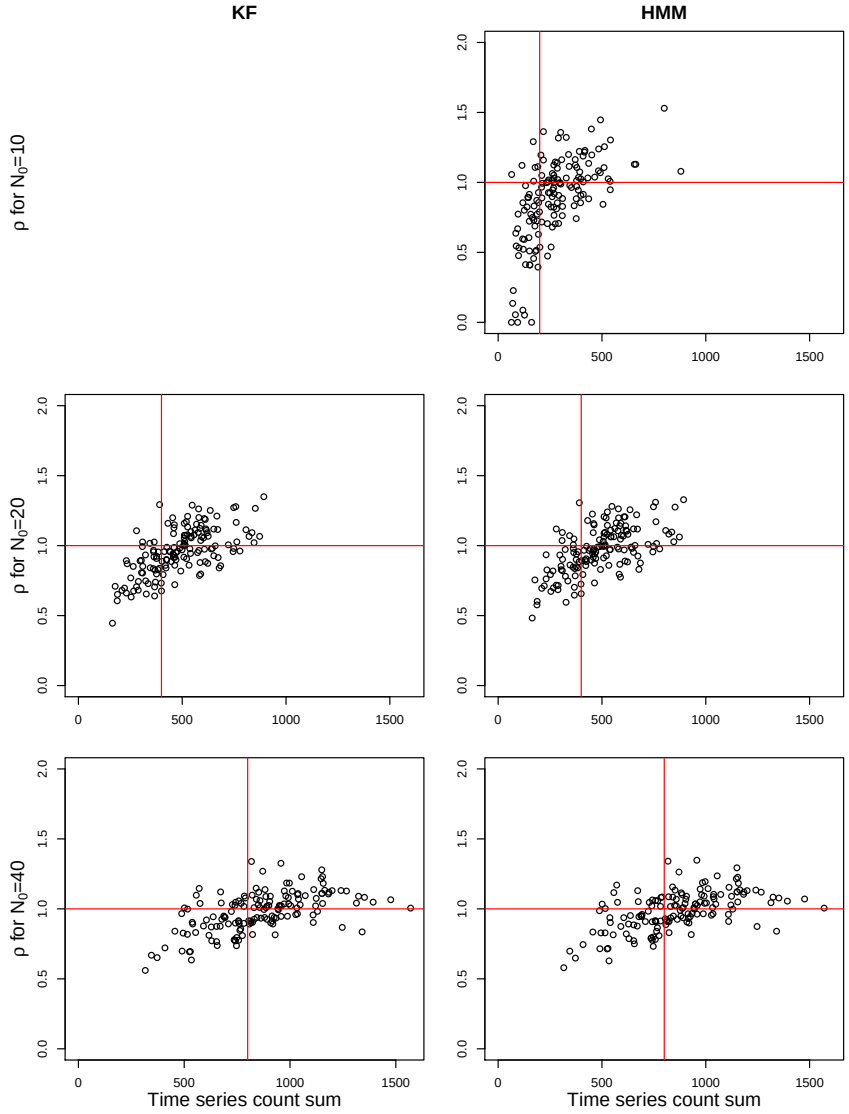

Fig. C.2 Simulation results for the productivity parameter, ρ, against the time series count sum for different population sizes for 20 years of study. The horizontal red lines in each plot represent the true value of ρ, and the vertical red lines represent the expected sum of the counts of the time-series observed in the 20 years of study.

C.2.1 Simulation of the Binomial-Poisson Non-Stationary Convolution

This section shows plots for the binomial, Poisson distributions and binomial-Poisson convolution.

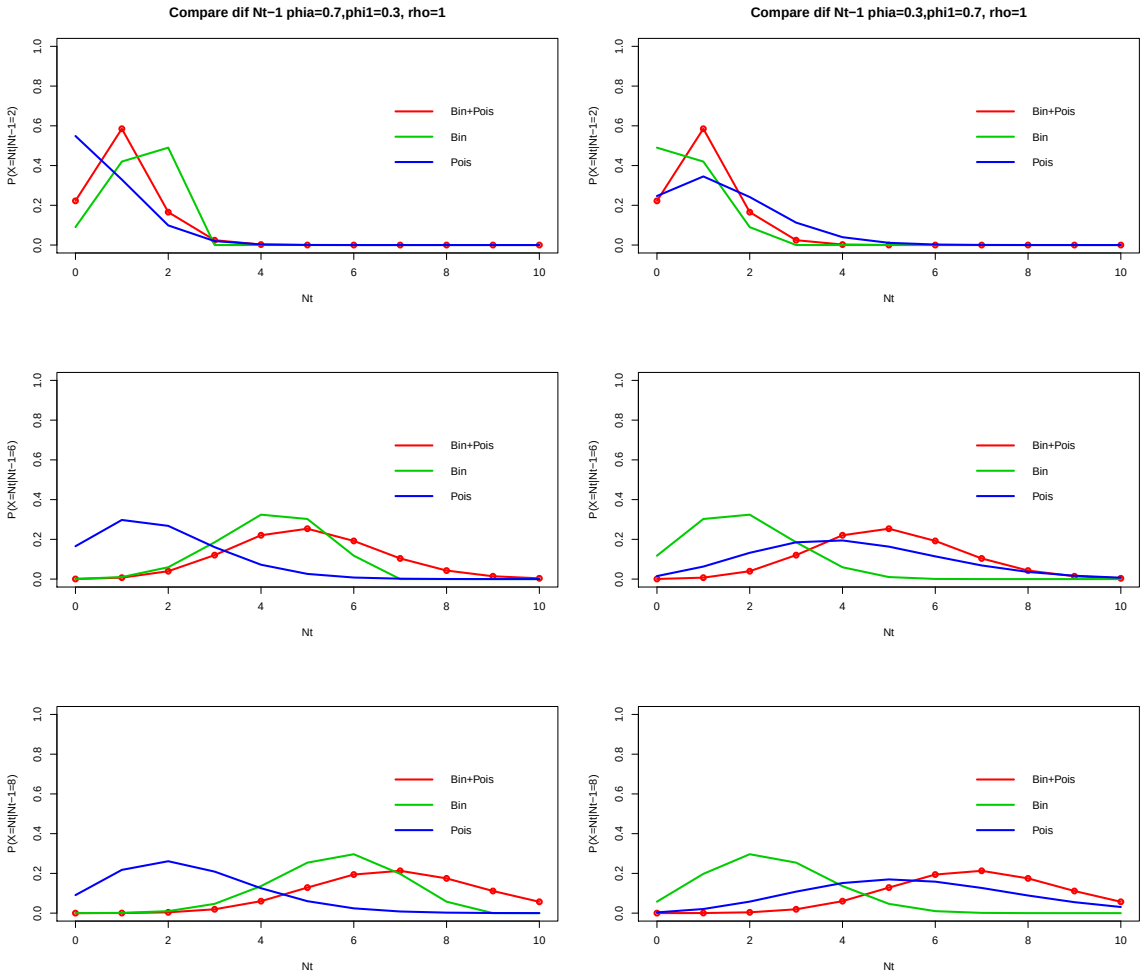

Fig. C.3 Binomial-Poisson non-stationary convolution for a stable population with $N_0 = 10$. The results on the left show a stable population with $\phi_1 = 0.30$, $\phi_a = 0.70$ and $\rho = 1$, on the right we invert the survival probabilities so they are $\phi_1 = 0.70$, $\phi_a = 0.30$. The red line shows the binomial-Poisson convolution. The green line represents the binomial distribution with probability $p = \phi_a$. The blue line shows the Poisson distribution where the mean $\theta = \phi_1\rho$. The first row shows the distributions when they are evaluated at the value 2, the second and third rows show the distributions when they are evaluated at 6 and 8.

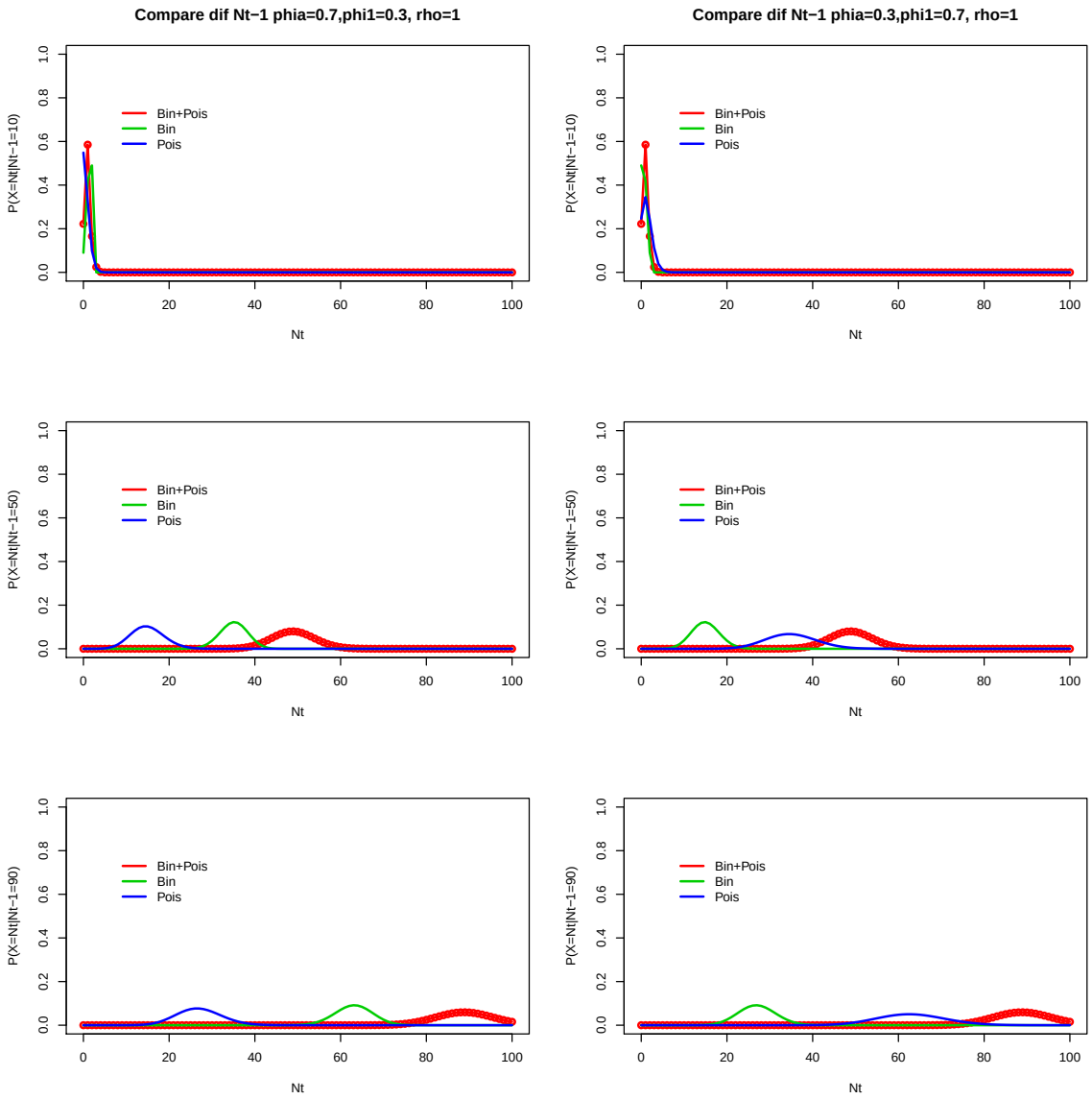

Fig. C.4 Binomial-Poisson non-stationary convolution for a stable population with $N_0 = 100$. The results on the left show a stable population with $\phi_1 = 0.30$, $\phi_a = 0.70$ and $\rho = 1$, on the right we invert the survival probabilities so they are $\phi_1 = 0.30$, $\phi_a = 0.70$. The red line shows the binomial-Poisson convolution. The green line represents the binomial distribution with probability $p = \phi_a$. The blue line shows the Poisson distribution where the mean $\theta = \phi_1\rho$. The first row shows the distributions when they are evaluated at the value 10, the second and third rows show the distributions when they are evaluated at 50 and 90.

C.2.2 The Non-stationaty Poisson Distribution for Time-Series SSMs.

This section provides further simulation results to support the findings described in 4.6.2.

Table C.6 Median relative bias for a non-stationary Poisson distribution with mean, $\theta = 1$ for a time series of size 20.

N_0	$\theta = 1.00$
5	-0.1177
10	-0.0806
20	-0.0299
40	-0.0106

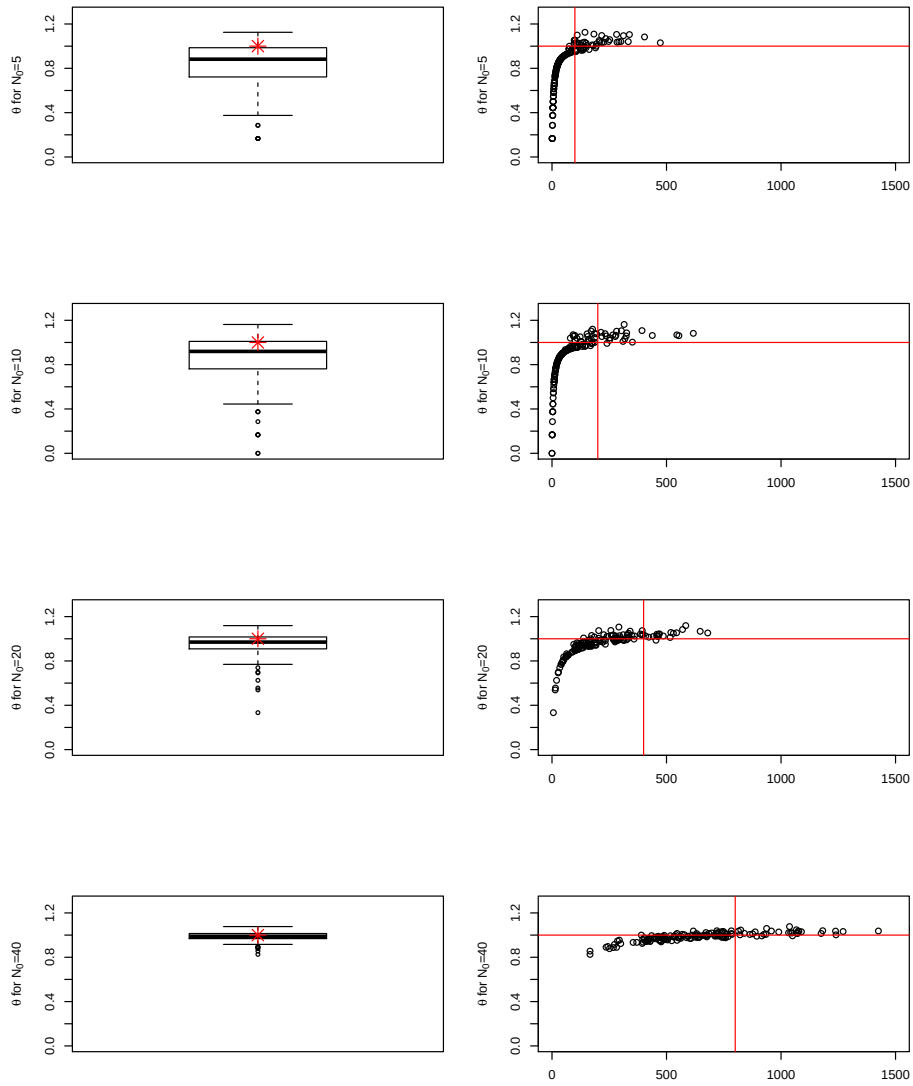

Fig. C.5 Simulation results for a non-stationary Poisson process with 10 years of data. On the left we present the boxplots containing the simulation results for the mean parameter, θ. The thick middle black line represents the median estimated value, and the red star the real value of θ. On the right we can observe the results for the mean parameter, θ, against the time series count sum for different population sizes for 10 years of study. The horizontal red lines in each plot represent the true value of θ, and the vertical red lines represent the expected sum of the counts of the time-series observed in the 10 years of study.

C.3 Combining Multiple Time-Series Data Sets—Effect on Bias

This section provides further simulation results to support the findings described in 4.6.4.

Table C.7 shows simulation results from combining several time-series data sets with different sizes in an IPM. The time-series fitted using the KF have $N_0 = 60$, and the time-series fitted using the HMM $N_0 = 10$. Table C.7 shows that overall having larger counts decreases the bias. Moreover, increasing the number of data sets in the analysis also decreases the bias.

Table C.7 Median relative bias for a stable population in the productivity parameter, ρ for IPMs that combine ring-recovery data with several time-series data sets which contain large and small counts. The time-series with large counts have $N_0 = 60$ and are fitted using the KF. The time-series with small counts have $N_0 = 10$ and are fitted using HMMs. Column 1 indicates the number of large data sets used and column 2 the number of small data sets used, and column 3 the bias for ρ. The first row indicates the data used and the combinations fitted.

large KF	small HMM	RR+large+small RR+KF+HMM
0	1	-0.3030
1	0	-0.0716
1	1	-0.0710
0	5	-0.0443
5	5	-0.0169
10	5	-0.0085
20	5	-0.0015
0	10	-0.0148
5	10	-0.0111
10	10	0.0062
20	10	0.0015
0	20	-0.0257
5	20	-0.0279
10	20	-0.0068
20	20	-0.0061
5	0	-0.0256
10	0	-0.0183
20	0	-0.0202

Appendix D

Supporting Information for Chapter 5

This appendix provides data and additional results to support the findings in Chapter 5.

D.1 Starling Data

In this section we provide the ring-recovery m-arrays for starling data. These data are part of the BTO Ringing Scheme, which is funded by a partnership of the British Trust for Ornithology, the Joint Nature Conservation Committee (on behalf of: Natural England, Natural Resources Wales and Scottish Natural Heritage and the Department of Agriculture, Environment and Rural Affairs (Northern Ireland), The National Parks and Wildlife Service (Ireland) and the ringers themselves. Table D.1 contains the ringing and recovery totals for the birds ringed as first-year birds. Table D.2 contains the ringing and recovery totals for birds ringed as adults respectively.

Table D.1 Ring-recovery data for starlings ringed in their first year of life for the years 1990-1999.

Year of ringing	Year of recovery 1	2	3	4	5	6	7	8	9	10	Total ringed
Ringed as first-year birds											
1990	48	26	5	7	4	5	1	1	0	0	4648
1991		47	18	6	2	4	2	0	1	3	5489
1192			27	13	9	5	0	3	2	2	3646
1993				37	21	11	4	3	2	1	4700
1994					23	13	10	6	1	1	4268
1995						44	13	11	4	3	5405
1996							35	17	4	1	4327
1997								22	16	4	4164
1998									24	14	4577
1999										15	3957

Table D.2 Ring-recovery data for starlings ringed as adults for the years 1990-1999.

Year of ringing	Year of recovery 1	2	3	4	5	6	7	8	9	10	Total ringed
Ringed as adults											
1990	9	19	7	4	4	1	2	0	2	0	1698
1991	0	7	10	5	2	3	0	3	0	0	1659
1992			6	7	6	1	1	0	0	1	1235
1993				2	9	8	4	5	0	2	1846
1994					5	10	6	4	3	0	1578
1995						4	5	3	7	3	1984
1996							5	7	4	1	1986
1997									5	3	1272
1998									2	7	1315
1999										3	1061

D.2 Comparison between IPMs and Separate Models

In this section we present a comparison between the IPMs, SSMs and RR models for the starling data. For this, we compare the best models in terms of AIC presented in Table 5.7 for each step of the "forward selection" procedure. In such a way, we start by comparing the model in which all parameters are kept constant (step 1). Then we compare the models in which one covariate (latitude) is added to ϕ_a (step 2). We continue by providing a comparison for the best models in steps 3-5. The SSM is parameter redundant. Therefore, we have to reparameterise it by introducing a new parameter, $\beta = \phi_1\rho$ (Section 1.2.2). We provide a comparison in all of the steps for the IPMs and the RR models. However, for the SSMs we can only provide a comparison for steps 1 and 2, as in step 3 we add a covariate to ϕ_1.

Table D.3 shows a comparison for the models in which all the parameters are kept constant. Here, there is a slight variation in the parameter estimate values obtained for the IPM in comparison with the RR. In the IPM these values are slightly smaller. However, the standard errors for both models are identical. Additionally, Table D.3 shows that the estimate for ϕ_a is at the boundary, and has a very with a very large standard error. Moreover, here β is estimated at 0.957 which is significantly higher than the result that we would obtain from the product between the values of ϕ_1 and ρ from the IPM. This demonstrates that the SSM alone provides poor estimates of the parameters, as well as not being able to estimate ϕ_1 and ρ separately.

Tables D.4- D.7 show the results for the models in which spatial dependencies have been added to the survival parameters ϕ_1 and ϕ_a. Here, we observe that the estimates related to these parameter change between the IPM and the RR models. Additionally, for these models, the IPMs provide smaller standard errors than the RR models. This is true, in both cases, when the IPMs estimates the parameters higher and lower than the RR models.

Table D.3 Comparison between the IPM, SSM and RR models with all parameters kept constant. Parameter estimates, with standard errors given in parentheses. Here, $\beta = \phi_1\rho$. This reparameterisation is needed in the SSM as otherwise the model is parameter redundant.

Pars	IPM	SSM	RR
ϕ_a	0.660(0.018)	0.001(0.118)	0.676(0.019)
ϕ_1	0.546(0.021)	-	0.551(0.021)
ρ	0.550(0.050)	-	-
β	-	0.957(0.119)	-
σ_η	17.838(2.263)	16.454(2.205)	-
μ	15.523(1.550)	15.342(1.584)	-
λ	0.016(0.001)	-	0.016(0.001)

Table D.4 Comparison between the IPM, SSM and RR models. Parameter estimates, with standard errors given in parentheses, for the models in which ϕ_a is dependent on latitude and the remaining parameters are kept constant. Here, $\beta = \phi_1 \times \rho$. This reparameterisation is needed in the SSM as otherwise the model is parameter redundant.

Pars		IPM	SSM	RR
ϕ_a	α_1	0.781(0.087)	-2.038(0.932)	0.838(0.094)
	β_{lat_1}	0.343(0.067)	1.003(0.655)	0.301(0.089)
ϕ_1		0.562(0.021)	-	0.565(0.021)
ρ		0.521(0.049)	-	-
β		-	0.854(0.083)	-
σ_η		17.236(2.166)	15.867(2.132)	-
μ		15.136(1.524)	14.966(1.562)	-
λ		0.016(0.001)	-	0.016(0.001)

Table D.5 Comparison between the IPM and RR models. Parameter estimates, with standard errors given in parentheses, for the models in which ϕ_a is dependent on latitude, ϕ_1 is dependent on the urban type of land cover and the remaining parameters are kept constant. Note that it is not possible to fit the SSM alone, even with reparameterisation, due to parameter redundancy.

Pars		IPM	RR
ϕ_a	α_1	0.861(0.092)	0.927(0.093)
	β_{lat_1}	0.362(0.068)	0.423(0.078)
ϕ_1	α_2	0.807(0.135)	0.912(0.142)
	β_{urban}	-0.060(0.011)	-0.072(0.013)
ρ		0.506(0.050)	-
σ_η		16.777(2.088)	-
μ		14.827(1.505)	-
λ		0.017(0.001)	0.017(0.001)

Table D.6 Comparison between the IPM and RR models. Parameter estimates, with standard errors given in parentheses, for the models in which ϕ_a is dependent on latitude with linear and quadratic terms, ϕ_1 is dependent on the urban type of land cover and the remaining parameters are kept constant. Note that it is not possible to fit the SSM alone, even with reparameterisation, due to parameter redundancy.

Pars		IPM	RR
ϕ_a	α_1	0.707(0.100)	0.710(0.117)
	β_{lat_1}	0.213(0.081)	0.126(0.132)
	$\beta_{lat_1^2}$	0.137(0.046)	0.174(0.063)
ϕ_1	α_2	0.856(0.131)	0.916(0.138)
	β_{urban}	-0.065(0.011)	-0.072(0.013)
ρ		0.524(0.050)	-
σ_η		16.664(2.042)	-
μ		14.994(1.519)	-
λ		0.017(0.001)	0.017(0.001)

Table D.7 Comparison between the IPM and RR models. Parameter estimates, with standard errors given in parentheses, for the models in which ϕ_a is dependent on latitude with linear and quadratic terms, ϕ_1 is dependent on the urban and farm types of land cover and the remaining parameters are kept constant. Note that it is not possible to fit the SSM alone, even with reparameterisation, due to parameter redundancy.

Pars		IPM	RR
ϕ_a	α_1	0.668(0.101)	0.708(0.117)
	β_{lat_1}	0.160(0.083)	0.127(0.132)
	$\beta_{lat_1^2}$	0.170(0.048)	0.180(0.063)
ϕ_1	α_2	1.041(0.151)	1.055(0.162)
	β_{urban}	-0.057(0.011)	-0.064(0.013)
	β_{farm}	-0.011(0.004)	-0.009(0.005)
ρ		0.535(0.050)	-
σ_η		16.520(2.037)	-
μ		14.941(1.517)	-
λ		0.017(0.001)	0.017(0.001)

D.3 Results for Starling Data

In this section we provide the results obtained from fitting the SE-IPM to additional models to those presented in 5.4.

Table D.8 shows some additional models fitted. In Table D.8 we see that the AIC values for all the models here are always higher than that obtained for the best model in terms of AIC from the "forward selection" procedures.

Table D.8 Additional models and model comparison for spatially-explicit IPMs fitted for the starling data for the years 1990-1999.

Model	No. pars	AIC
$\phi_{a,1(farm)}$	8	11,903.20
$\phi_{a,1(grass)}$	8	11,917.59
$\phi_{a,1(urban)}$	8	11,886.17
$\phi_{a,1(water)}$	8	11,915.46
$\phi_{a,1(wood)}$	8	11,912.26
$\phi_{a,1(long+long^2)}$	10	11,900.83
$\phi_{a,1(lat+long)}$	10	11,883.80
$\phi_{a,1(farm+urban)}$	10	11,881.49
$\phi_{a,1(farm+grass)}$	10	11,902.53
$\phi_{a,1(grass+urban)}$	10	11,886.05
$\phi_{a(farm+lat+long)}, \phi_{1(farm+lat)}$	11	11,880.87
$\phi_{a(grass+lat+long)}, \phi_{1(grass+lat)}$	11	11,880.46
$\phi_{a(urban+lat+long)}, \phi_{1(urban+lat)}$	11	11,868.27
$\phi_{a(water+lat+long)}, \phi_{1(water+lat)}$	11	11,885.38
$\phi_{a(wood+lat+long)}, \phi_{1(wood+lat)}$	11	11,882.50
$\phi_{a,1(lat+long+farm)}$	12	11,882.07
$\phi_{a,1(lat+long+grass)}$	12	11,882.03
$\phi_{a,1(lat+long+urban)}$	12	11,870.25
$\phi_{a,1(lat+long+water)}$	12	11,886.80
$\phi_{a,1(lat+long+wood)}$	12	11,884.50
$\phi_{a,1(lat+long+lat^2+long^2)}$	12	11,863.88
$\phi_{a(farm+lat+long+lat^2+long^2)}, \phi_{1(farm+lat+lat^2)}$	14	11,866.34
$\phi_{a(grass+lat+long+lat^2+long^2)}, \phi_{1(grass+lat+lat^2)}$	14	11,872.19
$\phi_{a(urban+lat+long+lat^2+long^2)}, \phi_{1(urban+lat+lat^2)}$	14	11,858.68
$\phi_{a(water+lat+long+lat^2+long^2)}, \phi_{1(water+lat+lat^2)}$	14	11,872.17
$\phi_{a,1(farm+lat+long+lat^2+long^2)}$	16	11,862.69

Table D.8 – continued from previous page

Model	No. pars	AIC
$\phi_{a,1(grass+lat+long+lat^2+long^2)}$	16	11,866.47
$\phi_{a,1(urban+lat+long+lat^2+long^2)}$	16	11,860.55
$\phi_{a,1(water+lat+long+lat^2+long^2)}$	16	11,861.57
$\phi_{a,1(wood+lat+long+lat^2+long^2)}$	16	11,866.24
$\phi_{a,1(lat+long+lat^2+long^2+lat^3+long^3)}$	16	11,926.54

D.3.1 Heat Maps

In this section we provide probability heat maps for the survival parameters for the second to the fifth best models in terms of AIC.

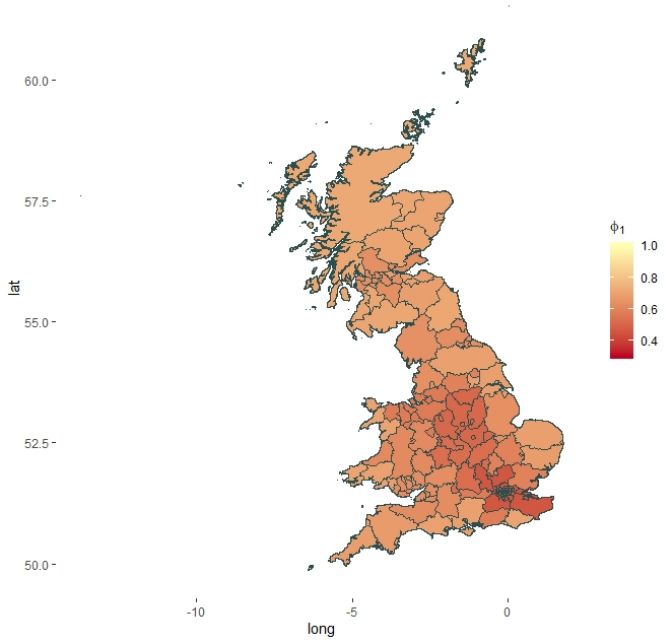

(a) First-year survival

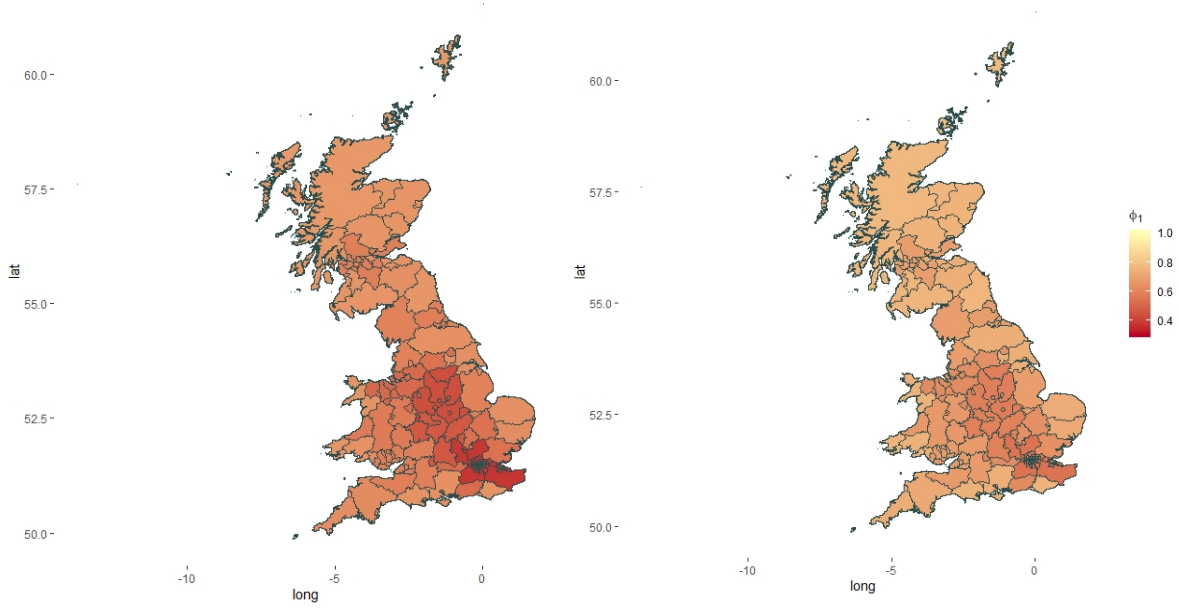

(b) Lower interval

(c) Upper interval

Fig. D.1 Heat maps for the second best model in terms of AIC: Survival probability and 95% confidence intervals for first-year starlings for the years 1990-1999.

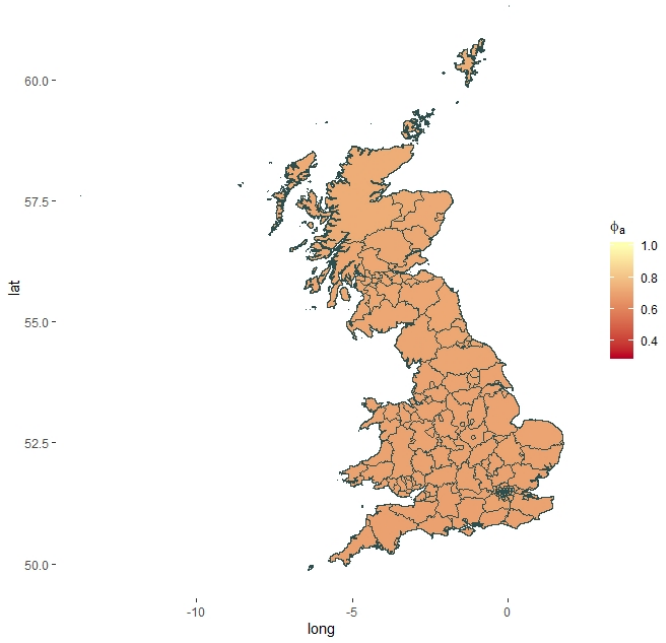

(a) Adult survival

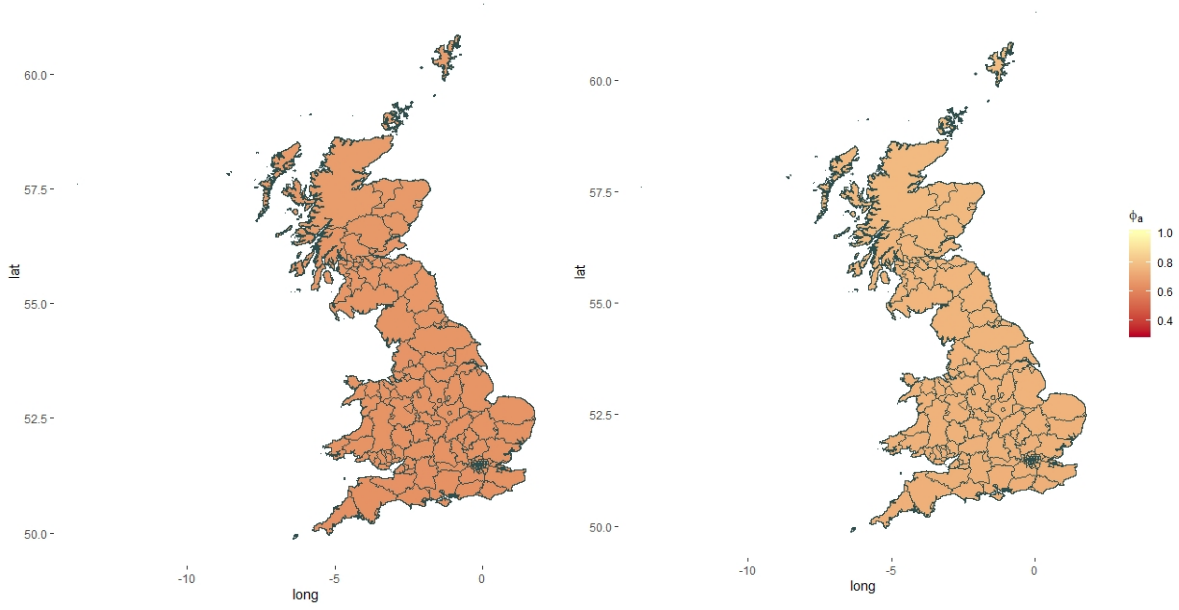

(b) Lower interval

(c) Upper interval

Fig. D.2 Heat maps for the second best model in terms of AIC: Survival probability and 95% confidence interval for adult starlings for the years 1990-1999.

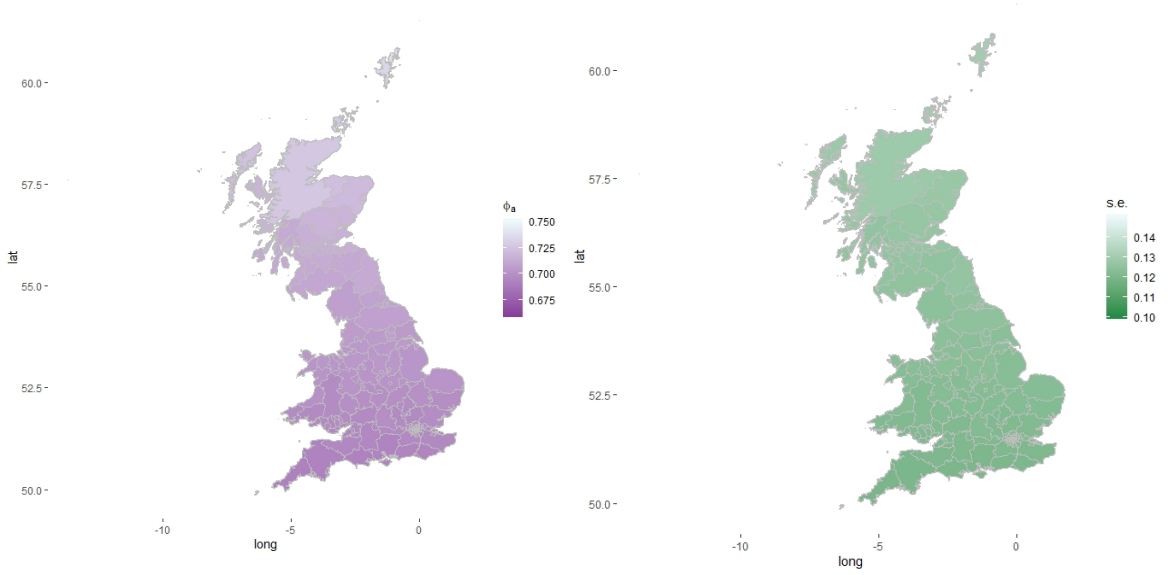

(a) Adult survival

(b) Standard errors

Fig. D.3 Adult survival probability and standard errors for the second best model in terms of AIC for starlings for the years 1990-1999.

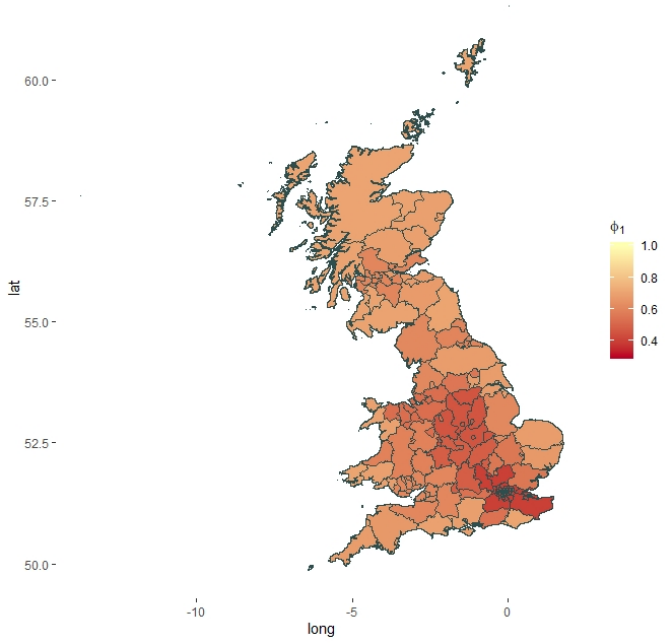

(a) First-year survival

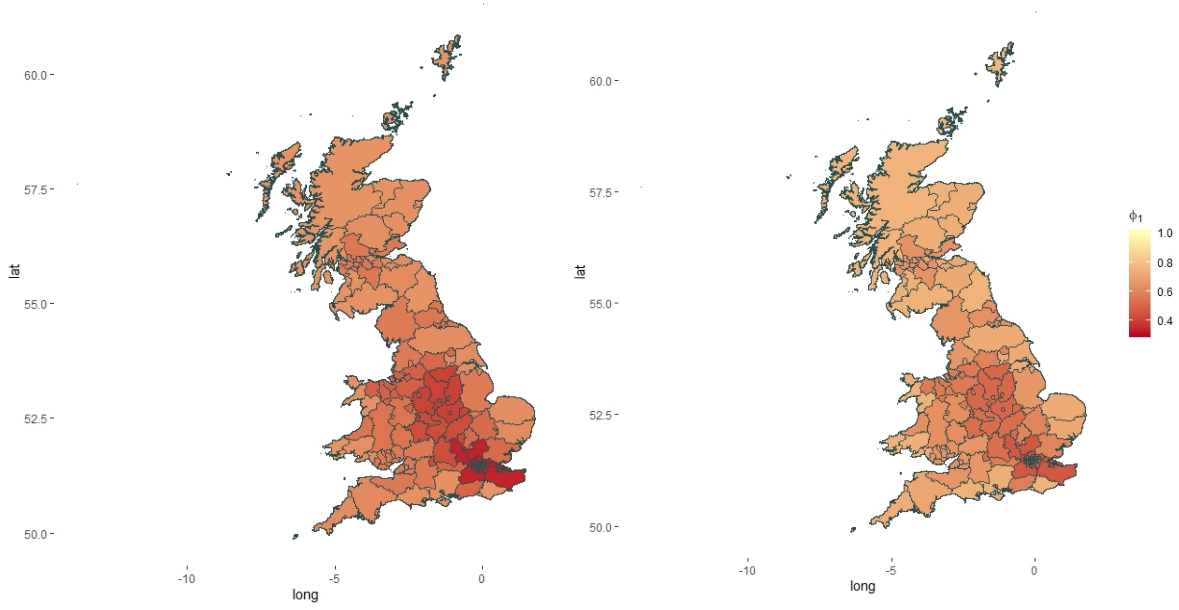

(b) Lower interval

(c) Upper interval

Fig. D.4 Heat maps for the third best model in terms of AIC: Survival probability and 95% confidence intervals for first-year starlings for the years 1990-1999.

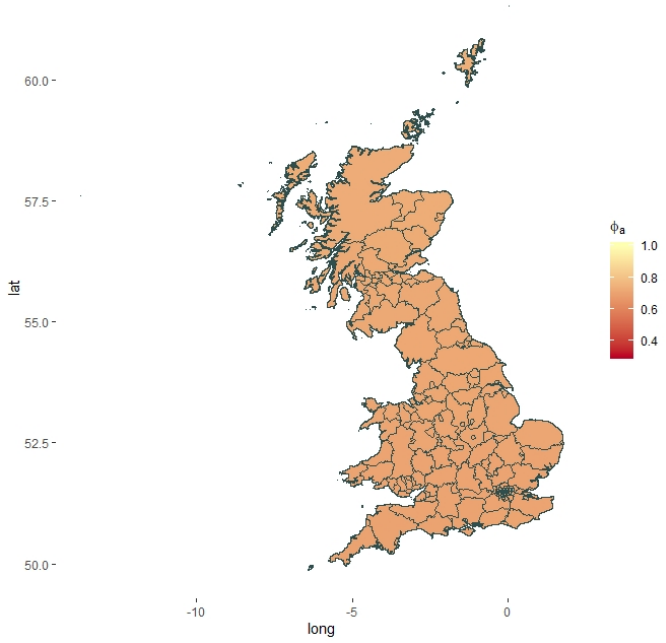

(a) Adult survival

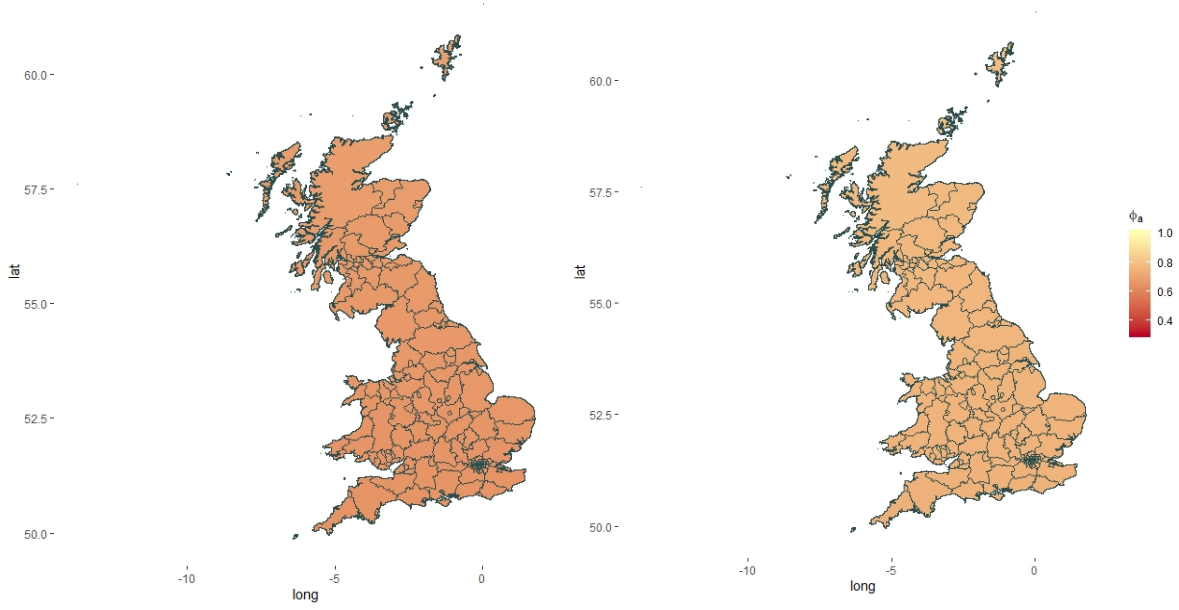

(b) Lower interval

(c) Upper interval

Fig. D.5 Heat maps for the third best model in terms of AIC: Survival probability and 95% confidence interval for adult starlings for the years 1990-1999.

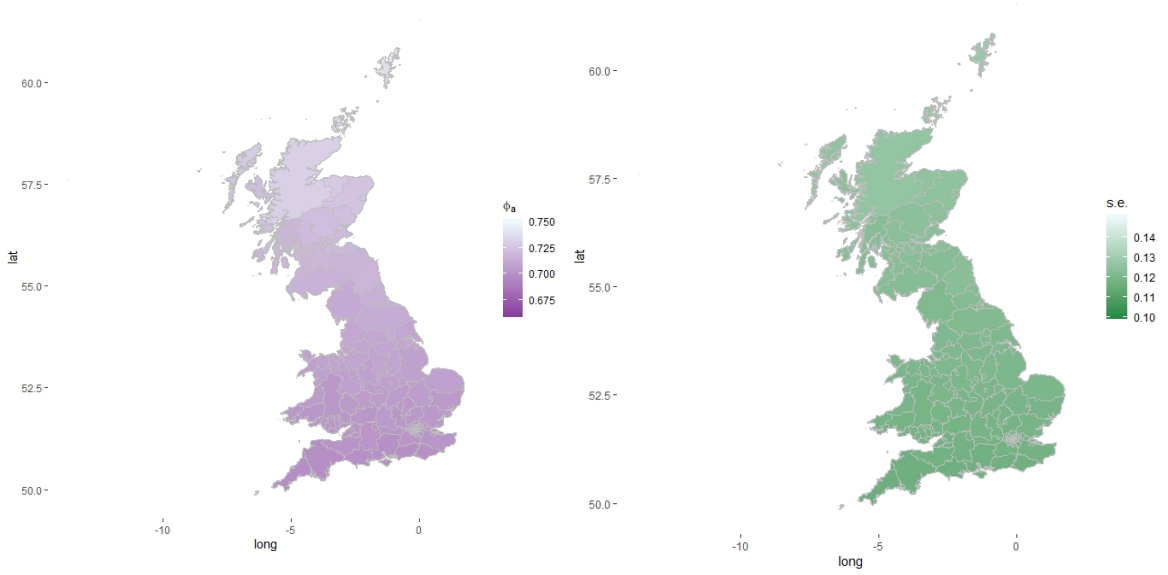

(a) Adult survival

(b) Standard errors

Fig. D.6 Adult survival probability and standard errors for the third best model in terms of AIC for starlings for the years 1990-1999.

D.3.2 Point Estimate Maps

In this section we provide the corresponding point maps to the heat maps provided in Sections 5.4 and D.3.1.

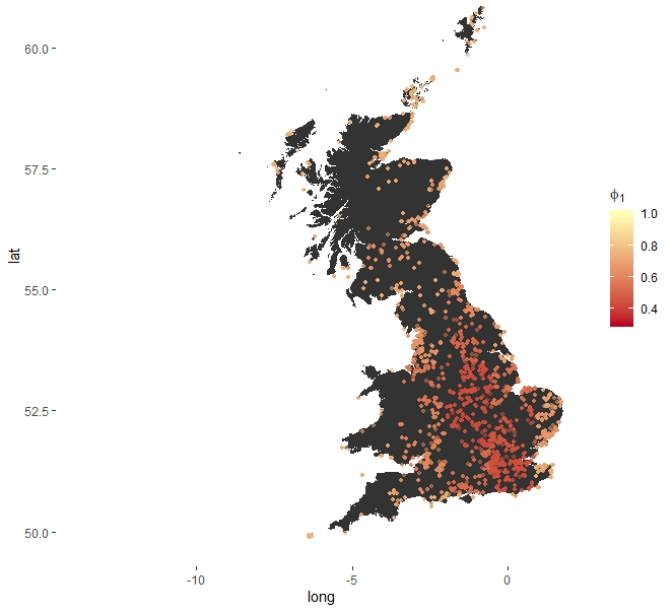

(a) First-year survival

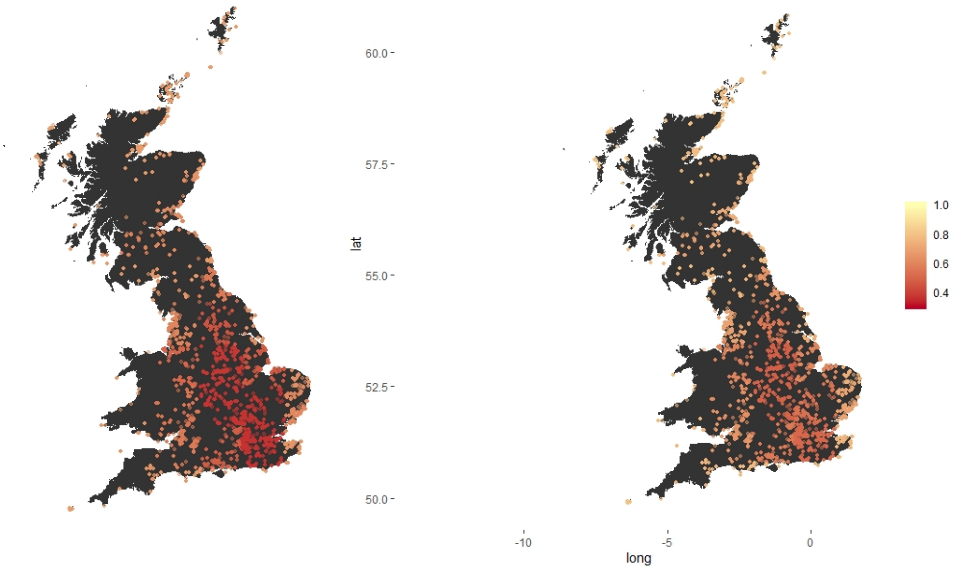

(b) Lower interval

(c) Upper interval

Fig. D.7 Point estimate maps for best model in terms of AIC: Survival probability and 95% confidence intervals for first-year starlings for the years 1990-1999.

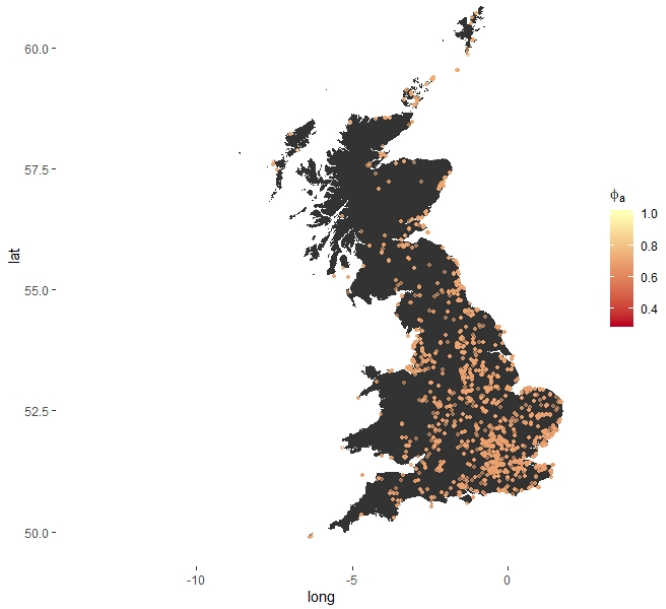

(a) Adult survival

(b) Lower interval

(c) Upper interval

Fig. D.8 Point estimate maps for best model in terms of AIC: Survival probability and 95% confidence intervals for adult starlings for the years 1990-1999.

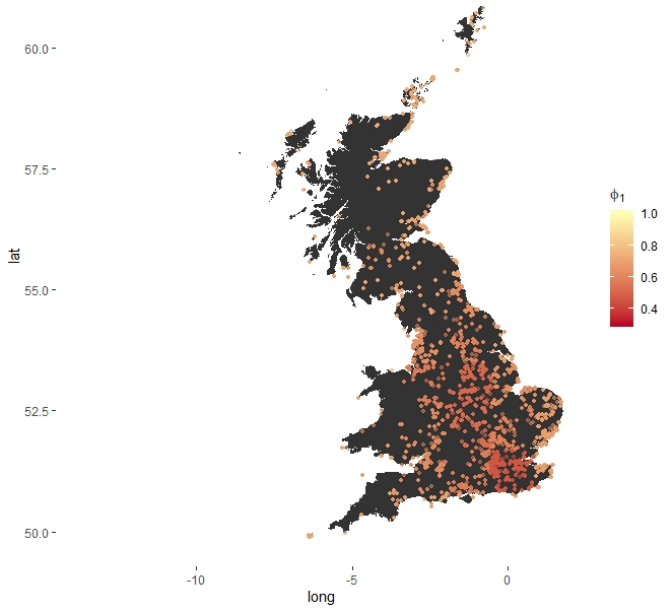

(a) First-year survival

(b) Lower interval

(c) Upper interval

Fig. D.9 Point estimate maps for the second best model in terms of AIC: Survival probability and 95% confidence intervals for first-year starlings for the years 1990-1999.

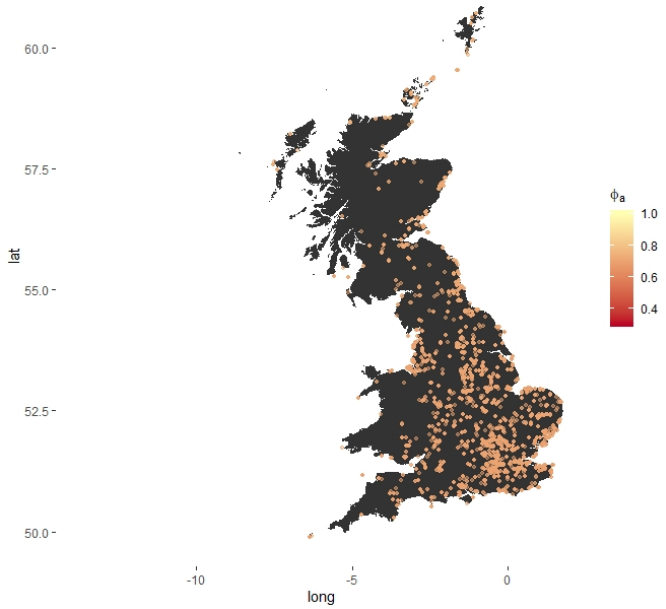

(a) Adult survival

(b) Lower interval

(c) Upper interval

Fig. D.10 Point estimate maps for the second best model in terms of AIC: Survival probability and 95% confidence interval for adult starlings for the years 1990-1999.

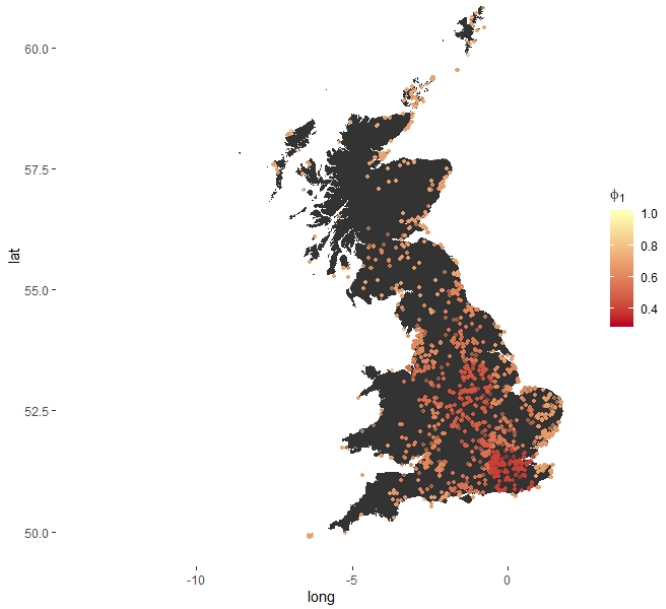

(a) Adult survival

(b) Lower interval

(c) Upper interval

Fig. D.11 Point estimate maps for the third best model in terms of AIC: Survival probability and 95% confidence interval for adult starlings for the years 1990-1999.

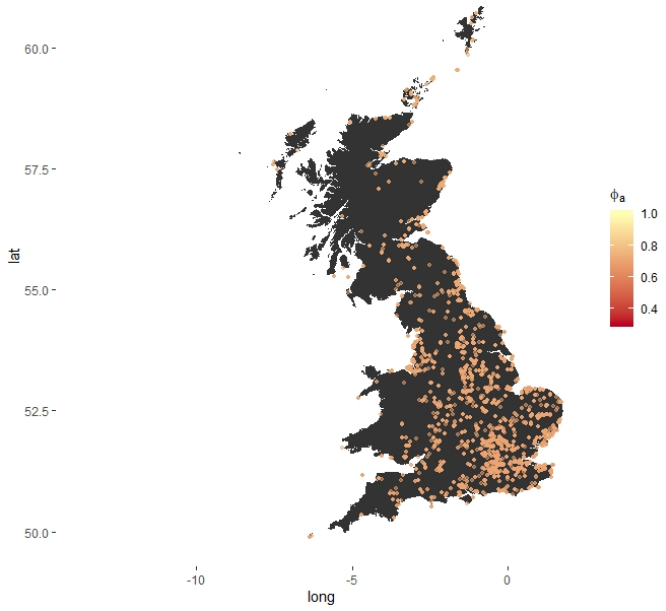

(a) Adult survival

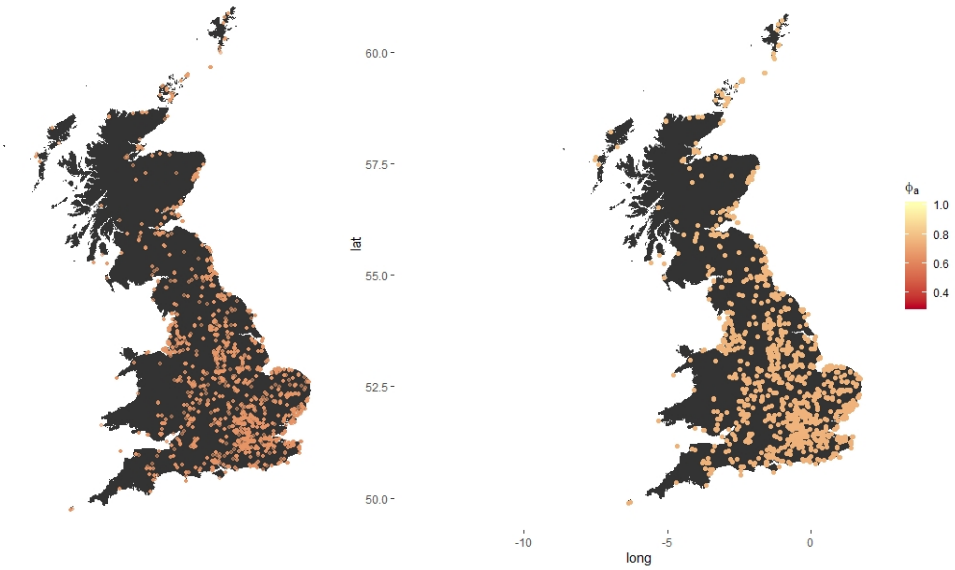

(b) Lower interval

(c) Upper interval

Fig. D.12 Point estimate maps for the third best model in terms of AIC: Survival probability and 95% confidence interval for adult starlings for the years 1990-1999.

D.4 Autocorrelation Results for the Starling Ring-recovery Data

In this section we provide additional autocorrelation results to those presented in Section 5.4. Dormann et al. (2007) describes different methods to recognise spatial autocorrelation, amongst these, they suggest to check for patterns in the residuals. We use the residual formula shown in Equation D.1 and adapt it to obtain the residuals for the ring-recovery data sets.

$$e_i = y_i - \hat{y}_i \,. \tag{D.1}$$

Let n_1 be number of years of ringing, and n_2 number of years of recovery. The total number of birds ringed at the start of year i is given by T_i, $R_{i,j}$ is the total number of birds ringed at the start of year i and recovered dead in year j, and $P_{i,j}$ are the cell probabilities of a multinomial distribution. Residuals formula adapted to the ring-recovery data per square,

$$e_s = \sum_{i=1}^{n_1} \sum_{j=i}^{n_2} T_i P_{i,j} - R_{i,j} \,. \tag{D.2}$$

Figure D.13 shows the distribution of the residuals for the ring-recovery model, this shows that there is not apparent pattern.

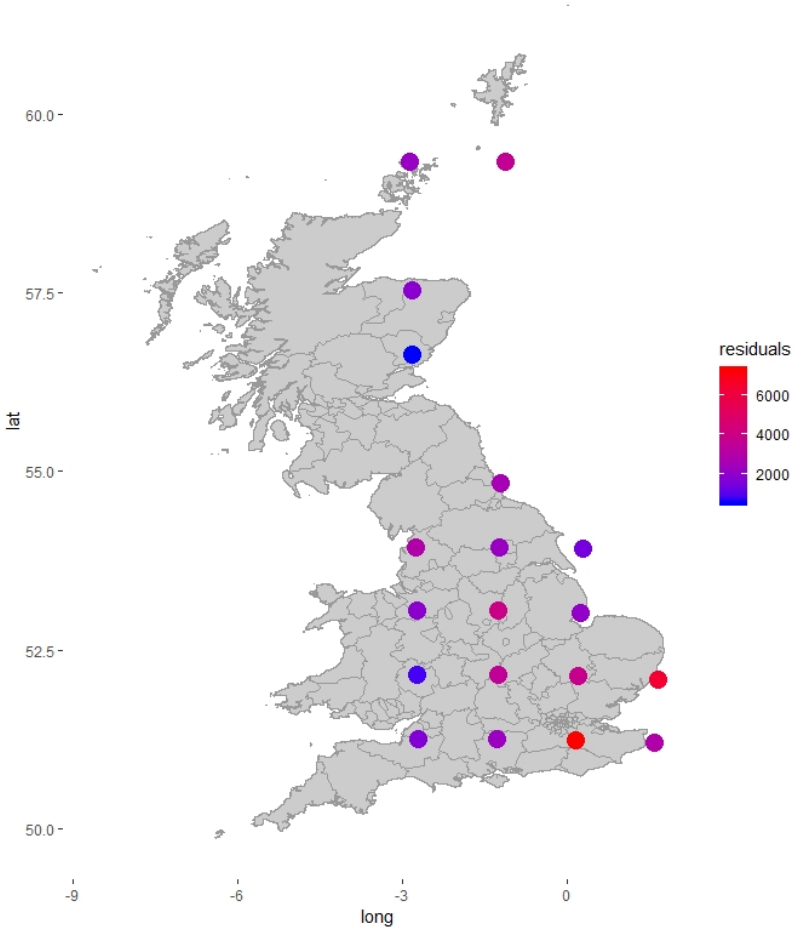

Fig. D.13 Distribution of residuals for the ring-recovery model for the starling data for the years 1990-1999.

Appendix E

List of Electronic Appendix

In this appendix we provide R code for the models developed in Chapters 2, 3, and 5. The R code can be accessed online via the link https://tinylink.net/KhxdU. The link gives access to the following folders:

E.1 Chapter 2

combined_model.r—Contains the code to fit the ring-recovery historical and historical combined data models from Chapter 2. As an example the blackbird data are provided within the code.

E.2 Chapter 3

Contains two folders with the R code for the capture-recapture models described in Chapter 3 for the entire sample and the female subsample.

E.2.1 Capture-Recapture Data

CaptureRecapture.r—Capture-recapture code for the capture-recapture sample; here models with time dependencies and categorical covariates such as sex and site can be added.

E.2.2 Female Nest Data

CaptureRecapture_femalenestdata.r—Capture-recapture code for the female nest capture-recapture sample; here models with categorical covariates such as sex and site, and continuous covariates, i.e. female presence data, can be added.

E.3 Chapter 5

SE_IPM_example.r—Contains the R code to fit the SE-IPM described in Chapter 5.